

University of Kentucky

UKnowledge

University of Kentucky Doctoral Dissertations

Graduate School

2010

PALINSPASTIC RECONSTRUCTION AROUND A THRUST BELT RECESS: AN EXAMPLE FROM THE APPALACHIAN THRUST BELT IN NORTHWESTERN GEORGIA

Brian Stephen Cook

University of Kentucky, b.cook@uky.edu

[Right click to open a feedback form in a new tab to let us know how this document benefits you.](#)

Recommended Citation

Cook, Brian Stephen, "PALINSPASTIC RECONSTRUCTION AROUND A THRUST BELT RECESS: AN EXAMPLE FROM THE APPALACHIAN THRUST BELT IN NORTHWESTERN GEORGIA" (2010). *University of Kentucky Doctoral Dissertations*. 5.

https://uknowledge.uky.edu/gradschool_diss/5

This Dissertation is brought to you for free and open access by the Graduate School at UKnowledge. It has been accepted for inclusion in University of Kentucky Doctoral Dissertations by an authorized administrator of UKnowledge. For more information, please contact UKnowledge@lsv.uky.edu.

ABSTRACT OF DISSERTATION

Brian Stephen Cook

The Graduate School
University of Kentucky

2010

PALINSPASTIC RECONSTRUCTION AROUND A THRUST BELT RECESS:
AN EXAMPLE FROM THE APPALACHIAN THRUST BELT
IN NORTHWESTERN GEORGIA

ABSTRACT OF DISSERTATION

A dissertation submitted in partial fulfillment of the
requirements for the degree of Doctor of Philosophy in the
College Arts and Sciences
at the University of Kentucky

By
Brian Stephen Cook

Lexington, Kentucky

Director: Dr. William A. Thomas, Hudnall Professor of Geological Sciences

Lexington, Kentucky

2010

Copyright © Brian Stephen Cook 2010

ABSTRACT OF DISSERTATION

PALINSPASTIC RECONSTRUCTION AROUND A THRUST BELT RECESS: AN EXAMPLE FROM THE APPALACHIAN THRUST BELT IN NORTHWESTERN GEORGIA

In a well-defined subrecess in the Appalachian thrust belt in northwestern Georgia, two distinct regional strike directions intersect at approximately 50°. Fault intersections and interference folds enable tracing of both structural strikes. Around the subrecess, tectonically thickened weak stratigraphic layers—shales of the Cambrian Conasauga Formation—accommodated ductile deformation associated with the folding and faulting of the overlying Cambrian–Ordovician regional competent layer. The structures in the competent layer are analogous to those over ductile duplexes (mushwads) documented along strike to the southwest in Alabama.

The intersection and fold interference exemplify a long-standing problem in volume balancing of palinspastic reconstructions of sinuous thrust belts. Cross sections generally are constructed perpendicular to structural strike, parallel to the assumed slip direction. An array of cross sections around a structural bend may be restored and balanced individually; however, restorations perpendicular to strike across intersecting thrust faults yield an imbalance in the along-strike lengths of frontal ramps. The restoration leads to a similar imbalance in the surface area of a stratigraphic horizon, reflecting volume imbalance in three dimensions.

The tectonic thickening of the weak-layer shales is evident in palinspastically restored cross sections, which demonstrate as much as 100% increase in volume over the restored-state cross sections. The cause of the surplus shale volume is likely pre-thrusting deposition of thick shale in a basement graben that was later inverted. The volume balance of the ductile duplex is critical for palinspastic reconstruction of the recess, and for the kinematic history and mechanics of the ductile duplex.

KEYWORDS: Appalachian thrust belt, geology of Georgia, recess, palinspastic restoration, ductile duplex

Brian Stephen Cook
Student's signature

July 21st, 2010
Date

PALINSPASTIC RECONSTRUCTION AROUND A THRUST BELT RECESS:
AN EXAMPLE FROM THE APPALACHIAN THRUST BELT
IN NORTHWESTERN GEORGIA

By

Brian Stephen Cook

Dr. William A. Thomas

Director of Dissertation

Dr. Alan E. Fryar

Director of Graduate Studies

July 21st, 2010

DISSERTATION

Brian Stephen Cook

The Graduate School
University of Kentucky

2010

PALINSPASTIC RECONSTRUCTION AROUND A THRUST BELT RECESS:
AN EXAMPLE FROM THE APPALACHIAN THRUST BELT
IN NORTHWESTERN GEORGIA

DISSERTATION

A dissertation submitted in partial fulfillment of the
requirements for the degree of Doctor of Philosophy in the
College Arts and Sciences
at the University of Kentucky

By
Brian Stephen Cook

Lexington, Kentucky

Director: Dr. William A. Thomas, Hudnall Professor of Geological Sciences

Lexington, Kentucky

2010

Copyright © Brian Stephen Cook 2010

This dissertation is dedicated to God,
who has blessed me with a wonderful family

ACKNOWLEDGMENTS

First, I would first like to thank my advisor, Dr. William A. Thomas, for his insight and guidance during the course of this research project. Also, I would like to thank my committee: Dr. James Drahovzal, Dr. Michael Kalinski, Dr. Kieran O'Hara, and Dr. Edward Woolery. I would also like to thank my outside examiner Dr. Richard Sweigard, who agreed to help at my defense on very short notice. Every one of the above improved this dissertation tremendously with their suggestions.

I wish to also thank all the sources of funding that helped to get this project off and running. A considerable part of this research project was funded by the EDMAP component of the National Cooperative Geologic Mapping Program of the United States Geological Survey. The University of Kentucky Department of Earth and Environmental Sciences provided funding through the Brown-McFarlan and Ferm Funds. The University of Kentucky Graduate School provided funding through the student support program. Funding was also provided by the American Association of Petroleum Geologists and the Geological Society of America.

Many other faculty members here have helped me through the years, especially those for whom I taught as an assistant. I wish to thank Dr. Rick Bowersox, Dr. Alan Fryar, and Dr. David Moecher. You taught me so much!

I wish to also thank my colleagues through the years, and especially my friends and officemates. Mike Solis took the raw contour lines for my models and transformed them into the finished product included in this dissertation. Liz Dodson and Carrie Kidd helped to keep me sane. Most of all, I wish to thank Dr. Matt Surles for his help and friendship, and for knowing the words to "Georgia on a Fast Train."

It would take pages upon pages for me to thank all the people who helped me get to this place in my life. I wish I could name them all. I have been blessed with a wonderful family, and I want to thank all of them for their love and support. Many of my closest family members are no longer here. I wish I could share this time in my life with my mother, Martha Melton, and her parents, Calvin and Lois, who will always be such an important part of the person I am (at least the good parts!). Words cannot express how I miss you all. I also want to thank my father, Gary Cook, his mother, Irene Cook, and my aunt, Linda Melton.

Finally, I wish to thank Lois Yoksoulion for her love and friendship over the last few years. Thank you for the laughs and the quality time with the cats.

TABLE OF CONTENTS

| | |
|------------------------------------------------------------------------------------|-----------|
| Acknowledgments..... | iii |
| List of Tables | vii |
| List of Figures..... | viii |
| List of Files | xi |
| CHAPTER I: INTRODUCTION..... | 1 |
| CHAPTER II: BACKGROUND STRUCTURAL GEOLOGY | 7 |
| 2.1 ALONG-STRIKE BENDS IN THRUST BELTS | 7 |
| 2.1.1 Controls on formation and development of salients | 7 |
| 2.1.1.1 Mechanisms in basin-controlled salients | 7 |
| 2.1.1.2 Mechanisms in salients related to irregularities of colliding margins..... | 9 |
| 2.1.1.3 Other mechanisms controlling thrust belt curves..... | 10 |
| 2.1.2 Paucity of research on recesses..... | 11 |
| 2.1.3 Possible causes of bends in thrust belts | 12 |
| 2.1.4 Structural problems of bends in thrust belts | 14 |
| 2.1.4.1 Problems with palinspastic restoration around bends in thrust belts..... | 14 |
| 2.1.5 Recesses in the Appalachian thrust belt..... | 15 |
| 2.1.5.1 New York recess..... | 15 |
| 2.1.6 Examples of structural intersections in other thrust belts | 22 |
| 2.2 DUCTILE DUPLEXES IN THRUST BELTS | 22 |
| 2.2.1 Ductile duplex case study in Alabama..... | 23 |
| 2.3 STRATIGRAPHIC CONTROLS ON STRUCTURES..... | 23 |
| <u>CHAPTER III: REGIONAL STRATIGRAPHY OF NORTHWESTERN GEORGIA</u> | <u>33</u> |
| 3.1 INTRODUCTION TO REGIONAL STRATIGRAPHY | 33 |
| 3.2 CAMBRIAN SYSTEM | 34 |
| 3.2.1 Lower Cambrian Shady Dolomite | 35 |
| 3.2.2 Upper Lower Cambrian Rome Formation | 36 |
| 3.2.3 Middle to Lower Upper Cambrian Conasauga Formation | 38 |
| 3.2.3.1 Maynardville Limestone Member of the Conasauga Formation..... | 42 |
| 3.3 UPPER CAMBRIAN AND LOWER ORDOVICIAN KNOX GROUP | 43 |
| 3.3.1 Copper Ridge Dolomite | 46 |
| 3.3.2 Chepultepec Dolomite | 47 |
| 3.3.3 Longview Limestone | 49 |
| 3.3.3.1 Sandstones in the Knox Group | 49 |
| 3.3.4 Newala Limestone | 50 |
| 3.3.5 Alternate interpretations/correlations in the upper Knox Group | 51 |

| | |
|--------------------------------------------------------------------------------|-----|
| 3.8.3.1 Lithology of the Mississippian-Pennsylvanian boundary | 107 |
| 3.8.3.2 Data from fossils | 108 |
| 3.8.3.3 Associated problem with the Pennington-Raccoon Mountain boundary | 109 |
| 3.8.3.4 Summary and commentary | 110 |
| 3.9 SUMMARY OF REGIONAL STRATIGRAPHY | 110 |
| | |
| <u>CHAPTER IV: REGIONAL STRUCTURAL GEOLOGY OF NORTHWESTERN GEORGIA</u> | 122 |
| 4.1 INTRODUCTION TO REGIONAL STRUCTURAL GEOLOGY | 122 |
| 4.1.1 Review of regional thrust sheets and thrust faults | 122 |
| 4.2 REGIONAL SETTING OF SOUTHERN APPALACHIAN STRUCTURES IN GEORGIA | 123 |
| 4.3 STRUCTURE OF THE SMALL-SCALE RECESS IN NORTHWESTERN GEORGIA | 125 |
| 4.3.1 Kingston-Chattooga anticlinorium | 125 |
| 4.3.2 Little Sand Mountain-Horn Mountain fold train | 126 |
| 4.3.3 Simms Mountain-Horseleg Mountain fold train | 128 |
| 4.4 BASEMENT FAULTS IN NORTHWESTERN GEORGIA | 131 |
| | |
| <u>CHAPTER V: CROSS SECTIONS, SUBSURFACE STRUCTURE, VOLUME BALANCE</u> | 148 |
| 5.1 CROSS SECTIONS AND SUBSURFACE STRUCTURE | 148 |
| 5.2 VOLUME BALANCE IN THE DUCTILE DUPLEX | 151 |
| 5.2.1 Analogy with structures in Alabama | 154 |
| 5.2.2 Interpretation for structures in Georgia | 155 |
| | |
| <u>CHAPTER VI: INTERPRETATIONS AND DISCUSSION</u> | 174 |
| 6.1 STRUCTURAL INTERFERENCE IN THE GEORGIA SUBRECESS | 174 |
| 6.2 IMPLICATIONS OF DUCTILE DUPLEX VOLUME BALANCE | 175 |
| | |
| <u>CHAPTER VII: SUMMARY AND CONCLUSIONS</u> | 178 |
| | |
| REFERENCES | 181 |
| | |
| VITA | 194 |

LIST OF TABLES

| | |
|----------------------------------------------------------------------------------------------------------|-----|
| Table 5-1, Calculations from the ductile duplex models | 159 |
| Table 5-2, Calculations of shortening magnitudes from cross sections..... | 159 |
| Table 5-3, Calculations of ductile duplex surface area from cross sections | 160 |
| Table 5-4, Calculations of thrust sheet surface area from cross sections as shown in Figure 5-10..... | 160 |

LIST OF FIGURES

| | |
|---------------------------------------------------------------------------------------------------------------------------------------------------------------------------------------------------|-----|
| Figure 1-1, Map of the Appalachian thrust belt drawn in 1893 by Bailey Willis..... | 3 |
| Figure 1-2, Detail of outline structural geology map of the Appalachian thrust belt | 4 |
| Figure 1-3, Structural outline map of the Appalachian thrust belt in Alabama and Georgia..... | 5 |
| Figure 1-4, Geologic map of the subrecess in Georgia..... | 6 |
| Figure 2-1, Idealized end-member models of salient development..... | 25 |
| Figure 2-2, Sample calculations of implied tangential strain around a salient and a recess..... | 26 |
| Figure 2-3, Location map of the structural analyses of Geiser and Engelder (1983) | 27 |
| Figure 2-4, Location map of the abrupt bend in the Appalachian thrust belt of central western Virginia and major structural features..... | 28 |
| Figure 2-5, Location map of the Appalachian thrust belt of central western Virginia | 29 |
| Figure 2-6, Diagram of the transfer of displacement within a thrust fault system | 30 |
| Figure 2-7, Regional map of the southwestern Appalachian orogen and the eastern Ouachita orogen..... | 30 |
| Figure 2-8, Diagrams illustrating the evolution of the Late Proterozoic Cartersville transfer fault into an oblique footwall ramp during late Paleozoic Alleghanian collisional events..... | 31 |
| Figure 3-1, Generalized stratigraphic column for the Paleozoic succession in northwestern Georgia..... | 112 |
| Figure 3-2, Comparative stratigraphic column for the Paleozoic succession in northwestern Georgia..... | 113 |
| Figure 3-3, County location map for northwestern Georgia..... | 113 |
| Figure 3-4, Comparative stratigraphic column for the Knox Group in Alabama and Tennessee..... | 114 |
| Figure 3-5, Cross sections of the Middle and Upper Ordovician showing the two dominant facies | 115 |
| Figure 3-6, Subdivisions of the Chickamauga Supergroup | 116 |
| Figure 3-7, Diagrammatic stratigraphic cross sections and correlations for the Mississippian succession in northwestern Georgia..... | 117 |
| Figure 3-8, Alternate interpretations of the Mississippian succession in northwestern Georgia..... | 118 |
| Figure 3-9, Correlation chart noting evolution of nomenclature of the Pennsylvanian succession in northwestern Georgia..... | 119 |
| Figure 3-10, General columnar sections of the Upper Mississippian and Lower Pennsylvanian succession in northwestern Georgia | 120 |
| Figure 3-11, Details of biostratigraphic markers in the Lower Pennsylvanian and Upper Mississippian..... | 121 |
| Figure 4-1, Rose Diagram of bedding on Taylor Ridge monocline | 134 |
| Figure 4-2, Equal-area stereoplots of poles to bedding on Taylor Ridge monocline..... | 134 |
| Figure 4-3, Equal-area stereoplots of poles to bedding on Taylor Ridge monocline without small-scale fold..... | 135 |
| Figure 4-4, Equal-area stereoplots of poles to bedding on Taylor Ridge monocline small- scale fold..... | 135 |

| | |
|------------------------------------------------------------------------------------------------------------------------------------------------------------------------------------------|-----|
| Figure 4-5, Equal-area stereoplot of poles to bedding on Little Sand Mountain–Horn Mountain fold train | 136 |
| Figure 4-6, Equal-area stereoplot of poles to bedding on Little Sand Mountain syncline | 136 |
| Figure 4-7, Equal-area stereoplot of poles to bedding on Dick Ridge anticline | 137 |
| Figure 4-8, Equal-area stereoplot of poles to bedding on Horn Mountain anticline | 137 |
| Figure 4-9, Equal-area stereoplot of poles to bedding on Turkey Mountain anticline | 138 |
| Figure 4-10, Equal-area stereoplot of poles to bedding on Simms Mountain–Horseleg Mountain fold train | 138 |
| Figure 4-11, Equal-area stereoplot of poles to bedding on Simms Mountain anticline (northeastern end) | 139 |
| Figure 4-12, Equal-area stereoplot of poles to bedding on Simms Mountain anticline (southwestern end) | 139 |
| Figure 4-13, Equal-area stereoplot of poles to bedding on Rock Mountain syncline | 140 |
| Figure 4-14, Equal-area stereoplot of poles to bedding on Lavender Mountain anticline near northeastern end | 140 |
| Figure 4-15, Equal-area stereoplot of poles to bedding on Horseleg Mountain anticline | 141 |
| Figure 4-16, Equal-area stereoplot of poles to bedding on Strawberry Mountain anticline along topographic crest | 141 |
| Figure 4-17, Equal-area stereoplot of poles to bedding on Strawberry Mountain anticline along roadcut | 142 |
| Figure 4-18, Equal-area stereoplot of poles to bedding on Strawberry Mountain anticline along northwestern part of roadcut | 142 |
| Figure 4-19, Equal-area stereoplot of poles to bedding on Strawberry Mountain anticline along southeastern part of roadcut | 143 |
| Figure 4-20, Equal-area stereoplot of poles to bedding on Taylor Ridge monocline west of intersection with Strawberry Mountain anticline | 143 |
| Figure 4-21, Equal-area stereoplot of poles to bedding on Taylor Ridge monocline north of intersection with Strawberry Mountain anticline | 144 |
| Figure 4-22, Equal-area stereoplot of poles to bedding on Taylor Ridge monocline south of intersection with Strawberry Mountain anticline | 144 |
| Figure 4-23, Equal-area stereoplot of poles to bedding on Taylor Ridge monocline farther north of intersection with Strawberry Mountain anticline | 145 |
| Figure 4-24, Equal-area stereoplot of poles to bedding on Taylor Ridge monocline farther north of intersection with Strawberry Mountain anticline (omitting point from small fold) | 145 |
| Figure 4-25, Equal-area stereoplot of poles to bedding on Strawberry Mountain anticline at intersection with Dick Ridge anticline | 146 |
| Figure 4-26, Basement fault map of northwestern Georgia, from Rich (1992) | 147 |
| Figure 5-1, Seismic reflection profile of the ductile duplex | 161 |
| Figure 5-2, Simplified palinspastic restoration of cross section A–A' | 163 |
| Figure 5-3, Isopach map of the deformed-state ductile duplex | 165 |
| Figure 5-4, Three-dimensional surface model of the deformed-state ductile duplex | 166 |
| Figure 5-5, Isopach map of the restored-state ductile duplex using a simple line-length balance method for the base of the Knox Group (Unit 2) | 167 |

| | |
|-----------------------------------------------------------------------------------------------------------------------------------------------------------------------------------|-----|
| Figure 5-6, Three-dimensional surface model of the restored-state ductile duplex | 168 |
| Figure 5-7, Sequential cross sections illustrating a basement graben that is interpreted to be the source of the surplus volume of Unit 1 shales in the subrecess in Georgia..... | 169 |
| Figure 5-8, Isopach map of the graben-state ductile duplex..... | 171 |
| Figure 5-9, Three-dimensional surface model of the graben-state ductile duplex | 172 |
| Figure 5-10, Calculations made from actual measurements on cross sections D–D' and L–L' in comparison with the simplistic model in Figure 2-2..... | 173 |

LIST OF FILES

Plate 1, Geologic map illustrating the surface geology of the Georgia subrecess, [plate1.pdf](#), 2676 KB.

Plate 2, Geologic cross sections illustrating the structural geometry of the Georgia subrecess, [plate2.pdf](#), 788 KB.

Chapter I:

INTRODUCTION

Sinuuous curves in the gross-scale structural trend of the Appalachian fold-and-thrust belt have been recognized for well over 100 years (Figure 1-1; Willis, 1893). The curves in the Appalachian orogen have since been related to the geometry of the pre-orogenic continental margin (*cf.* Thomas, 1977). The continental margin can be defined as a zigzag array of transform faults and rifts (Figure 1-2) that form promontories that are concave toward the continent and embayments that are convex toward the continent. During subsequent thrusting, broad, sweeping curves called salients are formed at embayments (Figure 1-2). In some places, the change in structural trend is more abrupt and is expressed as a more pronounced bend, rather than a sinuous curve. As illustrated in Figure 1-2, these abrupt trend changes in recesses are at the along-strike ends of salients of the Appalachian thrust belt, and correspond to the promontories of the pre-orogenic continental margin.

The thrust belt of the southern Appalachians includes Cambrian to Pennsylvanian strata in thrust sheets that generally are imbricated northwestward and strike northeastward. In northwestern Georgia, the Appalachian thrust belt includes the gradually curved Tennessee salient, convex toward the craton in the direction of thrust translation, and the composite Alabama recess, which is concave toward the craton (Figure 1-3). In the northeastern part of the composite Alabama recess, at a subrecess in northwestern Georgia (Figure 1-3, and also labeled as **A** in Figure 1-2), north-northeastward-striking thrust faults and related folds in the southern arm of the Tennessee salient intersect east-northeastward-striking thrust faults and related folds that diverge from the predominant strike of the eastern arm of the Alabama recess (Figure 1-4).

The structural problems posed by along-strike bends in thrust belts are multifold. Mechanical and kinematic questions about the formation and evolution of thrust belt bends remain to be answered. Primarily, the argument hinges on whether thrust belt bends are the product of one primary deformation direction or of multiple episodes of deformation, including at least two thrust directions. Furthermore, the palinspastic

restoration of a non-parallel array of cross sections around a thrust belt bend leaves substantial volume-balance problems.

The focus of this research is to investigate the lithostratigraphy and structure of the Georgia subrecess in northwestern Georgia to gain some insight into the formation of the subrecess through the study of both structural trends and the interaction between them. During the course of the field research, a geologic map (Plate 1) and an array of palinspastically restored cross sections have been assembled (Plate 2). The purpose of this dissertation, along with the map and cross sections from this project, is to present the reader with an understanding of the Georgia subrecess in three dimensions and of the general elements of evolution.

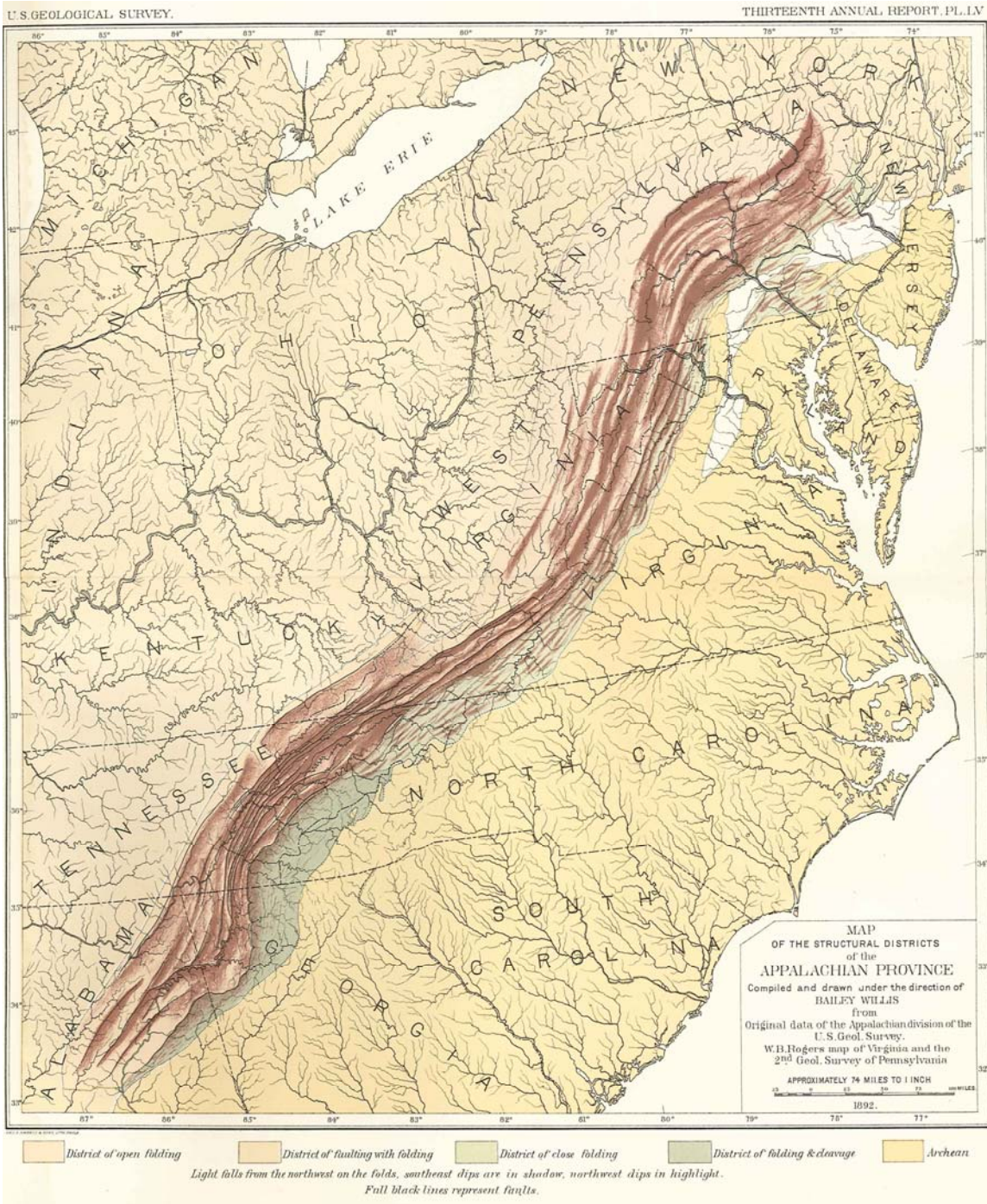


Figure 1-1. Map of the Appalachian thrust belt drawn in 1893 by Bailey Willis, who used shading to emphasize morphology. The salients and recesses of the orogen are unmistakably—and artistically—illustrated on this map.

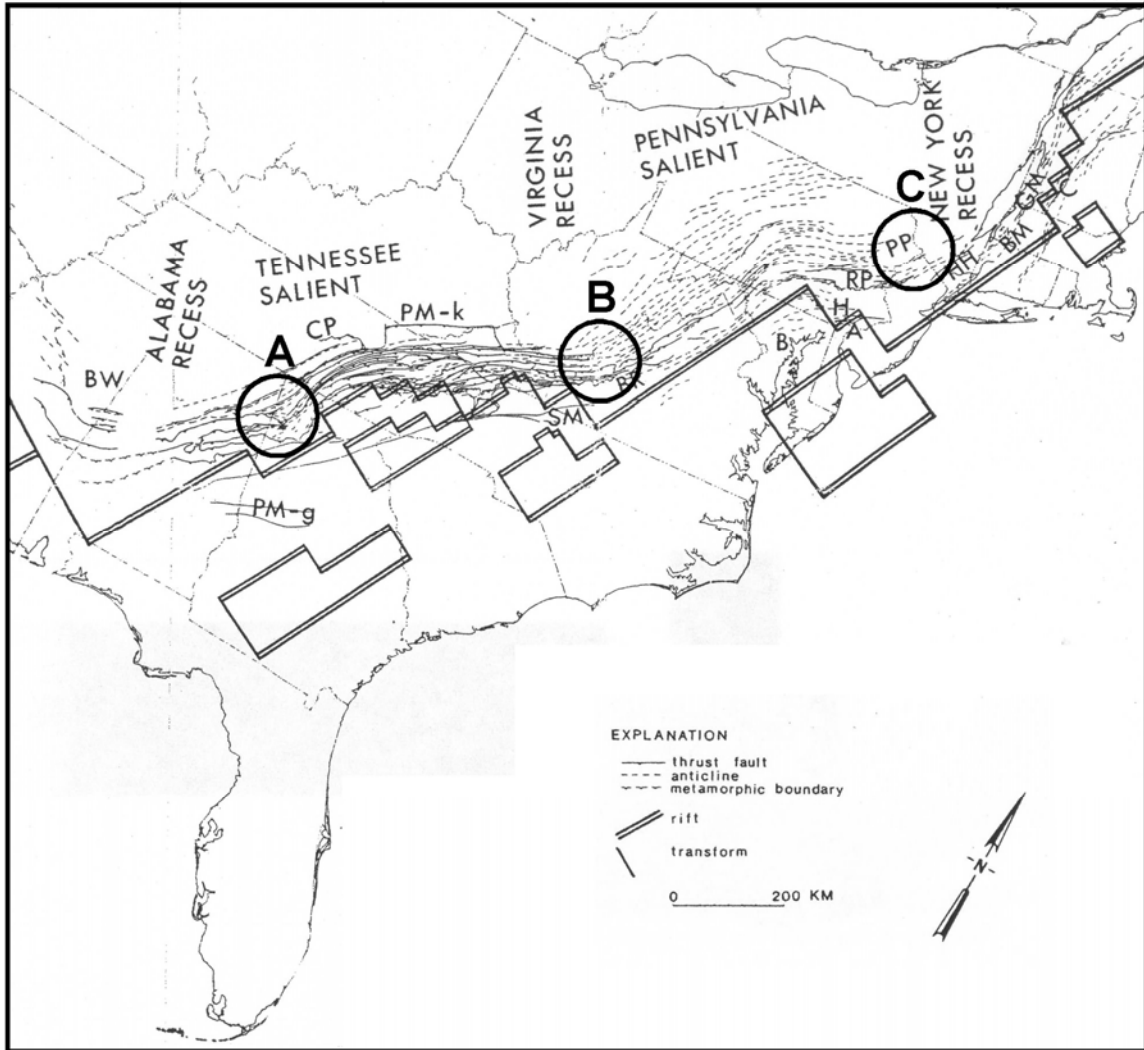


Figure 1-2. Detail of outline structural geology map of the Appalachian thrust belt indicating the locations of abrupt changes in the structural trend, as well as interpretation of shape of the pre-Appalachian Iapetan rifted margin, from Thomas (1977). The bends in strike are labeled as **(A)** northwestern Georgia, **(B)** central western Virginia, and **(C)** northeastern Pennsylvania/southeastern New York. Also note the prominent salients and recesses, and their location with respect to the promontories and embayments of the continental margin.

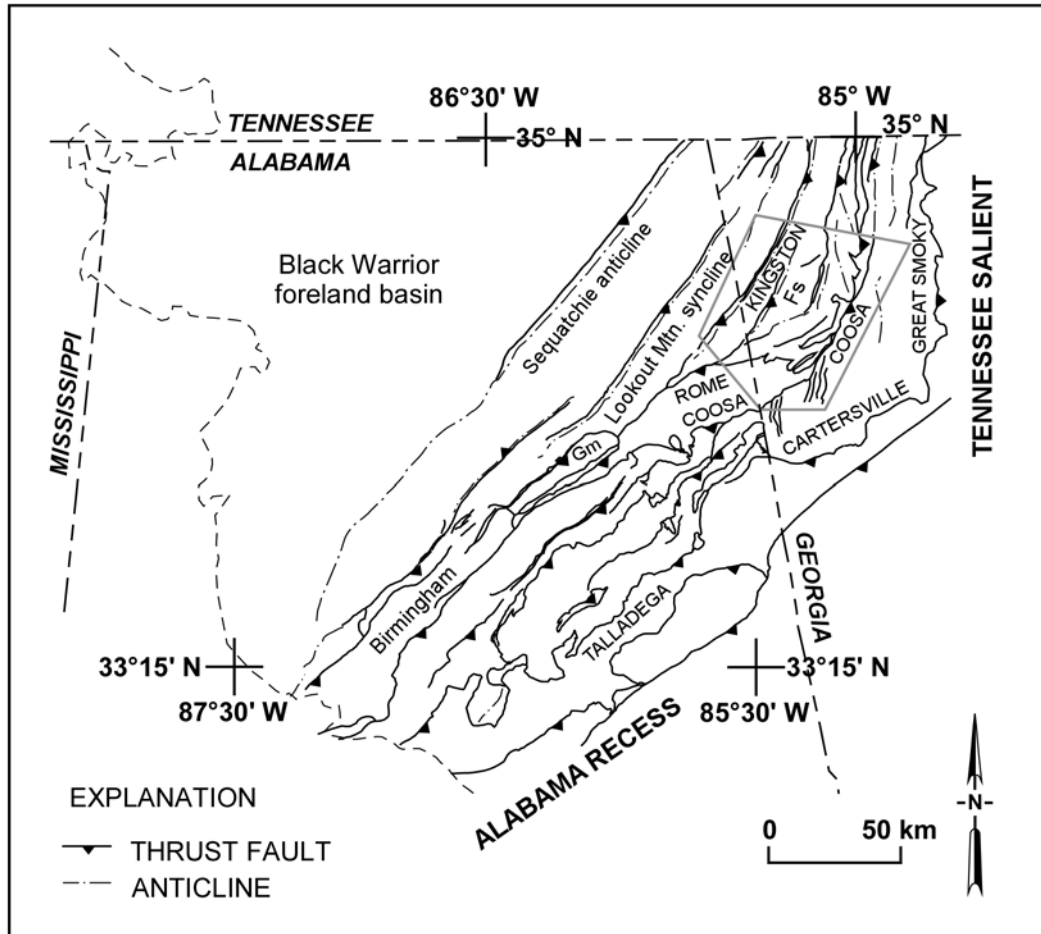


Figure 1-3. Structural outline map of the Appalachian thrust belt in Alabama and Georgia, adapted from Thomas (2007). The gray polygon shows the location of the more detailed map in Figure 1-4. Names of faults are in all capital letters. The Floyd synclinorium is labeled as Fs, Gadsden mushwad as Gm. The label “Birmingham” shows the location of both the surface thin-skinned Birmingham anticlinorium and the subsurface Birmingham basement graben.

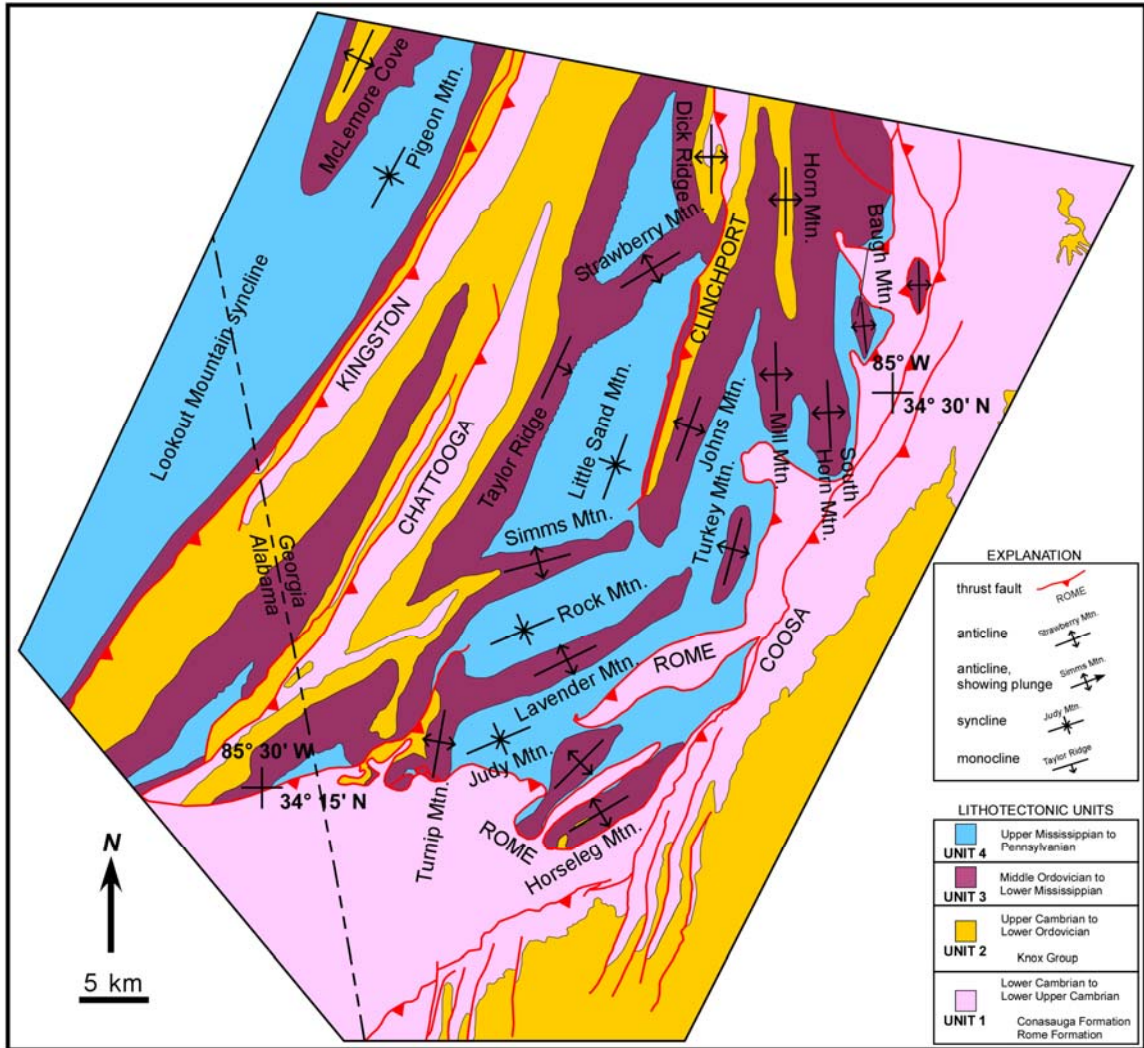


Figure 1-4. Geologic map of the subrecess in Georgia, compiled from field data of the author, as well as Butts (1948), Cressler (1963, 1964a, b, 1970, 1974); Georgia Geological Survey (1976), Thomas and Cramer (1979), Osborne *et al.* (1988), and Thomas and Bayona (2005). Plunge directions of fold hinges are denoted by closed arrows and the major folds are labeled. Fault names are in all-capital letters. The Kingston–Chattooga anticlinorium is the structurally high outcrop area dominantly of Units 1 and 2 between Lookout Mountain syncline and Taylor Ridge monocline. The Floyd synclinorium (including Little Sand Mountain, Rock Mountain, and Judy Mountain synclines, as well as other unnamed folds) encompasses the entire outcrop area of Unit 4 southeast of the Kingston and Chattooga faults.

Chapter II:
BACKGROUND STRUCTURAL GEOLOGY

2.1 ALONG-STRIKE BENDS IN THRUST BELTS

Map-view curves in trends of mountain belts were recognized more than 200 years ago on some of the first geographic maps of mountains; a study by Marshak (2004) includes a concise history on this subject. Curves in the characteristically sinuous map traces of orogenic thrust belts can be classified as either salients or recesses. Salients are broad, sweeping curves, which are convex in the direction of thrust transport; recesses are more angular bends that are concave in the direction of thrust transport.

2.1.1 *Controls on formation and development of salients*

Thrust-belt salients have been studied fairly widely over the last few decades, and much of the research has focused on defining the controls on the formation and development of salients. Macedo and Marshak (1999) documented details of the shapes and geologic settings of salients in various locations and noted that, for most salients, the apex is coincident with the pre-thrusting sedimentary depocenter in the basin from which it formed, as demonstrated by Thomas (1977). Marshak (2004) noted that although most thrust belt curves are “basin controlled,” other controls on thrust belt curves include interactions with obstacles or indenters. Marshak (2004) also noted that not all curved thrust belts are true “oroclines,” and that “orocline” should refer only to specific thrust belts in which some segments have been rotated on a vertical axis.

2.1.1.1 Mechanisms in basin-controlled salients

Many studies have shown that the geometry of basins that underlie some salients affects the formation and development of the salient. Macedo and Marshak (1999) documented along-strike change in depth to detachment as the controlling factor for salients forming within thick sedimentary successions; in such places, the salients form over deeper passive-margin basins and tend to propagate along the axes of the borders of the basins, which are at high angles to the thrust belt (*cf.* also Thomas, 1977). The width of the thrust belt varies as a function of depth to the detachment and thus maintains volume for a given angle of critical taper; this concept was demonstrated by Marshak and Wilson (1992) using simple sandbox models. Examples of salients formed at basins with

thick sedimentary successions include the Pennsylvania salient (Gray and Stamatakos, 1997; Macedo and Marshak, 1999) and the Sulaiman salient in Pakistan (Davis and Lillie, 1994; Macedo and Marshak, 1999). The Nackara salient in the Adelaide thrust belt in southern Australia formed along a rift axis at a high angle to the thrust belt (Marshak and Flötmann, 1996).

Along-strike changes in the strength of the detachment also control formation of a salient. Davis and Engelder (1985) and Jaumé and Lillie (1988) noted that width of a thrust belt is dependent on the strength of the detachment horizon, because the angle of critical taper decreases as the detachment strength decreases. For example, for a given magnitude of shortening, a thrust belt over a strong detachment (which sustains a higher critical taper angle) will be narrower than that over a weak detachment (Callasou *et al.*, 1993). Thus, a thrust belt over a weak horizon, such as a “glide horizon” in an evaporite, will protrude farther into the foreland. This mechanism may also work in union with the depth-to-detachment mechanism because evaporites are more common in basins with thicker sedimentary successions (Marshak, 2004). Frey (1973) documented that the Pennsylvania salient in the Appalachians coincides with detachments in the evaporites of the Silurian Salina Formation. The Sulaiman salient in Pakistan (Davis and Lillie, 1994) is also an example of a salient that is localized over a weak sedimentary glide horizon; also, the widest segments of the Zagros Mountains in southern Iran coincide with the presence of salt diapirs (Talbot and Alavi, 1996; McQuarrie, 2004). Other examples include the Monterrey salient in the Cordillera Occidental in Mexico (Marrett, 1995; Melnyk and Cameron, 1998), the Salt Range in Pakistan (Jaumé and Lillie, 1988; McDougall and Khan, 1990), and the Jura Mountains in Switzerland (Laubscher, 1972, 2008).

Along-strike changes in dip of the basal detachment cause the width of a thrust belt to change and, as a result, control formation of a salient (*e.g.*, Boyer, 1995; Mitra, 1997). A steeper detachment dip yields a wider thrust belt because the critical-taper angle of a wedge is the sum of the dip of the basal detachment and the slope of the wedge surface (Marshak, 2004). Consequently, a steeper basal detachment may correspond to a deep basin, so that these two mechanisms may work in conjunction. Boyer (1995) and

Mitra (1997) cited the Wyoming and Provo salients in the Sevier thrust belt in Utah as examples of salients that are controlled by detachment dip.

Along-strike change in the strength of the thrust wedge itself is a factor in formation of a salient (*e.g.*, Boyer, 1995; Mitra, 1997). Thrust wedges of stronger rocks have greater critical-taper angles than thrust wedges of weaker rocks; thrust wedges of weaker rocks are thus wider and protrude farther into the foreland for a given magnitude of shortening (Marshak, 2004). For example, Marshak (2004) mentioned facies changes in a basin, such as a well-cemented sandstone grading laterally into a weak organic shale would lead to curvature during thrust translation; he also noted that thick-skinned thrust belts tend to be narrower because of the inclusion of strong basement rocks. On a related note, Marshak (2004) postulated that along-strike changes in heat flow (and thus, changes in rheology) could conceivably have the same effect (*i.e.*, hotter, weaker rocks would have a lower angle of critical taper).

2.1.1.2 Mechanisms in salients related to irregularities of colliding margins

The shape of an indenter can also be a factor in the formation of a salient. Marshak (2004) noted that the “impression of a promontory or of an exotic crustal block of limited along-strike [extent] into a sedimentary basin generates a salient to the foreland of the collision,” as illustrated by simple sandbox models. In indenter-controlled salients, thrust translation begins at the apex of the indenter and magnitude of translation decreases away from the apex; as a result, curvature is related to differential displacement along the length of the indenter. Marshak (2004) illustrated that structural trend lines converge at the apex of indenter-controlled salients, which contrasts with the configuration in basin-controlled salients (Macedo and Marshak, 1999). Laubscher (1972) noted that curved faults form in advance of an indenter. The shape of an indenter-controlled salient is a function of the shape of the indenter; Macedo and Marshak (1999) demonstrated from sandbox models that a rounded indenter creates a parabolic curve and a rectangular indenter yields a flat curve. Indenters that collide obliquely create asymmetric salients (Marshak, 2004).

Margin-controlled salients were first hypothesized by Dana (1866). In his textbook, Dana (1866) suggested that curves in mountain belts were formed where the mountains were molded along an uneven margin of a preexisting craton. Although Dana

would not have understood the origin of the tectonic stresses involved, his hypothesis of how promontories and embayments control thrust belt shape is still valid. This idea was updated greatly by Rankin (1976), Thomas (1977), and Thomas and Whiting (1995), and was applied by these authors to the salients and recesses of the Appalachian thrust belt. Another example of a margin-controlled salient was proposed by Royden and Burchfiel (1989) for the curvature of the Carpathian range along the southern margin of Europe. Essentially, the effects of margin geometry on the geometry of thrust belts works much like that of the basin controls. Salients form in embayments of the continental margin where passive-margin sedimentary successions are thicker and wider, and recesses form over the promontories of the continental margin where the basin is shallower and more narrow (*cf.* Thomas, 1977).

Obstacles, such as foreland basement highs, also form curves in thrust belts. Kulik and Schmidt (1988) demonstrated that the interference structures in the Rocky Mountain foreland are largely controlled by the interaction of basement structures with predominantly eastward-directed thrusting. Montgomery (1993) and Paulsen and Marshak (1999) further showed that pre-thrusting stratigraphic thinning--also interacting with basement structures--may account for the abrupt curvature to the north and south of the Provo salient, in Idaho-Wyoming and Utah, respectively (*i.e.*, the Uinta recess, *etc.*). In the Provo salient itself, however, Kwon and Mitra (2004) demonstrated three different superposed transport directions on the basis of orientations of plastic deformation and fractures. Marshak (2004) further noted that recess margins evolve into strike-slip fault systems where the edge of the obstacle is steep and into gradual curves where the edge of the obstacle is characterized by a gentle slope.

2.1.1.3 Other mechanisms controlling curves in thrust belts

Curves are also formed at the intersections of non-parallel thrust belts. Marshak (2004) noted that different segments of a thrust belt “may form at different times, either because convergence or collision occurs at different parts of a margin at different times during a single orogenic event, or because different [parts of the thrust belt] form in response to entirely separate collisional or convergent events.” Marshak and Tabor (1989) noted “intersection oroclinal” at locations where faults of two non-parallel salient segments overlap. Marshak (2004) cites the New York and Virginia recesses of the

Appalachian thrust belt as examples of intersection oroclinal curves. Such curves also have been described in the Brasilia belt in east-central Brazil (Araújo and Marshak, 1997) and in the Cape fold belt of southern Africa (de Beer, 1992).

Curves in thrust belts can also be formed where strike-slip fault zones intersect. An example of strike-slip fault motion superposed on thrust belts is documented where the Makran thrust belt in southern Pakistan intersects the Chaman strike-slip system, which is the transform fault that bounds the western part of India (Lawrence *et al.*, 1981; Marshak, 1988).

Marshak (2004) noted that some curves “may not reflect rotation of structural trends around a vertical axis but may instead be an artifact of the erosion of a regional-scale plunging fold [with an axis that trends obliquely] to the thrust front.” Such folds have been documented from tangential buckling over the intersections of frontal and oblique ramps in the footwall of the Wyoming salient (Apotria *et al.*, 1992; Apotria, 1995) and of the Appalachian thrust belt in Alabama (Cook and Thomas, 2009). Such folds may also form in thrust belts that are buckled in subsequent folding episodes; for example, Burg *et al.* (1997) suggest that the Nanga Parbat syntaxis in the northwestern Himalayas is a suture that was folded and subsequently exhumed. Similarly, Paulsen and Marshak (1998) proposed that uplift and erosion intensified the curvature of the northern part of the Uinta recess.

Furthermore, one or more factors can contribute to the genesis of a bend in the structural trend of a fold–thrust belt. Lacquement *et al.* (2005) noted that the Meuse Valley recess in the Ardennes Variscan thrust belt in northern France and southern Belgium was formed by a combination of vertical axis rotation and oblique folding over a frontal-ramp–oblique-ramp intersection in the footwall.

2.1.2 Paucity of research on recesses

A literature search of the kinematics of curves in thrust belts demonstrates that salients have been studied far more extensively than recesses. At the time of this writing, a quick keyword search on GeoRef yielded 895 hits for the term “salient” and only 141 for the term “recess.” Macedo and Marshak (1999) documented details of shapes and geologic settings of salients in various locations. Although some recesses result from bending of strike in a thrust belt propagating around a foreland obstacle (*e.g.*, the Uinta

recess, *cf.* Paulsen and Marshak, 1999), many recesses are the intersections of the distal arms of two adjacent salients, implying that recesses are the consequence of curvature of salients.

2.1.3 Possible causes of recesses in thrust belts

Two alternative sets of solutions may be suggested for junctions of structural trends. One involves two temporally successive episodes of deformation, each with a different translation direction that corresponds to the observed structural trends, such that the younger set of structures overprints the other with compressional interference structures. In such models, the two translation directions correspond directly with the structural trends observed in the opposite arms of the recess. Geiser and Engelder (1983) noted two phases of deformation from layer-parallel shortening (LPS) fabrics in Pennsylvania and New York. A similar study by Dean and Kulander (1978) demonstrated two discrete deformation events recorded by stylotized joints in the Greenbrier Limestone in the Alleghany plateau of southwestern West Virginia. They found an early LPS fabric normal to the general trends of the southern Appalachians, and this fabric was later refolded about trends of the central Appalachians. In contrast, the other solution set involves a single episode of deformation. Kulander and Dean (1986) demonstrated that bends in thrust belts can be generated by differential displacement. Differential displacement may result from gradients in displacement magnitude (along faults within one fault system or as a transfer among different fault systems), or a transfer of displacement mechanism (*i.e.*, efficiency of accommodation of shortening, perhaps between predominant thrust faulting and predominant folding). A drastic along-strike increase in plastic deformation would represent another possible transfer of deformation mechanism.

In the Appalachian thrust belt, the abrupt angular intersections in structural trends are at the ends of salients in the thrust belt (Figure 1-2, also *cf.* Thomas, 1977). Perhaps these bends are, in part, the necessary results of the intersections of the active salient segments of the Appalachians. Furthermore, the style of salients and how the individual faults evolve (*cf.* Kwon and Mitra, 2004) must also be considered. Five idealized end-member models of salients are shown in Figure 2-1, and each involves different along-strike variations in compression and thrust-front translation, displacement paths, rotations

of translation directions and fault orientations, *etc.* The models in Figure 2-1, however, do not address the along-strike ends of the salients. Thus, the deformation at the boundary between any of the various types of salients must also determine—at least in part—the nature of the interstitial recess (*i.e.*, the boundary conditions of the salients are also factors in the evolution of the recess).

Interference patterns of folds, according to Ramsay (1962), result from the relationship between direction of second-phase motion and the orientation of the earlier folds. Further, Stewart (1993) demonstrated dual-phase deformation and described possible accommodation structures, such as faults superposed on folds. He also states, however, that this is analogous to deformation observed over frontal-ramp–oblique-ramp intersections in the footwall (*cf.* Alvarez-Marrón, 1991; Lacquement *et al.*, 2005; also see preliminary discussions by Butler, 1982a, b), for which only one phase of deformation/transport is necessary. Second-order structures result from single-phase deformation that involves translation of rocks over a footwall structure, such as the intersection between a frontal ramp and an oblique or lateral ramp (Apotria *et al.*, 1992; Apotria, 1995; Cook and Thomas, 2009). These second-order structures are produced over the corner of the footwall structure, which corresponds to the intersection of the structural trends at the surface, and the nature of the second-order structures is dependent upon the footwall geometry. Compressional structures (such as higher order folds or thrust faults) are generated if the footwall structure is concave with respect to regional transport. Conversely, extensional structures (such as tear faults) are formed if the footwall structure is convex with respect to the direction of thrusting.

Stauffer (1988) demonstrated that some interference patterns are affected by bends in rock layers that form at fold intersections, to which he referred as “coaptation folds”. Lisle *et al.* (1990), however, stressed the influence of layer thickness and competence in constraining the formation and geometry of such folds. Lisle *et al.* (1990) concluded that such “coaptation folds” are actually topologically necessary at the flanks of domes and basins, and should thus be called “curvature-accommodation folds”. Stewart (1993) further refined these ideas by creating a model that accounts for volume of rock that must be accommodated at fold intersections.

2.1.4 Structural problems of bends in thrust belts

The problems presented by marked changes in structural trends are multifold. The primary problem is defining whether the present structures were generated by a single deformational episode or by multiple phases of deformation. The proposed explanations for abrupt changes in structural trends are, in turn, also numerous. Several studies demonstrate multi-phase deformation—and thus, interference patterns—in the Appalachians (*e.g.*, Dean and Kulander, 1978; Murray and Skehan, 1979; Drake and Lyttle, 1980; McMaster *et al.*, 1980; Mosher, 1981; Wise, 2004). In contrast, many explanations involve a single phase of deformation (*e.g.*, Dahlstrom, 1969, 1970; Kulander and Dean, 1986; Gray and Stamatakos, 1997; Marshak, 2004). Furthermore, if thrust translation is perpendicular to structural trends, then one must consider a space problem at bends in thrust belts that necessitates along-strike strain. Thus, palinspastic restoration of the volume of rock in the regional thrust sheets must account for strains out of the planes of cross section and possible multi-directional thrust translation.

The primary problem of bends in thrust belts involves the nature of deformation—basically how many stages were involved. This can be determined by close examination of local structures—both mesoscopic and microscopic. If the deformation did, in fact, occur in two phases, then interference structures (*i.e.*, fold overprint or accommodation structures, such as superposed thrust faults) should be apparent. Contrarily, if there were one single transport direction, then an altogether different—yet no less complex—set of structures must result, such as a gradient in displacement or deformation mechanism.

A secondary problem involves defining how (and to what magnitude) deformation and/or strain are accommodated in the rocks at such an intersection during tectonic transport. This problem is more important, however, for single-phase deformation, for which accommodation cannot be explained by interference structures.

2.1.4.1 Problems with palinspastic restoration around bends in thrust belts

Palinspastic restorations of cross sections along bends in thrust belts can be problematic (Thomas, 1989). A space problem arises if cross sections are restored perpendicular to the strike of intersecting fault sets (assuming that slip is perpendicular to strike). If the bend in strike is concave towards the foreland (*i.e.*, a recess), the fault trace lengthens when restored. Conversely, the restored fault trace shortens if the bend is

convex toward the foreland (*i.e.*, a salient). Figure 2-2 illustrates the calculation of the amount of tangential extension or shortening associated with translation through a salient or recess. Thus, there is an inherent distortion of volume, although each cross section within an array of cross sections across a structural bend may be balanced individually. There are two main solutions to this problem. The first involves treating the ends of the fault segments as fault tips, such that displacement diminishes to zero toward the fault tip. The second involves restoration of a wedge-shaped block (*i.e.*, with sides bounded by cross sections perpendicular to the two regional structural trends) such that higher order compression or extension must be accommodated within the block by other mechanisms (*i.e.*, superposed folds and/or faults, diffusive mass transfer, *etc.*).

2.1.5 Recesses in the Appalachian thrust belt

Pronounced, abrupt bends in the strike of the Appalachians in the United States are in recesses in northeastern Pennsylvania, central western Virginia, and across Alabama (the Pennsylvania, Virginia, and Alabama recesses, respectively, in Figure 1-2). The Alabama recess is the most complex and the least studied of the three recesses in the Appalachian thrust belt. At the northeastern end of the Alabama recess in northwestern Georgia, structural trends the trailing thrust sheets bend abruptly (Figures 1-2 and 1-3). The most abrupt bend in frontal structures is observed in western Alabama and eastern Mississippi (Figure 1-2). The structural intersection in northwestern Georgia is the focus of the present research and is herein referred to as the Georgia subrecess.

2.1.5.1 New York recess

In the New York recess in northeastern Pennsylvania, the trend of the Appalachian thrust belt curves abruptly southwestward from approximately 030 to 075 (Figure 1-2), and marks the loosely defined boundary between the central Appalachians and the northern Appalachians. The former trend continues northward and curves northeastward around the Quebec salient, the latter trend continues southwestward around the Pennsylvania salient into Virginia.

Macedo and Marshak (1999) described the Pennsylvania salient as a basin-controlled and a margin-controlled salient, the development of which is related to a thick underlying sedimentary succession, as well as evaporites deposited in the basin. Gray and Stamatakos (1997) compiled paleomagnetic data from various studies and concluded

that those data are consistent with oroclinal bending of the Pennsylvania salient. Both of these models only require one general direction of tectonic transport. In a study to the contrary, Geiser and Engelder (1983) compiled, correlated and interpreted orientation data from various deformation structures such as “mechanical twins, solution cleavage, crenulation cleavage, pencils, joints, and deformed fossils” to investigate and quantify layer-parallel shortening in this region (in the area shown in Figure 2-3). In this study, Geiser and Engelder (1983) demonstrated two discrete, major phases of Alleghanian deformation (the Lackawanna phase and the Main phase) that occurred during a time of sustained plate interactions. Lastly, the authors noted that these pulses are likely to be diachronous with respect to each other, and that the sequence of overprinting is consistent at all locations, although the data are sparse.

The Lackawanna phase is manifest by structures that denote generally northwestward displacement, although the deformation is kinematically complex and includes regional strike-slip components. Geiser and Engelder (1983) estimated the associated deformation to be early Late Pennsylvanian or younger in age, and they conclude that it represents an early phase of the Alleghanian orogeny. The authors interpreted the Lackawanna phase to have a component of strike-slip motion, possibly between the North American craton and the Avalon microcontinent. The authors suggested some possible tectonic interpretations for this phase including: (a) initial lateral motion caused by a rigid indenter; and (b) initial oblique subduction.

The Main phase results from a displacement directed predominantly east-west in eastern Pennsylvania. To the north, the displacement was rotated clockwise as it translated around the northeastern end of the Pennsylvania salient (*i.e.*, the phase is directly affected by the regional structural trends). This phase is estimated to be early Permian or younger in age (Geiser and Engelder, 1983). This episode is interpreted as the final closure of—and possible contact between—the rigid plates of Africa and North America, which is considered to be the Alleghanian orogeny *sensu lato*.

Later studies by Wise (2004) and Wise and Werner (2004) proposed a different model that incorporates two directions of tectonic shortening at times that differ from the two phases of Geiser and Engelder (1983). The phases in the model of Wise (2004) and

Wise and Werner (2004) are called the Reading Prong stage, which is directed to ~325 and the Nittany-Juniata stage, which is directed to ~290–295.

It is debatable whether either of these two-phase models really explains the bend in strike. Geiser and Engelder (1983) noted that they could not determine whether their two phases actually represented two distinct translations or were part of a single, continuous rotation of tectonic translation. Furthermore, the two orientations of these two-phase models may only reflect the deformation corresponding to the salient arms on either side of the recesses.

2.1.5.2 Virginia recess

In the Virginia recess of central western Virginia, the trend of the Appalachian thrust belt curves abruptly southwestward from approximately 030 to 060 (Figure 2-4). To the northeast of this change, the Appalachian structural trend consistently curves northeastward through the Pennsylvania salient into Pennsylvania and New York. To the southwest, the structural trend curves consistently through the Tennessee salient into Georgia. Kulander and Dean (1988) illustrated that this area of abrupt trend change defines a structural recess (the Virginia recess of Thomas, 1977), and stated that it marks the boundary between the southern Appalachians and central Appalachians. In the recess, key southern Appalachian structures—such as the Saltville and St. Clair faults—terminate northeastward. To the northeast of this juncture, shortening of the sedimentary cover rock is increasingly accommodated by folding, leading to a gross-scale increase in fold frequency and widening of the fold belt (Figure 2-5). The northwestern segment of the Virginia recess is also underlain by the southeasternmost extent of the evaporites of the Silurian Salina Formation. The change from folds on the northeast to faults on the southwest, however, may reflect a difference in the level of the thrust belt exposed at the present surface, and thus may be more apparent than real. The faults on the southwest may represent a structurally/stratigraphically lower level of exposure than the folds. The folds on the northeast may represent detachment folds above a deeper detachment with frontal ramps similar to those faults to the southwest. The change in deformation style may be attributed to causes such as the effects of the continental-margin geometry and changes in stratigraphic thicknesses (*e.g.*, the thickening Devonian section to the northeast, *cf.* discussion of Catskill–Pocono clastic wedge in Thomas, 1977). The general

differences in style of deformation between the southern and central Appalachians are described by Rodgers (1970), and the primary geological and geomorphological contrasts are outlined by Lowry (1971).

The Massanutten-Blue Ridge and Pulaski thrust sheets are bounded by the North Mountain-Pulaski fault system (Figure 2-4) and were translated as a composite sheet, which spans across the Virginia recess of Thomas (1977), as well as the change in Appalachian trend around the recess (Kulander and Dean, 1988). Kulander and Dean (1988) stated that displacement magnitude of the “master” thrust sheet is constant throughout this region, and that there is no evidence for “abrupt or irregular changes” in displacement along strike. They further stated that the mechanism of displacement is transferred gradually between the primary thrust faults on a regional scale. Along the leading edge of the composite thrust sheet, the displacement on the North Mountain fault decreases toward the southwest, whereas the displacement along the Pulaski fault increases markedly southwestward (see cross sections in Kulander and Dean, 1988). This mechanism of fault displacement transfer (Figure 2-6) is described in detail by Dahlstrom (1969, 1970). Thus, according to Kulander and Dean (1988), the regional bend in Appalachian structural trends here results from the change in deformation style rather than magnitude of translation.

2.1.5.3 Alabama recess and the Georgia subrecess

The Alabama recess is a more composite recess, and is structurally distinct from the other two Appalachian recesses. In northwestern Georgia, north-striking structures that curve northeastward around the Tennessee salient into central Virginia intersect and interfere with northeast-striking structures that extend eastward from Alabama (Figure 1-2), thereby defining the Georgia subrecess. The northeastward-striking segment extends, as a nearly linear feature, southwestward across Alabama to the Ouachita structures in the subsurface in Mississippi, where there is another sharp bend in structural trends (Figures 1-2 and 1-3).

In northwestern Georgia and northeastern Alabama, frontal structures such as the Sequatchie anticline and the Lookout Mountain syncline are nearly straight and strike approximately 040 (Figure 1-3). Intermediate structures such as the Kingston, Peavine, Chattooga and Opossum Valley/Jones Valley faults and the Kingston–Chattooga

anticlinorium are nearly straight, but have slight cratonward-concave curvature and some are offset at lateral ramps in Alabama. The eastern (trailing) end of the Kingston–Chattooga anticlinorium is defined by Taylor Ridge monocline, which dips into the Floyd synclinorium. Interior structures in the region have the most abrupt bend in strike, and bend southwestward from approximately 020 to 070. These structures include the Helena, Western Coosa, and Eastern Coosa (or Coosa) faults in the area of study (Figure 1-4) as well as the Talladega–Cartersville–Great Smoky fault (the leading metamorphic thrust sheets of the Appalachian Piedmont) to the southeast. In the footwall of the Coosa fault in Georgia, an interference pattern is defined by the sinuous trace of the Rome fault and two main fold trains that plunge into the depression of the Floyd synclinorium (Figures 1-3 and 1-4). The trends of the two fold trains correspond to the approximately 020 and 070 strikes in the Georgia subrecess, and they intersect and interfere throughout the area of the Floyd synclinorium (Figure 1-4). An abrupt change in strike marks the Georgia subrecess, from which displacement is absorbed toward the foreland such that structures like the Kingston fault are not affected. To the southwest of the Georgia subrecess, Appalachian structures curve gently from approximately 070 to 090 in the subsurface of eastern Mississippi (Figures 1-3), where they intersect and truncate Ouachita structures. This intersection defines the Alabama recess at the thrust front, whereas the Alabama recess is defined in trailing structures in northwestern Georgia in the subrecess.

The most prominent bend in strike is the intersection between the Talladega–Cartersville fault and the Great Smoky fault. Tull and Holm (2005) reviewed the area in terms of what they call the Cartersville transverse zone, and reinforced the idea of an oblique/lateral ramp at the Rising Fawn transverse zone by presenting evidence based on the differences in the Appalachian thrust belt on either side of the transverse zone (Figures 2-7 and 2-8). The authors cited the absence of the rift-fill rocks of the Ocoee basin across the Alabama promontory (or southwest of the Rising Fawn transverse zone), and the lack of the thick clastic succession caused a contrast in mechanical properties that is marked by the abrupt change in structural style at the Rising Fawn transverse zone (*i.e.*, the large-scale isoclinal folding of the Blue Ridge to the northeast that is absent in the Talladega belt to the southwest—perhaps as a result of the more massive basement).

They mentioned that the abrupt change in stratigraphic level of the Cartersville–Great Smoky fault further suggests a continental-margin transform fault. Tull and Holm (2005) also mentioned the difference in distribution of metamorphic isograds and mafic metaigneous rocks across the transverse zone.

The southern Appalachian thrust belt commonly is interpreted in the context of a break-forward sequence of thrusting and unidirectional northwestward thrust translation (*e.g.*, Boyer and Elliott, 1982; Thomas, 1985; Woodward and Gray, 1985, *etc.*) with break-back sequences (*e.g.*, Thomas, 2001; Thomas and Bayona, 2005, *etc.*). Upon closer inspection, however, the idea of unidirectional displacement may not be applicable everywhere.

This area was first mapped and discussed by Hayes (1891, 1894), who conducted the earliest geologic research in northwestern Georgia. Both the accompanying maps to these studies clearly show the two structural trends in northwestern Georgia. Hayes (1891) noted that variation in “rigidity” in the stratigraphic succession in the Southern Appalachians directly correlates to deformation style (*i.e.*, folding in weaker rocks, faulting in stronger rocks). Hayes (1894) specifically noted the Cambrian “soft shales and limestones” in the area around Rome (in contrast to “great masses of conglomerate and quartzite” of the Cambrian to the north in Tennessee) as the cause of the concentration of folding in the region.

The area was later mapped at greater detail by Hayes (1902) and Butts (1948). Cressler (1964a, b, 1970) later depicted this area on 1:62,500-scale county geologic maps on planimetric bases of Floyd, Chattooga, and Walker Counties, Georgia, and described the general geology. Cressler (1970) also noted high-angle southwest-trending faults to the south of the interfering folds. These faults are splays of the Coosa fault and are the southwesternmost structures that follow the general structural trend prominent to the northeast of this bend in the Appalachians. Kesler (1975) further described the general geology of this area, and emphasized the local change in trend of the Rome and Coosa faults.

Later publications refined the general understanding of this region. The geologic map published by the Georgia Geological Survey (1976) clearly depicts how the structural trends are distributed within and partitioned among the thrust sheets. Both the

north-northeast and the east-northeast trends are visible in the interference folds within the composite Kingston–Chattooga–Clinchport thrust sheet and on the trace of the Rome fault (the leading edge of the Rome thrust sheet). The map also clearly shows the southwest-trending splays of the Coosa fault, which extend into the hanging wall, the Coosa thrust sheet. Furthermore, it shows a cross fold in the hanging wall of the Clinchport fault, which is the northernmost clearly defined structure that follows the general east-northeast trend prominent to the southwest of this bend in Appalachian structural trends. The map also illustrates that the bend in structural trend does not affect the rocks in the footwall of the Kingston and Chattooga faults and is more pronounced to the southeast at the Cartersville–Great Smoky fault. Thomas (1990) defined this bend in the trend of the Appalachian thrust belt as the Rising Fawn transverse zone. A later mapping project by Baldwin and Thomas (1997, and unpublished map) showed a general tightening of folds in the zone of interference.

More recent research has more clearly defined some of the details of the regional geologic structures. Bayona *et al.* (2003) demonstrated local vertical-axis rotation in this region, and stated that it may be attributed to differential slip related to rheology contrasts between detachment levels at oblique/lateral ramps, the ramp geometry, and gradients in the depth to basement. From paleomagnetic data, the authors calculated a clockwise rotation of $25 \pm 7.8^\circ$ in the Kingston–Chattooga–Clinchport thrust sheet south of the interference folds, which is insufficient to cause the entire bend. Bayona *et al.* (2003) further illustrated thin-skinned structures overlying regional northeast-striking basement faults offset by northwest-striking basement faults at transverse zones, and also emphasized the folding and refolding of the Rome fault in the area of the interference folds. Thomas and Bayona (2005) described the regional details of the Rising Fawn transverse zone. Of particular interest, they also noted the highly sinuous nature of the Rome fault in this region, indicating a subhorizontal folded fault surface. Folds in the footwall are coaxial with the folds in the fault surface. The authors further stated that the footwall folds are truncated by the fault, and the folds were subsequently tightened, folding both the footwall rocks and the Rome thrust sheet. Thus, the deformation in this region is evidently multiphase, and the phases may or may not be co-directional. Thomas and Bayona (2005) also described the change in trend of the Cartersville–Great Smoky

fault. They further noted that segments of the Coosa fault in Alabama follow the southwest trends seen in the splays in Georgia. The Eastern Coosa fault bends to the southwest and terminates, and farther to the west, the hanging wall of the Western Coosa fault includes southwest-trending splays. Even farther to the west, the Western Coosa fault bends to the southwest, where it truncates the Helena fault (Thomas and Bayona, 2005).

From all these previous studies, the two sets of regional structural trends are readily apparent; however, at the scale of existing maps, no well-defined map patterns or structures clearly define the nature of interference at the intersection. Consequently, more research on the structures in the zone of interference is necessary to determine the structural history of the thrust belt in this area, to more fully analyze the deformation mechanisms, and to resolve the number of deformation episodes.

2.1.6 Examples of structural intersections in other thrust belts

Intersections of regional structures are common at bends in orogenic belts. Interference structures have been described in the Rocky Mountain foreland (*e.g.*, Kulik and Schmidt, 1988; Montgomery, 1993; Paulsen and Marshak, 1999; Kwon and Mitra, 2004), in the Cantabrian zone of the Asturian Arc (Hercynian Cordillera) in northwestern Spain (*e.g.*, Julivert, 1981; Julivert and Marcos, 1973; Alvarez-Marrón, 1991; Van der Voo, 2004), and in the Salt Ranges in northern Pakistan (*e.g.*, Stewart, 1993; McDougall and Khan, 1990).

These thrust-belt bends, however, are not all located in recesses, and the structures therein may be produced by mechanisms that differ from those in the Appalachian intersections (*cf.* discussion of the Uinta recess in section 2.1.1.2). Julivert and Marcos (1973) described the interference structures in the Cantabrian zone as the result of superposed flexural deformation episodes. On the contrary, Van der Voo (2004) presented evidence of large-scale rotation on the basis of paleomagnetic data. Stewart (1993) concluded that the fold interference structures in northern Pakistan are a result of footwall ramp intersections (*cf.* Apotria *et al.*, 1992; also see discussion of this area in McDougall and Khan, 1990).

2.2 DUCTILE DUPLEXES IN THRUST BELTS

A brittle duplex is defined by brittle “horses” that are bounded by coherent thrust faults, which connect the floor and roof thrusts. A ductile duplex is also defined by a roof thrust and a floor thrust. In contrast, the volume between the roof thrust and floor thrust in a ductile duplex is filled with ductilely deformed rocks from a thick weak layer in the stratigraphy during thrust translation. Ductile duplexes are characterized by small-scale disharmonic folds, small faults, and the lack of coherent brittle horses. The necessary weak layer typically is a shale-dominated succession that may include some thin-bedded intervals of more competent rocks. The essential ideas of ductile duplexes and how they are formed are summarized in the study of Thomas (2001). The combined function of the state of stress and the mechanical properties of a regional stratigraphic succession are considered to be the primary control on structural style of folds and faults within a thin-skinned thrust belt (*e.g.*, Jamison, 1992). Thomas (2001) noted that the “geometry of both thrust-fault surfaces and fault-related folds is closely controlled by mechanical properties of stratigraphic units.” The fold form of detachment folds is defined by a rigid layer, and a detachment anticline is filled with ductilely deformed rocks from a weak layer (Thomas, 2001). A detachment anticline generally forms in a rigid layer over the tip of a thrust fault within an underlying weak unit (Thorbjornsen and Dunne, 1997). A relatively greater volume of weak-layer rocks can be tectonically thickened, which elevates and distorts an overlying rigid layer (*e.g.*, Stewart, 1999); and subsequent deformation can propagate into the foreland and incorporate footwall rocks (Ramsay, 1992). Both of these mechanisms operate in the development of ductile duplexes.

2.3 STRATIGRAPHIC CONTROLS ON STRUCTURES

The bulk stratigraphy of a thrust sheet is directly related to the mechanical properties of the sheet and is a primary factor in how the thrust sheet deforms. The alternate rigid layers and weak layers control partitioning of brittle and ductile deformation, respectively, with respect to depth within a thrust sheet (*cf.* Wiltschko and Geiser *in* Hatcher *et al.*, 1989).

A comprehensive analysis of the regional stratigraphy is therefore important to the problems addressed in the present study. Any kinematic and mechanical investigation of geologic structures, such as that included herein for the recess in northwestern Georgia, must include research of the mechanical properties of the stratigraphic succession. Furthermore, the mechanical properties of the thrust sheets are directly related to the deformation styles observed both at the surface and in the subsurface. The present investigation intends to demonstrate the relation of regional stratigraphy to the clearly defined structural interference pattern in Georgia.

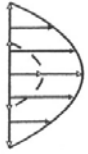
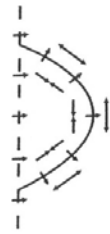
| A BOW-AND-ARROW RULE | B OROCLINE | C DIVERGENT TRANSPORT | D TEAR FAULT BOUNDARIES | E LATERAL OR OBLIQUE RAMP BOUNDARIES |
|-------------------------------------------------------------------------------------------------------------------------------------------------------------------------------------------|------------------------------------------------------------------------------------------------------------------------------------------------------------------------------------------------------------------------------------------------------------------------------------|----------------------------------------------------------------------------------------------------------------------------------------------------------------------------------------------------------------------------------------------------------------------------------------------------------------------------------------------------------|---------------------------------------------------------------------------------------------------------------------------------------------------------------------------------------------------------------------------------------------------------------------------------------------------|---------------------------------------------------------------------------------------------------------------------------------------------------------------------------------------------------------------------------------------------------------------------------------------------------------------------------------------------------------------------|
|  |  |  |  |  |
| <p>Primary differential parallel transport; No vertical-axis rotation of transport; No vertical-axis rotation of fault; Maximum thrust-front advance in middle of salient</p> | <p>Primary uniform parallel transport; Passive vertical-axis rotation of transport during bending; Vertical-axis rotation of fault (i.e. folding of fault); Extensional strain on the outer side of salient; Contractional strain on the inner side of salient</p> | <p>Primary differential transport with divergent trajectories; No vertical-axis rotation of fault; Maximum thrust-front advance in middle of salient; Stretching parallel to the regional transport in the leading portion of the salient; Stretching perpendicular to the regional transport in the trailing portion of the salient</p> | <p>Primary uniform parallel transport; Uniform thrust-front advance; Uniform shortening; Strike-slip faults at ends; No vertical-axis rotation of transport; No vertical-axis rotation of fault; No tangential extension; Original foreland-convex basin geometry</p> | <p>Primary parallel transport; Uniform or nonuniform thrust-front advance; Vertical-axis rotation of transport at edges due to lateral-ramp or oblique-ramp-related structures; No vertical-axis rotation of fault; Contractional deformation at the edges of salient; No tangential extension; Original foreland-convex basin geometry</p> |
| <p>Elliott (1976); Ferill and Groshong (1993) Sussman et al. (2003)</p> | <p>Carey (1955); Marshak (1988); Marshak et al. (1992); Ferill and Groshong (1993); Hindle and Burkhard (1999) Sussman et al. (2003)</p> | <p>Argand (1924); Marshak (1988); Marshak et al. (1992); Hindle and Burkhard (1999) Sussman et al. (2003)</p> | <p>Marshak (1988); Marshak et al. (1992); Ferill and Groshong (1993)</p> | <p>Argand (1924); Marshak (1988); Marshak et al. (1992); Casas et al. (1992); Apotria (1995); Hindle and Burkhard (1999); Macedo and Marshak (1999)</p> |

Figure 2-1. Idealized end-member models of salient development illustrating the evolution of the faults in each case, from Kwon and Mitra (2004). The dashed lines are pre-deformational material lines, the solid lines are the same material lines after thrust translation. Black arrows represent thrust transport directions and open arrows represent fault propagation directions. Double-headed arrows represent tangential extension.

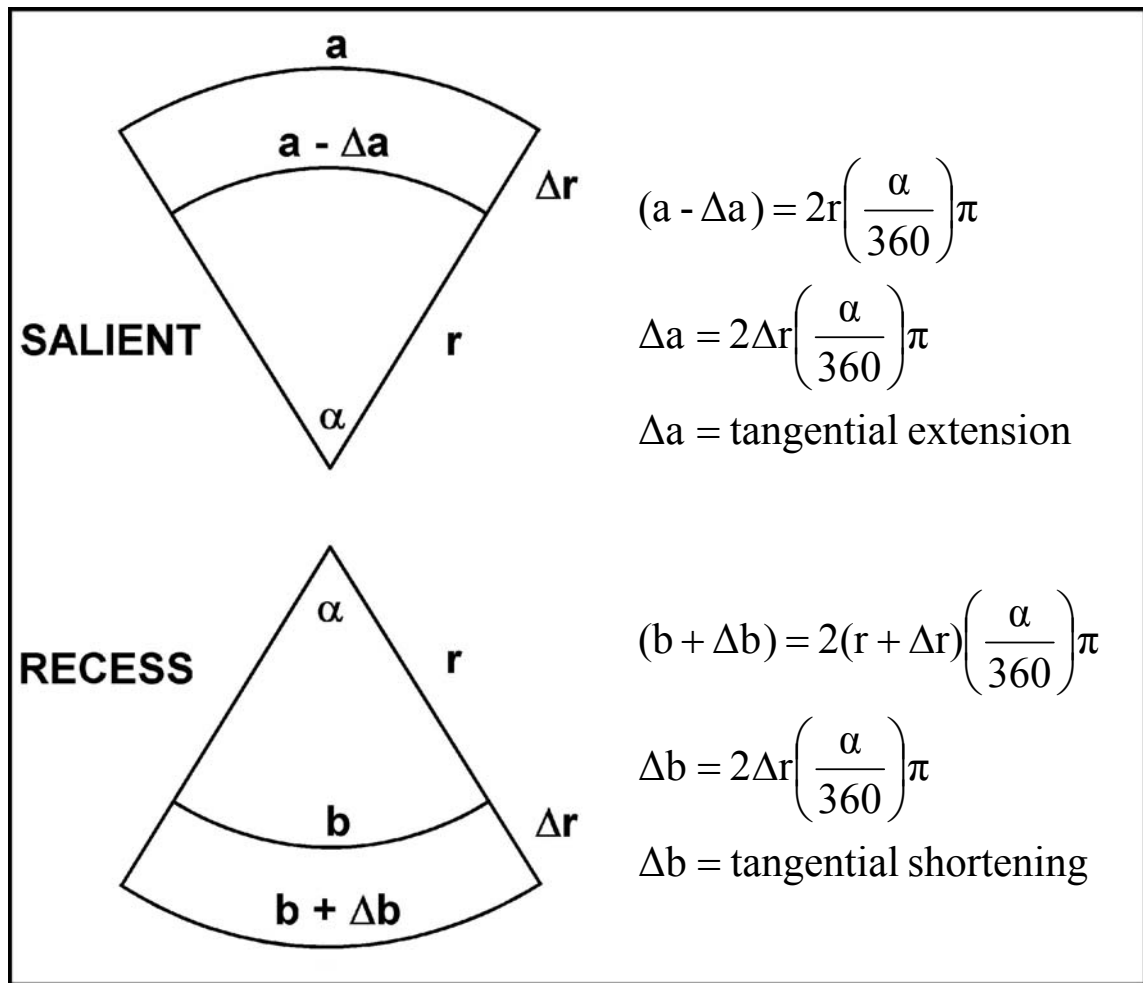


Figure 2-2. Sample calculations of implied tangential strain around a salient and a recess, adapted from Thomas (1989). Note that the sense of extension/shortening is reversed for palinspastic reconstructions.

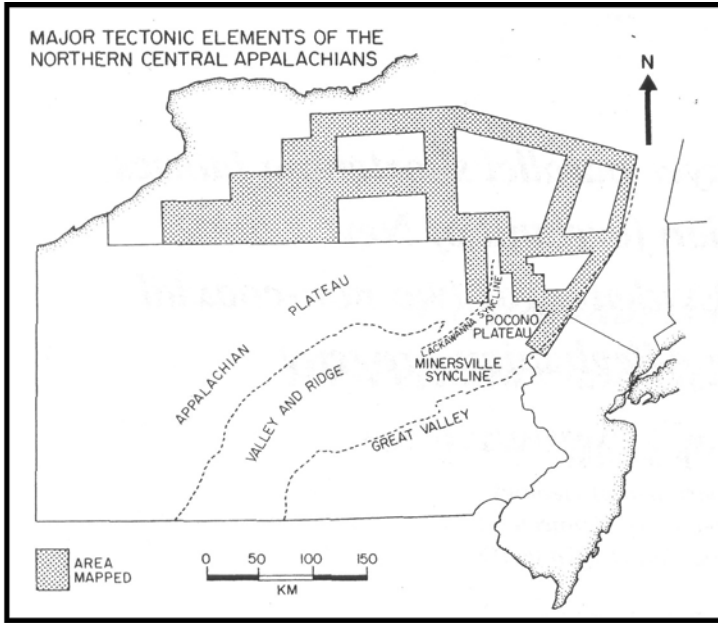


Figure 2-3. Location map of the structural analyses of Geiser and Engelder (1983).

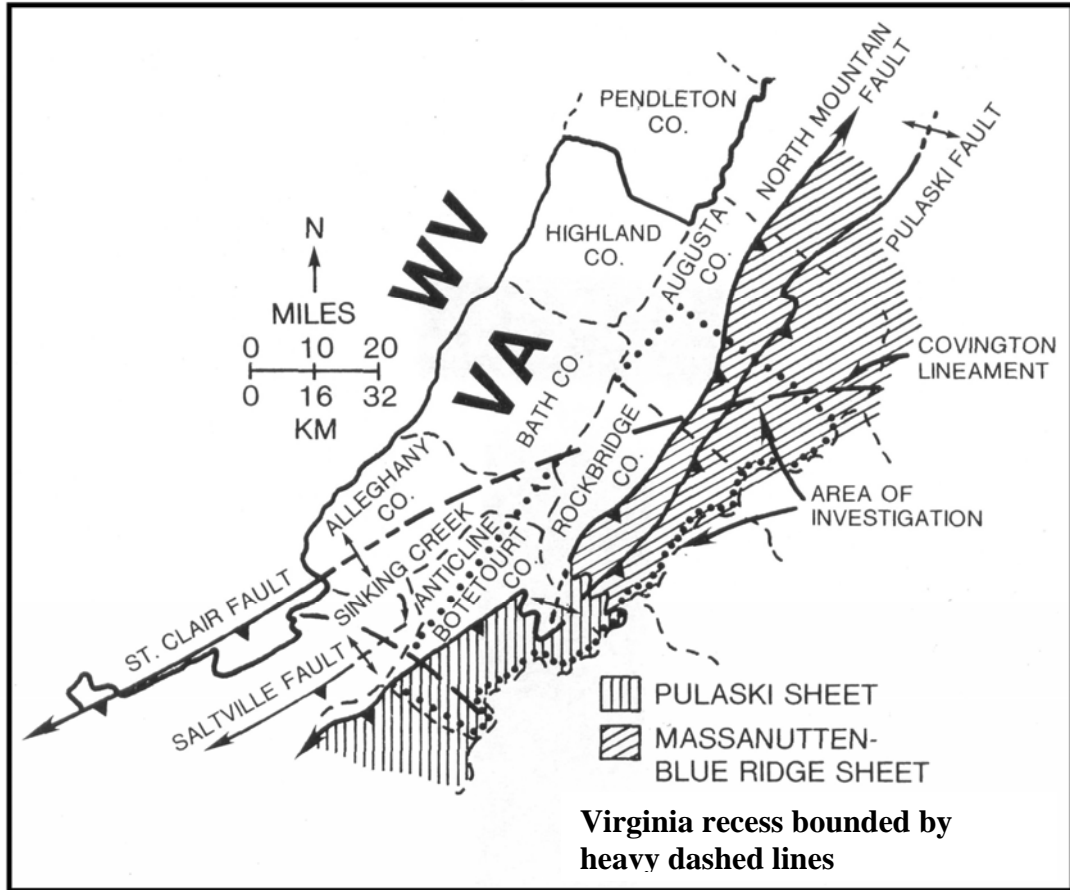


Figure 2- 4. Location map of the abrupt bend in the Appalachian thrust belt of central western Virginia and major structural features, from Kulander and Dean (1988). Note the composite Pulaski/Massanutten–Blue Ridge thrust sheet and bounding fault system (the North Mountain and Pulaski faults). Also note the termination of the Saltville and St. Clair faults near the Virginia recess.

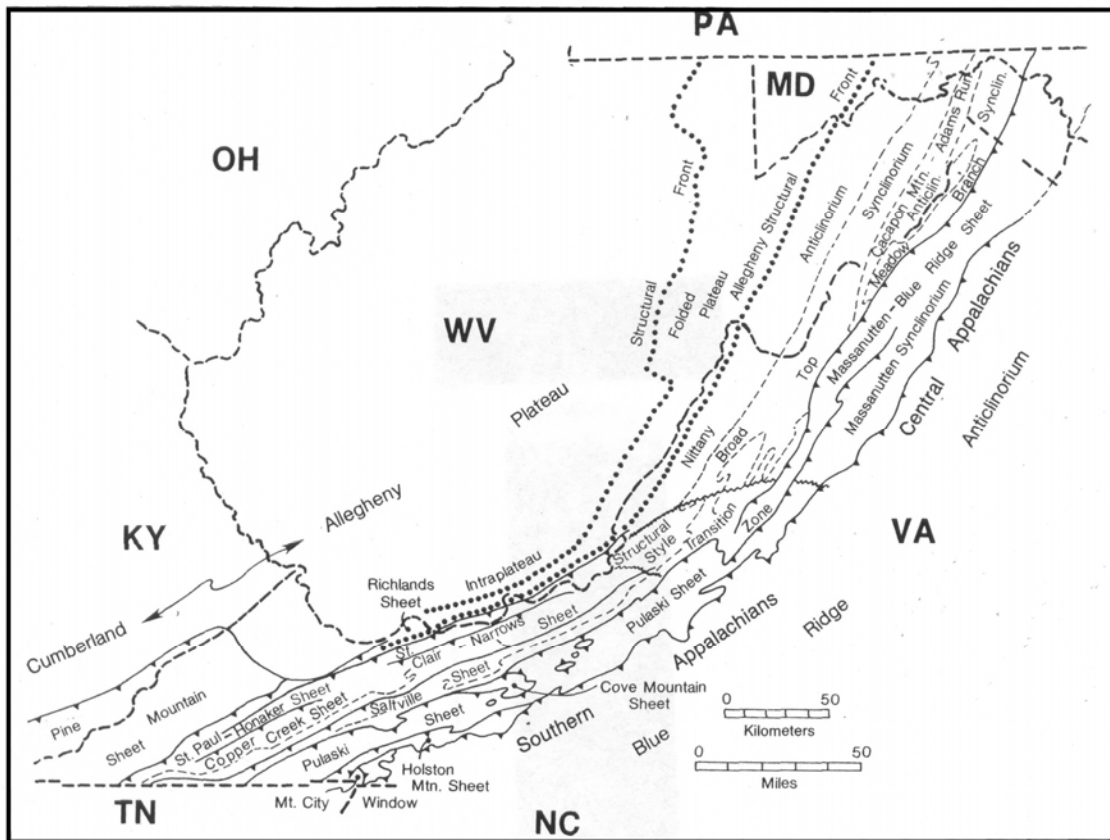


Figure 2-5. Location map of the Appalachian thrust belt of central western Virginia illustrating the widening of the thrust belt to the northeast of the bend in strike, from Kulander and Dean (1986).

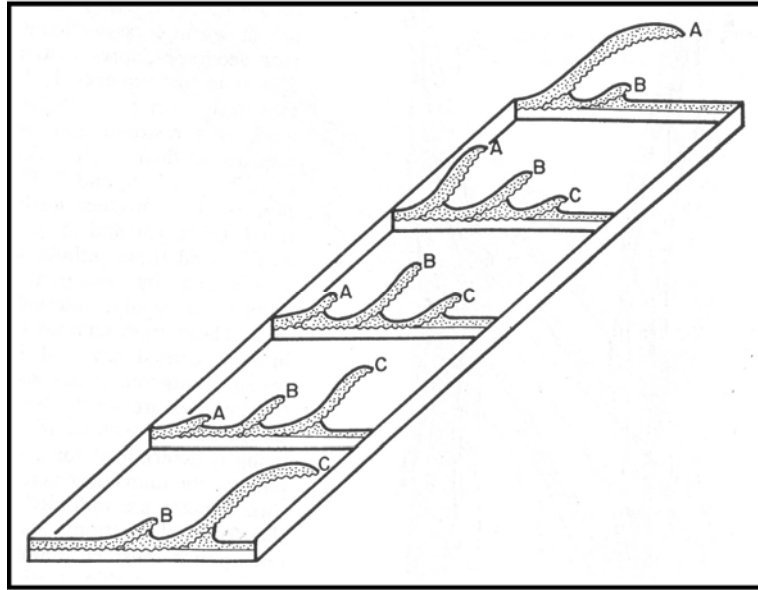


Figure 2-6. Diagram of the transfer of displacement within a thrust fault system, from Dahlstrom (1969).

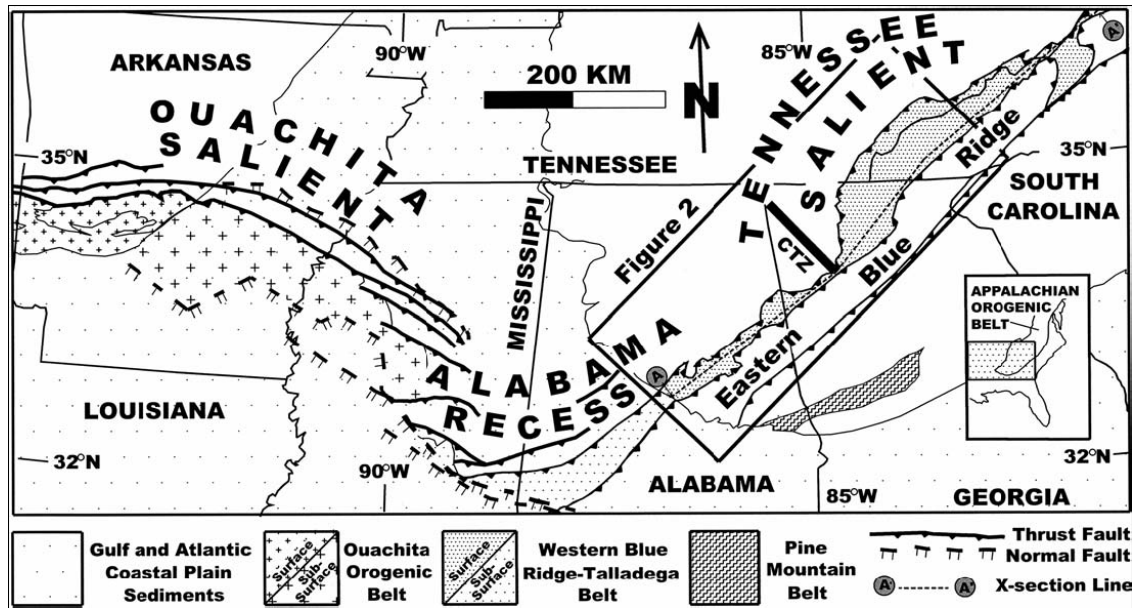


Figure 2-7. Regional map of the southwestern Appalachian orogen and the eastern Ouachita orogen, marking the location of a proposed transverse zone (labeled as CTZ) in northwestern Georgia, from Tull and Holm (2005). Also shown here is the location of cross section A-A' from Figure 2-8.

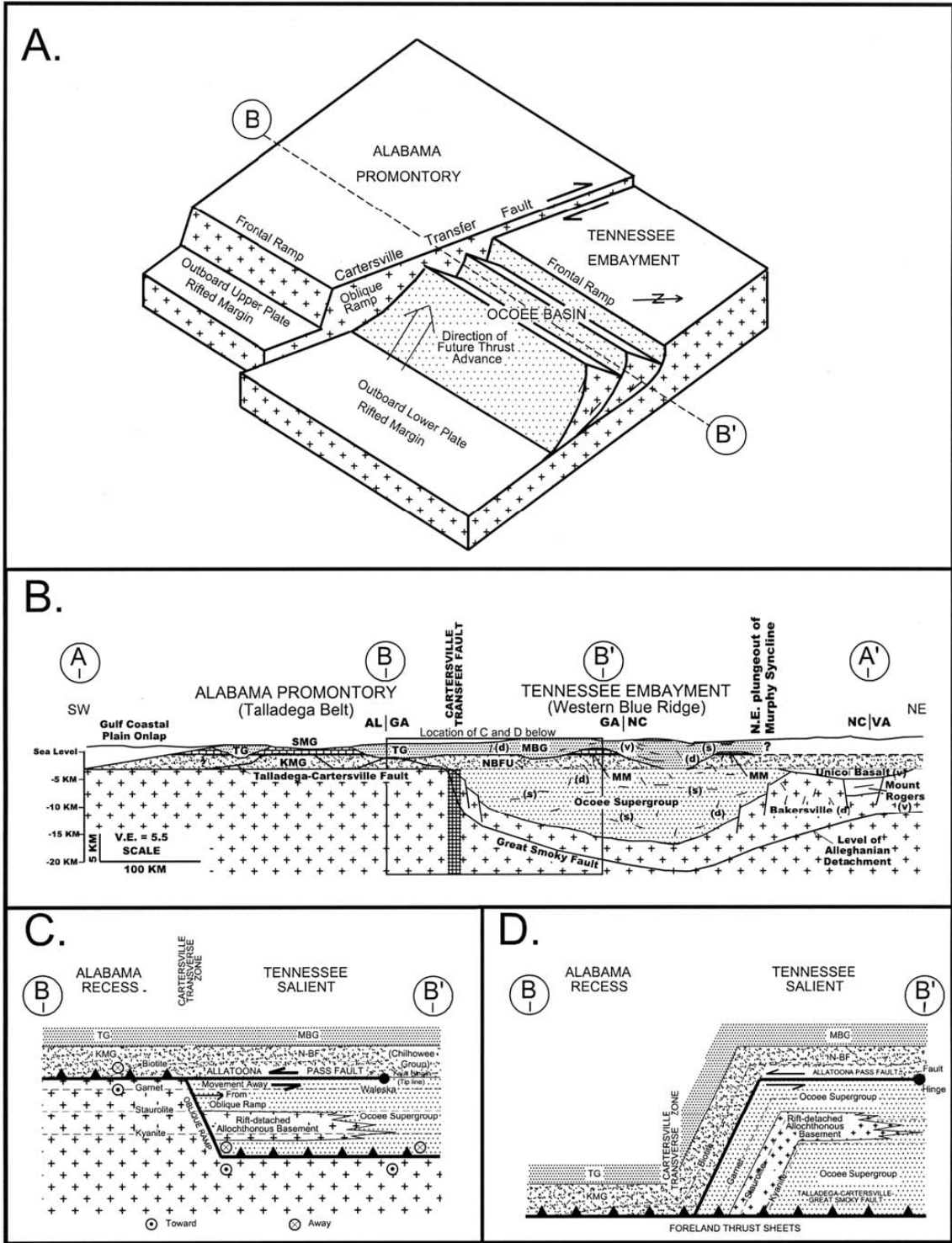


Figure 2-8. (previous page) “Diagrams illustrating the evolution of the Late Proterozoic Cartersville transfer fault into an oblique footwall ramp during late Paleozoic Alleghanian collisional events, from Tull and Holm (2005).

(A) Schematic block diagram of the Late Proterozoic rifted-margin configuration at the junction between the Alabama promontory (upper plate rifted margin) and the Tennessee embayment (lower plate rifted margin). (B) Schematic along-strike (SW–NE) cross section (location in Figure 2-7) prior to Paleozoic deformation and metamorphism from the Gulf Coastal Plain in Alabama to the North Carolina–Virginia border illustrating the configuration relative to the Cartersville transfer fault of the rift-facies sequence (Ocoee Supergroup), drift-facies sequences (Chilhowee Group = Kahatchee Mountain Group [KMG] = Nantahala-Brasstown Formations undifferentiated [NBFU], and Sylacauga Marble Group [SMG] and Murphy Marble [MM]), and clastic wedge sequences (Talladega Group [TG] and Mineral Bluff Group [MBG]). Post-Iapetus rifting mafic igneous suite in the Tennessee salient shown as short line segments representing dikes (d), sills (s), and volcanic rocks (v). (C) Schematic along-strike diagram following regional metamorphism and isoclinal folding and just prior to the advance of the WBRTB allochthon over frontal and oblique ramps seen in A, showing the configurations of stratigraphic sequences in B, metamorphic isograds, and the initial trajectories of Alleghanian faults. Stratigraphic units and faults dip toward the viewer, whereas metamorphic isograds dip away from the viewer. (D) Configuration in C following advancement of the WBRTB allochthon over the oblique ramp and a large frontal ramp (shown in A) north of the CTZ, illustrating arching of the Blue Ridge and metamorphic isograds along the Tennessee salient.”

Chapter III:
REGIONAL STRATIGRAPHY

3.1 INTRODUCTION TO REGIONAL STRATIGRAPHY

In northwestern Georgia, the Paleozoic stratigraphy is comprised of rocks from the Cambrian up to the Pennsylvanian (Figure 3-1). Some of the first general surveys and discussions of the Paleozoic stratigraphy in Georgia were conducted by Hayes (1891, 1894, 1902). Spencer (1893) also reviewed the Paleozoic stratigraphy in northwestern Georgia, and recorded detailed accounts of the stratigraphy in ten individual counties. Spencer (1893) also compared and correlated his Paleozoic section to those of Hayes (*e.g.*, 1891) in Georgia, Smith (*e.g.*, 1876, 1890) in Alabama, and Safford (*e.g.*, 1869) in Tennessee (Figure 3-2). Similarly, Maynard (1912) summarized the Paleozoic succession and also recorded county-scale details of the stratigraphy in northwestern Georgia; his report paid particular attention to carbonate rocks and the resources thereof. The study by Butts (1948) contains a detailed map (scale 1:250,000) and concise report, on which almost all research on the geology of northwestern Georgia has been based in years since. Butts (1948) also extended his paleontological research into Georgia in this report, and his biostratigraphic data are still used at present. Later county-scale maps (scale 1:62,500) and reports were prepared for the region in cooperation with the United States Geological Survey by Cressler (1963, 1964a and b, 1970, and 1974) and Croft (1963), who also included fossil and hydrogeologic data in their studies; these reports contain the most recent mapping at this scale. In 1976, the Georgia Geological Survey published a geologic map of the entire state of Georgia at a scale of 1:500,000. More recently, Chowns (1989) briefly outlined the Paleozoic stratigraphy in Georgia and discussed distribution of lithofacies with respect to the regional thrust sheets and depositional environments. Most recently, the study of Thomas and Bayona (2005) is similar to that of Chowns (1989), but covers a much larger area, is more detailed on a broad scope, and also includes details of the tectonic implications and interactions of the Paleozoic succession in both Georgia and Alabama.

The following sections in this chapter provide a systematic summary of the Paleozoic succession in the region of study. Local lithologic details are described where

applicable. Many exposures were poor and/or both upper and lower contacts were not exposed, which precludes any precise measurements of thickness. County locations are shown in Figure 3-3.

3.2 CAMBRIAN SYSTEM

The oldest rocks exposed in the study area are dolostones of the Lower Cambrian Shady Dolomite; the oldest rocks that are most widely exposed in the region are fine-grained clastic rocks of the upper Lower Cambrian Rome Formation. The hanging wall of the regional décollement, however, cuts up-section in the direction of transport and includes older rocks in the more interior thrust sheets (Thomas and Bayona, 2005). The regional décollement is within the Cambrian Chilhowee Group under the Great Smoky/Cartersville thrust sheet, cuts upward and flattens near the base of the Rome Formation (and locally includes Shady Dolomite) under the Coosa thrust sheet, and cuts upward and flattens farther northwestward into the Conasauga Formation under the more frontal thrust sheets (Thomas and Bayona, 2005). The only well drilled to basement in Georgia was located near the northwestern corner of the state in Dade County; this well showed Rome Formation resting on basement (*cf.* Ortiz and Chowns, 1978; Coleman, 1988). Thus, although the regional décollement includes older rocks on the southeast (*i.e.*, Chilhowee Group and more of the Shady Dolomite) elsewhere, the sub-décollement Rome Formation evidently laps down onto basement rocks toward the northwest in the area of this study.

The Cambrian succession of Shady Dolomite–Rome Formation–Conasauga Formation thins northwestward, and the Shady Dolomite pinches out (Kidd and Neathery, 1976). The Rome Formation–Conasauga Formation succession generally is incompetent and contains the regional décollement; as a result, this succession typically is pervasively faulted and folded to an extent that precludes accurate thickness measurements. In the southwest of the study area near Rome, the Rome Formation–Conasauga Formation succession is estimated to be complete and is approximately 600–750 m thick (Cressler, 1970). To the northwest, west of the Sequatchie Valley in Alabama, the combined thickness of the same succession is estimated to be 520 m (Kidd

and Neathery, 1976); this area marks the foreland tip of the décollement structures (Chowns, 1989).

3.2.1 Lower Cambrian Shady Dolomite

The Lower Cambrian Shady Dolomite was originally named Shady Limestone by Keith (1903) for Shady Valley in Johnson County, Tennessee, and renamed by Stose (1923) because of the predominant lithology. The formation typically overlies the clastic succession of the Weisner Formation at the top of the Chilhowee Group, but this contact has not been found in Georgia (Butts, 1948). Butts (1948) characterized the formation in Georgia as bluish-gray, medium- to coarse-crystalline dolostone, which he noted was lithologically similar to the Shady Dolomite in Alabama. Butts (1948) further noted that the upper contact of the formation is not exposed in Georgia, which suggests that the outcrops of Shady Dolomite in the study area are contained in fault-bounded horses along the Coosa fault. The carbonate rocks of the Shady Dolomite are the upper part of a transgressive succession that records early “post-rift subsidence of a passive margin along the Blue Ridge rift of southeastern Laurentia (North America)” (Thomas and Bayona, 2005; *cf.* Thomas, 1991). According to Maples and Waters (1984), the formation represents an offshore shelf deposit with reefs.

Cressler (1970) noted dolostone in Floyd County that he correlated with the Shady Dolomite because of stratigraphic position and similar lithology; the contact with the overlying Rome Formation, according to Cressler (1970), is apparent at some of the exposures. The Shady Dolomite in Alabama thins and pinches out northwestward toward the foreland because of onlap (Kidd and Neathery, 1976); no evidence to the contrary has been documented for Georgia. Cressler (1970) documented only a few outcrops of Shady Dolomite in the study area, all of which are located in the immediate hanging wall of the Coosa fault, and, thus, the total thickness cannot be measured. The Shady Dolomite in these exposures is comprised of approximately 6 m of a lower dolostone and about 3.0–4.5 m of an upper, mainly shaly, dolostone that is thinly to massively bedded; these dolostone units are separated by approximately 3 m of dark shale and very thinly bedded “earthy” dolostone that weathers to shale. The upper dolostone is overlain by about 1.5 m of dark-gray shale that grades “abruptly upward into maroon shale and siltstone” of the Rome Formation. The dolostone primarily is medium- to dark-gray and very thickly to

massively bedded; it is commonly characterized by silt or clay that “weathers out as shale or accumulates on the surface as an olive-gray, tan, or yellowish-brown crust” (Cressler, 1970). The Shady Dolomite is also characterized by numerous fractures filled with fine-crystalline, light-gray quartz; these veins produce a “boxwork” relief pattern, especially on weathered surfaces. According to Cressler (1970), the formation in northwestern Georgia is completely free of chert.

3.2.2 Upper Lower Cambrian Rome Formation

The upper Lower Cambrian Rome Formation was named by Hayes (1891) for outcrops to the south of Rome, Georgia; the author did not specify a type section. In the study area, the formation is presumed to overlie the Shady Dolomite conformably in the more southeastern thrust sheets and to rest unconformably on basement beneath the more northwestern thrust sheets. The Rome Formation typically consists of shale, siltstone, and sandstone that are interbedded with minor amounts of limestone and dolostone (Butts, 1948; Thomas and Bayona, 2005). Butts (1948) described the sandstone as fine-grained and generally green or red; he described the shale as gray, pinkish, or yellowish where weathered, and presumed the shale to be naturally green in color. Cressler (1970) mentioned quartzite that is mainly in the upper half of the Rome Formation. In the subsurface in Alabama, the Rome Formation also includes evaporites, and the distribution of the evaporites is constrained by synrift basement faults (Thomas *et al.*, 2001). No evaporites have been documented in the Rome Formation in Georgia. Thomas and Bayona (2005) noted that the “abrupt appearance of clastic sediment above the transgressive Shady carbonates indicates a new source of detrital sediment on the passive-margin shelf, and marks an interruption in the stability of the shelf” subsequent to the onlap of the Shady Dolomite facies. The initial deposition of clastic Rome Formation succession roughly corresponds to the initiation of the Ouachita rift, which is a “late stage of crustal extension and rifting recorded in the basement faults of the Birmingham graben” (Thomas and Bayona, 2005; *cf.* Thomas, 1991). Chowns (1989) stated that the Rome Formation, from the limited available data, appears to represent peritidal deposition during a regression.

The Rome Formation in Floyd County holds up an array of knobby ridges in the hanging wall of the Coosa fault. In these outcrops, a large proportion of the shale, as well

as thin-bedded sandstone and siltstone, is bright red, purple, green, yellow, and brown in color; thicker sandstones are generally pale gray and weather to tan or rusty brown (Cressler, 1970). Cressler (1970) also noted that alternate layers of multi-colored rocks are distinctive to the formation. The Rome Formation ranges from 150 m to more than 300 m in thickness in the type locality in Floyd County, which is the only place in the study area where the base of the formation is exposed (and therefore a presumably complete section can be estimated).

Most of the outcrops of the Rome Formation have been identified in the hanging wall of the Coosa fault, and are limited to Floyd and Gordon Counties in this study. In Floyd County, outcrops of the formation were found in an abandoned quarry near GA Highway 27 southeast of Horseleg Mountain and in horsetail splays of the Coosa fault in or near roadcuts along US 411/GA 53 west of Cave Spring. Southeast of Horseleg Mountain, the Rome Formation is rusty red and yellow, and grayish tan shale that is pervasively folded and intensely folded in places into tight meter-scale folds. At the largest roadcut in the Coosa fault splays, the exposure is comprised of rusty red, yellowish-tan, and greenish gray shale, mudstone, siltstone and fine-grained sandstone. This exposed section is approximately 75 m thick, but accurate measurement is not possible because of some intensely folded beds and short (about 1 m) covered intervals. Furthermore, some parts of the section have been weathered to saprolite (primarily the shale). In the next splay to the west, about 1.5 km away, an outcrop of the formation is comprised of about 10 m of red, yellow, and greenish-tan saprolitic shale interbedded with meter-thick units of tan mudstone, siltstone, and very fine-grained sandstone in beds about 1 to 5 cm thick; the shaly saprolite appears to be disharmonically folded between the two largest siltstone intervals. The Rome Formation in Gordon County is in scattered outcrops, where it is irregularly laminated. One outcrop noted is comprised of approximately 20–30 m of rusty-reddish-brown shale interbedded with very fine-grained, thin-bedded sandstone that is weathered to a tan color; total thickness could not be determined accurately because of pervasive ductile deformation that primarily was concentrated in the shale. Another outcrop is comprised of about 4–5 m of deformed purplish-red and yellowish shale. In yet another such location, the formation is exposed in a low railroad cut as medium- to dark-gray shale that is weathered to tan and red.

Cressler (1974) described the Rome Formation in Gordon County as approximately 90–150 m thick and lithologically similar to the formation in the type locality, except that it contains much less sandstone and the sandstone beds are generally thinner (no thicker than about 2.5 to 5.0 cm).

The only other documented exposure in the area of study is in a belt in the hanging wall of the Clinchport fault in eastern Walker County and southwestern Whitfield County (Cressler, 1964b, 1974). Cressler (1964b) stated the Rome Formation in Walker County generally is sandstone, siltstone, and claystone. He described the sandstone as fine grained; green, brown, red, dark-gray, or nearly white; and in beds primarily less than 10 cm thick. He described the siltstone and claystone facies as fissile and green, yellow, brown, and red (Cressler, 1964b). Cressler (1964b) also noted pervasive, tight folds and steeply dipping to vertical beds in almost all the exposures of the Rome Formation in this locality, which, in addition to the base of the formation not being exposed, precludes an estimate of total thickness. Cressler (1974) described the Rome Formation in Whitfield County as similar to the formation as exposed in Floyd County in terms of character and thickness.

3.2.3 Middle to Lower Upper Cambrian Conasauga Formation

The Middle to lower Upper Cambrian Conasauga Formation was named by Hayes (1891) for outcrops along the Conasauga River in Whitfield and Murray Counties in Georgia; Hayes did not specify a type section. The formation is presumed to conformably overlie the Rome Formation (via a gradational contact) where exposed in the area of study (Cressler, 1970; Chowns, 1989). Butts (1948) described the Conasauga Formation as greenish shale that weathers to pale yellowish-gray or pinkish color and is interbedded with blue limestone. According to Chowns (1989), limestones in the Conasauga Formation in Georgia are more predominant toward the southeast, as has been documented in Tennessee by Rodgers (1953). Butts (1948) also noted that the presence of the limestone facies, in combination with an absence of red shale and sandstone, are the primary criteria for distinguishing (and also establishing the boundary) between the Conasauga Formation and the Rome Formation. Rodgers (1953) divided the Conasauga Formation into six recognized subdivisions to the north of the study area in Tennessee; these subdivisions were made on the basis of six alternate units of shale and limestone.

Munyan (1951) mentioned the regional members of the Conasauga Formation but was not able to map any of them separately because of poor exposure around Dalton; he did mention, however, correlation to the uppermost Maynardville Limestone Member. Cressler (1970, 1974) mapped subdivisions of the Conasauga Formation in places on the basis of predominant lithology (*e.g.*, mostly shale, or greater proportion of shale to limestone and vice versa); and the Georgia Geological Survey (1976) mapped comparable subdivisions on the basis of lithology, but also suggested possible correlations with the subunits of the Conasauga Formation in Tennessee. The Conasauga Formation represents an upward gradation from the clastic facies of the underlying Rome Formation into the carbonate facies of the overlying Knox Group; the transition, however, ranges with location from near the base to near the top of the formation (Thomas and Bayona, 2005). Hasson and Haase (1988) noted that the lithofacies of the Conasauga Formation throughout Tennessee is “consistent with a shelf–intrashelf–basin–carbonate ramp” environment.

The shaly facies of the Conasauga Formation hosts the regional décollement, but the uppermost, dominantly carbonate facies functions mechanically as a stiff layer in cooperation with the overlying Knox Group carbonate succession (Thomas and Bayona, 2005). Where the formation is exceptionally thick and dominated by shale, ductile deformation of the Conasauga Formation fills cores of detachment folds and ductile duplexes (Thomas and Bayona, 2005; Cook and Thomas, *in press*).

The general thickness of the Conasauga Formation is controlled systematically by a set of basement faults, which indicates movement along these late synrift faults (Thomas *et al.*, 2000). More recently, Cook and Thomas (*in press*) have demonstrated a similar setting in northwestern Georgia, in which the Conasauga Formation deposited in a basement graben is thicker than the average regional thickness.

Cressler (1970) divided the Conasauga Formation in Floyd County into two belts. Each belt has a distinct lithologic succession, and the rocks therein represent different depositional environments.

The eastern belt is in the hanging wall of the Coosa fault. The lower part of the eastern belt is composed of more than 30 m of medium-gray massive-bedded limestone overlain by “several hundred feet” of olive and tan shale (Cressler, 1970). The middle

part is composed of “thick, apparently discontinuous layers of massively bedded, medium-gray, oolitic and non-oolitic limestone that grades into and is interbedded with olive and tan shale” (Cressler, 1970). The upper part is composed of “several hundred feet of calcareous olive-gray and tan shale interbedded with thick sections of massively bedded, blue-gray ribboned limestone” with some gray dolostone (Cressler, 1970). In a low outcrop along US 411/GA 53 northeast of Cave Spring, an exposure of the formation is about 2–3 m of light- to medium-gray shale that is weathered to tan, brown, and pale olive-gray. Poor exposure and numerous faults (and probable pervasive ductile deformation) preclude accurate thickness measurements of the eastern belt of the Conasauga Formation; Cressler (1970) estimated a total thickness of approximately 450 m.

The western belt of the formation in Floyd County is exposed in the hanging walls of the trailing imbricates of both the Kingston and Chattooga faults; the western belt is poorly exposed, which precludes accurate measurement of total thickness. This western belt is divided by Cressler (1970) into three distinct, successive units. The lower unit is composed of olive-green silty shale that weathers to tan or pinkish orange and is interbedded with fine- to medium-grained sandstone that weathers to rusty brown. The middle unit is composed of medium- to dark-gray massively bedded limestone that is interbedded with olive-gray to tan shale. The upper unit is composed of “olive and tan shale containing a large quantity of thin-bedded limestone and calcareous siltstone” that is overlain by a zone of “dark olive-gray, somewhat silty, shale containing abundant mica flakes” (Cressler, 1970).

The Conasauga Formation in Chattooga County underlies valleys located in the hanging walls of both Kingston fault splays (wider outcrop at trailing splay), a narrow outcrop in the hanging wall of the leading Chattooga fault splay and a wide outcrop in the hanging wall of the trailing Chattooga fault splay, and in a synclinal “arm” off the wide outcrop that plunges out south of the southwestern end of the Taylor Ridge monocline. According to Cressler (1964a), the Conasauga Formation in these exposures consists primarily of calcareous siltstone and claystone that weathers to shale; he also noted a limestone unit near the top of the formation that is characterized by numerous stylolites. Although not mentioned by Cressler, this limestone unit presumably correlates to the

Maynardville Limestone Member. The limestone is characterized by light- to dark-gray color, commonly thick to massive beds, and abundant silt and clay; it is about 90 m thick and is also characterized by numerous stylolites (Cressler, 1964a). Cressler (1964a) noted that this limestone was well exposed in a US27/GA1 roadcut northeast of Trion, however, exposure at this outcrop is currently poor. The siltstone and claystone facies of the Conasauga Formation are light-gray to olive-gray and weather to brown; the siltstone is very thin-bedded where weathered and medium-bedded where unweathered (Cressler, 1964a). About 1.5 km south of Lyerly in the hanging wall of the trailing Chattooga fault splay, the exposure shows about 0.5 m of light-gray to tan, calcareous (possibly dolomitic) claystone in beds about 0.1 m thick. The claystone also contains abundant veins of microcrystalline calcite.

The Conasauga Formation in Walker County is exposed in a wide outcrop in a valley in the hanging wall of the trailing Kingston fault splay, a narrow outcrop in the valley along strike from the northern end of the trailing Chattooga fault splay, and along the Clinchport fault west of Villanow in a valley in the hanging wall and in a small fold in the footwall. The Conasauga Formation in these outcrops generally is siltstone, claystone, shale, and limestone; and the lower part of the formation is dominantly siltstone and claystone with a few scattered limestone beds (Cressler, 1964b). According to Cressler (1964b), the uppermost part of the formation is characterized by approximately 90 m of light- to dark-gray, limestone in thick beds (about 0.3 to 2.0 m thick) that have a ribboned appearance because of bands of clay and silt that “stand in relief” on weathered surfaces; this limestone unit is correlated by Cressler (1970) with the Maynardville Limestone Member. The siltstone and claystone are calcareous and weather to a shaly rock that is brown or green; the green-colored rock appears more clay-rich than the brown (Cressler, 1964b).

The Conasauga Formation makes up a significant amount of the hanging wall of the Coosa fault at the surface in Gordon County. Cressler (1974) describes the formation there as alternating layers of shale and limestone that are thick enough to control topography. The Conasauga Formation in Gordon County is observed as medium-gray, medium- to coarse-crystalline limestone (grainstone) interbedded with dark-gray shale; it

is also exposed as a light-gray, slightly shaly mudstone in a quarry in the northwestern corner of the county.

Cressler (1970, 1974) mapped the distribution of subdivisions of the Conasauga Formation on the basis of dominant lithology (*i.e.*, shale, limestone, dolostone, *etc.*). The western belt of the Conasauga Formation generally is distributed such that the uppermost subunit is mapped in the immediate hanging wall of the Rome fault, the lower subunit in the immediate footwall of the Coosa fault (trailing part of the Rome thrust sheet), and the middle subunit between. There is no apparent pattern of distribution in the eastern belt of the Conasauga Formation of Cressler (1970).

3.2.3.1 Maynardville Limestone Member of the Conasauga Formation

The only part of the Conasauga Formation that is mentioned or mapped separately in Georgia is the uppermost Maynardville Limestone Member (*e.g.*, Munyan, 1951; Georgia Geological Survey, 1976; Chowns *et al.*, 1992; Wilson, 1992); these studies mainly documented the lithologic contrast to the overlying Knox Group strata as a basis of placing the upper contact. The Maynardville Limestone was named by Oder (1934) for exposures in Union County, Tennessee, and was later considered as the uppermost member of the Conasauga Formation (Munyan, 1951). Munyan (1951) correlated the “uppermost, heavy limestone” of the Conasauga Formation with the Maynardville Limestone as defined by Rodgers (1953). Wilson (1992) basically stated only that the upper contact is placed at the top of a succession of light-gray chert-free beds (see also description of lower contact of Copper Ridge Dolomite in section 2.3.1). Munyan (1951) further noted a “tripoli zone” at the base of cherty limestone, which he assigned to the base of the overlying Knox Group. Chowns *et al.* (1992) described the formation in an incomplete section near Graysville as “massive weathering, crudely bedded, bioturbated” dolomitic limestone; they described the limestone as medium- to dark-gray, very thin-bedded, chert-free micrite, which is interbedded with tan-weathering dolostone partings that increase toward the top. Chowns *et al.* (1992) estimated the thickness of the Maynardville Limestone Member as approximately 119 m.

Cressler (1964a, b, 1974) mapped the Maynardville Limestone Member separately. It is shown on those maps along the base of the Knox Group throughout the Kingston–Chattooga anticlinorium in Chattooga and Walker Counties, in McLemore

Cove in Walker County, and in central Gordon County. Cressler (1970) does not map the unit separately, but noted in the text that the uppermost (approximately 60–90 m) of limestone and dolostone in the eastern outcrop belt are equivalent to the Maynardville Limestone Member. Similarly, Cressler (1963) describes the uppermost unit in the Conasauga Formation as approximately 90 m of massive-bedded, gray limestone, and notes in the stratigraphic explanation on the accompanying map that this unit is probably equivalent to the Maynardville Limestone Member. The Georgia Geological Survey (1976) mapped the Maynardville Limestone Member in the hanging wall of the Coosa fault.

3.3 UPPER CAMBRIAN AND LOWER ORDOVICIAN KNOX GROUP

The middle Upper Cambrian to Lower Ordovician Knox Group was named by Safford (1869) for exposures in Knox County, Tennessee. The Knox Group is a thick succession of massive dolostone, limestone, and chert. In the region of this study, it is presumed to conformably overlie the Conasauga Formation; in the area around Dalton, Munyan (1951) noted that the contact between the Maynardville Limestone Member and the Copper Ridge Dolomite appeared to be conformable such that “only a time hiatus might exist” at the plane. In Georgia, the Knox Group consists of four formations in succession upward: the Copper Ridge Dolomite, the Chepultepec Dolomite, the Longview Limestone, and the Newala Limestone. The contact between the Copper Ridge Dolomite and the Chepultepec Dolomite is assumed to approximate the Cambrian-Ordovician boundary. Butts included detailed descriptions of these units in his report of Alabama (Butts, 1926), but not for Georgia (Butts, 1948). Butts (1948) stated that although these units had been recognized in Georgia, “the conditions of exposure and scarcity of fossils make their accurate separation impossible without much more detailed investigation” than time permitted for his report. In several studies, the Newala Limestone is mapped as a distinct unit in Georgia and the other formations are mapped as undifferentiated Knox Group (*e.g.*, Butts, 1948; Munyan, 1951; Cressler, 1963, 1964a, b, 1970, 1974). The Georgia Geological Survey (1976) mapped both the Copper Ridge Dolomite and the Newala Limestone separately in some locations, but the Knox Group is shown as an undifferentiated unit in most places. Cressler (1970) mapped the Newala

Limestone as a unit separate from the Knox Group, and Butts (1948) considered it to be the basal unit of the overlying Chickamauga Limestone. To date, the most comprehensive study of the formation in this region is that of Raymond (1993) on the Knox Group of Alabama. The top of the Knox Group is characterized by a regional unconformity that locally preserves significant topographic relief on the ancient Knox erosional surface (*cf.* reference list in Milici and Smith, 1969). The post-Knox unconformity is correlative with the craton-wide sequence unconformity at the base of the Middle Ordovician between the Sauk and Tippecanoe sequences as described by Sloss (1963).

The carbonate succession of the Knox Group represents passive-margin deposition (Thomas and Bayona, 2005). Chowns (1989) noted that numerous carbonate bank environments are present throughout the formation, although the depositional fabric largely has been “destroyed by late diagenetic dolomitization.”

Chowns (1989) described the Knox Group as the “thickest, most homogeneous rock unit” in northwestern Georgia. Consequently, the Knox Group is the regional mechanical rigid layer, which controls the structural geometry of the thrust sheets (Thomas and Bayona, 2005). In Georgia, the Knox Group typically is transported above the décollement (separated by the upper carbonate-dominated part of the underlying succession) or is cut by major thrust faults (Cook and Thomas, *in press*).

Exposure of the Knox Group in the study area is poor, and it is also poorly exposed on local scales across the region. Butts (1948) stated that a reliable thickness measurement for the Knox Group in Georgia was impossible. Furthermore, because of the scarcity of carbonate rock exposures, chert residuum commonly is all that remains to mark the Knox Group. Munyan (1951) noted the absence of complete sections and scattered outcrops to the north of the study area around Dalton, Georgia. Wilson (1992) documented the same to the north of the study area in Tennessee. Butts (1948) estimated thickness of the individual units as 610 m for the Copper Ridge Dolomite, 305 m for the Chepultepec Dolomite, and 152 m for the Longview Limestone. The only reference sections in Georgia are from wells in Dade County, in which the Knox Group is approximately 1270 m thick (Ortiz and Chowns, 1978), and from outcrops at Graysville Gap in Catoosa County, where the estimated thickness of the group is 1223 m (Chowns *et*

al., 1992). The study of Chowns *et al.* (1992) presents a further discussion of the Knox Group exposures at Graysville Gap, which includes descriptions of incomplete sections in the area. Wilson (1992) described outcrops of the Knox Group to the north of Graysville Gap across the Tennessee state line; he estimated the total thickness at 850 m but noted that it increases southward to approximately 1080 m near the state line. The more complete sections of the Knox Group are located to the north of the area of structural interference that is the focus of the present research.

In Walker County, the undifferentiated Knox Group is mapped in the core of McLemore Cove anticline and in an anticline between Dick Ridge and the Clinchport fault. It is also mapped in the valleys on either side of Johns Mountain and in outcrop bands southeast of the Kingston fault; these map patterns extend southward into Chattooga County. In Floyd County, the undifferentiated Knox Group is mapped in an extensive area southeast of the Coosa fault.

In many locations throughout the study area, the Knox Group is exposed only as residual, massive white chert that weathers in places to tan, gray, and rusty brown. The chert residuum in some locations is bedded, banded (alternating white and gray), or slightly silty. Outcrops that include other rocks (mainly carbonate) were observed, however, in various locations throughout Chattooga County. In one roadcut just west of Lyerly, the Knox Group is exposed as approximately 1 m of white, massively-bedded chert in beds about 5–20 cm thick overlying approximately 2 m of pale-gray, medium- to coarse-grained sandstone that is cemented with dolomite in beds about 2–30 cm thick. The sandstone is interbedded with gray chert nodules (1–10 cm in diameter) and stringers (1–5 cm thick). About 3.5 km southeast of Lyerly, the group is exposed as 4–5 m of medium-gray, very fine to fine-crystalline dolostone in beds that range from 5 cm to about 1 m thick. The thickest (~1 m) bed is laminated; the laminations are about 2 mm thick. One layer in this outcrop includes dark-gray and black chert nodules as thick as 10 cm that are laterally continuous across most of the exposure. To the northeast of Trion near the western flank of Taylor Ridge, the group is exposed as approximately 20–30 m of pale- to medium-gray, mostly very fine- to fine-crystalline dolostone in beds that range from 10 cm to about 1 m thick. The dolostone at this location is interbedded with white and light-gray chert nodules and stringers that range 1–25 cm in thickness. The most

extensive outcrop of the Knox Group is exposed in an abandoned quarry about 2.5 km north of Trion. The exposure in this quarry exceeds at least 30 m, but the base of the outcrop is under water. The Knox Group in this quarry is light- to medium gray, thin- to thick-bedded, micritic to fine-crystalline limestone and dolostone in beds that range from about 1 cm to about 1 m thick. The carbonate rocks are interbedded with massive, primarily white chert beds and nodules.

3.3.1 Copper Ridge Dolomite

The middle Upper Cambrian Copper Ridge Dolomite was named by Ulrich (1911) after exposures in northwestern Knox County, Tennessee, on the prominent ridge of the same name. Butts (1926) described the Copper Ridge Dolomite as generally thick-bedded, light-gray, fine- or coarse-grained and “presumably siliceous” dolostone and noted that exposures of the formation are characterized by dense, hard, white or yellowish gray chert float with irregular edges in a deep-red soil. Munyan (1951) documented similar lithology in outcrops in the Dalton quadrangle, in Georgia and Tennessee. The descriptions of Wilson (1992) are also similar, and he added that some of the chert pieces are as thick as 60 cm. Butts (1948) did not describe any specific outcrops of the formation in Georgia. Cressler (1970) described the formation in Floyd County as “light- to medium-gray, fine- to coarse-grained, thickly to massively bedded cherty [dolostone], and brownish-gray, medium- to coarse-grained, asphaltic [dolostone] that has a distinctive fetid odor on fresh breaks”; he also noted that the brownish-gray dolostone is predominant in the lower part of the formation, and the light-gray is predominant in the upper part. Cressler (1970) also noted the highly siliceous chert both in layers and as “boulder-like chunks” and that it is light-gray or dark-gray in color depending on amount of weathering. The formation commonly is deeply weathered and covered by a mantle of residual chert and clay that generally is 15–60 m thick but exceeds 90 m in thickness (Cressler, 1970).

In the Graysville Gap exposures, the Copper Ridge Dolomite is comprised of approximately 747 m of massive, thick-bedded cherty dolostone, which is mostly covered; the dolostones are generally light to medium/dark gray, fine to medium grained, and locally bituminous (Chowns *et al.*, 1992). The base is taken to be below the lowest massive dolostone (Maynard, 1912), which is in contrast to the limestones and thin-

bedded dolostones of the underlying Conasauga Formation; although the rocks are similar in color. Chowns *et al.* (1992) interpreted the transition from limestone to dolostone as indicative of a shift from subtidal carbonates to peritidal deposits. Wilson (1992) estimated a thickness of about 300 m for the Copper Ridge Dolomite on the basis of residuum in his study area just to the north. Cressler (1970) noted that the formation is approximately 914 m thick in Catoosa County and suggested that a comparable thickness is possible for Floyd County.

Carbonate outcrops of the Copper Ridge Dolomite are rare. Cressler (1970) demonstrated that the rocks of the Knox Group exposed on Horseleg Mountain belong to the Copper Ridge Dolomite. From this location, he noted various specimens of the gastropod *Scaevogyra*, one of which is indicative of a thin zone in the Upper Cambrian succession (Cressler, 1970, citing a personal communication from Ellis L. Yochelson of the United States Geological Survey). The map of the Geological Survey of Georgia (1976) shows only Copper Ridge Dolomite (and no other Knox Group rocks) on Horseleg Mountain.

3.3.2 *Chepultepec Dolomite*

The Lower Ordovician Chepultepec Dolomite was named by Butts (1926) for exposures near the town of Chepultepec (later renamed Allgood) in Blount County, Alabama. Butts (1926) described the Chepultepec Dolomite as dolostone and limestone that is characterized by chert and abundant fossils, primarily gastropods; Butts (1948) noted these gastropods include *Sinuopea* and *Chepultepecia* and the guide fossil *Helicotoma uniangulata*. He noted that the residual chert is characteristically “a peculiar soft, mealy, cavernous chert, which looks like worm-eaten wood” (Butts, 1926). Commonly, the more ubiquitous index fossils, such as *Sinuopea*, in cavernous chert residuum are presumed to define Chepultepec Dolomite outcrops. Rodgers and Kent (1948) noted a thin, but extensive sandstone layer marking the base of the Chepultepec Dolomite; and this was later described in Georgia (Cressler, 1963, 1974; Wilson, 1992). Munyan (1951) also mentioned sandstone in the Knox Group around Dalton and described some exposures; although, he did not find any other sufficient evidence in the chert for “definite identification” of the Chepultepec Dolomite. Munyan (1951) further noted that he was able to confirm the identification of the formation as mapped by Butts

(1948) on the basis of the cavernous chert residuum in other locations, but that his attempts to trace the zone “with any degree of accuracy” were unsuccessful and thus did not warrant documentation.

In the Graysville Gap outcrops, the Chepultepec Dolomite is comprised of “repetitious cycles of subtidal to peritidal carbonates” that are extensively dolomitized (Chowns *et al.*, 1992). The rocks generally are dark gray near the bases of the cycles and light gray near the tops, but the color is also dependent on amount of bituminous matter (Chowns *et al.*, 1992). This description is similar to that of the underlying Copper Ridge Dolomite; some limestone, however, is present in the lower part of the Chepultepec Dolomite. The tops of the cycles are also characterized by “chaotic, vuggy paleosols partly replaced by chert and infilled with microquartz and agate,” and the pedogenic features include solution collapse breccias (Chowns *et al.*, 1992). As a result, agate and mealy or vuggy chert typify the residual soils of the formation. Chowns *et al.* (1992) made no mention of the sandstone at the base of the formation, but did denote part of the sequence as covered in their stratigraphic column.

Wilson (1992) described the Chepultepec Dolostone as approximately 270–300 m of medium- to thick-bedded, light-gray, fine- to medium-grained dolostone, of which exposure is limited. He also noted the presence of a few beds of dark-gray dolostone that are primarily limited to the lower third of the formation, and thin sandstone beds at the base that separate the formation from the underlying Copper Ridge Dolomite. Wilson (1992) described the chert in the lower part of the formation as porous and characterized by dolomite rhomb molds; in the upper part of the formation, the chert is more massive. Wilson (1992) also noted that fossils in the Chepultepec Dolomite are rare, but documented “occasional” *Lecanospira compacta* specimens in the residual chert.

The Chepultepec Dolomite in Catoosa County consists primarily of “light- to medium-gray [dolostone] in thick to massive layers” that is interbedded with sparse beds of gray and tan, micritic limestone (Cressler, 1963). Thin sandstone beds are present near the base and also in the middle of the Chepultepec Dolomite, and locally are present in small pieces in the soil. The formation there is approximately 150 m thick (Cressler, 1963).

3.3.3 Longview Limestone

The Lower Ordovician Longview Limestone was named by Butts (1926) for exposures in the town of Longview in Shelby County, Alabama. Raymond (1993) described the Longview Limestone as “medium- to thick-bedded, light- to medium-gray cherty limestone and lesser amounts of interbedded [dolostone]”; the limestone generally is peloidal grainstone to mudstone, locally mottled with dolostone (compiled from various references in Raymond, 1993). The most distinctive characteristic of the Longview Limestone in Alabama is the presence of quartz sand, which is more abundant than in other units of the Knox Group; the sand generally is scattered grains, thin laminae, or thin local beds (Raymond, 1993). The formation is also characterized by “thin-bedded stromatolitic chert and nodular chert”, which yields abundant dense, blocky chert residuum (Raymond, 1993). According to Butts (1926, 1948; also *cf.* Twenhofel *et al.*, 1954; Raymond, 1993, and references therein), the presence of the diagnostic gastropod *Lecanospira* confirms the identification of the Longview Limestone in outcrop. This gastropod is ubiquitous throughout the Longview Limestone, in which fossils are otherwise sparse (Raymond, 1993).

In limited exposures in Floyd County, the Longview Limestone consists mainly of “massively bedded medium- to light-gray [dolostone]” that is interbedded with thickly bedded light- to medium-gray micritic to medium-grained limestone (Cressler, 1970). The Longview Limestone includes chert layers as thick as 2 m, and the commonly thick residuum is characterized by “large chunks and pieces” of tough, angular chert with a small amount of sandstone (Cressler, 1970). Cressler (1970) also documented that roughly half of the upper part of the Longview Limestone in Catoosa County is limestone, but nearly all of the formation is dolostone to the southeast in Polk County.

3.3.3.1 Sandstones in the Knox Group

Various thin sandstones have been documented in the Chepultepec Dolomite and Longview Limestone formations of the Knox Group. In the county geologic reports of Cressler that mention sandstone in the Knox Group (1963, 1964b, 1970, 1974), however, there is little consistency in terms of occurrence and at what stratigraphic level within the two formations. It may be concluded that the thin sandstone intervals in this part of the Knox Group are, in essence, sporadically distributed and laterally discontinuous. As a

result, no attempts were made in this research to differentiate formations of the Knox Group in the field on the basis of sandstone outcrops.

3.3.4 *Newala Limestone*

The Lower Ordovician Newala Limestone was named by Butts (1926) for outcrops near the Newala Post Office in Shelby County, Alabama. Butts (1926) described the Newala Limestone as composed of “much limestone and proportionately little [dolostone]” and estimated the thickness as 300 m. Butts (1926) further described the limestone as “thick-bedded, compact or noncrystalline or textureless, dark gray, pearl gray, and bluish gray. The pearl-gray color perhaps predominates and is most characteristic.” The dolostone, according to Butts (1926), is found in thick coarse-grained beds or as mottling in the limestone. In his description, Butts (1926) differentiated the Newala Limestone from the underlying Longview Limestone by the purity and lack of chert.

The Newala Limestone is mapped by Butts (1948) on both limbs of McLemore Cove anticline in Walker and Catoosa County, in the footwall of the Kingston fault in northwestern Catoosa County, west of Ringgold in northern Catoosa County, in a syncline in the footwall of the Coosa fault in Murray County, and in the southeastern corner of Floyd County. The Newala Limestone as mapped by Butts (1948) is also shown on maps by Cressler (1963, 1964a, b, 1970, 1974) and the Georgia Geological Survey (1976). Munyan (1951) shows a similar outcrop pattern for the formation as Butts (1948) in Murray County, but it is more restricted in extent. Munyan (1951) mapped most of the Newala Limestone of Butts (1948) in this area as Knox Group.

Butts (1948) described outcrops of the Newala Limestone in Georgia as “a rather thick-bedded, pure, blue limestone” that is “massive, thick, or moderately thick-bedded...[with some] blue-gray, finely crystalline, and some compact dove layers (vaughanite).” Butts (1948) also noted that the weathered outcrops are characterized by “nodules, stringers, and thin partings” of black chert. He further asserted that this description is consistent in all the outcrops throughout the state, made mention of exposures scattered around northwestern Georgia, and, particularly in the area of study, cited good exposures in Walker County. Coincidentally, Butts (1948) described the Murfreesboro Limestone (which overlies the Newala Limestone in his account of the

Chickamauga Supergroup) as “dove-colored or blue, compact or crystalline, fossiliferous limestone” that is characterized by local “black, ropy” chert. Cressler (1963, 1964a, b) mapped the Newala Limestone as a separate unit between the Knox Group and the Chickamauga Supergroup in Catoosa County, but did not describe it except to mention that he included it in the Chickamauga Supergroup rather than the Knox Group because of lithologic similarity and that it “includes much [dolostone]” in the lower part.

In Floyd County, the Newala Limestone consists primarily of equal proportions of interbedded limestone and dolostone; the limestone is slightly more abundant in the upper part (Cressler, 1970). The limestone is light to medium/dark gray and is thickly to massively bedded; the beds commonly are approximately 0.30 to 1.25 m thick, although some beds are thinner (Cressler, 1970). The dolostone is light to medium gray and fine to coarse grained, and is characterized by massive beds that are thicker than about 2 m in some localities (Cressler, 1970). The Newala Limestone typically contains “either widely scattered chert nodules or a few thin discontinuous chert beds,” and locally contains abundant nodular and bedded chert (Cressler, 1970). In some places, the top of the formation is marked by a conglomerate of argillaceous limestone clasts in a matrix of pure limestone. Cressler (1970) estimated that the thickness of the Newala Limestone is at least 90 m.

3.3.5 *Alternate interpretations/correlations in the upper Knox Group*

Chowns *et al.* (1992) and Wilson (1992) employed the Kingsport Formation and Mascot Formation subdivisions (as used to the north in Tennessee), for the rocks above the Chepultepec Dolomite as suggested by Harris (1969) and Wilson (1979). The Kingsport Formation as used by Chowns *et al.* (1992) and Wilson (1992) contains the entire Longview Limestone as described and also includes some overlying rocks; only Wilson (1992) mentioned any further details by indicating inclusion of a limestone facies and a finely crystalline dolostone facies in addition to the Longview Limestone as previously mapped. On the contrary, unpublished field investigations of G. A. Cooper and B. N. Cooper in the years 1944 to 1947 (*cf.* Twenhofel *et al.*, 1954) in Tennessee demonstrated the Kingsport and Mascot Formations overlying the Longview Limestone in the upper Knox Group; this organization of the Knox Group was also used by Rodgers and Kent (1948). Furthermore, Cressler (1963) used the Copper Ridge-Chepultepec-

Longview nomenclature of Butts (1948) in his report for Catoosa County, which includes the area studied by Chowns *et al.* (1992).

3.3.5.1 Kingsport Formation

The Lower Ordovician Kingsport Formation was named by Oder and Miller (1945) for exposures near Kingsport in Sullivan County, Tennessee. In the type section, they described the formation in four parts (from base to top) as: 1) approximately 55 to 65 m of predominately brown limestone that is locally altered to crystalline dolostone, interbedded with light- to dark-gray, fine-grained dolostone with abundant chert layers; 2) approximately 10 to 12 m of light- to dark-gray and brownish, fine-grained or finely crystalline dolostone with some brown limestone; 3) approximately 13 to 15 m of light brownish gray to almost white, fine-grained dolostone; and 4) approximately 31 to 41 m of light to dark, fine-grained dolostone with some brown limestone interbeds (Oder and Miller, 1945). Chowns *et al.* (1992) estimated the thickness of the Kingsport Formation as 81 m, and Wilson (1992) estimated 68–75 m on the basis of topographic expression. Whether Chowns *et al.* (1992) and Wilson (1992) consistently placed the upper and lower contacts for formation at the same stratigraphic position is ultimately unclear, but the lithologic successions both should correspond roughly to the Longview Limestone and the lower part of the Newala Limestone (Figure 3-4).

The Kingsport Formation of Chowns *et al.* (1992) is composed primarily of light-gray, micritic limestone, which “ranges from peloidal mudstone to packstone with some intraclastic and sandy intraclastic beds.” The limestones commonly are fossiliferous; they also include isolated dolomite euhedra and grade into coarse-grained “sucrosic” dolostone, which is interpreted to be “late diagenetic in origin” (Chowns *et al.*, 1992). The authors also mentioned that chert nodules, which are red in some locations, are common in the limestone and dolostone; the chert is locally accumulated in irregular masses that may be related to solution collapse breccias (Chowns *et al.*, 1992). Compared with the two underlying formations in the Knox Group, the Kingsport Formation is “lighter in color (less bituminous), less dolomitic, and texturally less complex” according to Chowns *et al.* (1992); the authors also noted that the spongy, dolomitic chert residuum as described in the Chepultepec Dolomite is lacking in the Kingsport Formation.

Wilson (1992) described the formation simply as “light-gray, aphanitic limestone” in the lower part and medium-gray, coarsely crystalline (“recrystalline”) dolostone in the upper part. He also mentioned that chert residuum is rare, but the float is chalky and blocky or in small nodules where present. Wilson also noted that the outcrop belt of the Kingsport Formation “forms a shallow valley or low hills downdip from the massive cherts of the Chepultepec [Dolomite] and in front of higher elevations produced by the Mascot [Formation],” and commonly is characterized by a row of depressions, indicating geologically recent karst solution collapse.

3.3.5.2 Mascot Formation

The Lower Ordovician Mascot Formation (originally Mascot Dolomite) was named by Oder and Miller (1945) for exposures near Mascot in Knox County, Tennessee. In the type section, they described the formation as approximately 150 to 200 m of light- and dark-gray dolostone and limestone that is moderately cherty; a chert-matrix sandstone at the base is about 0.2 m thick (Oder and Miller, 1945). The Mascot Formation as used by Chowns *et al.* (1992) and Wilson (1992) evidently corresponds roughly to the upper part of the Newala Limestone (Figure 3-4).

Chowns *et al.* (1992) described the Mascot Formation as predominately light-gray dolostone interbedded with partially dolomitized limestone; the limestones are described as micritic and peloidal, and grade into coarse-grained “late diagenetic” dolostone. The formation is lithologically similar to the underlying Kingsport Formation, except that dolostones are more abundant than limestones, and chert is less common. Chowns *et al.* (1992) also noted subdued topography in outcrop belts of the Mascot Formation with respect to other formations in the Knox Group because of the lack of chert; the authors also mentioned a lack of continuous exposure.

According to Wilson (1992), the base of the Mascot Formation is indicated by several thin beds of sandstone that is cemented in a matrix of light-colored chert. He further described the lower part of the Mascot Formation as light- to dark-gray, fine-grained dolostone that, toward the south, is increasingly interbedded with light-gray, medium-bedded, dense limestone. The formation as described by Wilson (1992) also includes light-gray, coarse-grained dolostone; dolostone beds in the upper part of the formation locally “show a distinctive pink to yellowish and maroon clouding” (Wilson,

1992). The residual chert of the Mascot Formation is bedded or nodular. The nodules are commonly red in color and banded, and some of the bedded chert is locally dark in color and weathers to small fragments (Wilson, 1992). The formation is well exposed in the National Cemetery in Chattanooga, and Wilson (1992) noted “distinct zones of breccia, which are interpreted as solution-collapse features related to the unconformity” at the top of the Mascot Formation.

Chowns *et al.* (1992) estimated the thickness at 50 m, and Wilson (1992) asserted that the thickness varies between about 135 and 150 m. Chowns *et al.* (1992) ascribed this difference to the lower stratigraphic level of the Mascot boundary drawn by Wilson (1992), as well as to variation in truncation of the upper Knox Group below the unconformity.

3.3.5.3 Problems with Newala Limestone

The map of Butts (1948) shows outcrop belts of the Newala Limestone in the area around Chickamauga. Successive studies have reinterpreted this succession as discussed by Milici and Smith (1969) and summarized by Chowns *et al.* (1992). Milici and Smith (1969) pointed out that the Newala Limestone as described by Butts (1948) only referred to “one lithologic type of the very complex formation, and did not recognize the basal dolostone and chert-pebble conglomerates and the extensive development of red shales, variegated dolomitic limestones, and ‘red-mottled’ limestone that occur within the formation” in the vicinity of Chickamauga. Butts (1948) did identify “red or red-mottled limestone interbedded with blue or dove beds” in eastern belts west of Lafayette and west and north of Ringgold. According to Milici and Smith (1969), however, Butts (1948) possibly erroneously included these with the Murfreesboro Limestone.

Milici and Smith (1969) asserted that the Newala Limestone of Butts (1948) in the area around Chickamauga is above the post-Knox unconformity, and should thus be included within the Pond Spring Formation. Both the studies of Milici and Smith (1969) and Chowns *et al.* (1992) stated that the “Newala” as mapped by Butts (1948), must include some Lower Ordovician rocks on a more regional scale and therefore straddles the unconformity and should be divided. Furthermore, Butts (1948) documented abundant specimens of the gastropod *Ceratopea* in his Newala Limestone, on which he based a correlation with upper Beekmantown (Kingsport and Mascot Formations), thus

indicating Lower Ordovician rocks. Cressler (1970) further discussed *Ceratopea* as a guide fossil to the Newala Limestone. Milici and Smith (1969), however, noted that their map was sufficiently similar to that of Butts (1948) to indicate that specimens of *Ceratopea* described in both studies near Chickamauga are above the post-Knox unconformity (and thus the basal Chickamauga Supergroup must therefore include some Lower Ordovician rocks). Chowns *et al.* (1992) maintained that in the Graysville area, the lower part of this Newala as mapped by Butts (1948) should be assigned to the Mascot Formation and the upper part to the Pond Spring Member of the Stones River Formation (as part of the Chickamauga Supergroup).

If the upper part of the Newala Limestone of Butts (1948) cannot be demonstrated to be of Middle Ordovician age via biostratigraphic markers, then perhaps the only evidence available is the stratigraphic position relative to the poorly exposed post-Knox unconformity. Munyan (1951) found the Newala Limestone to be unconformably overlain by Ordovician sandstone (*i.e.*, below the post-Knox unconformity) and consequently noted that some of the Newala Limestone of Butts (1948) in the area around Dalton to the east of Chickamauga is correctly placed, and thus is part of the Knox Group.

3.3.5.4 Summary of problems in mapping the upper Knox Group

No consensus has evolved for mapping the succession of rocks in the upper Knox Group between the base of the Chepultepec Dolomite and the post-Knox unconformity in Georgia. Butts (1948) favored the Longview Limestone–Newala Limestone configuration that he also used in Alabama (1926). More recent studies in northern Georgia appear to prefer the Kingsport Formation–Mascot Formation nomenclature from Tennessee (as described in section 3.3.5.3). Furthermore, the uncertainty that has surrounded the mapped Newala Limestone indicates the difficulty in mapping the Knox Group in this region.

The biostratigraphic markers, such as fossil specimens of *Sinuopea* and *Lecanospira*, have been used to distinguish respective lithostratigraphic units in the Knox Group, but there is some disagreement or uncertainty (*i.e.*, Munyan, 1951). According to Ed Osborne, director of the Geologic Investigations Program, at the Geological Survey of Alabama (personal communication, 2010), all of the many specimens of *Lecanospira* he

has found are at the stratigraphic level of the Longview Limestone; some of the specimens, however, were in cavernous chert that is more indicative of Chepultepec Dolomite (but presumably at the Longview stratigraphic level). As an aside, one should note that Butts (1948) did not document both chert type and fossil content for any location in the area of this study.

According to John Repetski of the United States Geological Survey, identification of such fossils, even at the genus level, is challenging as a result of the different preservation modes such as certified (perhaps only partially) molds and casts, *etc.* (personal communication, 2010). Also, one should note that the base of the Ordovician was officially raised by the International Commission on Stratigraphy (ICS) in 2001 (*cf.* www.stratigraphy.org); thus some rocks considered Lower Ordovician in pre-2001 literature are now “officially” part of the Upper Cambrian.

Both of the sets of nomenclature/interpretation fit loosely to the rocks of the Knox Group in Georgia given the poor quality of exposure; thus these interpretations may not be mutually exclusive. Neither of these interpretations, however, appears to be consistently traceable outside of scattered locations (*cf.* lack of contacts on significant portion of map by Chowns *et al.*, 1992), and correlation between them has not proved possible. As a result, mapping the entire Knox Group as an undifferentiated unit is suggested for regional studies such as that contained in the present research.

3.3.6 Top of the Knox Group

Throughout much of the study area, the Knox Group is approximately 660 m thick in the hanging wall of the Kingston fault. This thickness is based on seismic reflection profiles and surface data such as outcrop widths and bedding orientations. This total thickness would only accommodate the Copper Ridge Dolomite and, perhaps in places, some of the lower part of the Chepultepec Dolomite. Biostratigraphic evidence presented by Cressler (1970) from the Knox Group at Horseleg Mountain (*cf.* section 3.3.1) indicates that the Copper Ridge Dolomite is overlain unconformably by the Middle Ordovician Greensport Formation and that the Longview Limestone, Chepultepec Dolomite, and possibly some of the upper part of the Copper Ridge were eroded prior to Middle Ordovician. He also noted that significant amounts of the upper Knox Group “also may have been eroded from other areas west and north of the Rome fault as is

suggested by the extreme narrowness of the outcrops there,” and by the presence of the Attalla Chert Conglomerate Member that everywhere indicates the unconformity (Cressler, 1970).

On the contrary, Butts (1948) cited biostratigraphic evidence for upper units within the Knox Group in the study area. For example, he found various specimens of *Sinuopea* and *Lecanospira*. There is uncertainty, however, about the exact age of these fossils (c.f. discussion in Section 3.3.5.4).

Furthermore, lithologic boundaries should not be treated as reliable time boundaries. Commonly, the type of residual chert (*e.g.*, mealy or cavernous chert in the Chepultepec Dolomite) is used as a diagnostic for positive identification of units within the Knox Group (*e.g.*, Butts, 1948; Oder, 1934; Cressler, 1963, 1970; Chowns *et al.*, 1992), and that may not be reliable (*cf.* Munyan, 1951). Some of the units of the Knox Group are possibly thinner in the region because of diminished carbonate accumulation. Also, solution collapse has been documented in the Knox (*e.g.*, Garry, 2001), which could also preserve rocks at a lower stratigraphic position than expected. Two categories of solution collapse may be present: 1) paleokarst features associated with the Middle Ordovician erosion surface, and 2) present erosion and/or geologically recent solution collapse structures. Either or both of these types of solution collapse may be present in the Knox Group in northwestern Georgia. Lastly, Repetski (1992) in a study of conodonts in the Knox Group at Graysville concluded that “a considerable part of the Chepultepec [Dolomite] at Graysville and elsewhere” actually should be reassigned to the Upper Cambrian on the basis of ages of conodont zones as defined at that time.

The post-Knox unconformity is a highly irregular erosional surface characterized by locally high topographic relief caused by solution collapse structures (*e.g.*, Butts, 1926; also see more recent details and descriptions by Munyan, 1951; Drahovzal and Neathery, 1971; Garry, 2001; Bayona, 2003; Thomas, 2007). On a regional scale, the general stratigraphic level of the unconformity truncates more of the Knox Group succession southward through Georgia.

Chowns *et al.* (1992) ascribed some of the variation in thickness of the Mascot Formation to karst topography on the post-Knox unconformity (*i.e.*, sinkholes and other solution collapse features). The formation ranges in thickness from 135 to 150 m around

Chattanooga, Tennessee (Wilson, 1992); it is approximately 107 m thick in the well in Dade County, Georgia; and ranges from about 30 to 50 m thick in the area around Graysville, Georgia (Chowns *et al.*, 1992). Chowns *et al.* (1992) noted three cave-fill structures in two quarries in their study area that are roofed by the Mascot Formation but “clearly connect” with the unconformity. One of these is located in the Stone Man quarry and is approximately 6 m below the unconformity. A similar collapse breccia crops out elsewhere in the study area of Chowns *et al.* (1992) near the unconformity. The authors further noted that the upper part of the Mascot Formation is particularly fractured and “infiltrated by greenish-gray shales” that locally penetrate as far down as the limestones of the Kingsport Formation; they also posited that some of the “solution collapse and silicification” in the Kingsport Formation could possibly be related to the unconformity (Chowns *et al.*, 1992).

In an evident regional trend, the post-Knox unconformity truncates progressively more of the upper Knox Group southward along strike in Georgia. On the north, approximately 13 km south of Ringgold in Catoosa County, the Mascot Formation is absent and the basal Middle Ordovician Pond Spring Formation of the overlying Chickamauga Supergroup rests directly on the Kingsport Formation (Chowns *et al.*, 1992). Approximately 16 km south-southwest of Chickamauga in Walker County, Butts (1948) documented *Sinuopea* and *Chepultepecia* near the top of the Knox Group, which suggests that the beds below the unconformity are in or near the Chepultepec Dolomite. Farther to the south, at “several points” west of Trion and Summerville (presumably in Chattooga County), Butts (1948) suggested that the Middle Ordovician rests on Longview Limestone on the basis of *Lecanospira* specimens. Farther south, the Middle Ordovician directly rests on Copper Ridge Dolomite on Horseleg Mountain (*cf.* section 3.3.1).

Furthermore, Munyan (1951) noted that all of the Newala and Longview Limestones and part of the Chepultepec Dolomite apparently are absent in the area west of Dalton, where the post-Knox unconformity probably overlies Chepultepec Dolomite. The upper units of the Knox Group reappear in the stratigraphy farther to the east near Dalton (Munyan, 1951), farther to the northwest near the Tennessee state line in the area of Graysville (Chowns *et al.*, 1992) and to the west in the footwall of the Kingston fault

(Wilson, 1992). Cressler (1970) noted that the upper units of the Knox Group are absent in the area around Rome, but that all three formations of his Knox Group are present to the southeast in the hanging wall of the Coosa fault. Cressler (1970) documented Copper Ridge Dolomite on the basis of massive chert residuum with fossil cryptozoa adjacent to the Conasauga Formation in “much of southern and eastern Floyd County” and large parts of Polk County; he also noted Longview Limestone on the basis of *Lecanospira* in chert in Polk County and in southeasternmost Floyd County adjacent to Newala Limestone. In areas between, Cressler (1970) noted “an unusual amount of soft, cavernous chert” and some bedded sandstone indicative of Chepultepec Dolomite; he did not, however, attempt to differentiate these formations because of time constraints in his field work.

3.4 MIDDLE AND UPPER ORDOVICIAN

The Middle and Upper Ordovician succession in northwestern Georgia was summarized by Chowns and McKinney (1980; *cf.* also Chowns, 1972, specifically for details of the Upper Ordovician), who identified three major facies suites. Two of these facies suites are mapped in the area of the present study (Figure 3-5). Generally, the shallow-water carbonates of the Middle Ordovician Chickamauga Limestone predominate in the northwest and grade southeastward into peritidal clastic redbed facies of the Middle and Upper Ordovician Greensport and Sequatchie Formations (Allen and Lester, 1957). In some parts of the study area, the Greensport and Sequatchie Formations are divided by the intervening coarse clastic sedimentary succession of the Colvin Mountain Sandstone. Chowns and Carter (1983a) demonstrated that the facies boundaries generally coincide with major thrust faults: the carbonates are northwest of the Kingston fault, the peritidal deposits are between the Clinchport and Rome faults, and the gradation between the two facies spans primarily between the Kingston and Clinchport faults. The Middle and Upper Ordovician succession overlies the post-Knox unconformity and is overlain by another unconformity (Drahovzal and Neathery, 1971; Chowns, 1989). Bayona (2003) noted that the facies distribution of the succession is indicative of subsidence of and deposition into a Taconic foreland basin.

3.4.1 *Chickamauga Limestone*

The Middle Ordovician Chickamauga Limestone was named by Hayes (1891) for outcrops along the West Chickamauga Valley south of Chattanooga, Tennessee, near Ringgold, Georgia, and consists of a complex of silty to argillaceous limestone and calcareous siltstone. Hayes (1894) included all rocks from the top of the Knox Group to the base of the Rockwood Formation (now mainly Red Mountain Formation) in the Chickamauga Limestone. In a detailed study, Milici and Smith (1969) expanded the nomenclature to the Chickamauga Supergroup, which they subdivided into the lower Stones River Group and upper Nashville Group, as well as the respective subdivisions of both groups (Figure 3-6). Milici and Smith (1969) noted that the Chickamauga Supergroup exceeds 440 m in thickness in the type section. Milici and Smith (1969) also described the unconformable contact between the base of the Chickamauga Limestone and the underlying Knox Group with attention to degree of truncation of the Knox Group; they also listed several other references on this subject.

With the exception of the Pond Springs Formation, the names of the formations in the Chickamauga Supergroup as defined by Milici and Smith (1969) are borrowed from rocks units with type sections in central Tennessee (*cf.* Wilson, 1949). Wilson (1949, and references therein) defined this carbonate succession as the Chickamauga Group in Tennessee, and subsequent lateral correlations of have proven to be difficult. Wilson (1949) noted a particular problem with lateral variation between the Bigby and Cannon Limestones in central Tennessee, which had previously been considered individual units in the same stratigraphic position. In his report, Wilson (1949) referred to “Bigby facies” and Cannon “facies” and combined this succession into the Bigby-Cannon Limestone. Furthermore, facies variations throughout the Middle Ordovician in the region combined with poor exposure precludes reliable tracing of any subdivisions of the Chickamauga Supergroup in the area of study. Carter and Chowns (1988) noted that “outside the type section in Georgia, and in Alabama,” the Stones River and Nashville are “more appropriately” considered as formations of a group as defined by Drahovzal and Neathery (1971). For these reasons, the entire carbonate succession between the post-Knox unconformity and the overlying Sequatchie Formation is referred to herein as the Chickamauga Limestone as opposed to using the “supergroup” or “group” nomenclature.

In Floyd County, the Chickamauga Limestone is exposed along an abandoned railroad cut through the southwestern end of Simms Mountain. There, the formation is exposed as massive medium-gray, micritic limestone weathered to pale, bluish gray, in beds 10–25 cm thick and in a 50-cm-thick interval of irregular beds approximately 2 cm thick.

In Chattooga County, the Chickamauga Limestone is exposed on the southeastern flank of Lookout Mountain, in the core of a syncline west of Summerville (east of Lookout Mountain), in a belt on the west side of Taylor Ridge and Simms Mountain, and on the flanks of Kincaid Mountain. On Taylor Ridge, in an abandoned quarry along a hiking trail in Floyd State Park, the formation is exposed as more than 10 m of light-gray and reddish brown micritic limestone in thin beds ranging from less than a centimeter to approximately 20 cm. Some of the beds in this quarry have a waxy sheen.

In Walker County, the Chickamauga Limestone is exposed in the area around Lookout and Pigeon Mountains. Cressler (1964b) described the formation there as flaggy limestone and estimated the thickness to be approximately 425–640 m; this description, however, includes all the rocks between the Knox Group and the Red Mountain Sandstone. On the northwestern flank of Pigeon Mountain near the northeastern end, the Chickamauga Limestone crops out in several locations; this area is likely the type area for parts of the formation. In this area, it is exposed as light-gray, bioclastic packstone intervals in thick beds about 25 cm in thickness or in thin beds about 2–5 cm thick that are interbedded with shale. The formation in this area is also exposed as light- to medium-gray, flaggy, calcareous mudstone interbedded with medium- to dark-gray micritic limestone with some dolomitic laminae. Near the intersection between Lookout Mountain and Pigeon Mountain (Daugherty Gap), the formation is exposed as light- to medium-gray bioclastic packstone with abundant brachiopods. The Chickamauga Limestone also crops out along GA136 west of Maddox Gap. The formation there is medium- to dark-gray, bioclastic packstone that is interbedded with light- to medium-gray micrite and nodular-bedded, light-gray micrite.

3.4.1.1 Attalla Chert Conglomerate Member

The post-Knox unconformity is marked locally by the Attalla Chert Conglomerate Member, which was named by Butts (1910) for exposures near the town of Attalla in

Etowah County, Alabama. The formation generally is comprised of “subangular to rounded pebbles, cobbles, and boulders” of chert and rare quartz and dolostone in a matrix of sand-sized granular chert and quartz (Drahovzal and Neathery, 1971). It is considered the basal member of the Chickamauga Limestone in Alabama by Butts (1910, 1926) and similarly the basal member of the Stones River Group in Alabama (Drahovzal and Neathery, 1971; and Neathery, 1988). Chowns and Carter (1983b), however, refer to the formation as the basal part of the Greensport Formation. The thickness of the Attalla Chert Conglomerate ranges from 0 to about 33 m in Alabama (Drahovzal and Neathery, 1971).

Cressler (1970) identified the Attalla Chert Conglomerate on Horseleg Mountain, where it is approximately 0.2 to 0.6 m thick and composed of round to angular reworked chert clasts from the underlying Knox Group. The clasts range in size from that of a sand grain to about 2 cm in diameter, and are cemented in a matrix of mudstone or limestone. The matrix of the formation on Horseleg Mountain grades upward into overlying red mudstones and red shaly limestones, which are assigned to the Greensport Formation by Chowns and Carter (1983b).

Cressler (1970) found the Attalla Chert Conglomerate to be thick enough to map in only one location in the study area, which is near the southwestern end of Lavender Mountain in Floyd County. The formation is exposed as chert conglomerate of uncertain (but not great) thickness at this locality. In the Floyd County report, Cressler (1970) also mentioned that the Attalla Chert Conglomerate is well developed in southern Chattooga County; the formation is not mentioned, however, in his report for Chattooga County (Cressler 1964a) or shown on the map therein.

During the present study, the Attalla Chert Conglomerate was observed underlying Greensport Formation in northernmost Floyd County (Furnace Valley as labeled by Cressler, 1970) as float beside the road west of Calhoun Gap on Horn Mountain. The formation here is composed of coarse- to very coarse-grained conglomeratic sandstone with clasts of vitreous, sand-sized quartz grains and chert clasts about 1–2 mm in diameter.

3.4.1.2 Pond Spring Formation

The Middle Ordovician Pond Spring Formation was named by Milici and Smith (1969) for exposures near Pond Spring near the town of Chickamauga in Walker County, Georgia. It is a succession dominated by tidal-flat carbonates and red clastic rocks that is 76–92 m thick (Carter and Chowns, 1988). The Pond Spring Formation also includes a basal conglomerate that is generally less than 1 m thick. The conglomerate is comprised of light-gray dolostone pebbles and boulders as large as 0.3 m in diameter in a porous, light-gray or light greenish-gray dolosiltite matrix, which grades upwards into red mudstones and silty limestones (Milici and Smith, 1969). Milici and Smith (1969) included this unit in the Chickamauga Supergroup as the basal formation of their Stones River Group; Carter and Chowns (1988) included the unit as the basal member of their equivalent Stones River Formation of the Chickamauga Group.

According to Chowns *et al.* (1992), a more complete section of the Pond Spring Member can be found in a quarry opened in 1989 (Stone Man Quarry) about 5 km southeast of Graysville in Catoosa County. The formation in the quarry is comprised of three units: a basal multicolored, conglomeratic dolostone; a middle light-gray, micritic limestone; and an upper reddish-gray, bioturbated limestone. The total thickness is estimated to be 59 m (Chowns *et al.*, 1992).

In the Stone Man quarry, the basal dolostone is fine- to coarse-grained, generally gray mottled with red and green, and interbedded locally with red and green clay shales (Chowns *et al.*, 1992). The base of this unit contains angular limestone, dolostone, and chert clasts that are derived from the underlying Mascot Formation, according to Chowns *et al.* (1992). The basal unit varies in thickness, and locally drapes into solution depressions on the post-Knox unconformity; it predominantly consists of “colluvium and paleosols [that] mantle the unconformity” (Chowns *et al.*, 1992).

The overlying middle limestone in the Stone Man quarry is a light-gray, slightly dolomitic, fossiliferous peloidal mudstone or wackestone; the predominant fauna include “ostracods, gastropods, thin-shelled bivalves, and encrusting solenoporoid algae” (Chowns *et al.*, 1992). The unit (primarily in the lower part) includes both “bioturbated subtidal and laminated peritidal facies capped by intraclastic exposure surfaces”; and the upper part is described as shaly and bioturbated, and includes abundant small, knobby

chert nodules. Chowns *et al.* (1992) noted that this unit is lithologically similar to limestones of the upper Knox Group, and thus careful mapping of the unit is necessary.

The upper unit in the quarry is comprised of reddish-gray, bioturbated, shaly limestone that is “interbedded and interburrowed” with red, green, gray, and black shales; it exceeds 30 m in thickness in the cores from the Stone Man quarry (Chowns *et al.*, 1992). The fauna of this unit is similar to that of the underlying limestone, but also includes some trilobites and articulate and inarticulate brachiopods. The unit suggests a “restricted subtidal-lagoonal environment,” and grades upward into “more open-marine gray, shaly, bioturbated limestones” that probably correspond to the base of the overlying Murfreesboro Member of the Stones River Group (Chowns *et al.*, 1992).

3.4.1.3 Correlation of rocks directly above the post-Knox unconformity

Milici and Smith (1969) demonstrated that the difficulty in mapping the post-Knox unconformity has led to inaccuracies that have obscured various stratigraphic relationships and features. For instance, the basal Middle Ordovician rocks rest on different levels of the Knox Group in different places.

Across the region, chert-pebble conglomerates are present in places where the Middle Ordovician rests directly on Mascot Formation, such as around Graysville (Chowns *et al.*, 1992) and Chickamauga (Milici and Smith, 1969). Also, Bridge (1955) noted extensive Middle Ordovician chert and dolostone conglomerate overlying the Mascot Formation to the north in Jefferson County, Tennessee; he also described local collapse structures filled with about 3 to 5 m of dolostone “rubble” in a dolomitic matrix, which grades upward into the conglomerate. According to Chowns *et al.* (1992), such breccias are more common, however, where the Kingsport Formation and Chepultepec Dolomite are both truncated. The authors attributed this to the erosion of these “cherty” formations as a source for the chert pebbles, which they asserted is the origin of the Attalla Chert Conglomerate Member, especially in Alabama. Moreover, Cressler (1970) suggested that the Attalla Chert Conglomerate Member in Georgia is also quite well developed where the Middle Ordovician rests on the very chert-rich Copper Ridge Dolomite in Floyd County. The stratigraphic level of the Knox Group underlying the chert conglomerate in the valley west of Calhoun Gap is not known.

Chowns *et al.* (1992) examined pebbles from both the Pond Spring Formation and the Attalla Chert Conglomerate Member and concluded that, with the exception of some coarse-grained “late diagenetic” dolostones, the “lithologic character of the Knox Group was already established before the Middle Ordovician transgression.” The authors further noted that pebbles of fine- to medium-grained dolostone, chert, and even “agate from silicified paleosols” are present in these rocks (Chowns *et al.*, 1992).

Both the Attalla Chert Conglomerate Member and the Pond Spring Formation have been interpreted to be deposits of “transitional environments during transgression over an eroded karstic surface of Knox Group dolostones” (Carter and Chowns, 1988). Drahovzal and Neathery (1971) illustrated this idea in more detail and mentioned various types of conglomerates that mark the post-Knox unconformity, as well as the ambiguity caused by poor exposure at the unconformity.

The ambiguity about the exact lithology and age of the conglomerates is reiterated by Chowns and Carter (1983b), who noted variable details in chert-clast and dolostone-clast conglomerates over the unconformity; each of these varieties has its own implications for timing of origin. The Middle Ordovician conglomerate facies by nature is not laterally continuous, and also is likely to be of different ages in different locations. Thus, the facies can only be generally correlated in terms of stratigraphic position; no regional detailed correlation is possible or necessary. More importantly, one must consider the nature and paleoenvironment of the unconformity (*i.e.*, length of time of exposure, development of karst topography, formation of soils, *etc.*), as well as the age and lithology (including source of sediment) of the overlying rocks, as the primary factors in the formation of the conglomerate types. Cressler (1970) described the matrix for the Attalla Chert Conglomerate in Floyd County as “identical to material forming the basal bed of the succeeding Middle Ordovician formation,” and this explanation can be applied throughout the area of study. The present study suggests using the Attalla Chert Conglomerate Member nomenclature for the Middle Ordovician conglomerate facies for all locations, regardless of overlying lithofacies, in the interest of convenience of mapping and in stratigraphic description.

In summary, the Attalla Chert Conglomerate Member is a distinctive marker above the post-Knox unconformity, and the amount of clastic detritus that comprises the

unit is thin and laterally variable. The unit is overlain by Middle Ordovician limestones. One notable exception is at Horseleg Mountain, where the lower Middle Ordovician limestone is unconformably absent and the Attalla Chert Conglomerate Member is overlain by the upper Middle Ordovician Greensport Formation redbed succession. There, the Greensport Formation contains clasts that are lithologically similar to those in the underlying Attalla Chert Conglomerate Member.

3.4.2 *Sequatchie Formation*

The Middle to Upper Ordovician Sequatchie Formation was named by Ulrich (1911) for exposures in the Sequatchie Valley in Tennessee, and Milici and Wedow (1977) later assigned the type section of the formation as defined by Ulrich (1911) to an exposure at Hicks Gap in Marion County, Tennessee. The Sequatchie Formation is comprised mainly of red clastic rocks that locally include limestone and gray shale (Carter and Chowns, 1988). Milici and Wedow (1977) also demonstrated that the Sequatchie Formation grades southward into a gray fossiliferous limestone facies in the southern part of the Sequatchie Valley and Lookout Valley in Tennessee; they named this equivalent formation the Shellmound Formation. Chowns (1972) and Rindsberg (1983) proposed subdivisions for the Sequatchie Formation. Rindsberg and Chowns (1986) subdivided the Sequatchie Formation in northwestern Georgia into three named member units (Ringgold, Shellmound, and Mannie Shale Members, in ascending order), and Chowns and Zeigler (1989) added a fourth member on the southeast (Dug Gap Member) that is an equivalent to the upper two members on the northwest.

The base of the Sequatchie Formation has been demonstrated to be time-transgressive (Drahovzal and Neathery, 1971; Carter and Chowns, 1988). Carter and Chowns (1988) noted that in the northwestern outcrops of the formation in Georgia, approximately 92–122 m (on average) of Chickamauga Limestone is present between the T-4 bentonite horizon and the base of the Sequatchie Formation. To the southeast, however, the same bentonite has been placed just below the base of the Sequatchie Formation (Carter and Chowns, 1988).

The Sequatchie Formation is composed of red very fine-grained sandstone, siltstone and shale, which locally includes gray limestone and shale (Carter and Chowns, 1988). Carter and Chowns (1988) estimated a thickness of less than 60 m for the

formation in the northwestern part of the study area. To the southeast, the formation comprises approximately half of the red clastic facies, and thickness ranges from approximately 60 to 120 m (Carter and Chowns, 1988). The Sequatchie Formation thins to the north and west in Georgia (Figure 3-5), and the stratigraphic position atop the Chickamauga Limestone suggests that progradation of clastic sediments from the east stifled carbonate deposition (Carter and Chowns, 1988). The depositional environments indicated by the Sequatchie Formation are related to tidal flats (*cf.* discussion in Chowns and Carter, 1983a); Martin (1992) elaborates on the depositional environments in much more detail.

In Floyd County, the Sequatchie Formation is exposed along an abandoned railroad cut at the southwestern end of Simms Mountain as reddish brown siltstone interbedded with fine- to medium-grained sandstone that is weathered to tan. The beds in these outcrops range in thickness from 0.5–1.0 m. In this outcrop area, the intertonguing with the Chickamauga Limestone can be observed (as demonstrated in Figure 3-5). The formation is also exposed as float in contact with the overlying Red Mountain Formation at the southwestern end of Lavender Mountain, where it is gray, fine-grained sandstone and rusty brown shale weathered to tan. The Sequatchie Formation is also exposed on Horseleg Mountain, where it is gray and dark, rusty red mudstone and tan, thin-bedded siltstone that is interbedded in places with saprolitic, rusty red and yellow shale.

In Chattooga County, the Sequatchie Formation is exposed on Taylor Ridge along a roadcut of US27 and along the road through Hammond Gap east of Trion. Cressler (1964a) described the formation at these locations as approximately 76 m of calcareous shale and fine-grained, thick-bedded, brown sandstone with some quartz conglomerate. In the roadcut along US27, the formation is medium-gray shale weathered to light gray near the top and rusty red, coarse-grained sandstone near the base. At Hammond Gap, the formation is exposed as several meters of massive, reddish brown mudstone interbedded with fine- to medium-grained sandstone in beds ranging from 1 cm to 1 m in thickness and thin, weathered, gray shale.

In Walker County, the Sequatchie Formation is exposed on Taylor Ridge along roadcuts near Maddox Gap and Smith Gap. At Maddox Gap, the formation is exposed as several meters of mostly thick-bedded to massive, gray mudstone and siltstone

interbedded with some thick intervals (1-3 m thick) of dark, rusty reddish-brown, fine- to coarse-grained sandstone in beds about 1 cm to 1 m thick. Some of the mudstone in these outcrops is slightly shaly and some of the sandstone is cemented with calcium carbonate. At Smith Gap, the formation is exposed as approximately 4 m of dark, rusty red mudstone that is slightly shaly in places.

In Gordon County, the Sequatchie Formation is exposed on the western flank of Horn Mountain along the roadcut through Calhoun Gap. In this outcrop, the formation is exposed as weathered maroon shale that is demonstrably stratigraphically higher than the underlying Colvin Mountain Sandstone.

3.4.3 Greensport Formation

The Middle Ordovician Greensport Formation was named by Drahovzal and Neathery (1971) for exposures at Greensport Gap in Etowah County, Alabama. The formation is comprised of red shales that are interbedded with micritic limestone beds that are also generally red and shaly, and red sandstones. Despite the paucity of sedimentary structures and fossils in the Greensport Formation, the red coloration and general lithology suggests that it was deposited in a peritidal environment (Carter and Chowns, 1988). In Floyd County, the Greensport is composed of a lower unit of reddish gray, shaly, micritic limestone, a middle unit of red shale, and an upper unit of interbedded red shale and sandstone (Chowns, 1983a, b, and c; Bayona, 2003). The thickness of the formation is approximately 83 m (Chowns, 1983a).

The Greensport Formation is exposed in Floyd County on Horseleg Mountain and on the western flank of Johns Mountain near Dunaway Gap. At Horseleg Mountain, the formation is exposed as dark, rusty red, fine- to medium-grained sandstone that is weathered to red, yellow and tan and is interbedded with rusty red shale. Near the base, the formation is exposed as rusty red, purple, greenish brown and gray, and bluish gray calcareous siltstone and mudstone interbedded with rusty red shale. These exposures range in thickness from approximately 20 cm to about 5 m.

The Greensport Formation is exposed in Chattooga County in a roadcut on the western flank of Johns Mountain and along the US27 roadcut through Taylor Ridge. At Johns Mountain, the formation is exposed as more than 5 meters of rusty red and brown mudstone with small, green reduction spots in places. Along the US27 roadcut, the

lowermost part of the formation is exposed as over 10 m of rusty red, slightly shaly mudstone and some rusty brown siltstone that is weathered to tan in places. The beds in this outcrop average about 25 cm thick. The upper part of the formation (in contact with the overlying Colvin Mountain Sandstone) is exposed at this location as about 3 m of purplish red mudstone and siltstone interbedded with greenish very fine- to fine-grained sandstone.

In Walker County, the formation is exposed on the flank of Taylor Ridge in a roadcut along GA136 west of Maddox Gap and along the road through Smith Gap. At Maddox Gap, the formation is exposed as approximately 1.5 m of dark, rusty-red mudstone, in beds that are about 5–10 cm thick and are slightly shaly in places; the mudstone is overlain by approximately 0.5 m of rusty red, fine-grained sandstone weathered to brown in beds about 3–5 cm thick. At Smith Gap, the formation is exposed as weathered purple and green mudstone and shale. In Gordon County, the formation is exposed on the western flank of Horn Mountain at Calhoun Gap as saprolitic maroon and yellow shale.

3.4.4 *Colvin Mountain Sandstone*

The Middle Ordovician Colvin Mountain Sandstone was named by Drahovzal and Neathery (1971) for exposures through Colvin Mountain at Alexander Gap in Calhoun County, Alabama, and is comprised of approximately 1–23 m of quartz arenite and conglomerate. The Colvin Mountain Sandstone observed in Georgia has a distinctive yellowish color on some weathered surfaces, and is also weathered to tan and rusty red in places. No body fossils have been found in the formation, but vertical burrows are common in some of the sandstone beds (Drahovzal and Neathery, 1971; Carter and Chowns, 1988). Outcrops of the Colvin Mountain Sandstone invariably include one or two bentonite layers, which have been correlated to the T4 and T3 of Tennessee (Munyan, 1951; Chowns and Carter, 1983a), and thus the formation is likely isochronous with and correlative to the Stones River Group–Nashville Group boundary to the northwest (Carter and Chowns, 1988). Jenkins (1984) cites the common herringbone cross-bedding as an indication that the Colvin Mountain Sandstone was deposited in a wave- or tidal-dominated nearshore environment.

The Colvin Mountain Sandstone is exposed most extensively in the southern part of the study area in Floyd County. Near the southwestern end of Horseleg Mountain in Floyd County, it is white fine- to very coarse-grained (mostly coarse- to very-coarse), quartzose sandstone in beds that range from 5 cm to 1 m thick (most beds greater than 25 cm thick). Locally, the formation contains well defined cross-beds and bi-modal ripple marks; some surfaces are slickensided or have a polished appearance. Gradational upper and lower contacts are apparent in the exposures on Horseleg Mountain. The formation is redder, finer grained, and more thinly bedded in the lower part, where it is interbedded with red shales of the underlying Greensport Formation. Near the top of the formation, it is interbedded with gray shale and brown mudstone presumably of the Sequatchie Formation. At Calhoun Gap on the western flank of Horn Mountain at the Floyd/Gordon County line, it is white coarse- to very-coarse-grained, quartz sandstone that is weathered to yellow and gray in beds that are approximately 50 cm thick.

In Chattooga County, the Colvin Mountain Sandstone is exposed along the US27 roadcut through Taylor Ridge and in a roadcut on the western flank of Johns Mountain. In the Taylor Ridge exposures, the formation is white, medium- to very coarse-grained sandstone and conglomerate that has a yellowish tint on weathered surfaces. Some of the sandstone near the upper and lower contacts is weathered to rusty red and tan. The sandstone is mostly coarse- to very coarse-grained and the blocks in the float range from 3 cm to just under 1 m (most blocks range from 5–25 cm). In the Johns Mountain roadcut near Dunaway Gap, the formation is exposed as yellow and white, medium- to very coarse-grained sandstone that is weathered to tan and gray.

In Walker County, the Colvin Mountain Sandstone is exposed in a roadcut along GA136 west of Maddox Gap, where it is observed in contact with the underlying Greensport Formation. At this location, it is exposed as approximately 3.5 m of brown, medium- to coarse-grained sandstone in beds that range in thickness from 2 cm to about 1 m. The coarse-grained sandstone in this outcrop has a yellowish tint. The formation is also exposed at Smith Gap through Taylor Ridge, where it is dark, rusty red, medium- to coarse-grained sandstone.

One of the only fairly complete sections of the Middle Ordovician red-bed succession in Georgia is at the southwestern end of Horseleg Mountain in Floyd County

(Chowns and Carter, 1983a, c). In the vicinity of Rome, in different places, the Greensport Formation directly overlies the karst surface at the top of the Knox Group or a thin carbonate unit separates the two (Chowns and Carter, 1983b, c). In these localities, Cressler (1970) notes two outcrops that are approximately 180 m apart (that possibly correspond roughly to the outcrops described by Chowns and Carter, 1983b and c) with different lithologies overlying the post-Knox unconformity. At one outcrop, a yellow calcareous mudstone that grades up into red mudstone is present, and can be attributed to the Greensport Formation. At the other outcrop, the basal yellow mudstone is replaced with about 15 m of light- to medium-gray, thick-bedded micrite that is overlain by red mudstone. If this carbonate layer underlying the Greensport Formation mudstones is part of the Chickamauga Supergroup, then perhaps it is a further indication of the extent and nature of the intertonguing between the two lithofacies. Furthermore, Cressler (1970) asserts that the cherty dolostones just below the unconformity belong to the Cambrian Copper Ridge Formation, which would indicate the absence of the entire Lower Ordovician succession.

3.4.5 Alternate nomenclature and interpretations

The Middle Ordovician Moccasin Formation and Middle and Upper Ordovician Bays Formation nomenclature has also been imported from Tennessee for use in Georgia. The Moccasin Limestone was named by Campbell (1894) for exposures along Moccasin Creek in Scott County, Virginia. The formation generally is comprised of red argillaceous limestone that grades upward into the bluish flaggy limestones of the overlying Chickamauga Limestone. Butts (1948) extended the Moccasin Limestone into Georgia as a “red facies” of the Lowville Limestone; this Lowville-Moccasin unit overlies the Lebanon Limestone of the Chickamauga Group or directly overlies the Knox Group where the “Newala and Stones River Group” are absent. Milici (1973) revised the name to Moccasin Formation and included it within the Chickamauga Group as defined in Tennessee (Wilson, 1949).

The Bays Sandstone was named by Keith (1895) for exposures in the Bays Mountains in Hawkins and Greene Counties, Tennessee; the formation is described as red calcareous and argillaceous sandstone in which the calcareous content increases from the

type section southwestward toward Knoxville. Milici (1973) revised the name to Bays Formation within the Chickamauga Group in eastern Tennessee.

The Middle and Upper Ordovician succession is mapped by the Georgia Geological Survey (1976) as part of a Middle and Upper Ordovician undifferentiated unit in places and as Moccasin Limestone–Bays Formation undifferentiated in other places. Both these map units also include rocks of the Sequatchie Formation.

Cressler (1964a, b) mapped the entire Middle and Upper Ordovician succession between the Knox Group and Red Mountain Formation as Chickamauga Limestone in Chattooga and Walker Counties. He divided the Chickamauga Limestone into two facies: a near-shore facies that is composed of approximately 700 m of siltstone and claystone, which is probably the Greensport and Sequatchie Formations, and an off-shore facies that is composed of approximately 425–640 m of flaggy limestone, which is probably the Chickamauga Limestone (Cressler, 1964b). Cressler assigned the Middle and Upper Ordovician succession near Johns Mountain to the near-shore facies and the remaining exposures (farther to the west) to the off-shore facies. Thus, from his location of the near-shore facies and from his lithologic descriptions, one can conclude that the off-shore and near-shore facies he described are a reflection of the northwest-to-southeast, carbonate-to-clastic facies change. The undifferentiated Middle and Upper Ordovician succession of Cressler (1964a, b) reflects the difficulty in defining distinguishable units within the carbonate-to-clastic facies change, in addition to the poor exposure of this succession.

Cressler (1970) mapped the Middle and Upper Ordovician succession as an undifferentiated unit in Floyd County. From his description, however, one can deduce that he designated the Chickamauga Limestone–Greensport Formation–Colvin Mountain Sandstone succession as Murfreesboro, Ridley, and Moccasin Limestones, and labeled rocks of the Sequatchie Formation as Bays Formation. Cressler (1970) described the Murfreesboro Limestone on Horseleg Mountain as calcareous mudstone that is yellow at the base and grades upward through pink and into red flecked with yellow; he also noted that, in a nearby location, the mudstone of the Murfreesboro is replaced by approximately 15 m of limestone. Cressler (1970) did not include any description or much discussion of the Ridley Limestone. The Murfreesboro and Ridley Limestones are formations in the

Chickamauga Supergroup in Georgia as described by Milici and Smith (1969). Carter and Chowns (1988) have since demonstrated the intertonguing of the Chickamauga Limestone carbonates into the Greensport Formation–Colvin Mountain Sandstone succession (see also other discussions in Chowns and Carter, 1983a, and Chowns, 1989). This intertonguing of the facies was noted during the field research of this project at an outcrop along an abandoned railroad cut at Simms Mountain, where micritic limestone of the Chickamauga Limestone is interbedded with brown sandstone that is likely Sequatchie formation.

Similarly, Cressler (1974) assigns the rocks from the Clinchport fault westward to the Kingston fault (predominantly carbonate and red-bed facies) to the Moccasin Limestone, and the rocks to the east of the Clinchport fault (dominated by more clastic facies) to the Bays Formation.

In the more eastern outcrop belt, the lithologic similarities between the upper part of the Greensport Formation and the lower part of the Sequatchie Formation make the identification of the Colvin Mountain Sandstone essential for assigning boundaries. Thus, in the absence of Colvin Mountain Sandstone outcrops, Chowns and Carter (1983) proposed mapping this succession as a single unit, the Bays Formation. For the sake of simplicity, the present study suggests mapping this as Greensport–Colvin Mountain–Sequatchie Formation undifferentiated or as part of a larger undifferentiated Middle and Upper Ordovician succession.

3.5 SILURIAN SYSTEM

The Silurian system in Georgia is comprised entirely by the Lower Silurian Red Mountain Formation, which was named by Smith (1876) for exposures on Red Mountain east of Birmingham, Alabama. The Red Mountain Formation in Georgia was first mapped as Rockwood Formation (*e.g.*, Hayes, 1891; Spencer, 1893), which also included rocks of the Sequatchie Formation (Butts, 1948). Chowns (1972b; 2006), Chowns and McKinney (1980), Rindsberg and Chowns (1986), and Chowns *et al.* (1999) documented more details of the formation. To date, the most comprehensive description of the entire Red Mountain Formation in Georgia is that of Chowns (*in press*). Chowns (2006) noted depositional environments on the basis of three facies categories, which he defined as

outer shelf, inner shelf, and shoreface facies. As defined at present, the formation disconformably overlies the Upper Ordovician succession and disconformably underlies the Devonian succession (Chowns, 1989).

The Red Mountain Formation generally is composed of interbedded, rusty red shale, siltstone, sandstone, and conglomerate that weather to tan and rusty brown. In Floyd County, the formation is composed of a basal succession of massively bedded coarse-grained sandstone and quartz-pebble conglomerate, a middle succession of shale, siltstone, and medium- to coarse-grained sandstone, and an upper succession of interbedded shale, siltstone, and fine-grained sandstone (Cressler, 1970). Bedding thickness in the Red Mountain ranges from less than a centimeter in the shales to approximately 2 m in the massive sandstones and conglomerates. The formation varies in thickness from 75 m near the northwestern corner of Georgia to a maximum of 375 m in the Clinchport thrust sheet (Chowns, 1989). Cressler (1970) estimated the thickness of the formation as approximately 180 to 365 m in Floyd County (1970), approximately 305 m at Taylor Ridge in Chattooga County (1964a), and as approximately 305 m in Walker County (1964b). Rock from this formation has been developed as an important iron ore in Alabama and to a lesser extent in Georgia (Cressler, 1970). The Red Mountain Formation is resistant to weathering and holds up many of the highest topographic features in the study area, including Taylor Ridge, Dick Ridge, and Dirtseller, Horn, Horseleg, Johns, Lavender, Mill, and Simms Mountains. The proportion of shale to sandstone increases to the west, where the Red Mountain outcrops are more associated with low, rolling hills such as Shinbone Ridge.

3.5.1 Lower contact of Red Mountain Formation

Chowns and Carter (1983a) comment on the contact between the Red Mountain Formation and the underlying Sequatchie Formation. In particular, they object to placing the contact at the base of the approximately 30 m thick succession of rusty red, medium- to coarse-grained sandstone and conglomerate, as suggested by Cressler (1970, 1974) at Horn, Johns, Turkey, Turnip, and Heath Mountains. Chowns and Carter (1983a) noted that the Greensport, Colvin Mountain, and Sequatchie Formations include coarse-grained sandstones and assert that this 30-m-thick coarse clastic succession grades downward into the red beds of the Sequatchie Formation as they observed on Rocky Face Mountain at

Dug Gap, and thus should be included with the Upper Ordovician lithofacies. The authors further suggested that this boundary is more correctly placed where the coarse clastic succession is overlain by shales with thin distal turbidite sequences. This interpretation follows the argument for a late Ordovician erosional unconformity (Rindsberg, 1983) followed by a major marine transgression during the early Silurian, during which the Red Mountain Formation was deposited. The prescription of Chowns and Carter (1983) for assigning the Sequatchie Formation–Red Mountain Formation boundary was applied during the field work of the author with limited success. At Hammond Gap east of Trion, the contact between the upper Sequatchie Formation and the lower part of the Red Mountain Formation is clearly gradational, and thus any placement of the boundary would be arbitrary. The succession of coarse sandstone described by Chowns and Carter (1983) can also be observed to grade upwards into rocks that more clearly fit the description of the Red Mountain Formation.

3.6 DEVONIAN SYSTEM

The Devonian system in Georgia is characterized by scattered accumulations of chert and sandstone in the Lower and Middle Devonian succession (Armuchee Chert and Frog Mountain Sandstone formations) overlain by an extensive, but generally thin, accumulation of Upper Devonian black shale (Chattanooga Shale). Ferrill and Thomas (1988) noted that the Chattanooga Shale and the overlying, thin, Lower Mississippian Maury Shale may represent distal synorogenic sediment from Acadian tectonism. Chowns (1989) noted that the Chattanooga Shale represents low sedimentation rates in a broad intracratonic shelf under shallow anoxic water.

Over a large part of the map area, the thin formations that separate the Devonian Armuchee Chert and the Mississippian Fort Payne Chert (*i.e.*, the Devonian Chattanooga Shale and Mississippian Maury Shale) are not well exposed. As a result, the Devonian and Mississippian chert formations are mapped as an undifferentiated unit (*e.g.*, Cressler 1964a, b, 1970).

3.6.1 Lower to Middle Devonian

The Lower and Middle Devonian succession in Georgia is comprised of the Armuchee Chert and the Frog Mountain Sandstone, which primarily appears as a thin

layer within the Armuchee Chert. Nunan (1972) described both of these formations as shallow-marine shelf deposits.

3.6.1.1 Armuchee Chert

The Lower to Middle Devonian Armuchee Chert was named by Hayes (1902) for outcrops near Armuchee in Floyd County, Georgia. The base of the formation is an unconformity and the formation rests on the Red Mountain Formation throughout the extent in the study area. Although unclear, the type section presumably is the extensive exposure along Armuchee Creek where it intersects the end of Lavender Mountain (Cressler, 1970). The Armuchee Chert is composed primarily of white and medium- to dark-gray, thin-bedded to massive chert that weathers to light gray. The chert appears nodular in places and is locally sandy. It is also iron-rich in places, giving the chert a rusty, reddish brown color. Butts (1948) documented a fossil assemblage from the formation that confirms “Onondaga age,” which correlates to the lower part of the Middle Devonian. The Armuchee Chert ranges in thickness from approximately 30 to 45 m in the northern part of Floyd County, and from approximately 15 to 30 m in the central part of the county (Cressler, 1970). The formation forms hogbacks on the flanks of the high ridges on Red Mountain Formation.

In Floyd County, the Armuchee Chert can be identified at various roadcuts through Horseleg, Lavender, Simms, and Turkey Mountains. In two exposures on Horseleg Mountain, only white chert residuum was observed. In outcrops at the northeastern end of Lavender Mountain, the Armuchee Chert is pale- to dark-gray, purplish gray, unevenly bedded chert weathered to brownish-gray/tan and white, locally fossiliferous chert weathered to tan/gray in massive beds approximately 1 m thick or in thin, uneven beds less than about 5 cm thick; and black and tan/gray chert in nodular beds that are generally thinner than about 10 cm, but are as thick as approximately 20 cm. The Armuchee Chert at these outcrops is pervasively fractured and locally stained with iron oxide; the formation there also includes local white, slightly sandy chert. At the southwestern end of Lavender Mountain at the abandoned Central of Georgia Railway cut, the exposure of Armuchee Chert is several meters of white and tan/brown sandy chert and white massive chert that is characterized by some fossiliferous layers (predominantly brachiopods). Approximately 3 km northwest along Lavender Mountain

from the abandoned railroad cut in a roadcut through Fouche Gap, the formation exposed is approximately 0.5 m of white massive chert weathered to tan with a crust of iron oxide on some surfaces. The formation is also in a roadcut on the northeastern end of Simms Mountain, where it is exposed as approximately 2–3 m of white massive chert weathered to tan and rusty brown in wavy beds that range in thickness from 1–10 cm; the formation here is interbedded with weathered, pale gray shale near the contact with the Frog Mountain Sandstone. At the southern end of Turkey Mountain, the formation is irregularly bedded, nodular, massive, white and light-gray chert residuum that is weathered to tan and rusty red. In addition, Chowns (1983) documented Armuchee Chert in a roadcut through the southeastern flank of Turnip Mountain at the southern end of the mountain (GA20 in Floyd County). There, he attributes light-gray, nodular chert float to the formation at the western end of the roadcut.

In Chattooga County, the Armuchee Chert is exposed in the roadcut of US27/GA1 through Taylor Ridge monocline, where it is approximately 5 m exposed of white, massive chert. The formation is also exposed in a cut bank on the Pinhoti Trail on the northwestern flank of Strawberry Mountain anticline, just north of Subligna. There, the Armuchee Chert is white or pale- to medium-gray, chert in nodular beds approximately 5–10 cm thick. Also, on the southeastern flank of Taylor Ridge south of the intersection with Strawberry Mountain, the formation is exposed as white chert blocks in float.

In Walker County, the only outcrops identified are in the GA 136 roadcuts through Taylor Ridge at Maddox Gap and farther east through Dick Ridge. The Maddox Gap exposure is white, grainy or pock-marked chert that is weathered to tan, yellowish tan, and rusty yellowish brown. The Dick Ridge anticline exposure is white, sandy, pock-marked or porous chert that is weathered to yellowish tan.

The Armuchee Chert can be observed in contact with the Red Mountain Formation at a roadcut on the eastern flank of Horn Mountain at Calhoun Gap in Gordon County. There, the exposure is several meters of massive white/pale gray, irregularly bedded or nodular, iron-stained chert that is weathered to tan/brown or a pale purplish-gray in places; the beds generally are about 10 cm thick and are locally pitted or

furrowed. Cressler (1974) estimated the thickness of the formation here to be about 18 m and noted that both the upper and lower contacts can be identified.

3.6.1.2 Frog Mountain Sandstone

The Lower to Middle Devonian Frog Mountain Sandstone was named by Hayes (1894) for exposure on Frog Mountain in Cherokee County, Alabama. In Georgia, the Frog Mountain Sandstone primarily appears to be a clastic tongue extending northeastward into the middle and upper part of the Armuchee Chert (Figure 3-1). Butts (1948) noted “beds of calcareous, fossiliferous sandstone [that] weathers to a friable condition and brown color from the iron oxide present” in the Armuchee Chert exposed at Horseleg Mountain. It is composed of 1.5 to 7.5 m of fine- to medium-grained, light- to medium-gray sandstone (Cressler, 1970). The sandstone can be observed at the Central of Georgia Railway cut at the southeastern end of Lavender Mountain (Floyd County), where it is white, fine- to medium-grained, well-rounded, quartzose sandstone in ledges or boulders approximately 0.5 to 1.0 m thick that are weathered to tan or gray. Butts (1948) noted that the Armuchee Chert at the southwestern end of Lavender Mountain is overlain by approximately 4.5–6.0 m of sandstone that is similar to the Frog Mountain Sandstone. On Taylor Ridge, in a roadcut along GA136 east of Maddox Gap, the formation is exposed as a ledge of rusty yellow and red, fine- to medium-grained sandstone that is approximately 5–10 cm thick and locally contains some coarse grains. Also, on the southeastern flank of Taylor Ridge south of the intersection with Strawberry Mountain, the formation is exposed as irregularly-bedded, light- to medium-gray, fine-grained sandstone that is weathered to yellowish and greenish gray. In most of the outcrops in the central and eastern parts of the study area along Taylor Ridge, Dick Ridge, and Simms Mountain, the Frog Mountain appears in the Armuchee Chert as thin nodular-bedded vitreous rusty red/brown chert. This was described by Cressler as quartzite (1970). This rusty red/brown rock is exposed east of Hammond Gap on Taylor Ridge near where it intersects with Strawberry Mountain, where it is exposed as approximately 2–3 m of dark, rusty reddish brown, vitreous chert in slightly nodular beds that are about 1–3 cm thick. A similar rock is exposed, albeit significantly thinner, on Dick Ridge in a roadcut along GA136 and near the northeastern end of Simms Mountain; the vitreous chert in the Simms Mountain outcrop is dark, purplish red in color. In the

eastern part of the study area, Cressler (1974) noted that the Frog Mountain Sandstone facies is present only in scattered layers of ferruginous sandstone or very sandy chert in the Armuchee Chert, and is feldspathic in places. Thomas and Bayona (2005) noted that the formation is bracketed by unconformities.

3.6.2 Upper Devonian

The Upper Devonian Chattanooga Shale was named by Hayes (1891) for outcrops in Chattanooga, Tennessee. The base of the formation is an unconformity, and the formation rests on Armuchee Chert in the study area. The Chattanooga Shale consists of highly fissile black clay and slightly silty shale with local thin layers of siltstone and fine-grained sandstone; the rocks weather to brown, purplish-brown, or tan (Cressler, 1970). The formation is estimated to be as thick as 15 m near Menlo in Chattooga County (Cressler, 1964a) and perhaps elsewhere in far northwestern Georgia (Thomas and Bayona, 2005), but in thrust sheets to the southeast, the thickness diminishes to about 3 m (*e.g.*, in Floyd County according to Cressler, 1970). Although the thin Chattanooga Shale is poorly exposed apart from large but scattered roadcuts, it is presumed to be present everywhere in northwestern Georgia.

In Floyd County, the Chattanooga Shale is exposed at the northeastern end of Lavender Mountain. In these outcrops, it is black thin-bedded shale and also medium- to dark-gray shale that is interbedded with some silty shale weathered to tan. Also, Chowns (1983) measured approximately 2 m of Chattanooga Shale at the roadcut through the southern end of Turnip Mountain, which he described as black slickensided shale that is weathered to dark brown.

In Chattooga County, the Chattanooga Shale is present in the US27/GA1 roadcut through Taylor Ridge. There it is black shale with some sulfur stains, and Rich (1986a) estimated a thickness of about 9 m. The formation is also exposed in a cut bank on the Pinhoti Trail on the northwestern flank of Strawberry Mountain anticline, just north of Subligna. There, the Chattanooga Shale is black fissile shale weathered to chocolate brown. Thomas (unpublished field notes) measured 21 m of Chattanooga Shale in a roadcut through Shinbone Ridge on GA48 northwest of Menlo. The formation there is black, carbonaceous clay shale that is thinly fissile and is locally crumpled and slickensided, which suggests that the thickness of the formation here is likely a result of

tectonic thickening (Thomas, unpublished field notes). The formation has also been identified in lenticular bodies approximately 1 m long and 0.5 m thick in a chert quarry (Fort Payne Chert) near Silver Hill, but the shale is highly deformed and thickness there is unknown. The Chattanooga Shale is also exposed in some roadcuts farther north across Shinbone Ridge in Chattooga County and into Walker County, where it is exposed as approximately 1-2 m of dark gray or black shale weathered to dark chocolate brown.

In Walker County, Chattanooga Shale outcrops are also identified in the GA 136 roadcuts through Taylor Ridge at Maddox Gap and farther east through Dick Ridge. The Maddox Gap exposure is approximately 3 m of black shale that is weathered to chocolate brown. The Dick Ridge anticline exposure is black shale that is weathered to chocolate brown and purple in places; near the base of this exposure is approximately .25 m of light- to medium-gray, fine-grained sandstone that is weathered to greenish tan.

Most of the Chattanooga Shale exposed in the study area is deformed, and some has a carbonaceous, coaly sheen in appearance. For example, the formation has been identified in lenticular bodies approximately 1 m long and 0.5 m thick in a chert quarry (Fort Payne Chert) near the southwestern end of Simms Mountain at Silver Hill in Chattooga County, but the shale is highly deformed and thickness there is unknown. Similarly, the lens-shaped Chattanooga Shale bodies crop out in a quarry in northwestern corner of Gordon County, east of Horn Mountain near the Rome fault. There, the formation is exposed in lenticular forms (as seen in the chert pit near Silver Hill) that are as thick as 1 m. In a low roadcut near the northeastern end of Simms Mountain in Floyd County, the residuum of Chattanooga Shale is exposed as small chips of coal-like black shale. Similar chips of black shale with a coaly luster are exposed in a roadcut at the northeastern end of Strawberry Mountain near the intersection with Dick Ridge in Walker County.

3.7 MISSISSIPPIAN SYSTEM

The Lower and Middle Mississippian System in Georgia is distinctly marked by the laterally extensive Fort Payne Chert at the base, and the overlying succession is characterized by a regional-scale lithofacies change directed from dominantly carbonate on the northwest toward dominantly clastic on the southeast (Figure 3-7). The

Mississippian System in Georgia was first subdivided by Hayes (1891), and complete details of nomenclature evolution are described by Thomas (1979). Thomas (1979) remains the most comprehensive description of the Mississippian System in Georgia to date, and summarizes details of biostratigraphy and paleoecology, depositional and tectonic frameworks, and stratigraphic correlations to the Mississippian System in Alabama (a subject on which he is not just an expert, but also the damn king). Rich (1986b) summarized the Mississippian succession in Georgia, but utilized different correlations and subdivisions (Figure 3-8).

The Mississippian stratigraphy above the Fort Payne Chert generally can be subdivided into a northwestern carbonate facies and a southeastern clastic facies (Figure 3-7), both of which grade upward into the Pennsylvanian clastic succession of fine clastic rocks to massive sandstones (Thomas and Cramer, 1979). The carbonate facies is composed of high-energy shallow-marine limestones; the clastic facies is characterized by prodelta mud with lesser amounts of pro-delta sands. The clastic facies (essentially the Floyd Shale and Pennington Formation) progrades westward and intertongues with the carbonate facies (Monteagle and Bangor Limestones) toward the northwest (Thomas and Bayona, 2005). Similarly, Cressler (1964a, b) subdivides the Mississippian system in Chattooga and Walker Counties into two coeval facies. The eastern facies, which Cressler (1964a, b) assigned to the Floyd Shale, is exposed in a broad belt from the base of Taylor Ridge eastward to the Rome fault; this area also includes part of Floyd County. The thickness of the Mississippian succession east of Taylor Ridge at Little Sand Mountain is nearly 500 m (Thomas, 1979). The western facies, which is exposed on the southeastern flank of Lookout and Pigeon Mountains, is composed of approximately 245 m of limestone (corresponds to Monteagle and Bangor Limestones in ascending order) overlain by at least 60 m of shale (corresponds to Pennington Formation). The northwest-to-southeast change from thin, shallow-water shelf facies to thick, prograding clastic facies demonstrated by Thomas (1979) was interpreted by Rich (1992) to indicate late Paleozoic reactivation of down-to-southeast, steep basement faults.

Rich (1986b) estimated the thickness of the Mississippian system to be approximately 365 m in the northwest at Lookout and Pigeon Mountains; he estimated about 880 m to the southeast at Rock Mountain (Figure 3-8). The uppermost part of the

rocks he assigned to Pennington Formation, however, has been interpreted alternatively to be the lower part of the Upper Mississippian to Lower Pennsylvanian Raccoon Mountain Formation (McLemore, 1971; Thomas, 1979). Thus, these thickness values should be reduced, especially for the southeast facies where the Raccoon Mountain Formation is significantly thicker. Furthermore, the thickness of the Bangor Limestone in the interpretation of Rich (1986b) is estimated as approximately 50 m in the northwest and approximately 180 m in the southeast (Figure 3-8). This interpretation involves his correlation of the entire upper clastic unit of the Floyd Shale with the “Hartselle” interval that he used to mark the base of the Bangor Limestone, and thus all Monteagle Limestone equivalents are placed in the middle and/or lower units of the Floyd Shale. These correlations using sparse data are uncertain, and as such, the author prefers to map the Monteagle and Bangor Limestones as a single undifferentiated unit in the northwest and to not make any specific correlations to any part of the Floyd Shale as shown by Thomas (1979).

Thickness data for the southeastern clastic facies are sparse because of poor exposure (Thomas, 1979). Thomas (1979) estimated a thickness range of 360 to 460 m for the northwestern facies and a maximum thickness of 775 m for the southeastern facies in the Floyd synclinorium.

3.7.1 Lower Mississippian

3.7.1.1 Maury Shale

The Lower Mississippian Maury Shale was named by Safford and Killebrew (1900) for exposures in Maury County, Tennessee, and the type section is described in detail by Hass (1956). The Maury Shale is presumed to conformably overlie the Chattanooga Shale. The formation is considered only as an upper member of, or simply part of, the Chattanooga Shale by Butts (1948), Cressler (1963, 1964b, 1970, 1974), and Croft (1964). Cressler (1964a) did not report any Maury Shale lithotype in Chattooga County, but noted that the top of the Chattanooga Shale succession, where exposed, is usually covered by residuum from the overlying Fort Payne Chert. The Maury Shale is characterized by thin, greenish-gray glauconitic shale that is generally about 1 m thick, and commonly includes small phosphatic nodules (Thomas, 1979); it is laterally extensive and is a distinct marker horizon in the stratigraphy. Butts (1948) described the

upper part of the Chattanooga Shale (for which he mentioned possible correlation to the Maury Shale of Tennessee) as less than a meter of greenish clay with black nodules that are approximately 2 cm in diameter; he further noted that the nodules are presumably phosphatic. Thomas and Bayona (2005) noted that the Maury Shale is unconformably absent in many locations; the present research, however, has identified the formation at most of the few locations where the Chattanooga Shale is well exposed.

The formation can be identified at roadcuts on US27 through Taylor Ridge, where it is approximately 0.5 m of greenish gray shale with abundant concentric phosphate nodules that are less than about 1 cm in diameter. Rich (1986a) reported a thickness of about 1.2 m at this location. Thomas (unpublished field notes) measured 1.3 m of Maury Shale in a roadcut through Shinbone Ridge on GA48 northwest of Menlo in Chattooga County. The formation there is medium-gray and greenish-gray clay shale that is mottled green in places; part of the formation there is fissile and blocky (Thomas, unpublished field notes). The Maury Shale is also exposed in some roadcuts farther north across Shinbone Ridge in Chattooga and Walker Counties, where it is exposed as approximately 1 m of greenish gray, saprolitic shale weathered to tan or pale gray, with some phosphate nodules with diameters less than about 2 cm. Cressler (1970, 1974) reported nodules ranging from 0.5 to 15.0 cm in diameter, although 1–2 cm is more typical.

In a cut bank on the northwestern flank of Strawberry Mountain north of Subligna, the formation is exposed as faintly bluish, green-gray saprolitic shale. Chowns (1983) measured nearly 2 m of greenish gray clay shale at the roadcut through Turnip Mountain, which he attributed to the Maury Shale.

In Walker County, Maury Shale outcrops are also identified in the GA 136 roadcuts through Taylor Ridge at Maddox Gap and farther east through Dick Ridge. The Maddox Gap exposure is approximately 1 m of greenish shale that is weathered to tan with phosphate nodules less than about 1 cm in diameter. The Dick Ridge exposure is greenish gray shale that is weathered to tan with chalky white phosphate nodules that are about 1 cm or less in diameter.

In Walker County, Cressler (1964b) reported approximately 0.30–0.75 m of greenish clay shale with phosphatic nodules approximately 1.25–5.00 cm in diameter. In Floyd, Gordon, and Murray Counties, Cressler (1970, 1974) reported approximately

0.30–0.75 m of greenish clay shale with phosphatic nodules ranging from approximately 0.65 to 15.25 cm in diameter.

Incidentally, Cressler (1964a) did not recognize either Armuchee Chert or Maury Shale at the outcrop areas in Chattooga County (Taylor Ridge and Shinbone Ridge). If he included the Armuchee Chert with the overlying Fort Payne Chert, it is not apparent from his description.

3.7.1.2 Fort Payne Chert

The Lower to Middle Mississippian Fort Payne Chert was named by Smith (1890) for exposures in Fort Payne, Alabama. Presumably, the Fort Payne Chert conformably overlies the Maury Shale in the area of study, and the formation is a distinctive marker in the Paleozoic succession of Georgia. The Fort Payne Chert generally is characterized by light-gray or white chert in nodules or in irregular beds that are typically less than 25 cm thick; in Georgia, the thickness of the formation exceeds 60 m. Cherty dolostone and cherty limestone comprise a significant part of the formation (McLemore, 1971). Small quartz geodes (approximately 1–7 cm in diameter) are common in the formation, but are more abundant near the base (Cressler, 1964b); the geodes contain relict anhydrite crystals that are replaced by quartz and calcite (Chowns, 1972c). Weathered outcrops of the Fort Payne Chert commonly are littered with molds or silicified parts of echinoderm columnals and other fossils (pelmatozoans according to Rich, 1986b). Thomas (1979) stated that the formation is the weathering product of siliceous carbonates, during which the resistant silica was concentrated. Rich (1986b) noted that cores through the formation demonstrate “siliceous carbonate rock in chert nodules,” but that such subsurface samples are not as silica-rich as surface exposures. East of Pigeon Mountain, the formation evidently intertongues with and grades laterally into the Lavender Shale Member (Figure 3-1).

Rich (1986b) noted that the formation crops out in many places as a “resistant cap on dip slopes underlain by the Red Mountain Formation”; Shinbone Ridge is the most prominent example of such a ridge. Thomas (unpublished field notes) measured 29 m of Fort Payne Chert exposed in a roadcut through Shinbone Ridge on GA48 northwest of Menlo. The formation there is light-gray chert in beds approximately 0.3 m thick that are

nodular in places and characterized by clay partings; the lower 3 m is composed of dark gray chert (Thomas, unpublished field notes).

The Fort Payne Chert in Floyd County is composed of approximately 60 m of thin- and thick-bedded chert (Cressler, 1970) and is exposed at Turnip and Simms Mountains. Chowns (1983) measured approximately 4.5 m of Fort Payne Chert beneath the Lavender Shale Member at the GA20 roadcut through Turnip Mountain in Floyd County, which he described as dark gray thinly bedded (beds 3–15 cm thick) slightly nodular chert with shaly partings. At the northeastern end of Simms Mountain, the formation is exposed as approximately 6 m of white and gray chert weathered to tan in beds that are about 10 cm thick.

The Fort Payne Chert is well exposed on the flanks of Strawberry Mountain, on Taylor Ridge, and on Shinbone Ridge in Chattooga County. On Strawberry Mountain, the formation is exposed as white, nodular bedded chert that locally includes pale grayish purple geodes. At the Taylor Ridge roadcut along US27, the formation is comprised of about 45 m of gray-black, evenly bedded chert (beds 5–30 cm thick) that is dense and brittle (Cressler, 1964a). Farther southwest along Taylor Ridge near the intersection with Simms Mountain, the formation is exposed in an abandoned quarry, where it is light- to medium-gray dense chert in nodular beds that range 1–10 cm in thickness with some shaly partings. Total thickness of the Fort Payne is questionable in the quarry because of pervasive deformation. On Shinbone Ridge, the formation is exposed as white massive chert weathered to rusty brown and tan that is locally sandy and in beds that range 2–25 cm in thickness. In an abandoned quarry in Shinbone Ridge near Menlo, the formation is exposed as approximately 0.5 m of white, massive, irregularly or slightly nodular-bedded chert in beds about 5 cm thick. This chert exposure is overlain by approximately 10 m of red clay and saprolitic chert.

In Walker County, the formation is exposed on Pigeon Mountain, Dick Ridge, Shinbone Ridge, and Taylor Ridge, and is nearly 50 m thick (Thomas, 1979). The Fort Payne Chert there is composed of “stratified chert and dark compact calcareous shale or argillaceous limestone,” the latter of which can be attributed to the Lavender Shale Member. The beds range from 5 to 30 cm and the bedding surfaces are irregularly furrowed and, thus, the contacts appear uneven (Cressler, 1964b). In a roadcut along

GA193 across Pigeon Mountain, the formation is exposed as more than 10 m of massive, pale gray chert in beds and some nodules that range 5–25 cm in thickness. In Dick Ridge anticline near the intersection with Strawberry Mountain, the Fort Payne Chert is exposed as white, gray, and brown, deformed chert that is weathered to rusty red, yellow, and brown in places in thin, wavy or nodular beds. On Shinbone Ridge, the formation is exposed as massive, white chert weathered to rusty brown and tan in beds 2–25 cm thick. In a roadcut along GA136 across Taylor Ridge monocline near Maddox Gap, the formation is exposed as approximately 2 m of white chert weathered to tan with some rusty red and brown in wavy, irregular and nodular beds and nodules about 5–10 cm thick.

3.7.1.3 Lavender Shale Member of the Fort Payne Chert

The Lavender Shale Member of the Fort Payne Chert was named by Butts (1948) for roadcuts along the Central of Georgia Railway at the southwestern end of Lavender Mountain (approximately 0.6 km west of Lavender Station) in Floyd County, Georgia. The Lavender Shale Member is comprised of dark-gray, calcareous shale and argillaceous mudstone that weathers to “light-gray, greenish-gray, and yellowish-gray shale and mudstone” (Thomas, 1979). According to Cressler (1970), the formation at the type locality consists primarily of massive-bedded greenish-gray mudstone and shale, and also contains fossils including bryozoa and abundant crinoid columnals that are a centimeter or greater in diameter (*cf.* also Butts, 1948). Petrographic research by Hurst (1953) demonstrated that unweathered samples of typical Lavender Shale may contain as much as 75% carbonate and that it is more of a mudstone than a shale. The argillaceous and siliceous character observed at most exposures is thus likely to be a product of weathering (Rich, 1986b).

Thomas (1979) noted that the Lavender Shale does not constitute an individual unit; Cressler (1970) stated that rocks of the Lavender lithotype are distributed randomly within the Fort Payne Chert. The Lavender Shale also contains discontinuous chert beds. The formation possibly represents an easterly, more argillaceous facies of the Fort Payne Chert (Figure 3-1; *cf.* also Cressler, 1970; Thomas, 1979). Hurst (1953) noted a reciprocal relationship between the Fort Payne Chert and the Lavender Shale; the thickness of the Lavender Shale increases eastward in concert with the decrease in the

thickness of the more typical Fort Payne Chert lithotype. The Fort Payne Chert contains little argillaceous rock west of the Kingston–Chattooga anticlinorium, but is mostly replaced by Lavender Shale to the east of the anticlinorium (Figure 3-1). Thomas (1979) estimated the facies boundary between the Lavender Shale and the Fort Payne Chert to be a “very irregular north-trending line” through the Floyd synclinorium.

Near the depression of the Floyd synclinorium just northwest of Horseleg Mountain, the Lavender Shale Member is approximately 80 m thick (*cf.* Thomas, 1979). Thomas (1979) noted that it is not clear whether the top of the Lavender Shale Member is equivalent to the top of the Fort Payne Chert or whether the formation also includes equivalents of younger rocks.

In Floyd County, the Lavender Shale Member is exposed on the flanks of Turnip, Lavender, Turkey, and Simms Mountains. Chowns (1983) noted an incomplete section of the Lavender Shale Member at the GA20 roadcut through Turnip Mountain. At the eastern end of this roadcut, he attributed approximately 20 m (exposed) of gray to reddish gray weathered shales to the formation. At the northeastern end of Lavender Mountain, the formation is exposed as medium- to dark-gray calcareous shale that is weathered to light gray. At the southwestern end of Lavender Mountain, the formation is exposed as dark-gray to black, fossiliferous, calcareous shale that is interbedded with some dark chert. The formation is also exposed in roadcuts along GA140 through the southern end of Turkey Mountain. There, the Lavender Shale is exposed as approximately 10–20 m of massive-bedded, dark-gray shale and mudstone weathered to black and medium gray interbedded with some nodular-bedded light-gray chert. At the northeastern end of Simms Mountain, the formation is exposed as dark-gray, calcareous mudstone and shale in thin wavy beds that are generally less than 2 cm thick and in thick, blocky beds ranging 5–50 cm in thickness. These outcrops are a meter or more in total thickness and include local stringers and thin beds of black chert that is waxy in appearance and ranges 1–10 cm in thickness.

In Chattooga County, the Lavender Shale Member is exposed around Strawberry Mountain and Taylor Ridge. On the northwestern flank of Strawberry Mountain north of Subligna, the Lavender Shale is exposed as medium- to dark-gray mudstone weathered to pale gray in irregular or nodular beds. In the roadcut along US27 through Taylor Ridge,

the formation is exposed as more than 10 m of black and dark gray, siliceous mudstone in irregular or nodular beds that range from 5–10 cm in thickness. The mudstone is interbedded with dark gray shale in beds that are 1–3 cm thick.

In Walker County, the Lavender Shale Member is exposed around Dick Ridge. In the roadcut along GA136 through Dick Ridge, the formation is exposed as dark gray and black mudstone and chert weathered to purplish gray in nodular beds that are about 3–10 cm thick. Near the intersection between Dick Ridge anticline and Taylor Ridge monocline, the formation is exposed as approximately 4 m of black and dark gray chert and siliceous mudstone weathered to tan, medium gray, and white, in nodular beds that are about 1–3 cm thick.

3.7.2 Upper Mississippian northwestern carbonate facies

The northwestern carbonate facies of the Upper Mississippian succession (Figures 3-1, 3-7, and 3-8) can be divided into three successive subunits (Thomas, 1979). The basal unit is comprised of bedded chert and cherty carbonate rocks (Fort Payne Chert and Tuscumbia Limestone). The middle unit, which is the thickest, consists predominately of non-cherty limestone (Monteagle-Bangor Limestones). The uppermost unit is comprised of maroon, green, and gray mudstones and shales; and the mudstone/shale succession at the top grades upward into the shale, sandstone, and coal succession of the Lower Pennsylvanian (Pennington and Raccoon Mountain Formations).

Thomas and Bayona (2005) noted that the Fort Payne Chert and Tuscumbia Limestone represent the “last stage of passive-margin shelf deposition before the initial progradation of synorogenic clastic deposits from the Ouachita orogen into western Alabama and from the Alleghanian Appalachian orogen into northeastern Georgia” (*cf.* Thomas, 1974).

3.7.2.1 Tuscumbia Limestone

The Middle Mississippian Tuscumbia Limestone was named by Smith (1894) for exposures near the town of Tuscumbia in Colbert County, Alabama. It is composed of light-gray, medium- to thick-bedded bioclastic or micritic limestone with some beds that are partly oolitic. The Tuscumbia Limestone is distinguished by locally abundant light-gray or white chert nodules and concentrically banded chert concretions, but these chert-rich layers are not laterally continuous and thus do not serve as persistent marker beds

(Thomas, 1972). The formation commonly also contains beds of calcareous mudstone and finely crystalline dolostone; calcite pseudomorphs after gypsum are locally present in the dolomitic mudstones (McLemore, 1971). Thomas (1979) also noted rare argillaceous limestone and thinly bedded calcareous shale. The formation ranges in thickness from 35 to 65 m (Thomas, 1979); Rich (1986b) estimated approximately 61 m in thickness.

The upper and lower contacts of the Tuscumbia Limestone are gradational. The nodular chert of the Tuscumbia Limestone, however, contrasts with the bedded chert of the underlying Fort Payne Chert. The contact with the overlying Monteagle Limestone is characterized by a regional gradation from cherty limestone to predominantly non-cherty, oolitic limestone (Thomas, 1979). The contact is arbitrarily placed by McLemore (1971) above the highest cherty calcareous mudstone and below the lowest oolitic limestone of a considerable thickness. Thomas (1979), however, stated that thin cherty limestone commonly is present above this arbitrary contact, as are thin oolitic limestone beds below this “contact” in the Tuscumbia Limestone; thus, this contact as defined may not be extensively functional for detailed mapping.

The Tuscumbia Limestone in northwestern Georgia is restricted to the flanks of Lookout and Pigeon Mountains. The formation is mapped there as St. Louis Limestone by Croft (1964) in Dade County and Cressler (1964b) in Walker County, and by the Georgia Geological Survey (1976), using the nomenclature of Butts (1926, 1948). In McLemore Cove, near the intersection of Pigeon and Lookout Mountains (Walker County), the Tuscumbia Limestone is about 10 m exposed of light- to medium-gray, fine-crystalline grainstone and bioclastic packstone in beds approximately 0.2–0.5 m thick. The outcrop includes abundant brachiopod and bryozoa fossils in some layers. Dark-gray chert is also abundant in the exposure in nodules that are approximately 2–10 cm in diameter and in beds about 5 cm thick. In a roadcut of GA 193 on Pigeon Mountain in Walker County, the formation is about 1 m exposed of bluish-gray, massive micrite with abundant chert nodules; the limestone is underlain by light-gray chert residuum that is weathered to tan and white.

3.7.2.2 Monteagle–Bangor Limestones undifferentiated

The Upper Mississippian Monteagle Limestone was named for a section near the town of Monteagle in Franklin, Grundy, and Marion Counties, Tennessee. The name was

first proposed in a dissertation by Vail (1959) and first published by Peterson (1962); the type section was established by Stearns (1963). The Monteagle Limestone is generally characterized by light-gray, cross-bedded oolitic limestone in massive beds that are commonly greater than 3 m, with thick interbeds of bioclastic limestone (Thomas, 1972). The contact between the Monteagle Limestone and the overlying Bangor Limestone is clearly defined in Alabama by the intervening Hartselle Sandstone; the Hartselle Sandstone, however, pinches out eastward and does not continue into Georgia (*cf.* discussion of intervening Hartselle Sandstone and Pride Mountain Formation in Thomas, 1972). Rich (1986b) noted an argillaceous unit approximately 10.5 m thick at about the same stratigraphic level as the Hartselle Sandstone. Actual correlation to the Hartselle Sandstone has not been documented, and Thomas (1979) discussed difficulty in reliable tracing of the argillaceous limestone interval. Thomas also found additional argillaceous layers lower in the stratigraphy in other locations (personal communication, 2010); one of these layers is described by Thomas (1972) in his discussion of the Monteagle Limestone. As a result, the two limestone formations are mapped as Monteagle-Bangor Limestones undifferentiated in northwestern Georgia on the flanks of Lookout and Pigeon Mountains in Dade and Walker Counties (Figures 3-1 and 3-7). Croft (1964), Cressler (1964a, b), and the Georgia Geological Survey (1976) mapped the limestones as divided into Ste. Genevieve Limestone, Gasper Limestone, Golconda Formation, Hartselle Sandstone and Bangor Limestone, using the nomenclature of Butts (1926) for northeastern Alabama and Butts (1948) for northwestern Georgia. Croft (1964), however, notes that these formations are “lithologically similar and difficult to map separately” in Dade County.

The Upper Mississippian Bangor Limestone was named by Smith (1890) for exposures in the town of Bangor in Blount County, Alabama, and originally included all Mississippian rocks above the Fort Payne Chert. The Bangor Limestone is characterized by medium-gray, medium-bedded mainly bioclastic and oolitic limestone that includes local micrite, shaly argillaceous limestone, calcareous clay shale, and earthy dolostone; the upper part of the formation also includes interbeds of dusky-red and olive-green blocky mudstone (Thomas, 1972). Butts (1926) restricted the Bangor to carbonate rocks above the Hartselle Sandstone Member of the Floyd Shale and below the Pennington Shale.

The Monteagle–Bangor succession ranges in thickness from 135 to 275 m, and is mainly comprised of light-gray, massive beds of oolitic and bioclastic limestone with scattered, thin intervals of chert (Thomas, 1979). Cross-bedding is common in the thick oolitic limestone beds. Thin beds of dolostone comprise a small part of the succession, and gypsum crystals are very rare in the dolostone (only seen in core samples). Thin chert intervals throughout the formation contain scattered nodules; some of the intervals are laterally persistent over short distances, but none are sufficiently extensive to be used as stratigraphic markers (Thomas, 1979). Rich (1986b) noted that the Monteagle–Bangor succession is also characterized by ooid and skeletal grainstones. In the Bangor Limestone along Pigeon and Lookout Mountains, conspicuous shoaling-upward sequences capped by ooid grainstones have been documented (Rich, 1984, 1986c; Algeo, 1985).

The Monteagle–Bangor succession also includes a few beds of argillaceous limestone and calcareous shale; the shaly layers are generally less than 10 m thick and are randomly distributed throughout the succession (Thomas, 1979). Some of the shale intervals in the upper part of the succession include thin sandstone beds (Thomas, 1979). Two shaly units in the lower part of the succession (correlative to the Monteagle Limestone) can be traced for more than 25 km along Pigeon Mountain; most of the shaly intervals in the Monteagle–Bangor Limestones, however, have limited lateral extent in Georgia (Thomas, 1979). Intervals of gray calcareous shale interbedded with maroon and green mudstone characterize the top of the succession where the Monteagle–Bangor Limestones succession grades upward into the Pennington Formation (Thomas, 1979).

In McLemore Cove, near the intersection of Pigeon and Lookout Mountains (Walker County), the Monteagle–Bangor Limestones succession is about 6–7 m exposed of dark-gray, bioclastic packstone and some bioclastic wackestone in beds approximately 0.5–3.0 m thick. The outcrop includes some large calcite crystals in the wackestone layers. Farther upsection, the outcrop consists of about 3–4 m exposed of medium-gray, massive ooid grainstone in a micritic matrix; the grainstone is crossbedded in places and contains some concentric ooids. In a GA136 roadcut on the southeastern flank of Lookout Mountain in Walker County, the formation is about 4–5 m exposed of medium-gray, massive bioclastic packstone in beds approximately 0.5–1.0 m thick; the packstone

is interbedded with some intervals of calcareous shale that are 5–10 cm thick. Farther upsection, the outcrop consists of dark-gray bioclastic wackestone in beds approximately 0.25–1.00 m thick; fresh surfaces of the wackestone have an asphaltic odor.

3.7.2.3 Pennington and Raccoon Mountain Formations

The Upper Mississippian Pennington Formation was named by Campbell (1893) for exposures near Pennington Gap in Lee County, Virginia. The Pennington Formation above the northwestern carbonate facies rests gradationally on the Monteagle-Bangor Limestones. The lower part of the formation is comprised of maroon and green shale and mudstone that weathers to yellow-brown and coarsens upwards into dark-gray shale, siltstone, and fine-grained sandstone. The dark-colored sandy upper part of the facies presumably corresponds to part of the overlying Raccoon Mountain Formation (*cf.* Culbertson, 1963; McLemore, 1971; Thomas, 1979). The formation is characterized by abundant impressions of fenestrate bryozoa (Thomas, 1979). In northeastern Alabama and southern Tennessee, the base of the Pennington Formation is marked by a distinctive dolostone interval; although dolostone beds are present in the upper part of the Bangor Limestone in Georgia, the marker unit has not been identified (Thomas, 1979). Rich (1986b) noted a unit of skeletal limestone approximately 2.5 m thick at the base of the formation.

The Upper Mississippian-Lower Pennsylvanian Raccoon Mountain Formation was named by Wilson *et al.* (1956) for exposures on Raccoon Mountain near Whiteside, Tennessee, just north of the Georgia state line. The formation is the basal member of the Gizzard Group (*cf.* discussion in section 3.8). The Raccoon Mountain Formation above the northwestern carbonate facies is characterized by dark-gray shale, siltstone, fine-grained sandstone, and some coal; the sandstone beds are laterally discontinuous, and siderite nodules are common in the shaly intervals (Thomas, 1979). Several coal beds are documented in the formation on Sand Mountain near the northwestern corner of Georgia (Thomas, 1979). The formation also contains local maroon mudstone beds like the underlying Pennington Formation (Thomas, 1979). The contact between the Pennington and Raccoon Mountain Formations is “within a gradational [succession] that includes a variety of vertical arrangements of rock types” (Thomas, 1979). To the northeast in Tennessee, however, Milici (1974) documented that the basal sandstone of the Raccoon

Mountain Formation rests on a scoured surface. According to the Tennessee Division of Geology, the base of the Raccoon Mountain Formation is defined by the top of the highest limestone or maroon or green mudstone (Milici, 1974). The Raccoon Mountain Formation is overlain by a distinctive sandstone-conglomerate unit of the Lower Pennsylvanian succession, the Warren Point Sandstone of Culbertson (1963), *etc.*, and the “bluff-forming” unit of Cramer (1979).

In the northwestern part of the study area around Lookout and Pigeon Mountains, the Pennington–Raccoon Mountain succession is mapped together because of a lack of a consistently mappable contact (*cf.* Thomas, 1979). Farther to the southeast, the two formations are separated by a sandstone unit. Thomas (1979) noted that the thickness of the Pennington–Raccoon Mountain succession in the northwestern carbonate facies of the Upper Mississippian ranges from 65 to 130 m.

Along a GA 48 roadcut on the southeastern flank of Lookout Mountain in Walker County, a few outcrops of the Pennington–Raccoon Mountain succession are exposed. The lowermost is about 4–5 m exposed of yellowish-tan, slightly shaly claystone and siltstone in beds about 0.5–5.0 cm thick, which is weathered to white and rusty red. The next outcrop upsection consists of approximately 10 m exposed of medium-gray shale and thin siltstone beds (about 2 cm thick), weathered to dark gray, yellowish brown, and dark brown. Farther upsection, the formation consists of approximately 6–7 m exposed of deeply-weathered, yellowish-tan shale. Farther still upsection, the formation consists of approximately 6–7 m exposed of tan/brown, fine- to medium-grained sandstone in beds about 5–25 cm thick. Near the top of the succession (underlying about 2–3 m of covered interval below the base of the overlying Pennsylvanian sandstone), the formation is comprised by approximately 3 m of brown fine- to medium-grained sandstone in beds that generally are about 1–5 cm thick, but a few are as thick as 10 cm. The upper 2 m of this interval is interbedded with some shale.

Northeastward along the southeastern flank of Lookout Mountain in Walker County, a few outcrops of the Pennington–Raccoon Mountain succession are exposed in a GA136 roadcut. The lowermost is about 6 m exposed of massive, meter-thick ledges of yellowish-tan, finely-laminated, calcareous mudstone interbedded with some shale. The top of the succession (just below the contact with the overlying Pennsylvanian sandstone)

consists of approximately 5 m exposed of gray shale weathered to tan, white, and rusty red.

3.7.3 Upper Mississippian southeastern clastic facies

The southeastern clastic facies of the Mississippian succession in Georgia is dominated by shale, but also includes sandstone (Figures 3-1 and 3-7). The lower part of the clastic facies also includes bedded chert that is similar to that near the base of the carbonate facies to the northwest (nodular chert in the lower limestone of the Floyd Shale). The clastic facies contains interbeds of limestone that are similar to that in the middle of the carbonate facies.

The base of the southeastern clastic facies is comprised of the Fort Payne Chert and/or the Lavender Shale Member. The Floyd Shale overlies this interval and is characterized by a thick limestone unit at the base and a thick sandstone unit at the top. The Bangor Limestone tongue overlies the Floyd Shale, and is distinguished by a thick terrigenous unit in the middle. The overlying shale and sandstone succession of the Pennington and Raccoon Formations is similar to that in the northwestern carbonate facies, except that the two formations are separated by a distinctive sandstone unit (*cf.* interpretation of McLemore, 1971; Thomas, 1979). The upward gradation into the Lower Pennsylvanian succession is also similar to that in the northwestern carbonate facies. Incidentally, the Georgia Geological Survey (1976) mapped the entire Upper Mississippian succession east of Taylor Ridge between the Fort Payne Chert and the lowermost sandstone intervals on Rock and Little Sand Mountains as Floyd Shale (presumably following Butts, 1948).

Comparatively complete sections of the southeastern clastic facies have been documented at Little Sand Mountain (*e.g.*, McLemore, 1971; Thomas, 1979) and at Rock Mountain (*e.g.*, Thomas, 1979; Grainger, 1983; Rich, 1986b). Details of the section exposed at Rock Mountain have been greatly augmented by cores drilled by the Georgia Power Company Pumped Storage Project; data from the cores was integrated into the measured sections of Grainger (1983). Rich (1983) summarized details of the Floyd Shale in the area of Rome.

3.7.3.1 Floyd Shale

The Upper Mississippian Floyd Shale was named by Hayes (1891) for exposures in Floyd County, Georgia. The Floyd Shale is comprised predominately of dark-gray to black, locally silty shale that is partly calcareous and partly carbonaceous; the formation includes siltstone, sandstone, limestone, and local siderite nodules (Thomas, 1979). Cressler (1970) noted that the formation also includes a thick limestone near the base and sandstone layers near the top. Hayes (1902) referred to the uppermost sandstone as the Oxmoor Sandstone, and Cressler (1970) referred to the unit as the Hartselle Sandstone Member. Both of these names were extended from Alabama; the Oxmoor nomenclature, however, is no longer used there. Thomas (1979) discussed the problems with using the Hartselle Sandstone name for the sandstone at the top of the Floyd Shale in detail and referred to it as an “unnamed sandstone”; the problems with the Hartselle name mainly include the northeastward pinching out of the Hartselle Sandstone in Alabama about 45 km west of the Georgia state line and lateral discontinuities between sandstone layers. Rich (1983) approximated the thickness of the Floyd Shale in its type area around Rome to be 450 m; Grainger (1983) estimated the thickness as approximately 414 m at Rock Mountain. Thickness measurements of the various parts of the Floyd Shale in Thomas (1979) and Rich (1983) demonstrated that carbonate rocks make up a significant part of the formation as a whole, and likely more than shale; as a result, Rich (1983) suggested replacing the Floyd Shale name with Floyd Formation.

For the most part, the Floyd Shale consists of relatively little sandstone, but the predominantly shale succession grades upward into a unit of fine- to very fine-grained sandstone, that is characteristically interlaminated with clay (Thomas, 1979). Thomas (1979) stated that the sandstone generally is no thicker than 20 m throughout, but Cressler (1970) reported a thickness of approximately 90 m on Judy Mountain. Thomas (1979) further noted that the Judy Mountain outcrop is “isolated by erosion from other exposures” of the sandstone and, as a result, “correlation of the much thicker sandstone on Judy Mountain with the thinner sandstone elsewhere is uncertain.”

The lowermost part of the Floyd Shale as mapped in the depression of the Floyd synclinorium is comprised of a limestone unit (Figure 3-7) referred to as “unnamed lower limestone of clastic facies” by Thomas (1979). Thomas estimated that the thickness of

the basal limestone unit might exceed 180 m thick; Rich (1983) estimated a thickness of approximately 160 m. It is comprised of bioclastic grainstone and packstone, which contains some very coarse bioclasts and local black nodular chert. This interval also contains gray-to-black, very argillaceous, calcareous mudstones, which are similar to the Lavender Shale Member. These mudstones within the bioclastic limestone succession further suggest the intertonguing of the carbonate and clastic facies (Thomas, 1979).

The most complete succession of the lower limestone unit of the Floyd Shale was compiled from exposures and core samples in a quarry on the northern outskirts of Rome. This quarry is documented as the Florida Rock Industries Incorporated Rome quarry in Thomas (1979) and Rich (1983; 1986d) and as the Ledbetter quarry (as it was formerly called by former owners) by Cressler (1970). In the quarry, Rich (1983) subdivided the lower limestone unit into three subunits: a basal siliceous limestone unit, a middle shaly limestone unit, and an upper grainstone unit. The lower unit of cherty packstone and grainstone may be correlative to the chert-rich Tusculumbia Limestone to the northwest. Rich (1983) estimated a combined thickness of approximately 61 m exposed in the quarry.

The basal limestone of the Floyd Shale is exposed southeast of Strawberry Mountain in Chattooga County. A large outcrop of the unit is exposed at the southeastern base of the mountain in a creekbed near the main road north of Subligna. There, the unit is composed of medium- to dark gray, bioclastic wackestone; bedding surfaces contain some echinoderm columnals and are locally slickensided. Farther to the southeast, the unit is exposed in scattered outcrops. Along a forestry road, the unit is exposed as approximately 4 m of massive-bedded, medium-gray bioclastic packstone that is weathered to light gray and grades upward into dark-gray, faintly laminated (locally) micrite near the top of the outcrop that is weathered to a brownish gray. Bedding at this outcrop ranges from approximately 0.3 to 1.0 m thick. The float on top of the outcrop is composed of very finely laminated calcareous siltstone. The packstone contains abundant bioclasts of brachiopods and echinoderm columnals as much as 2 cm in diameter with some ooids throughout; fresh surfaces of the packstone have an asphaltic odor. In an outcrop just north of Subligna, the unit is exposed as approximately 5 m of medium- to dark gray, coarsely crystalline bioclastic packstone/wackestone in beds that

range in thickness from 10–50 cm and are shaly near the base. The outcrop contains abundant brachiopod fragments and echinoderm columnals with a few blastoid specimens. To the north in Walker County, the basal limestone unit is exposed east of Taylor Ridge in a roadcut near GA136 at Maddox Gap. There, the unit is exposed as approximately 3 m of light-gray, slightly shaly, calcareous mudstone and bioclastic packstone in beds 1–30 cm thick. The mudstone is rusty red and contains faint green reduction spots in places; the packstone contains abundant bryozoa fragments. In Floyd County, the basal limestone unit is exposed in the valley west of Little Sand Mountain. There, the unit is exposed as medium-gray, bioclastic wackestone and calcareous shale in beds that range from 0.3 to over 1.0 m in thickness. The unit is also exposed in a roadcut in the valley between Johns Mountain and the Rome fault, where it is exposed as approximately 5 m of light- to medium-gray, bioclastic wackestone that is interbedded with calcareous shale and weathers to tan. The unit is also exposed east of Turkey Mountain in Floyd County, just west of the Rome fault. There, the unit is exposed as approximately 5 m of medium-gray, coarsely crystalline, bioclastic packstone in thick ledges about 0.5–1.0 m thick; the packstone contains abundant fragments of echinoderm columnals, brachiopods, bryozoa, blastoids, and gastropods. The exposure includes a layer with abundant black chert nodules and stringers that resemble those in the Tusculumbia Limestone to the northwest.

The most complete succession of the Floyd Shale above the basal limestone unit was compiled from exposures and core samples from the Georgia Power Company project at Rock Mountain. Thomas (1979) estimated that this part of the Floyd Shale is as thick as 290 m. Rich (1983) estimated a thickness of 300 m, and Grainger (1983) estimated a thickness of 277 m. In the area around Rock Mountain, the basal limestone is overlain by calcareous shale; to the north, in the area around Little Sand Mountain, the basal limestone is overlain by a sandstone unit that is about 11 m thick (Thomas, 1979). The sandstone in the Floyd Shale characteristically is fine-grained, but the lower part generally consists of very fine-grained, ripple-laminated sandstone with argillaceous partings (Thomas, 1979). Thomas (1979) noted “small unidentified plant fragments” on bedding surfaces.

The Floyd Shale underlies large expanses of the valleys throughout the Floyd synclinorium, and exposure is poor and generally scattered in the outcrop area. Outcrops of the shale facies are rare, but Cressler (1970) documented a few locations. The shale in the formation exposed in the valley between Lavender Mountain and Judy Mountain is pervasively weathered dark-gray shale that is weathered to medium-gray, tan, and black in places. Outcrops of facies more resistant to weathering, such as the thick lower limestone or some of the thick limestone or sandstone units within the formation, create some topographic relief in the otherwise relatively flat areas underlain by the Floyd Shale. Furthermore, much of the exposed shale from the formation is interbedded with rocks that are more resistant to weathering, such as sandstone or limestone, and is sandy, silty, or calcareous in many places. One example is in outcrops along roads around Rock Mountain. There, the formation is exposed as medium- to dark-gray shale weathered to brownish tan and gray that is interbedded with thin, brown and gray siltstone and very fine- to medium-grained sandstone. The sandstone is locally iron-rich and stained to rusty red in places.

Outcrops of the sandstone unit previously correlated with the Hartselle Sandstone are best found in Floyd County on Judy Mountain and around Rock Mountain. This unit is also found in a low roadcut through Rock Mountain syncline, where it is exposed as approximately 3 m of massive-bedded, tan, fine- to medium-grained sandstone that is weathered and locally stained with iron oxide.

Other outcrops of sandstone in the Floyd Shale are located throughout Floyd County. In a roadcut along GA140 across the southern end of Turkey Mountain, the formation is exposed as approximately 50 cm of brownish gray, fine-grained sandstone in beds about 5 mm thick. On the west side of Turkey Mountain, the formation is exposed in a low roadcut as approximately 10 cm of tan, fine- to medium-grained sandstone weathered to buff and rusty red, interbedded with tan sandy shale. Near the intersection of Johns Mountain and Mill Mountain anticlines, the formation is exposed as approximately 1 m of purplish gray, slightly silty shale that is abundantly fractured and contains some yellowish, iron-stained bands. In the valley west of Little Sand Mountain, the formation is exposed as tan and brown, fine- to medium-grained sandstone weathered to rusty red or dull brown interbedded with some shale; the beds range in thickness from

a few centimeters to about 1 m in outcrops that range from about 20 cm to a few meters thick. To the southwest of Little Sand Mountain near the intersection of Taylor Ridge monocline and Simms Mountain anticline, the formation is exposed as rusty brown and yellow, iron-rich, fine- to medium-grained sandstone. The sandstone is interbedded with siltstone, mudstone, and shale; the shale and siltstone beds are pervasively folded and purplish brown in color in places. The sandstone beds in these outcrops range in thickness from about 1–20 cm, and the exposures range from about 50 cm to a few meters thick. Near the northeastern end of Lavender Mountain, the formation is exposed as a few m-thick intervals of dark gray shale interbedded with some thin lenses of fine-grained sandstone that are about 1 cm thick. Although the stratigraphic level of these sandstone layers is ultimately uncertain, no research has documented any success in lateral correlation of the layers throughout the sparsely outcrops in the study area. This suggests that these sandstones are not laterally continuous across the study area.

3.7.3.2 Bangor Limestone tongue

The Bangor Limestone in Floyd County is a tongue of the carbonate facies that extends southeastward into the clastic facies (Figures 3-7 and 3-8; *cf.* Thomas, 1979; Rich, 1986b). Butts (1948) noted a limestone unit in the Floyd Shale as he defined it that was similar in lithology and fossil assemblage to the Bangor Limestone, to which he referred to as “Bangor” (quotations his) because the limestone unit was significantly thinner than the general thickness of the formation. It is approximately 55 m thick in the northwest around Lookout and Pigeon Mountain and thickens to about 200 m in the Floyd synclinorium (Rich, 1986b). Thomas (1979) noted that the 200 m includes an interval of shale and sandstone. Grainger (1983) estimated a thickness of approximately 210 m at Rock Mountain. Conversely, Cressler (1970) estimated a thickness of about 90 m for the Bangor Limestone at Rock Mountain, where he described the formation as thick- to massive-bedded, gray and bluish gray, pure limestone. Cressler (1970) did not include the argillaceous limestone and calcareous shale below the limestone interval as part of the Bangor Limestone; he also did not include any of the overlying shale, which he attributed to a “thinned extension” of the Pennington Formation. The Bangor Limestone tongue is mapped separately only in the Little Sand Mountain and Rock Mountain areas. The formation can be divided into three members: lower, middle, and

upper (Rich, 1986b); Grainger (1983) described the Bangor Limestone at Rock Mountain in detail. The upper and lower members of the Bangor tongue are composed of bioclastic limestone (part of which contains localized nodules of dark chert) and argillaceous calcareous mudstone (Thomas, 1979). Thomas (1979) noted that the argillaceous mudstone weathers to massive clay that is characterized by abundant impressions of fenestrate bryozoa. The middle member is characterized by dark-gray clay shale interspersed with thin wavy beds of fine-grained sandstone with shaly partings (Thomas, 1979; Grainger, 1983). The clastic interbeds in this predominantly carbonate interval further indicate the intertonguing of facies (Thomas, 1979).

3.7.3.3 Pennington Formation

The Pennington Formation of the southeastern clastic facies primarily consists of dark shale that rests on the Bangor tongue, in the same stratigraphic position as observed to the northwest (Figures 3-7 and 3-8). The lower part of the formation is composed of thin-bedded claystone that weathers to brown and contains abundant brachiopod molds and siderite nodules; Thomas (1979) noted that this claystone may be weathered from argillaceous calcareous mudstone.

The upper part is characterized by laterally discontinuous, thin-bedded sandstone that increases in abundance toward the top. The sandstone is interbedded with shale and siltstone, and generally is clay rich (Crawford, 1986). Some of these sandstone beds are capped by micaceous, carbonaceous laminae and parts of the shale sequence contains abundant siderite nodules (Thomas, 1979). The upper part of the Pennington commonly includes marine invertebrate fossils, commonly as casts or molds in the sandstone slabs; plant fossils are mixed with the marine invertebrate fossils near the top of the formation, but generally are poorly preserved (Crawford, 1986). Thin limestone and calcareous sandstones, both of which are fossiliferous, are also common near the top of the Pennington Formation (Crawford, 1986).

At Rock Mountain, the Pennington Formation is approximately 175 m thick, but some of this is Raccoon Mountain Formation (Rich, 1986b). From the section measured by Grainger (1983), the Pennington Formation at Rock Mountain is approximately 117 m (using the sandstone to mark the base of the Raccoon Mountain as interpreted by Thomas, 1979).

3.7.3.4 Raccoon Mountain Formation

The Raccoon Mountain Formation of the southeastern clastic facies is characterized by a basal layer of very fine- to fine-grained, slightly argillaceous sandstone. This sandstone layer forms prominent ledges on Rock Mountain and Little Sand Mountain (Thomas, 1979); Crawford (1986, 1989) refers to this as the “lower” sandstone unit. Although lateral correlation of the sandstone unit overlying the shale is uncertain, the base of the lowest thick sandstone marks the top of the Pennington as interpreted by Thomas (1979). Thomas (1979) noted that a few thin coaly beds are present in the lower part of the unit; Crawford (1986) added that a thin carbonaceous zone commonly is present just above the basal sandstone unit and is characterized by “poorly preserved plant fossils (mostly stems and fruiting bodies).” The sandstone unit is overlain by dark shale that is similar to the shale below the sandstone unit in the underlying Pennington Formation (Thomas, 1979); the upper shale succession is interbedded with siltstone, thin sandstone beds, and a few thin limestone layers (Crawford, 1986). Thomas (1979) noted that the upper part of the formation commonly is characterized by siderite nodules.

Crawford (1986) described the lower sandstone as uniformly fine- to medium-grained quartz sandstone with commonly pervasive planar cross-beds in the lower part of the unit; he also noted common channels cut into the underlying succession of shale, siltstone, and lenticular sandstone. A peculiar feature of the lower sandstone is spherical-weathering voids on cm to m scale that are particularly common in the lower part (Crawford, 1986). The thickness range of the unit is consistent throughout exposures at both Little Sand and Rock Mountains; it is uncommonly less than 15 m and generally no greater than 30 m (Crawford, 1986).

The sandstone beds in the Raccoon Mountain Formation generally are thin, commonly characterized by shale partings, and some are ripple-laminated; the sandstone beds are capped by carbonaceous, micaceous laminae (Thomas, 1979). The sandstone is more quartzose toward the top of the unit. Thomas (1979) noted one sandstone bed that contains preserved echinoderm columnals, bryozoa fragments, and possible brachiopod fragments.

At Little Sand Mountain, the basal Raccoon Mountain Formation sandstone underlies the entire mountain and is the major cliff-forming unit. The vertical faces there are as thin as 1–2 m but generally exceed 15 m (Crawford, 1986). According to Crawford (1986), the estimated thickness of the part of the succession overlying the basal sandstone is approximately 91 m, and roughly the lower half of this succession is Upper Mississippian; Cramer (1979) measured this succession to be 26 m thick. In a few roadcuts on Little Sand Mountain, the basal sandstone is brownish tan, massive, medium- to coarse-grained sandstone in meter-thick beds. Farther upsection, the sandstone is pale tan or white in color and dominantly composed of quartz grains with some micaceous and feldspathic layers. The lower part of the sandstone is interbedded with sandy shale that is more abundant towards the base.

At Rock Mountain, the basal sandstone forms the lower of two ledges. It is well exposed at the top of the Georgia Power powerhouse excavation where Crawford (1986) noted thin carbonaceous layers in “channel rubble zones.” The measured section of Grainger (1983) lists the basal sandstone as approximately 15 m in thickness and the total thickness of the formation as approximately 132 m. Thus, the thickness of the overlying succession is approximately 117 m, and Crawford (1986) estimated that roughly the lower half of this succession is Upper Mississippian at Rock Mountain

3.7.4 Transition between northwestern carbonate facies and southeastern clastic facies

The lateral transition between the carbonate facies and the clastic facies is presumed to be one of intertonguing across the Kingston–Chattooga anticlinorium (Figures 3-7 and 3-8), as illustrated by the limestone “tongues” in the southeastern clastic facies (Thomas, 1979; Rich, 1986c). The extensive range of intermediate characteristics between the facies has not been documented, however, because of poor exposure and difficulty in correlation of stratigraphic units, particularly the sandstone or sandstones (Thomas, 1979). Furthermore, the Mississippian succession in the region of the Kingston–Chattooga anticlinorium has been removed by erosion. Thomas (1979) elaborated on the problematic facies transition and documented the details of sections to the north of the study area and their many interpretations. The intertonguing of the two lithofacies implies alternating episodes of delta progradation and delta destruction (Thomas and Cramer, 1979).

3.8 PENNSYLVANIAN SYSTEM

The Lower Pennsylvanian succession includes massive coarse sandstones and conglomerates, shale, and a few coal beds. The Pennsylvanian succession of Georgia was first subdivided by Hayes (1892) into two distinct units: the Lookout Sandstone below and the Walden Sandstone above (Figure 3-9). Comprehensive studies of the coal were published by McCallie (1904) and Johnson (1946), and other details can be found in reports of the United States Geological Survey and U.S. Bureau of Mines (Cramer, 1979). Butts (1948) mapped the Pennsylvanian succession as Pottsville Formation (with mention of the subdivisions of Hayes) as comprised of a basal massive bluff-forming sandstone unit that overlies the shales of the Pennington Formation. Later subdivisions by Johnson (1946) introduced the name Gizzard Member for the basal member of the Lookout Formation, which had been revised from the original Lookout Sandstone of Hayes (1892). More complete summaries and discussions of the evolution of Pennsylvanian nomenclature in Georgia are published by Culbertson (1963) and Cramer (1979). The Gizzard name was introduced as a locality by Safford (1869) for exposures on Little Fiery Gizzard Creek in Marion County, Tennessee. Nelson (1925) formally established the Gizzard nomenclature, which he expanded to the Gizzard Formation and divided it into three subformations. Wilson *et al.* (1956) named these subdivisions as follows: the basal Raccoon Mountain Formation, the Warren Point Sandstone, and the uppermost Signal Point Shale. Cressler (1964a, b, 1970) used subdivisions as correlated by Johnson (1946). The basic two-fold subdivision of Hayes is maintained on the 1976 geologic map of Georgia, except that the Lookout Sandstone is subdivided into the Gizzard Formation below and the Sewanee Conglomerate above; and the beds above the Sewanee are left undifferentiated. The Georgia Geological Survey (1976) mapped most of the Pennsylvanian System in northwestern Georgia as a single undifferentiated unit, except on the northwestern flank of Lookout Mountain and on Sand Mountain. In those locations the Lower Pennsylvania succession is called the Lookout Sandstone and is divided into Gizzard Formation below and Sewanee Sandstone above, and all the overlying Pennsylvanian rocks are mapped as an undifferentiated unit. Wilson *et al.* (1956) demonstrated that the distinctive massive sandstone near the base of the Pennsylvanian succession is formed by different stratigraphic units in different places.

Cramer (1979) outlined several problems in lateral correlation throughout the Pennsylvanian rocks in Georgia and consequently proposed considering the system as a “bluff-forming sandstone” and the vertical successions of rocks above and below the bluff-forming sandstone (Figure 3-9); as a result, it is difficult to resolve thickness estimates for individual formations from the measurements he documented. Grainger (1983) included a very detailed description of the stratigraphic succession at Rock Mountain on the basis of drill cores and surface and subsurface excavation associated with the construction of a pump storage facility there by the Georgia Power Company. Most recently, Crawford *et al.* (1989) published a concisely descriptive report on the Pennsylvanian stratigraphy in Georgia, and a study by Crawford (1989) is perhaps the most recent detailed report on the subject.

The base of the Lower Pennsylvanian is within a succession of shale that is conformable and continuous with that described for the shaly Upper Mississippian part of the Raccoon Mountain Formation in sections 3.7.2.3 and 3.7.3.4. Culbertson (1963) referred to the contact as an unconformity. Englund *et al.* (1985) noted that, although the underlying Upper Mississippian succession is essentially complete, an absence of beds containing lower Early Pennsylvanian fauna possibly indicates a hiatus. Crawford *et al.* (1989) contended, however, that there is “no clear physical evidence” for a Mississippian–Pennsylvanian unconformity.

Cramer (1979) noted that the Pennsylvania succession in Georgia suggests “continuous sedimentation during deposition of a prograding clastic wedge”; and that the succession above the Mississippian carbonate rocks grades upward from “marine and near-shore mudstone to massive barrier and (or) delta-front sandstones.” The westward-prograding clastic wedge interpretation of the succession carries implications of “identification of time-stratigraphic planes across temporally equivalent facies” (Cramer, 1979). Chowns (1989) noted that the sandstones of the Pennsylvanian succession suggest high-energy depositional environments such as “distributary channels and mouth bars, tidal inlets, and barrier beaches,” and that the shale and coal represent “bay and lagoon fills with marsh peats” (*cf.* also Hobday, 1974).

3.8.1 Lower Pennsylvanian succession northwest of the Kingston fault

The Lower Pennsylvanian rocks in Georgia crop out in wide expanses in the cores of the synclines that underlie Sand, Lookout, and Pigeon Mountains; and the Lower Pennsylvanian sandstones form the flat tops and prominent bluffs of these regionally extensive mountains (Figure 3-10). A stratigraphic section by Crawford *et al.* (1989) illustrates the Lower Pennsylvanian succession on Sand and Lookout Mountains.

The Raccoon Mountain Formation is a continuation of the same lithology as described at the top of the succession over the northwestern carbonate facies of the Mississippian (*cf.* section 3.7.2.3). According to the stratigraphic section of Crawford *et al.* (1989), the Raccoon Mountain Formation is approximately 125 m thick, and approximately 90 m of this succession is assigned to the Lower Pennsylvanian.

In the present research, the Lower Pennsylvanian succession in northwestern part of the study area was only investigated as high as the bluff-forming sandstone-conglomerate unit on Pigeon and Lookout Mountains. This upper sandstone-conglomerate unit (or Warren Point Sandstone) is approximately 151 m thick.

The Warren Point Sandstone is exposed in roadcuts along GA48 through the southeastern flank of Lookout Mountain in Chattooga County. The base of the unit is marked by approximately 1 m of conglomerate overlain by a ledge approximately 2 m thick of conglomerate and very coarse-grained white quartzose sandstone, which is overlain by about 1 m of medium- to coarse-grained sandstone beds that are approximately 25–50 cm thick. Farther upsection, the unit is white (locally iron oxide-stained), medium- to coarse-grained, cross-bedded, quartzose sandstone in meter-thick ledges and in intervals with beds ranging 1–25 cm in thickness.

Farther to the north, the Warren Point Sandstone is exposed in roadcuts along GA136 through the southeastern flank of Lookout Mountain in Walker County. The base of the unit is marked by a ledge of conglomerate that is approximately 2 m thick overlain by about 1.5 m of coarse-grained sandstone. Farther upsection, the unit is composed of white and tan, fine- to medium-grained sandstone that is weathered to buff and pale gray, in beds that range from 0.5 to 2.0 m in thickness.

3.8.2 Lower Pennsylvanian “outliers”

Outside of the regionally extensive mountains in northwestern Georgia, the Pennsylvanian system in the area of study is confined to the Pennsylvanian “outliers”, which include Rock Mountain in Floyd County and Little Sand Mountain in Chattooga County (Figure 3-10). Cramer (1979) and Crawford (1986) provided detailed stratigraphic descriptions, as did Grainger (1983) for the Rock Mountain area. Crawford (1986) divided the Pennsylvanian rocks in these locations with reference to a “lower” sandstone unit, and “upper” sandstone-conglomerate unit, and the rocks below, above, and between these markers. As described in section 3.7.3.4, the basal Lower Pennsylvanian succession includes roughly the upper half of the shaly succession (that overlies the basal sandstone unit) of the Raccoon Mountain Formation. For the Pennsylvanian outliers, the “upper sandstone-conglomerate” unit of Crawford (1986) equates to the “bluff-forming sandstone” unit of Cramer (1979); the unit distinctly marks the top of the Raccoon Mountain Formation.

Crawford (1986) described the upper sandstone-conglomerate succession of the Pennsylvanian outliers as massively bedded, fine- to coarse-grained, quartzose sandstone in which planar cross-beds are common. The basal unit is comprised of approximately 5–8 m of quartz-pebble conglomerate and conglomeratic sandstone (Crawford, 1986); this unit roughly correlates to the Warren Point Member as described by Culbertson (1963). Crawford (1986) also noted that the conglomeratic lithofacies is particularly well developed in channels that are cut into the underlying shales and siltstones

3.8.2.1 Little Sand Mountain

The upper sandstone-conglomerate section is present only on the southeastern end of Little Sand Mountain and is composed of approximately 15 m of quartz sandstone that is massively bedded at the base and more thinly bedded up-section (Cramer, 1979). The succession also includes conglomerate in distinct beds that contain quartz pebbles as large as 1 cm in diameter. The sandstone-conglomerate forms the rim of the highest part of the mountain and is overlain by an unknown thickness of gray shale; Cramer (1979) noted that this shale is at least 10 m thick.

3.8.2.2 Rock Mountain

The upper sandstone-conglomerate section (Warren Point Member) forms the prominent scarp on Rock Mountain and is comprised of approximately 30–45 m of light- to medium-gray, massively-bedded, fine- to medium-grained, cross-bedded sandstone (Grainger, 1983). Cramer (1979) noted that this succession is thinner bedded toward the top.

The section of rocks above the upper sandstone-conglomerate on Rock Mountain is composed of approximately 85 m of dark gray massive thin-bedded shale with sandstone laminae and thin sandstone beds (Grainger, 1983). In this succession, Crawford (1986) also noted siltstones and lenticular “partly calcareous” sandstones that contain zones of marine fossils toward the top. This succession roughly correlates to the Signal Point Member of Culbertson (1963).

3.8.3 Mississippian–Pennsylvanian boundary problem

Accurate location of the position of the Mississippian–Pennsylvanian systemic boundary has been a fairly long-standing problem. The problems include locating the boundary and assigning a mappable base of Raccoon Mountain Formation. Cramer (1979) noted that the boundary commonly had been placed at an arbitrary lithologic marker such as “the top of the highest maroon mudstone, below the lowest coal bed, at the base of the massive bluff-forming sandstone, or at the base of the lowest quartz-bearing sandstone.” Furthermore, Cramer (1979) eloquently stated that the primary problem is that such methods involve the application of rock-stratigraphic criteria to a horizon that is, by definition, time-stratigraphic. At the time of his study, Cramer (1979) stated that the identification of the Mississippian–Pennsylvanian boundary awaited “resolution of a maze of biostratigraphic and lithostratigraphic details.”

3.8.3.1 Lithology of the Mississippian–Pennsylvanian boundary

The Mississippian–Pennsylvanian boundary, as previously noted, has been documented within a gradational succession of shale and thin sandstone that has been assigned to either the Pennington Formation or the Raccoon Mountain Formation (*e.g.*, Thomas and Cramer, 1979; Crawford, 1986; Rich, 1986b; Crawford *et al.*, 1989). Crawford *et al.* (1989) maintained that there is no evidence for an unconformity at the base of the Lower Pennsylvanian succession in Georgia. Rich (1986b) stated that part of

the problem is that the boundary is within a succession that contains the upward gradation from carbonate into clastic deposits and from “marine units into predominantly non-marine” units. Furthermore, the succession that hosts the boundary is gradational in nature and thus there is no easily mappable lithologic contact. Cramer (1979) illustrated the uncertainty in the age of rock around this contact; for example, in his description of the succession at Little Sand Mountain, he noted that the “lowermost clastic rocks are considered Mississippian on the basis of regional facies considerations and paleontology... [and] the bluff-forming sandstone is considered Pennsylvanian” only on the basis of stratigraphic position. Cramer (1979) listed six distinct points (apart from the generally poor exposures) to explain why correlation in the Pennsylvanian succession is difficult.

Furthermore, Crawford *et al.* (1989) reiterated that the lowermost thick, massive, coarse-grained clastic rocks that form the cliffs on Sand, Lookout, Pigeon, Little Sand, and Rock Mountains are not all Pennsylvanian in age, and thus not necessarily the same lithologic unit. These clastic units exceed 30 m in thickness and several kilometers in length; some of these units, however, are lenticular in shape. For example, the basal sandstone in the Upper Mississippian part of the Raccoon Mountain Formation is not laterally continuous. As a result, Crawford *et al.* (1989) concluded that the basal sandstones of the Raccoon Mountain are not distinguishable from Pennsylvanian-age coarse sandstones and conglomerates via casual observation.

3.8.3.2 Data from fossils

For the Mississippian–Pennsylvanian boundary, biostratigraphic markers have been studied in detail (Figure 3-11). Cramer (1979) noted that lack of “detailed biostratigraphic data from this part of the section precludes precise identification” of the boundary. More recently, Crawford (1986) and Crawford *et al.* (1989) stated that ages have been better established on the basis of both marine and plant fossils.

Cramer (1979) noted that fossils “in the limestone sequence establish a Mississippian age, and plant fossils demonstrate a Pennsylvanian age in the coal above the massive sandstone.” A study by Wilson (1965) documented Upper Mississippian spores from a coal bed in the Raccoon Mountain Formation in Alabama, and Milici

(1974) noted Mississippian invertebrate fossils in the Raccoon Mountain Formation in Tennessee.

A study of Pennsylvanian plant fossils in Georgia by Gillespie *et al.* (1989) noted that the oldest Pennsylvanian fossils were collected from very similar lithologies to those from which the youngest Mississippian fossils were collected; they added that, in many locations, the fossiliferous horizons are separated only by a meter or a few meters. Crawford *et al.* (1989) asserted that coal beds are present only in the Pennsylvanian succession in Georgia and that Pennsylvanian fossils are invariably found in the lowermost coal bed; Gillespie *et al.* (1989) noted that the early Pennsylvanian ages for the coals were based on “plant compression, [florae], palynomorphs, and invertebrate marine assemblages.” Conversely, Crawford *et al.* (1989) noted that the uppermost limestone with a marine fossil “hash” contains an “abundant and diverse” Mississippian fauna. In consideration of these data, Crawford *et al.* (1989) concluded that the Mississippian–Pennsylvanian boundary is mappable, available, and reliably consistent, but that it is time-consuming to recognize.

3.8.3.3 Associated problem with the Pennington-Raccoon Mountain boundary

McLemore (1971) interpreted the lower sandstone as basal unit of the Raccoon Mountain Formation (see also Thomas, 1979). This interpretation requires that the Raccoon Mountain Formation must also include the uppermost Mississippian rocks, but provides a mappable contact. Stratigraphic columns in other reports (*e.g.*, Culbertson, 1963; Crawford, 1986; Crawford *et al.*, 1989; Grainger, 1983; Rich, 1986b), however, include the lower sandstone in the Pennington Formation and the Mississippian–Pennsylvanian boundary, which is higher in the stratigraphy, also serves as the boundary between the Pennington and Raccoon Mountain. The Mississippian–Pennsylvanian boundary is not easily identifiable and, thus, the formation boundary in this interpretation is not clearly mappable. Chowns (1989) noted that all of the carbonate rocks in the succession are Mississippian in age. The upper sandstone-conglomerate is the bluff-forming sandstone of Cramer (1979), and the succession includes coal, which places it definitively within the Lower Pennsylvanian (Chowns, 1989).

3.8.3.4 Summary and commentary

As Cramer (1979) mentioned, the attempts to assign a rock-stratigraphic marker to a time-stratigraphic horizon should be abandoned. Drahovzal and Neathery (1971) expressively illuminated this problem by emphasizing time-equivalence of facies as opposed to the idea of “time-separated units superimposed on one another” in a “layer-cake” stratigraphy. Cramer (1979) also noted that lateral facies variations must be considered in favor of the more simplistic “layer-cake” approach to stratigraphy as used in the past. Drahovzal and Neathery (1971) further emphasized that the spatial relationships are further complicated by crustal shortening from late Paleozoic thrust faulting, and that “new faunal data and new concepts in mapping help place each unit in its proper perspective.”

Lateral correlation difficulties aside, however, one certainly should consider the data of Crawford (1986) to be locally accurate (*i.e.*, in the vicinity of Little Sand Mountain or Rock Mountain). After considering all the available data, the author agrees with the method introduced by McLemore (1971; also used by Thomas, 1979) of using the “lower” sandstone as a mappable marker for the base of the Raccoon Mountain Formation, which, in this interpretation, straddles the Mississippian–Pennsylvanian boundary. The systemic boundary is not an easily recognizable horizon in the field, but can be assumed to be near the middle of the shaly interval in the Raccoon Mountain Formation between the lower and upper sandstone units as demonstrated by Crawford (1986). The fact that the Mississippian–Pennsylvanian systemic boundary is a time-stratigraphic horizon that is apparently located somewhere within a lithologically indistinguishable succession of thin argillaceous sandstones and sandy shale layers is consistent with continuous, uninterrupted deposition but exacerbates the problem of time correlation.

3.9 SUMMARY OF REGIONAL STRATIGRAPHY

The Paleozoic strata are divided into four lithotectonic units (Thomas 2001, 2007; Thomas and Bayona, 2005) on the basis of general stratigraphic characteristics and mechanical behaviour during deformation (Figure 1-4): **Unit 1**, the regional dominant weak layer, containing the regional décollement, encompasses Lower to lower Upper

Cambrian fine-grained clastic rocks and minor thin-bedded limestones (Rome and Conasauga Formations); **Unit 2**, the regional dominant competent layer, which controls ramp geometry, is an Upper Cambrian-Lower Ordovician massive carbonate unit (Knox Group); **Unit 3**, a relatively thin, laterally variable, heterogeneous Middle Ordovician to Lower Mississippian succession of limestone, shale, sandstone, and chert; and **Unit 4**, an Upper Mississippian-Pennsylvanian synorogenic clastic wedge dominated by shale in the lower part and generally coarsening upward into sandstone and shale. The detachment of the Kingston–Chattooga composite thrust sheet is persistently in shale-dominated facies of the Middle to lower Upper Cambrian Conasauga Formation (Unit 1). In northwestern Georgia, Units 3 and 4 primarily are deformed passively over the underlying regional competent layer (Unit 2). Topography in northwestern Georgia is largely controlled by stratigraphy: most ridges are on Unit 3, and topographic flats are predominantly on shale-dominated strata in Units 1 and 4. Interestingly, the idea of dividing the regional stratigraphy into layers on the basis of relative rigidity and the inferences of how they affect structures in the southern Appalachians were first discussed by Hayes in 1891.

| SYSTEM | STRATIGRAPHIC UNIT | | DOMINANT ROCK TYPES | |
|---------------|--------------------------------------|----------------------------|--------------------------------------------------------------------------------------|--------------------------------------|
| | NW | SE | NW | SE |
| PENNSYLVANIAN | LOWER PENNSYLVANIAN UNDIFFERENTIATED | | sandstone, conglomerate, shale, a few coal beds tan/white conglomeratic sandstone | |
| | RACCOON MOUNTAIN FORMATION | RACCOON MOUNTAIN FORMATION | sandstone and shale | sandstone and shale |
| MISSISSIPPIAN | PENNINGTON FORMATION | | sandstone and shale | sandstone and shale |
| | MONTEAGLE-BANGOR LIMESTONES | | limestone | limestone |
| | TUSCUMBIA LIMESTONE | | | sandstone and shale |
| | FLOYD SHALE | | | sandstone |
| | MAURY SHALE | | cherty limestone | bioclastic limestone |
| | FORT PAYNE CHERT | | white and gray chert | dark calcareous mudstone |
| DEVONIAN | CHATTANOOGA SHALE | | black shale | |
| | FROG MOUNTAIN SANDSTONE | ARMUCHEE CHERT | sandstone | white and gray chert |
| SILURIAN | RED MOUNTAIN FORMATION | | tan and reddish-brown shale, siltstone, and sandstone | |
| ORDOVICIAN | SEQUATCHIE FORMATION | | siltstone, sandstone, and shale that is locally calcareous, and some limestone | |
| | CHICKAMAUGA LIMESTONE | COLVIN MOUNTAIN SANDSTONE | argillaceous limestone and calcareous siltstone | quartzose sandstone and conglomerate |
| | GREENSPORT FORMATION | | red calcareous shale and mudstone | |
| CAMBRIAN | ATTALLA CHERT CONGLOMERATE | | chert-clast conglomerate | |
| | KNOX GROUP | | massive limestone, dolostone, and chert | |
| | CONASAUGA FORMATION | | gray calcareous shale and limestone | |
| | ROME FORMATION | | multi-colored shale and sandstone | |
| | SHADY DOLOMITE | | massive light-gray dolostone | |

Figure 3-1. Generalized stratigraphic column for the Paleozoic succession in northwestern Georgia.

| <u>System</u> | <u>Names of Formations in Georgia</u> | <u>Safford's Equivalents in Tennessee</u> | <u>Smith's Equivalents in Alabama</u> | <u>Hayes' Equivalents in Georgia</u> |
|----------------------|----------------------------------------|---------------------------------------------------------------------------|-----------------------------------------------------------------|-----------------------------------------|
| CARBONIFEROUS | Coal Measures | Coal Measures | Coal Measures | { Walden Sandstone Lookout Sandstone |
| | Mountain Limestone | Mountain Limestone | Bangor Limestone | Bangor Limestone |
| | Floyd Shales | | { Oxmoor Sandstone and Shales Fort Payne Chert | Floyd Shales |
| | Fort Payne Chert | Siliceous Group | | Fort Payne Chert |
| DEVONIAN | Chattanooga Black Shales | Black Shale | Black Shale | Chattanooga Black Shales |
| SILURIAN | Red Mountain | Dyestone Group, Whiteoak Mountain Sandstone and Clinch Mountain Sandstone | Red Mountain | Rockwood |
| ORDOVICIAN | Chickamauga (including Rockmart Slate) | Nashville Trenton Maclurea | Trenton or Pelham Limestone | Chickamauga Limestone |
| | Knox Dolomite | Knox Dolomite | Knox Dolomite | Knox Dolomite |
| CAMBRIAN | Oostanaula Shales | Knox Shales Knox Sandstone | { Montevallo Shales including Weisner Quartzite Coosa Shales | { Connesauga Shales Rome Sandstone |
| | ? | Chilhowie Sandstone Ocoee Conglomerate | | |

Figure 3-2. Comparative stratigraphic column for the Paleozoic succession in northwestern Georgia, adapted from Spencer (1893).

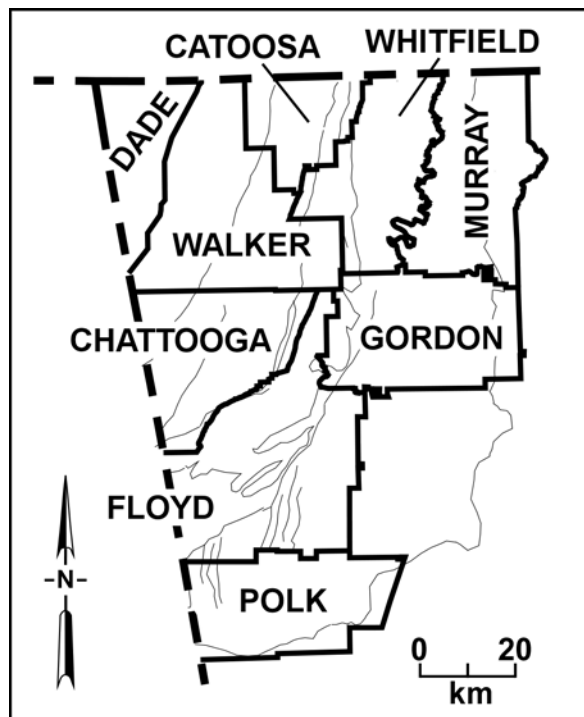


Figure 3-3. County location map for northwestern Georgia.

| SERIES | ALABAMA | TENNESSEE |
|-------------------|------------------------------------|------------------------------------|
| MIDDLE ORDOVICIAN | Middle Ordovician undifferentiated | Middle Ordovician undifferentiated |
| | | |
| LOWER ORDOVICIAN | Odenville Limestone | |
| | Newala Limestone | Mascot Dolomite |
| | Longview Limestone | Kingsport Formation |
| | Chepultepec Dolomite | Chepultepec Dolomite |
| UPPER CAMBRIAN | Copper Ridge Dolomite | Copper Ridge Dolomite |

Figure 3-4. Comparative stratigraphic column for the Knox Group in Alabama and Tennessee showing the relationship of the Mascot Dolomite and Kingsport Formation to the Longview Limestone and Newala Limestone, from Raymond (1993).

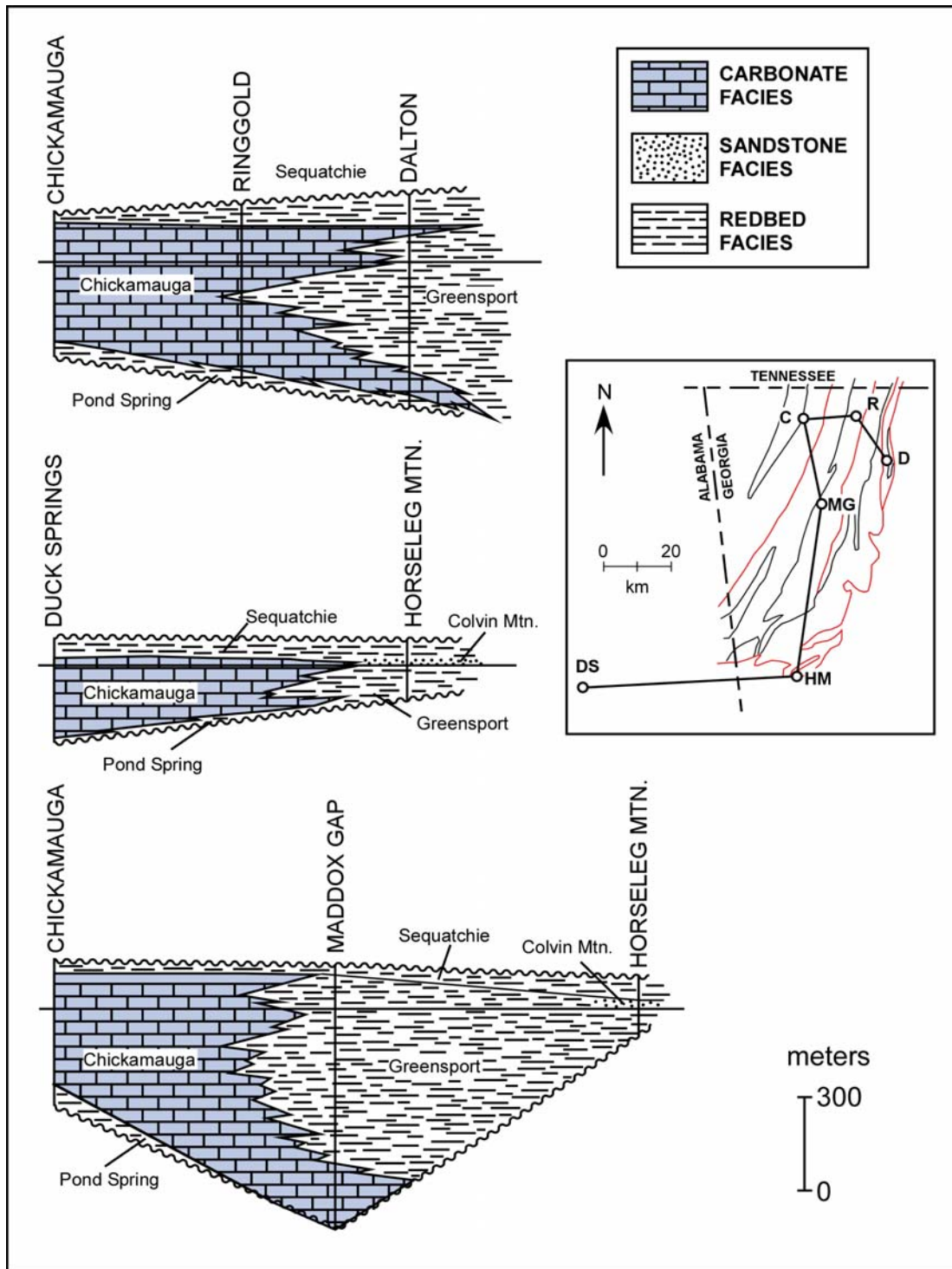


Figure 3-5. Cross sections of the Middle and Upper Ordovician showing the two dominant facies, modified from Carter and Chowns (1993) with field observations (thickness and correlation) for Maddox Gap. Generally, shallow-water carbonates of the Middle Ordovician Chickamauga Limestone predominate in the northwest and grade southeastward into peritidal clastic red bed facies of the Middle and Upper Ordovician Greensport and Sequatchie Formations.

| GEORGIA | | | | | TENNESSEE | | | GEORGIA | | |
|---------------|----------------|-------------------------------|---------------|-----------------|-------------------|---------------|--------------------|--------------|-----------------|------------|
| HAYES (1894) | MAYNARD (1912) | BUTTS AND GILDERSLEEVE (1948) | COOPER (1956) | CRESSLER (1964) | BASSLER (1932) | WILSON (1949) | SWINGLE (1964) | THIS REPORT | | |
| CHICKAMAUGA | FORMATION | SEQUATCHIE | | SEQUATCHIE | RICHMOND | SEQUATCHIE | SEQUATCHIE-JUNIATA | SEQUATCHIE | ORDOVICIAN | |
| | | MAYS-VILLE | | MAYSVILLE | LEIPERS | LEIPERS | LEIPERS | LEIPERS | | UPPER |
| | | TRENTON | | TRENTON | CATHEYS | CATHEYS | CATHEYS | CATHEYS | ORDOVICIAN | |
| | | TRENTON | | TRENTON | CANNON | BIGBY-CANNON | BIGBY-CANNON | CANNON | | SUPERGROUP |
| | | | | TRENTON | BIGBY | NASHVILLE | HERMITAGE | HERMITAGE | | |
| | | | | TRENTON | HERMITAGE | NASHVILLE | HERMITAGE | HERMITAGE | | HERMITAGE |
| | | LOWVILLE | | CARTERS | LOWVILLE-MOCCASIN | LOWVILLE | CARTERS | CARTERS | CARTERS | MIDDLE |
| | | LEBANON | | LEBANON | LEBANON | LEBANON | LEBANON | LEBANON | LEBANON | |
| | | LENOIR (RIDLEY) | | RIDLEY (PIERCE) | LENOIR | RIDLEY | RIDLEY | RIDLEY | RIDLEY (PIERCE) | |
| | | MOSHEIM | | MURFREESBORO | MOSHEIM | MURFREESBORO | MURFREESBORO | MURFREESBORO | MURFREESBORO | |
| MURFREESBORO | | MURFREESBORO | MURFREESBORO | MURFREESBORO | MURFREESBORO | MURFREESBORO | MURFREESBORO | | | |
| NEWALA | | NEWALA | NEWALA | WELLS CREEK | WELLS CREEK | POND SPRING | POND SPRING | | | |
| KNOX DOLOMITE | KNOX DOLOMITE | KNOX DOLOMITE | | KNOX GROUP | BEEKMANTOWN | KNOX DOLOMITE | KNOX GROUP | KNOX GROUP | LOWE ORDOVIC | |

Figure 3-6. Subdivisions of the Chickamauga Supergroup, from Milici and Smith (1969).

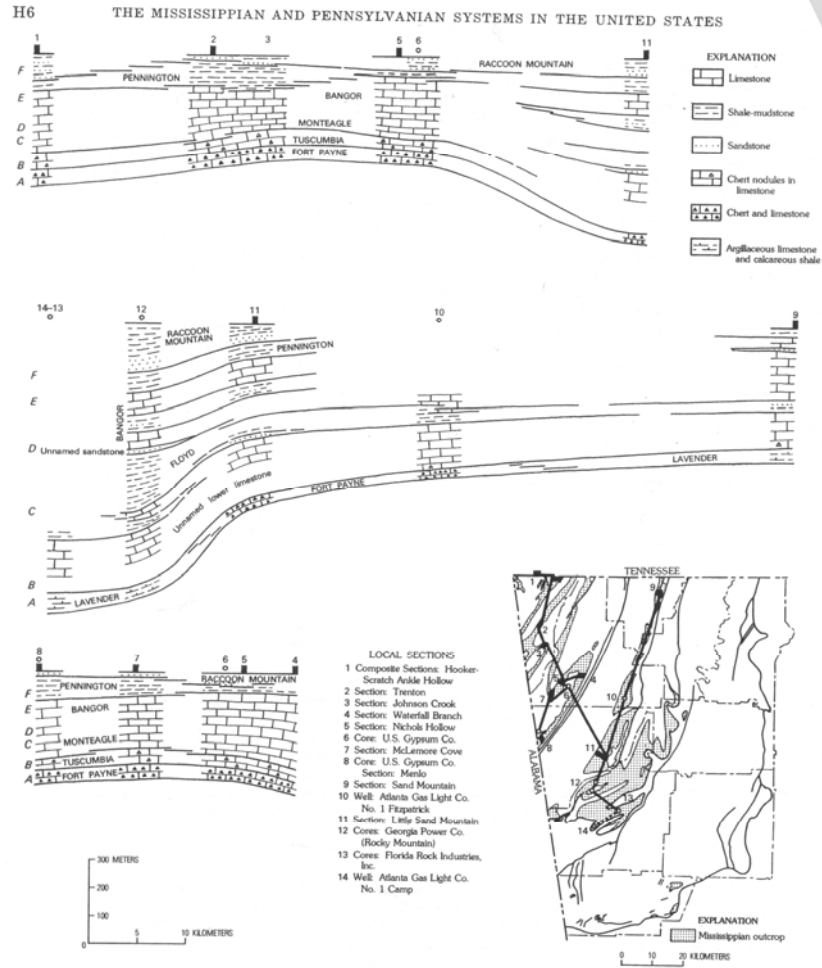
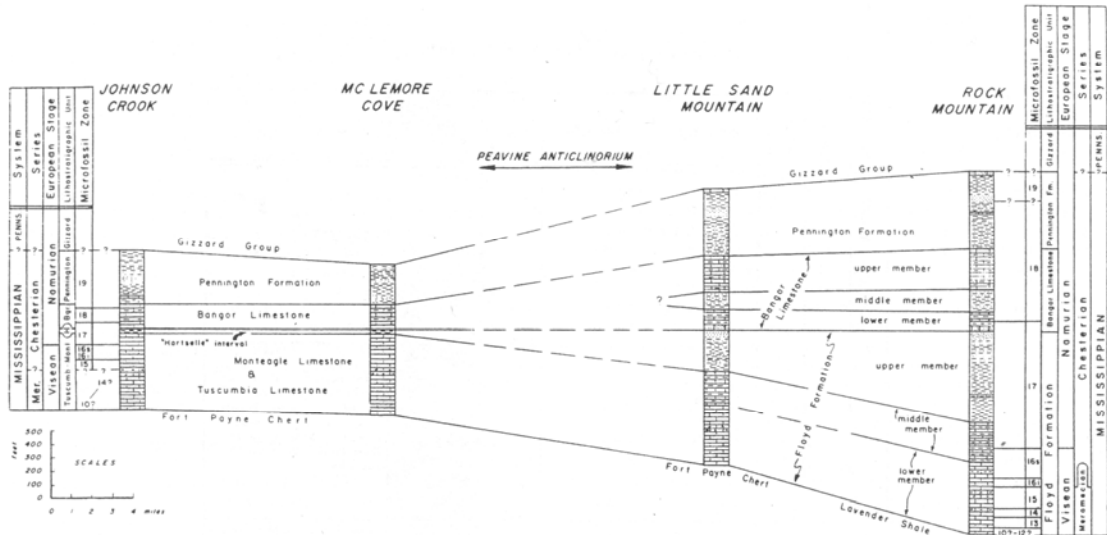


FIGURE 4.—Diagrammatic stratigraphic cross sections of Mis- Clement (1952) (section 3), Moore (1954) (section 2).

Figure 3-7. Diagrammatic stratigraphic cross sections and correlations for the Mississippian succession in northwestern Georgia, from Thomas (1979).



Mississippian Stratigraphy

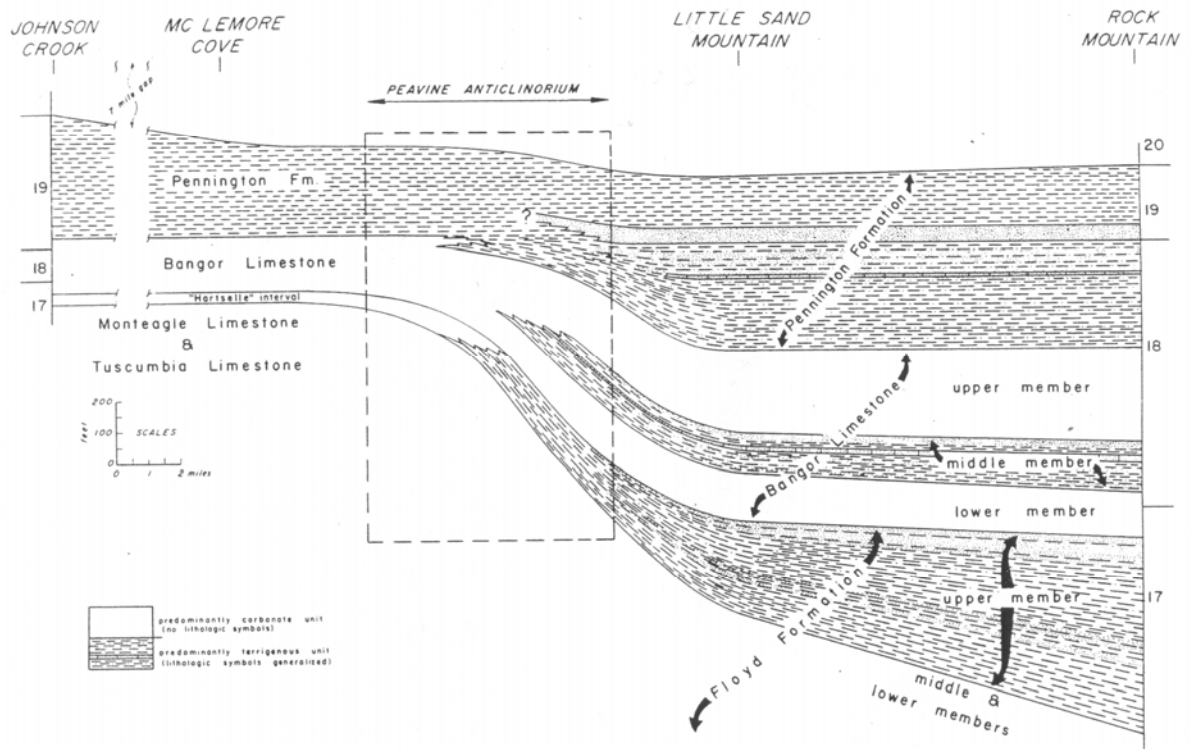


Figure 3-8. Alternate interpretations of the Mississippian succession in northwestern Georgia, from Rich (1986b).

| UNDERLYING ROCKS | PENNSYLVANIAN ROCKS | | | | | | | | AUTHOR AND DATE |
|-------------------------------------|--------------------------------|------------------------|------------------------|-------------------------------------|--------------------------------|----------------------|------------------|----------------------|------------------------------------------------|
| Upper Sub-Carboniferous | Coal Measures | | | | | | | | Little 1876 |
| Bangor Limestone | Lookout Sandstone | | | | Walden Sandstone | | | | Hayes 1892 |
| Pennington Formation | Pottsville Formation | | | | | | | | Georgia Div. of Mines, Mining and Geology 1939 |
| Pennington Formation | Lookout Formation | | | | Walden Formation | | | | Moore and others 1944 |
| | Unnamed | Lower Conglomerate | Unnamed | Upper Conglomerate | | | | | |
| Pennington Formation | Lookout Formation | | Whitwell Shale | Bonair Sandstone | Vandever Shale | Rockcastle Sandstone | | Johnson 1946 | |
| | Gizzard Member | Sewanee Member | | | | | | | |
| Pennington Formation | Lee Group | | | | | | | | Wanless 1946 |
| | Unnamed | Warren Point Sandstone | Gizzard Formation | Sewanee Conglomerate | Whitwell Shale | Eastland Sandstone | Newton Sandstone | | |
| Pennington Formation | Carboniferous (on map) | | | | | | | | Butts and Gilderleeve 1948 |
| | Pennsylvanian (in legend) | | | | | | | | |
| | Pottsville Formation (in text) | | | | | | | | |
| Pennington Formation | Pottsville Series | | | | | | | | Stearns and Mitchum 1962 |
| | New River Group | | | | | | | | |
| Pennington Formation | Gizzard Formation | | | | Crab Orchard Mountains Group | | | | Culbertson 1963 |
| | Raccoon Mountain Formation | Warren Point Sandstone | Signal Point Shale | Sewanee Conglomerate | Whitwell Shale | Newton Sandstone | Vandever Shale | Rockcastle Sandstone | |
| Pennington Formation | Gizzard Group | | | | Crab Orchard Mountains Group | | | | Wilson 1965 |
| | Norwood Cove Formation | Flat Rock | Warren Point Sandstone | Signal Point Shale | Sewanee Conglomerate | | | | |
| Pennington Formation | Interval A ₂ | | | | | | | | McKee and others 1975 |
| Pennington Formation | Lookout Sandstone | | | | Pennsylvanian undifferentiated | | | | Georgia Geological Survey 1976 |
| | Gizzard Formation | | | Sewanee Conglomerate | | | | | |
| Bluff-forming sandstone | | | | | | | | This paper | |
| Rocks below bluff-forming sandstone | | | | Rocks above bluff-forming sandstone | | | | | |

Figure 3-9. Correlation chart noting evolution of nomenclature of the Pennsylvanian succession in northwestern Georgia, from Cramer (1979).

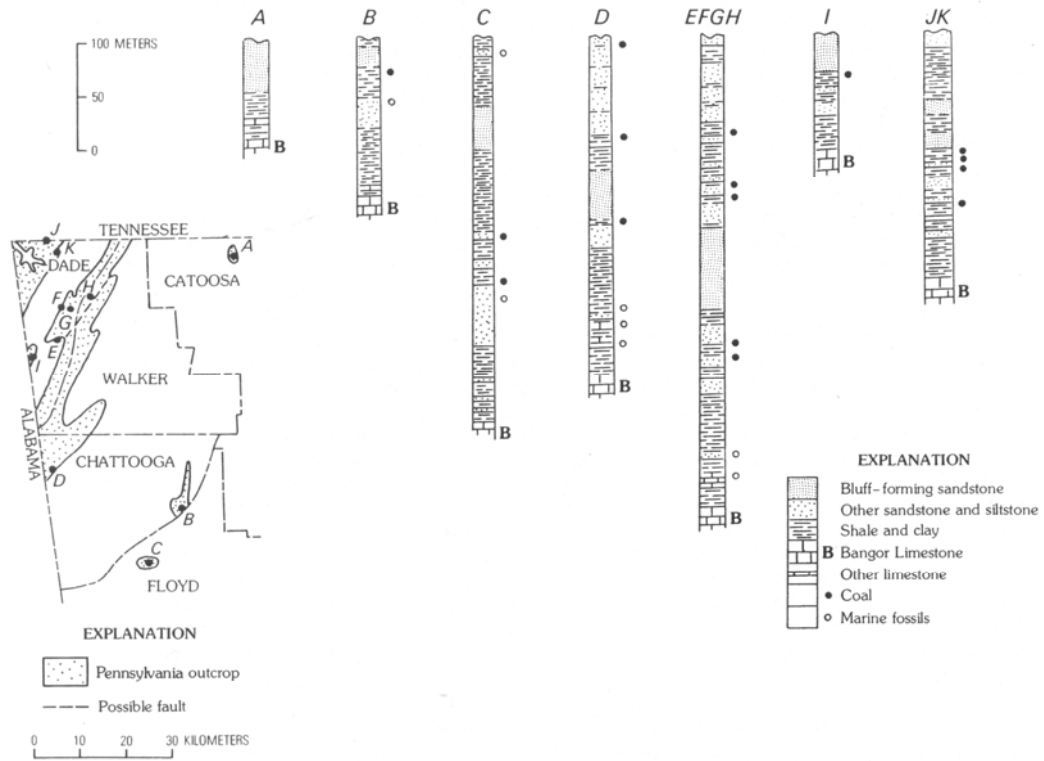


Figure 3-10. General columnar sections of the Upper Mississippian and Lower Pennsylvanian succession in northwestern Georgia, from Cramer (1979).

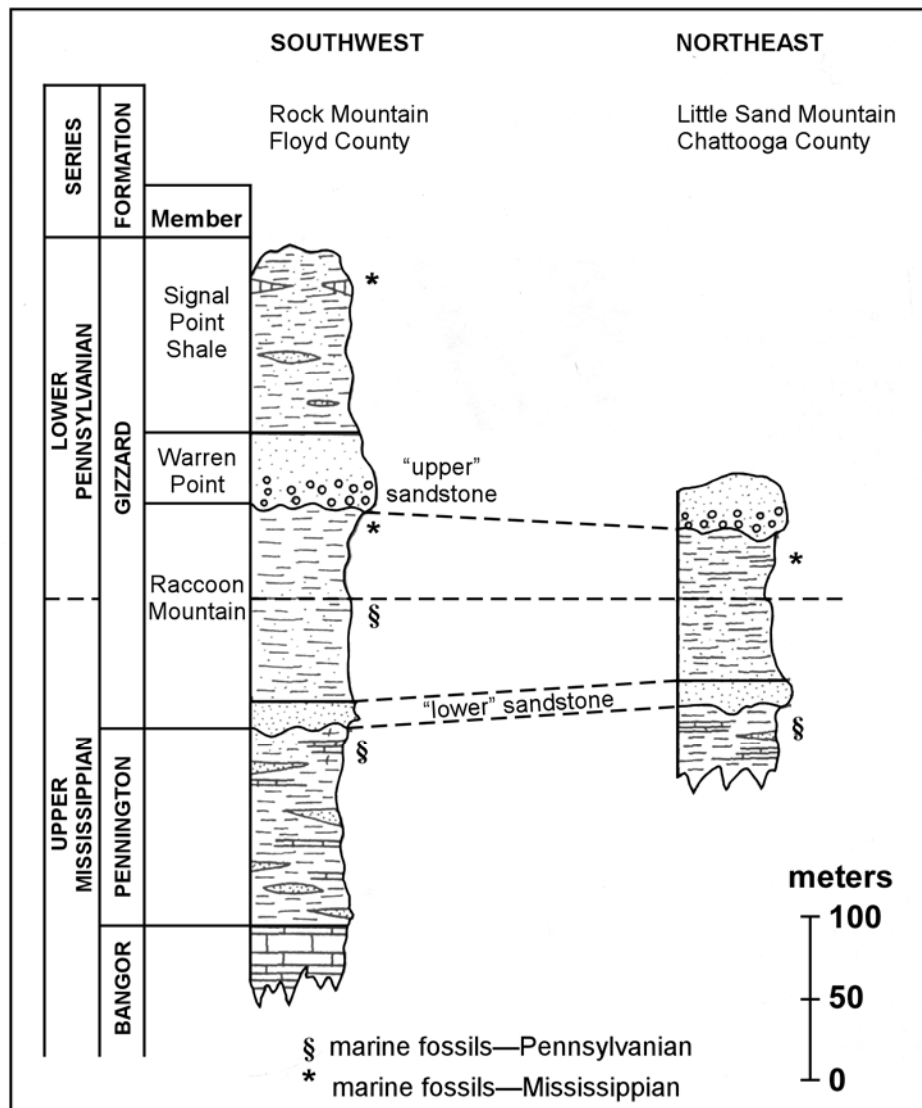


Figure 3-11. Details of biostratigraphic markers in the Lower Pennsylvanian and Upper Mississippian, adapted from Crawford (1989).

Chapter IV:
STRUCTURAL GEOLOGY OF NORTHWESTERN GEORGIA

4.1 INTRODUCTION TO REGIONAL STRUCTURAL GEOLOGY

Hayes first published studies of the southern Appalachian faults in northwestern Georgia (1891), and of the general structural geology of the region (1894) and in the area of Rome (1902). Spencer (1893) summarized the folds and major faults in each county in northwestern Georgia and noted bedding orientation measurements. Butts (1948) summarized the structural geology of northwestern Georgia particularly in the context of the major folds and thrust faults. Kesler (1975) documented the structural geology of northwestern Georgia with particular focus on the Rome and Coosa faults. Chowns (1989) summarized the structural geology of northwestern Georgia particularly in the context of the major thrust sheets and thrust faults, which he divided into the foreland thrust domain, the imbricate thrust domain, and the Rome–Coosa thrust domain. Rich (1992) documented a possible relation of major folds and faults in northwestern Georgia to a set of basement faults. Rich (1992) suggested that basement faults controlled location of folds and localized changes in stratigraphic thicknesses that directly affected changes in structural style. Most recently, Thomas and Bayona (2005) summarized the regional structural geology and documented details related to thrust sequences and palinspastic restorations of the major thrust sheets, and along-strike structural changes at transverse zones.

This chapter will integrate the past published work with new data collected as part of the current research. Parts of this chapter have been previously assembled for a manuscript by Cook and Thomas (*in press*).

4.1.1 Review of regional thrust sheets and thrust faults

In northeastern Alabama and northwestern Georgia, the frontal structures include the northeastward-striking Sequatchie anticline and Lookout Mountain and Pigeon Mountain synclines (Figures 1-3 and 1-4). Southeastward at the trailing edge of the Coosa thrust sheet, the approximately 070-striking Cartersville fault intersects the approximately 000-striking Great Smoky fault (Figure 1-3). These two structural strikes throughout the trailing structures define a subrecess of the Appalachian thrust belt in

northwestern Georgia. Just southeast of Lookout Mountain–Pigeon Mountain syncline, the composite Kingston–Chattooga–Clinchport thrust sheet bears interfering structures with the two regional trends (Figure 1-4). Farther southeast, at the trailing edge of the composite thrust sheet in the Georgia subrecess, the two regional trends are observed in the traces of the Rome fault and the Coosa fault (Figure 1-4).

4.2 REGIONAL SETTING OF SOUTHERN APPALACHIAN STRUCTURES IN GEORGIA

Regionally, the Appalachian thrust belt includes the gradually curved Tennessee salient, convex toward the craton in the direction of thrust translation, and the more angular bend of the Alabama recess, concave toward the craton. At the Georgia subrecess in northwestern Georgia, north-northeastward-striking thrust faults and related folds in the southern arm of the Tennessee salient intersect east-northeastward-striking thrust faults and related folds that diverge from the predominant strike of the eastern arm of the Alabama recess (Figure 1-3).

The Sequatchie anticline (Figure 1-3), along the northwestern structural front of the southern Appalachian thrust belt (Thomas and Bayona, 2005), has a remarkably straight axial trace trending approximately 040 and extending from the front of the Alabama recess on the southwest to a tangent near the apex of Tennessee salient on the northeast. The straight trace crosses the foreland with no deflection in strike at the Georgia subrecess. Parallel to and southeast of the Sequatchie anticline, the frontal Appalachian structures are characterized by narrow anticlines and broad flat-bottomed synclines, the southeasternmost of which is the Lookout Mountain syncline, and a southeastern branch, the Pigeon Mountain syncline (Figure 1-3).

In contrast, along the trailing edge of the Appalachian sedimentary thrust belt, the Cartersville and Great Smoky faults mark the leading edges of metamorphic thrust sheets and intersect at approximately 70° (Figure 1-3). In Alabama, the Cartersville and related Talladega faults generally parallel the regional 040 trend of the thrust belt; but in Georgia, the Cartersville fault bends to 070 and intersects the Great Smoky fault, which trends approximately 000 (Figure 1-3). The intersection of the Cartersville and Great

Smoky faults is the most pronounced surface expression of the two regional structural trends in the Georgia subrecess (Thomas and Bayona, 2005).

In the trailing part of the Appalachian sedimentary thrust belt (in the immediate footwall of the bend in the Cartersville/Great Smoky fault system), the trend of the Eastern Coosa fault bends abruptly from 020 on the north to 070 on the southwest, framing the Georgia subrecess (Figure 1-3). Where the fault bends abruptly in strike, several trailing splays extend southward, continuing along the direction of strike of the north-northeast-striking leading fault (Figure 1-4). The intersection between the Eastern Coosa fault and the trailing splays in the hanging wall defines a clear interference pattern between the two dominant strike directions of the leading fault. Farther southwestward in easternmost Alabama, the 070-striking segment of the Coosa fault merges into the predominant 040-trending Appalachian structures (Figure 1-3).

In intermediate structures between the sharply bent Eastern Coosa fault and the nearly straight frontal structures (*e.g.*, Lookout Mountain syncline), the bend in strike is absorbed by various intersecting and interfering folds and thrust faults in the Kingston–Chattooga–Clinchport composite thrust sheet (Figures 1-3 and 1-4). The distinct structural intersection in these intermediate structures, at an angle of approximately 50° between two distinct elements of regional strike, characterizes the Georgia subrecess. Structures striking 020 in the southern arm of the Tennessee salient and striking 070 in the eastern arm of the Alabama recess plunge from opposite directions into the depression of the Floyd synclinorium in the trailing part of the Kingston–Chattooga–Clinchport composite thrust sheet (Figures 1-3 and 1-4).

The Rome thrust sheet, consisting of Cambrian shale-dominated facies of the Conasauga Formation, bounds the southern and eastern sides of the subrecess (Figures 1-3 and 1-4). Trailing the eastern side of the subrecess, the Rome fault has a highly sinuous trace, indicating a folded, subhorizontal fault surface (Figures 1-3 and 1-4). Along the southern side, the Rome fault trace has an average trend of approximately 090 but is highly sinuous in detail (Cressler, 1970), indicating a subhorizontal envelope of folds of the fault surface that cuts obliquely across several thrust ramps and folds in the footwall. In addition to the irregular map trace, the shallow dip of the Rome thrust sheet is evident from the lack of seismic imaging of the near-surface fault (Thomas and Bayona, 2005).

Hayes (1891, 1902) and Butts (1948) cited the preservation of the Rome fault in synclinal structures as evidence for folding after the emplacement of the Rome fault hanging wall. The Rome fault truncates footwall folds that are coaxial with the folds of the fault surface; however, the fault-truncated footwall beds are folded more tightly than is the fault surface. The map relationships show that older footwall folds were truncated by an out-of-sequence Rome fault, and that the footwall folds were subsequently tightened, folding the Rome thrust sheet along with the footwall beds (Thomas and Bayona, 2005). Farther to the west in Alabama, the trace of the Rome fault curves to parallel the large-scale Appalachian structures (Figure 1-3).

4.3 STRUCTURE OF THE GEORGIA SUBRECESS IN NORTHWESTERN GEORGIA

Unique structural expressions distinguish three structural domains in the Georgia subrecess: 1) the Kingston–Chattooga anticlinorium, which includes the frontal structures of the thrust sheet; 2) the Little Sand Mountain–Horn Mountain fold train, which trends approximately 020 in the northern part of the Floyd synclinorium; and 3) the Simms Mountain–Horseleg Mountain fold train, which trends approximately 070 in the southern part of the Floyd synclinorium (Figure 1-4). The two distinctive structural trends are evident in Figure 4-1. Folds of both structural trends plunge into the depression of the Floyd synclinorium in the trailing part of the Kingston–Chattooga composite thrust sheet (Figures 1-3 and 1-4). An interference pattern in the structural intersection in the Georgia subrecess between east-northeastward- and north-northeastward-striking folds and faults enables the tracing of both strike directions through parts of the intersection. Graphical presentations (such as stereoplots and Rose diagrams) of the structural orientation data collected during the present research were prepared using GEOrient version 9.44 software package designed by Dr. Rod Holcomb.

4.3.1 *Kingston–Chattooga anticlinorium*

The northwestward-verging Kingston fault and a leading imbricate bound the southeastern limb of the Lookout Mountain syncline (Figure 1-4). Only a very gentle concave-cratonward curvature of the Kingston fault corresponds roughly to the more

angular recess between the fold trains within the Floyd synclinorium farther to the southeast. The Chattooga fault and a leading imbricate parallel the trailing limb of the Kingston thrust sheet and end northeastward along strike, indicating that the Chattooga fault is a splay in a composite thrust sheet from the detachment of the Kingston fault (Figure 1-4).

The leading part of the Kingston–Chattooga composite thrust sheet forms the structurally high Kingston–Chattooga anticlinorium exposed in Units 1-3 (Figure 1-4). The anticlinorium is deformed by internal folds and the two splays of the Chattooga fault. The trailing limb of the anticlinorium (the Taylor Ridge monocline) dips southeastward beneath the relatively deep Floyd synclinorium, which plunges into a regional depression within the recess between the oppositely plunging fold trains (Figure 1-4). The Taylor Ridge monocline is expressed at the surface primarily in Unit 3, striking approximately 025 on the map in Figure 1-4. The calculated average bedding plane is oriented 033 20 SE (Figure 4-2). Five bedding attitude readings from a small-scale fold exposed in the US27/GA1 roadcut through Taylor Ridge monocline, however, affect the calculations from the stereoplot; the small-scale fold orientations are removed from the data set in Figure 4-3. Figure 4-3 shows that the calculated average bedding plane is oriented 030 20 SE. The calculated girdle, which is a best-fit great circle that approximates the fold plane, is nearly vertical (Figure 4-3). The calculated β -axis, which is the pole to the calculated girdle and approximates the orientation of the fold axis, plunges 4° to a trend of 199 (Figure 4-3). Bedding orientations from only the small-scale fold in Taylor Ridge monocline are shown in Figure 4-4; the average bedding plane is oriented 303 56 SW, which shows that the fold is nearly orthogonal to the general trend of the monocline.

4.3.2 *Little Sand Mountain–Horn Mountain fold train*

To the north and east of the subrecess, south-southwestward-plunging flat-bottomed synclines and narrow, steep-sided anticlines approximately parallel the north-northeastward-striking Chattooga fault and Taylor Ridge monocline, and plunge south-southwestward into the depression of the Floyd synclinorium (Figure 1-4). Little Sand Mountain syncline, Horn Mountain anticline, and the intervening folds define a north-northeastward-trending fold train. Johns, Mill, and South Horn Mountain anticlines have the geometry of cylindrical folds, except at the southward-plunging ends which are more

conical folds. The folds in this fold train demonstrate a collective calculated girdle oriented 280 86 SW, and a calculated fold axis (β) that plunges 4° to a trend of 010, as shown in Figure 4-5. This north-northeastward plunge of the calculated fold axis is a reflection of irregularities in the shallow plunge of the fold axes of the cylindrical parts of these anticlines (particularly Horn Mountain anticline). Furthermore, although the conical plunging ends of the folds clearly plunge southward in map view (Figure 1-4), exposure of the down-plunge parts of the folds is poor, and thus little or no data were collected and included in the stereoplot. All of the anticlines rise steeply above the flat-bottomed synclines and have amplitudes of approximately 650 to 1500 m. Spacing between the anticlines is approximately 4 to 7 km.

The flat-bottomed Little Sand Mountain syncline, which is expressed at the surface in a sandstone in Unit 4, parallels the southeastern (downdip) side of the Taylor Ridge monocline, trending approximately 020 (Figure 1-4). The northwestward-verging Clinchport fault ramps through the trailing (southeast) limb of the Little Sand Mountain syncline, and northeastward along strike, obliquely truncates the 000-trending Dick Ridge anticline (Figure 1-4). The calculated fold plane for Little Sand Mountain syncline is vertical, as shown in Figure 4-6, and the calculated fold axis (β) trends 040.

Dick Ridge anticline is the most sinuous separate fold in the map area. In the northern part of the study area near the northeastern corner of Walker County, Dick Ridge anticline trends approximately 015 on the map in Figure 1-4. In this area, the northwestern limb of the anticline is exposed in a roadcut. The average bedding plane at this location is oriented 018 73 NW, and the calculated fold axis for the anticline there plunges 1° to a trend of 199 (Figure 4-7). Southward toward the southeastern end, the anticline curves into an intersection with the northeastern end of Strawberry Mountain (*cf.* section 4.3.3) and trends approximately 355 (Figure 1-4).

Johns Mountain anticline is a cylindrical ramp anticline in the hanging wall of the Clinchport fault exposed in Units 2 and 3, trending approximately 020 on the map in Figure 1-4. The Johns Mountain anticline ends in a southwestward-plunging, apparently conical fold associated with the southwestern end of the Clinchport fault (Figure 1-4).

Northeastward along strike, the Johns Mountain anticline merges with the up-plunge part of the 000-trending Horn Mountain anticline. The calculated fold axis for Horn Mountain anticline plunges 23° to a trend of 012 (Figure 4-8).

In the area where Horn Mountain anticline plunges southward, it intersects two smaller, 000-trending, doubly plunging anticlines: Mill Mountain and South Horn Mountain anticlines (Figure 1-4). In plan view, these two smaller anticlines are similar in shape to the smaller Turkey Mountain and Baugh Mountain anticlines and an unnamed fold just to the northeast in a window in the hanging wall of the Rome fault. Mill Mountain and South Horn Mountain anticlines, however, are higher in amplitude than these smaller anticlines. The amplitudes of Mill Mountain and South Horn Mountain anticlines are similar to that of Horn Mountain anticline, which makes the individual structures nearly indistinguishable near the area of intersection.

Turkey Mountain anticline, in the hinterland of the southwestern end of Johns Mountain anticline, is a doubly plunging anticline exposed in Unit 3, trending 015 (Figure 1-4). The calculated fold plane is nearly vertical, as shown in Figure 4-9, and the calculated fold axis trends 206.

4.3.3 *Simms Mountain–Horseleg Mountain fold train*

On the southern side of the subrecess, east-northeastward-plunging flat-bottomed synclines and narrow, steep-sided anticlines diverge from the north-northeastward-striking Chattooga fault and Taylor Ridge monocline, and plunge northeastward into the depression of the Floyd synclinorium (Figure 1-4). Simms Mountain anticline, Horseleg Mountain anticline, and the intervening folds define a north-northeastward-trending fold train. The folds in this fold train demonstrate a collective average fold axis that plunges 3° to a trend of 065, as shown in Figure 4-10. The anticlines rise steeply above the flat-bottomed synclines and have amplitudes of approximately 650 to 1000 m; spacing between the anticlines is approximately 4 to 7 km.

Simms Mountain anticline trends approximately 072 and plunges into the deepest part of the Floyd synclinorium (Figure 1-4). Southwestward up-plunge, Simms Mountain anticline shows distinct fold interference with the Taylor Ridge monocline (Figure 1-4). Near the northeastern plunging end, the fold plane is nearly vertical and the calculated fold axis plunges 5° to a trend of 062 (Figure 4-11). Near the southwestern end of Simms

Mountain anticline, the northwestern limb intersects Taylor Ridge monocline. In this area, along a road through the northwestern limb, numerous outcrop-scale folds can be observed. The outcrops at this location show a calculated fold axis plunges 33° to a trend of 072 (Figure 4-12). The steeper plunge near the structural intersection demonstrates lateral discontinuity of structures at this scale and suggests structural interference and/or overprint of the dip of Taylor Ridge monocline on the fold axis of Simms Mountain anticline.

The flat-bottomed Rock Mountain syncline is expressed at the surface in sandstones of Unit 4 and trends approximately 067 on the map in Figure 1-4. The average bedding plane observed for Rock Mountain is oriented 067 28 NW (Figure 4-13). The fold plane is nearly vertical, as shown in Figure 4-13, and the calculated fold axis trends 063.

Lavender Mountain anticline is a cylindrical fold, forming a ridge of Unit 3, trending approximately 064 in map view, and ending in a northeastward-plunging conical fold (Figure 1-4). Near the northeastern end of Lavender Mountain anticline, the fold plane is nearly vertical and the calculated fold axis plunges 5° to a trend of 080 (Figure 4-14). The northeasterly plunge is also represented in the average bedding orientation of 355 05 NE (Figure 4-14). The southwestern up-plunge end of the Lavender Mountain anticline shows fold interference with Turnip Mountain anticline, which is a ramp anticline exposed in Units 2 and 3, trending approximately 020 in map view, approximately parallel with the Taylor Ridge monocline in the footwall (Figure 1-4).

Judy Mountain syncline is expressed in a sandstone within Unit 4 immediately southwest of Lavender Mountain anticline. Judy Mountain syncline trends approximately 067 (Figure 1-4).

Horseleg Mountain anticline is exposed in Unit 3 and trends approximately 059 (Figure 1-4). The average bedding plane observed for Horseleg Mountain is oriented 062 58 NW (Figure 4-15). The calculated fold axis plunges 11° to a trend of 055 (Figure 4-15).

Strawberry Mountain anticline, which is approximately 17 km northwest of Simms Mountain anticline and on the opposite end of the Little Sand Mountain syncline, trends approximately 059 on the map in Figure 1-4, parallel with other anticlines in the

Simms Mountain–Horseleg Mountain fold train. Strawberry Mountain anticline ends in both directions along strike by interference with the Taylor Ridge monocline on the southwest and with Dick Ridge anticline and the Clinchport fault (part of the Simms Mountain–Horseleg Mountain fold train) on the northeast (Figure 1-4). Although the Strawberry Mountain anticline has the orientation of the Simms Mountain–Horseleg Mountain fold train, it is isolated within the Little Sand Mountain–Horn Mountain fold train, clearly showing interference between the two fold sets.

Bedding orientations near the crest of Strawberry Mountain anticline are accessible on a forestry road along the northwestern half of the mountain; the poles to these bedding planes are plotted in Figure 4-16. In the stereoplot, the calculated mean plane strikes 068 and dips 16° SE, and the calculated fold axis plunges 1° to a trend of 244. These measurements are in accord with the observed map-scale structures.

Bedding attitudes across part of Strawberry Mountain anticline near the southwestern end that intersects Taylor Ridge monocline are exposed in an approximately 2-km-long roadcut north of Subligna; poles to bedding through this roadcut are plotted in Figure 4-17. In this stereoplot, average bedding orientation is 075 05 NW, and the calculated fold axis (β) plunges 5° to a trend of 005. This trend is closer to that of Taylor Ridge monocline than that of Strawberry Mountain anticline; and, thus, it suggests some local structural overprint or interference between these two folds in the area near the intersection. Upon closer inspection, a marked change in strike can be observed along this roadcut; the data on either side of the abrupt change were subsequently separated into northwestern and southeastern populations. The northwestern population is plotted in Figure 4-18. In this stereoplot, the calculated mean plane strikes 034 and dips 7° NW, and the calculated fold axis plunges 3° to a trend of 014. The southeastern population is plotted in Figure 4-19. In this stereoplot, the calculated mean plane strikes 285 and dips 6° NE, and the calculated fold axis plunges 6° to a trend of 023. The differences between Figures 4-18 and 4-19 demonstrate the existence of two distinct populations of structural orientations, which correspond to two domains on either side of the abrupt change in strike along the roadcut. The more north-northwesterly calculated fold axis of the northwestern population suggests a stronger

overprint from the structural trend of Taylor Ridge monocline than is seen in the southeastern population.

Similarly, the structural orientations of bedding on Taylor Ridge monocline change near the intersection with Strawberry Mountain anticline. To the west of the intersection, bedding on Taylor Ridge monocline strikes 050 on average (Figure 4-20). In the adjacent areas to the north and south of the intersection, bedding on Taylor Ridge monocline strikes 027 and 038, respectively, on average (Figures 4-21 and 4-22). An outcrop farther to the north along Taylor Ridge monocline from the intersection with Strawberry Mountain anticline, which is shown in Figure 4-23, contains one bedding orientation that strikes 065 and dips 26° SE. The mean bedding plane for all these data strikes 025 and dips 17° SE. If the single more east-northeasterly bedding attitude measurement is omitted, the remaining data show a mean bedding orientation that strikes 020 and dips 17° SE (Figure 4-24), and the calculated fold axis plunges 1° to a trend of 022. These stereoplots demonstrate that the bedding at the outcrop is oriented along the primary structural trend of Taylor Ridge monocline. The more east-northeasterly bedding attitude, however, is only about 3 km from the center of the structural intersection with Strawberry Mountain anticline, and indicates a small-scale fold parallel with the general structural trend of the intersecting anticline.

The intersection between Strawberry Mountain anticline and Dick Ridge anticline also demonstrates structural interference. Bedding attitudes from outcrops in the area of the intersection are shown in Figure 4-25. In this stereoplot, the mean bedding orientation strikes 060 and dips 17° SE, and the calculated fold axis plunges 15° to a trend of 175. The mean bedding orientation is approximately the same as the structural trend of Strawberry Mountain anticline and the calculated fold axis is similar to the structural trend of Dick Ridge anticline. These data suggest that the bedding in this limb of Strawberry Mountain anticline may be locally overprinted with a fold that approximately parallels Dick Ridge anticline.

4.4 BASEMENT FAULTS IN NORTHWESTERN GEORGIA

Structural cross sections across northwestern Georgia by Woodward *in* Woodward and Gray (1985) depict the basement as relatively flat and, thus, do not

include any interaction between basement faults and the overlying stratigraphy or structures. Similarly, in a study of a seismic reflection profile across part of the Valley and Ridge in Tennessee, Harris (1976) attributed apparent broad folds in the lower part of the stratigraphic succession to “pull-ups” caused by acoustic velocity contrasts. In contrast, Thomas (1982) and Kaygi *et al.* (1983) suggested that basement faults with considerable offset along them influenced regional sedimentary deposition and structural styles in Alabama. These basement faults are related to Precambrian rifting along the continental margin as suggested by Thomas (1977). Rich (1992) noted that the displacement along the basement faults diminishes northeastward from Alabama and that the effects of large-displacement basement faults on the stratigraphy and structure in the Valley and Ridge of Tennessee is not yet evident; he also suggested that the seismic “pull-ups” cited by Harris (1976), however, likely indicate some basement relief below the décollement. Rich (1992) further noted that, as a result of the northeastward decrease in basement fault offset, Appalachian structures in Georgia may represent the transition from the structural styles in Alabama into those more characteristic in Tennessee. Moreover, Rich (1992) noted that thrust deformation in northwestern Georgia was directed primarily “uphill” over the reactivated basement faults and that duplex formation could have been “induced partly” by buttressing effects of the steep basement faults. Wiltchko and Eastman (1983, 1988) documented how basement warps and faults concentrate stress in the immediately overlying cover rocks. Along strike to the southwest in Alabama, Thomas (2001) demonstrated that basement faults localized a thicker deposit of Cambrian shales that later were deformed into ductile duplexes; Cook and Thomas (*in press*) later demonstrated a similar structure in northwestern Georgia.

Research by Rich (1992) documented the configuration of basement faults in northwestern Georgia (Figure 4-26) on the basis of the location and orientation of surface structures and Mississippian facies changes (Rich noted a lack of seismic reflection data in the report). Rich (1992) interpreted these steep basement faults to have been reactivated intermittently during the Paleozoic; and, thus, they significantly influenced the geometry and locations of Appalachian folds and faults, and the depositional framework, especially during the Mississippian (*cf.* section 3.7). The interpreted basement faults of Rich (1992) can be divided into two primary orientations, north-

northeast and east-northeast, which correlate directly with surface structures and with regional-scale facies changes.

According to the map of Butts (1948), the Clinchport fault ends southwestward along strike near the northeastern end of Simms Mountain. Rich (1992) interpreted a shift from horizontal displacement along the fault into a “disturbed zone” within the Floyd synclinorium, which functions as a displacement “transfer zone” (*i.e.*, of Dahlstrom, 1969) and continues southwestward under the Rome fault. Similarly, Chowns (1989) shows a speculative correlation of the Clinchport fault to a fault at the southwestern end of Lavender Mountain that is truncated on the southwestern end by the Rome fault. Chowns (1989) and Rich (1986c) suggested that the Clinchport fault is linked on the southwest with the Helena fault in Alabama. Rich (1992) concluded that if the two faults are linked, then the down-to-southeast basement faults were a “major causal factor in producing thrust slices that extended longitudinally over great distances along the Appalachian trend as relatively continuous tectonostratigraphic packages”; and that the different trends in the basement faults directly influenced shifts in direction of thrust deformation.

Rodgers (1970) noted that the Rome fault in the type area indicates a deep depression. Rich (1992) related the northern boundary of this depression to an east-northeast-directed basement fault, which parallels those that he interpreted to underlie Lavender and Simms Mountains.

More recently, studies by Bayona and Thomas (2003, 2006) and Thomas and Bayona (2005) documented the configuration of basement faults in northwestern Georgia, and their research included data from numerous seismic reflection profiles. The basement fault data from these studies were used to construct the cross sections included with the present research. Essentially, Bayona and Thomas (2006) show a transition in Georgia between two orientations of basement faults: one northeast-striking that corresponds to the Alabama promontory and one north-northeast-striking that corresponds to the southwestern flank of the Tennessee embayment.

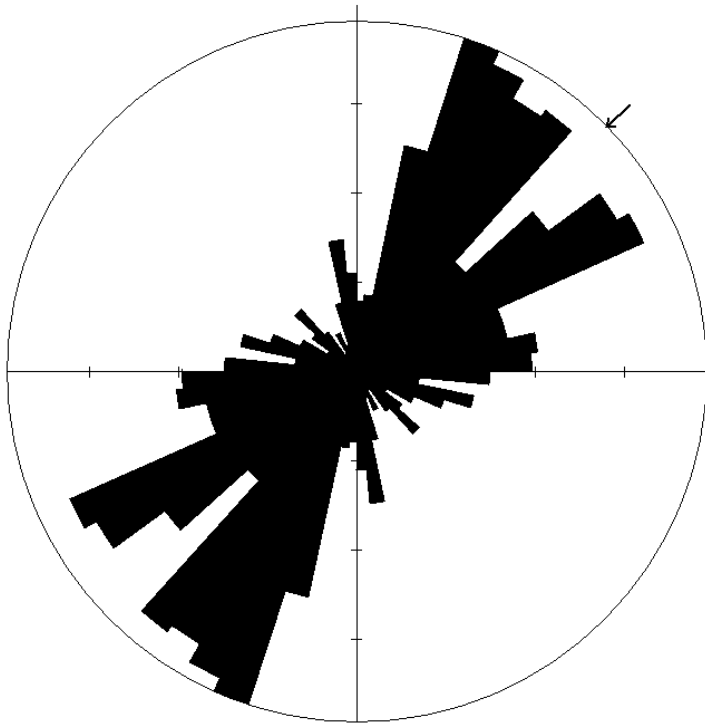


Figure 4-1
Rose Diagram of
bedding on
Taylor Ridge
monocline.

Number of data points
 = 639

Sector angle = 6°

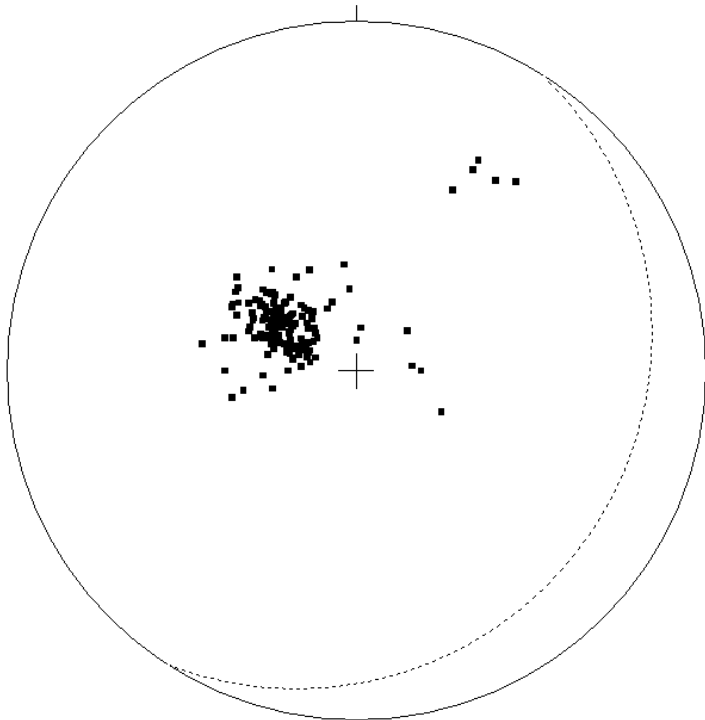


Figure 4-2
Equal-area stereoplot
of poles to bedding on
Taylor Ridge
monocline.

Number of data points
 = 172

Mean principal orientation
 = 033 20 SE

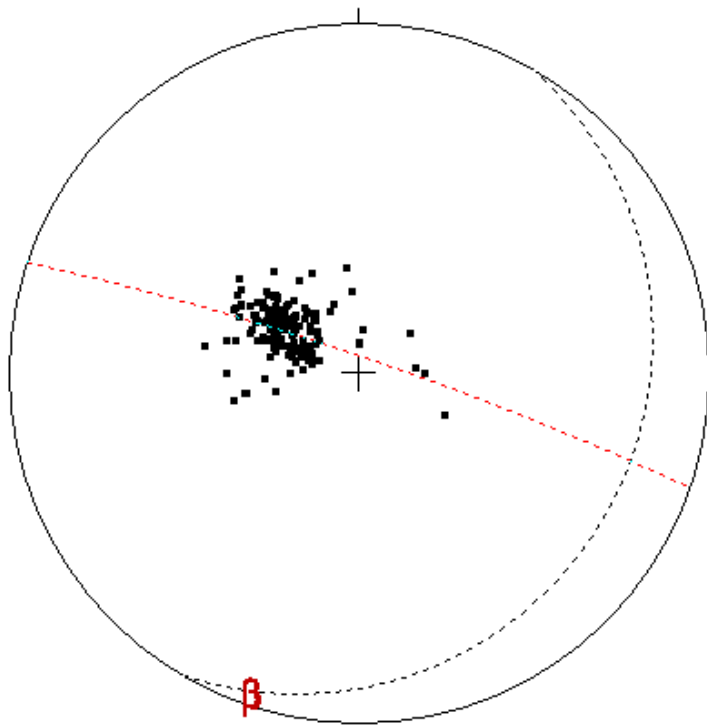


Figure 4-3
Equal-area stereonet plot
of poles to bedding on
Taylor Ridge
monocline without
small-scale fold

Number of data points
 = 167

Mean principal orientation
 = 030 20 SE

Calculated girdle:
 289 86 NE

Calculated beta axis:
 4, 199

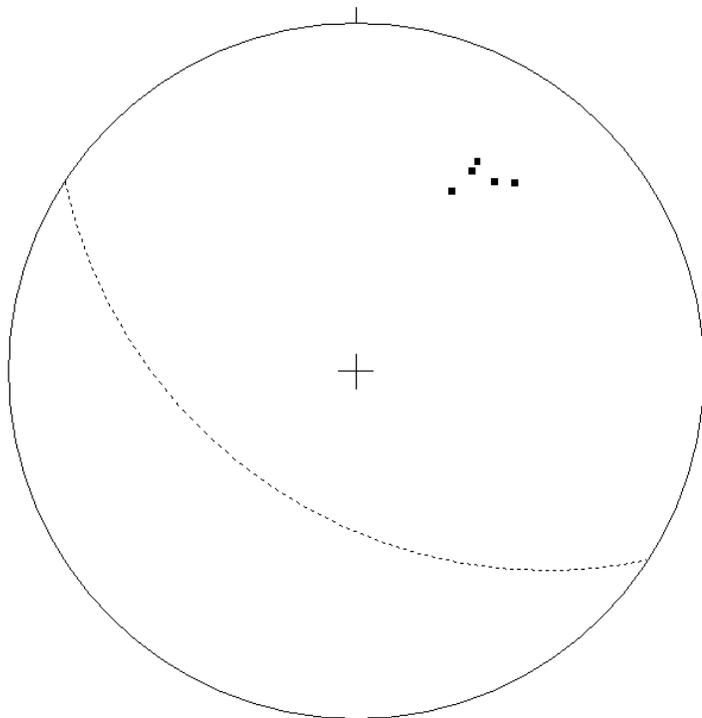


Figure 4-4
Equal-area stereonet plot
of poles to bedding on
Taylor Ridge
monocline small-scale
fold

Number of data points
 = 5

Mean principal orientation
 = 303 56 SW

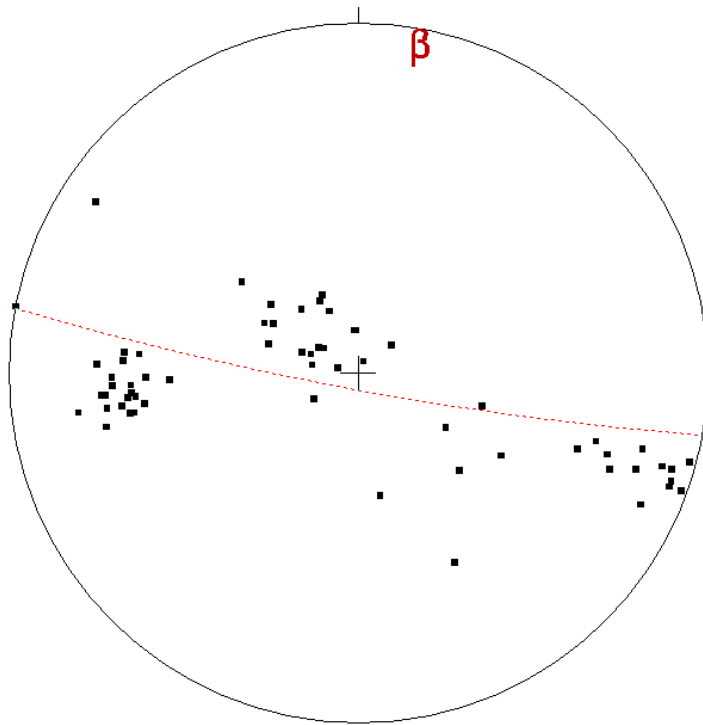


Figure 4-5
Equal-area stereonet plot of poles to bedding on Little Sand Mountain–Horn Mountain fold train

Number of data points = 65

Calculated girdle:
 280 86 SW

Calculated beta axis:
 4, 010

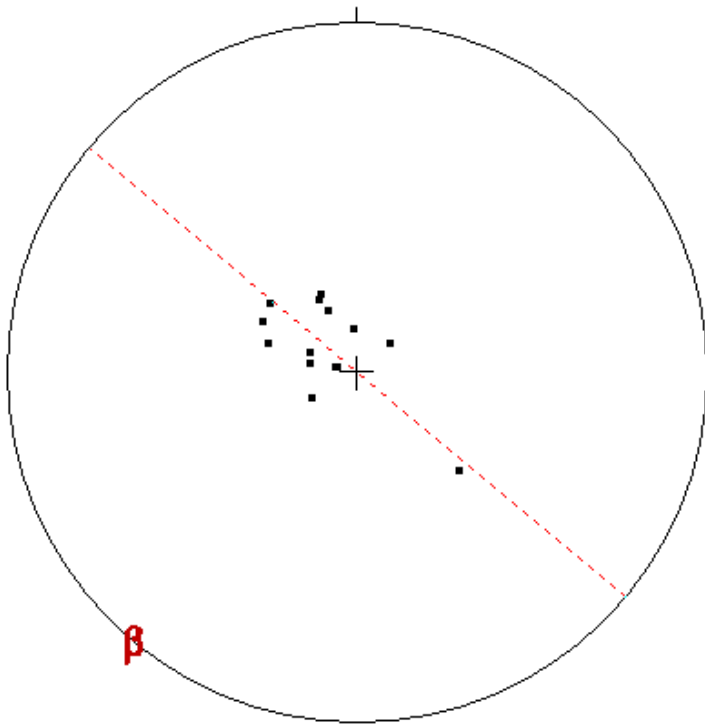


Figure 4-6
Equal-area stereonet plot of poles to bedding on Little Sand Mountain syncline

Number of data points = 15

Calculated girdle:
 310 90 NE

Calculated beta axis:
 0 220

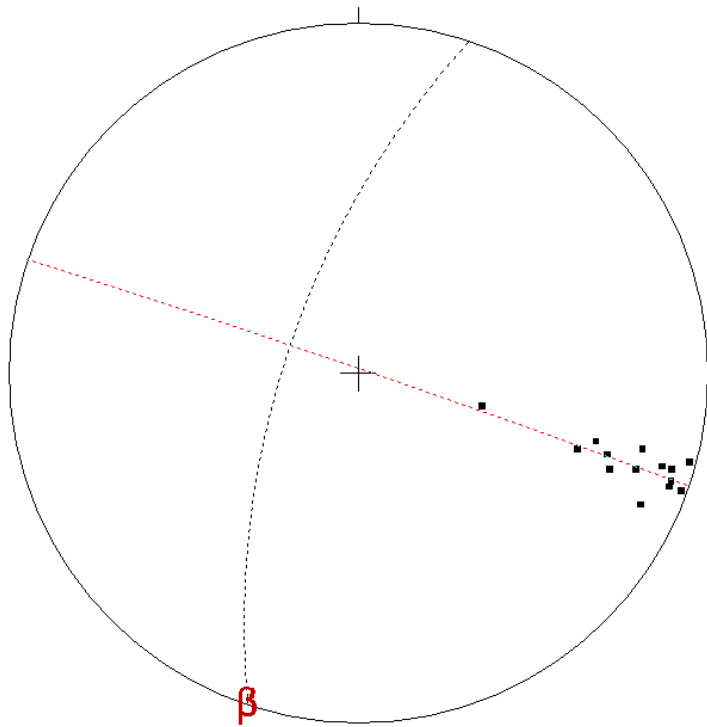


Figure 4-7
Equal-area stereonet
of poles to bedding on
Dick Ridge anticline

Number of data points
 = 14

Mean principal orientation
 = 018 73 NW

Calculated girdle:
 289 89 NE

Calculated beta axis:
 1, 199

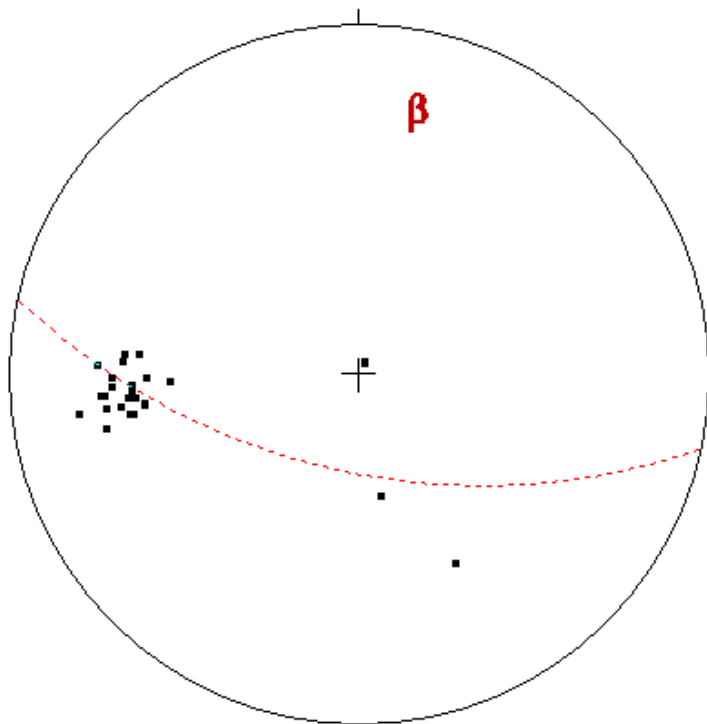


Figure 4-8
Equal-area stereonet
of poles to bedding on
Horn Mountain
anticline

Number of data points
 = 26

Calculated girdle:
 282 67 SW

Calculated beta axis:
 23, 012

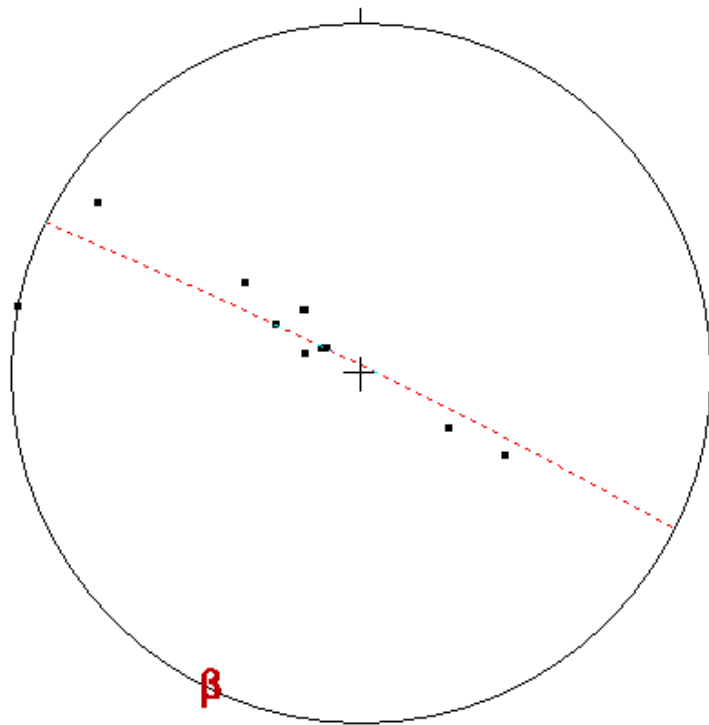


Figure 4-9
Equal-area stereonet plot of poles to bedding on Turkey Mountain anticline

Number of data points = 10

Calculated girdle:
 296 88 NE

Calculated beta axis:
 2, 206

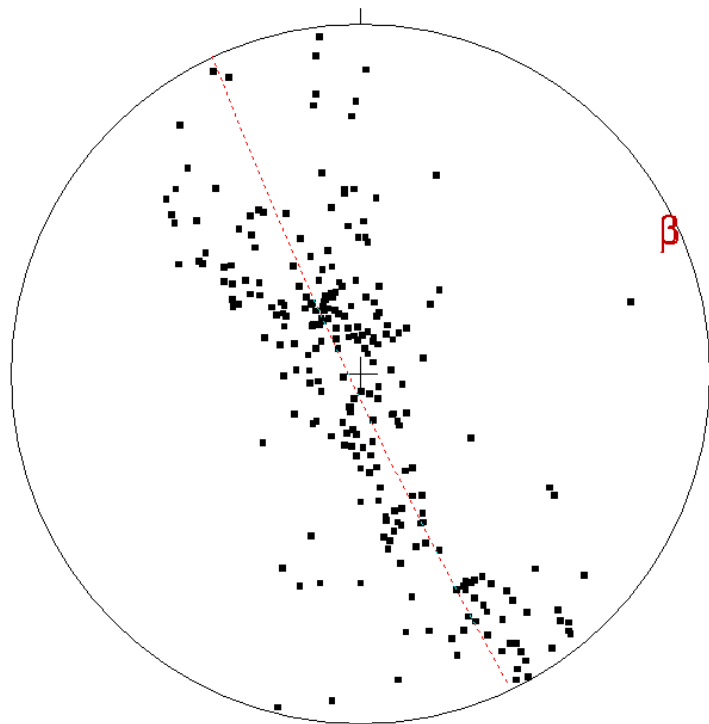


Figure 4-10
Equal-area stereonet plot of poles to bedding on Simms Mountain-Horseleg Mountain fold train

Number of data points = 252

Calculated girdle:
 335 87 SW

Calculated beta axis:
 3, 065

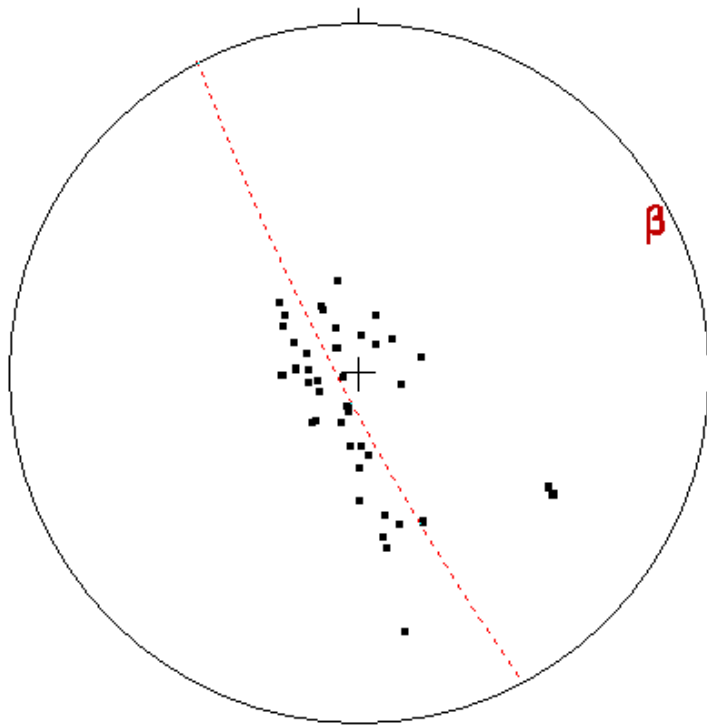


Figure 4-11
Equal-area stereonet plot
of poles to bedding on
Simms Mountain
anticline
(northeastern end)

Number of data points
 = 42

Calculated girdle:
 332 85 SW

Calculated beta axis:
 5, 062

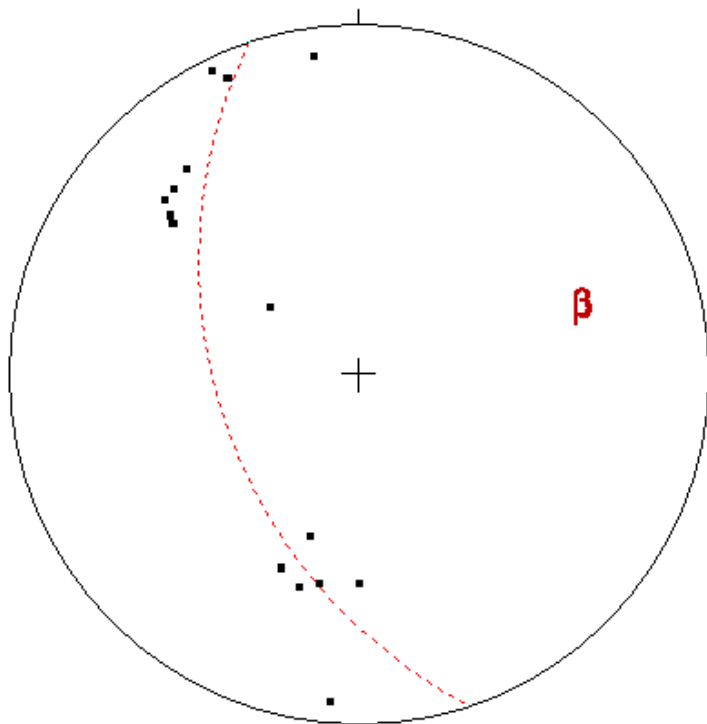


Figure 4-12
Equal-area stereonet plot
of poles to bedding on
Simms Mountain
anticline
(southwestern end)

Number of data points
 = 15

Calculated girdle:
 342 57 SW

Calculated beta axis:
 33, 072

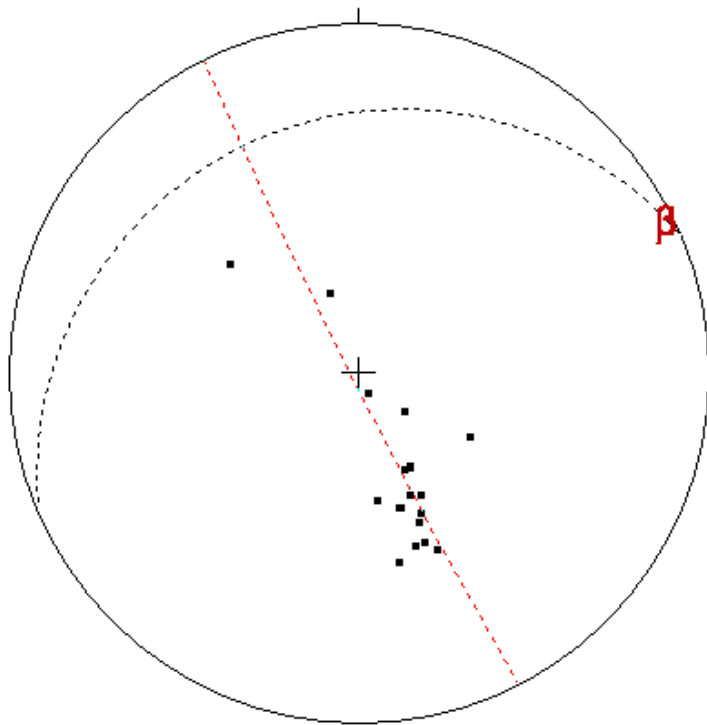


Figure 4-13
Equal-area stereonet plot
of poles to bedding on
Rock Mountain
syncline

Number of data points
 = 17

Mean principal orientation
 = 067 28 NE

Calculated girdle:
 333 88 SW

Calculated beta axis:
 2, 063

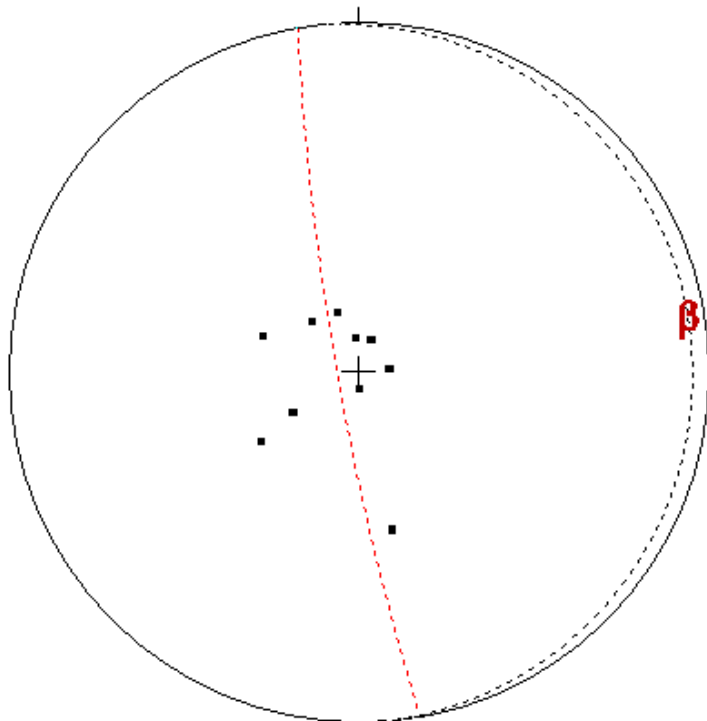


Figure 4-14
Equal-area stereonet plot
of poles to bedding on
Lavender Mountain
anticline near
northeastern end

Number of data points
 = 11

Mean principal orientation
 = 355 05 NE

Calculated girdle:
 350 85 SW

Calculated beta axis:
 5, 080

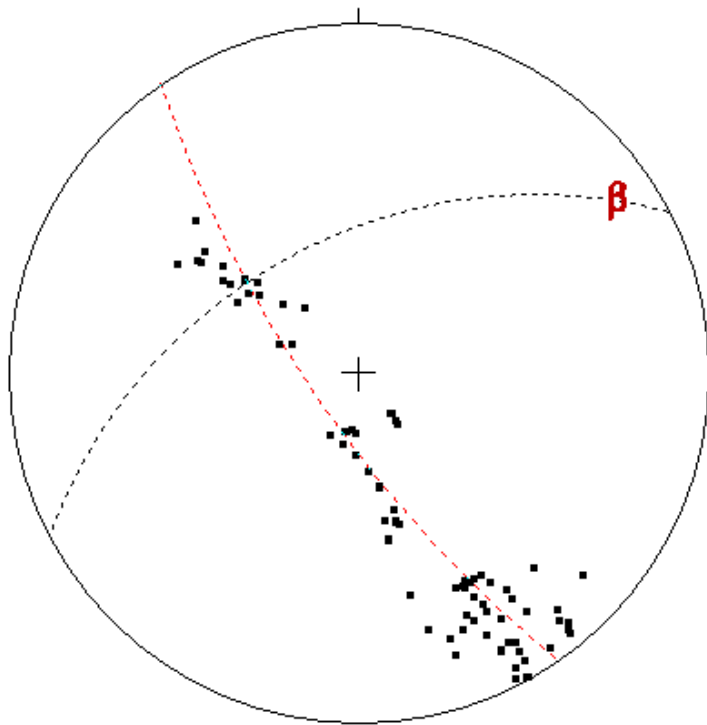


Figure 4-15
Equal-area stereonet plot
of poles to bedding on
Horseleg Mountain
anticline

Number of data points
 = 73

Mean principal orientation
 = 062 58 NW

Calculated girdle:
 325 79 SW

Calculated beta axis:
 11, 055

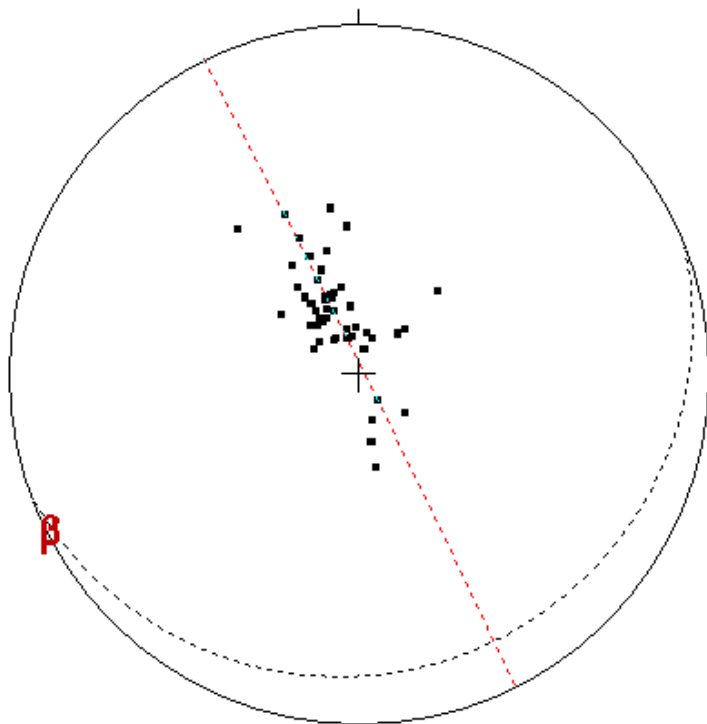


Figure 4-16
Equal-area stereonet plot
of poles to bedding on
Strawberry Mountain
anticline along
topographic crest

Number of data points
 = 49

Mean principal orientation
 = 068 16 SE

Calculated girdle:
 334 89 NE

Calculated beta axis:
 1, 244

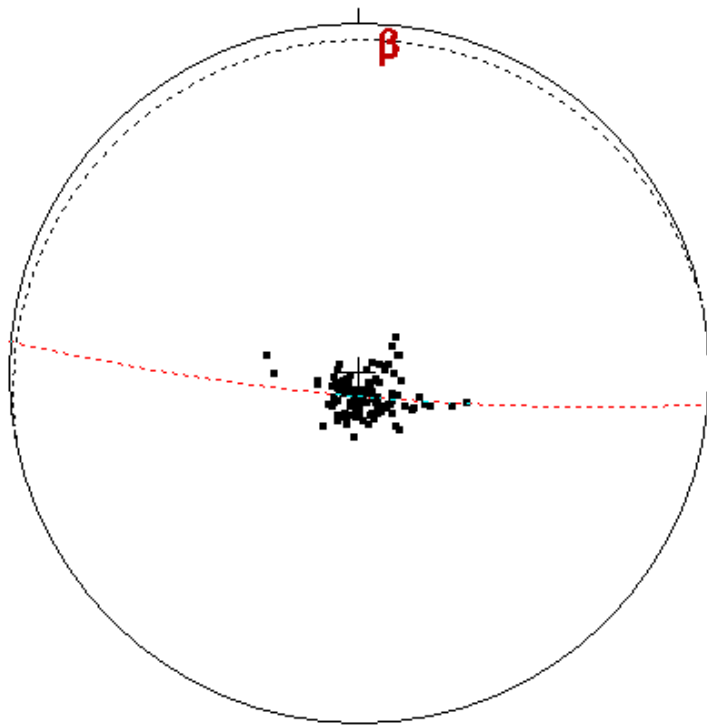


Figure 4-17
Equal-area stereonet plot
of poles to bedding on
Strawberry Mountain
anticline along roadcut

Number of data points
 = 114

Mean principal orientation
 = 079 05 NW

Calculated girdle:
 275 85 SW
 Calculated beta axis: 5,
 005

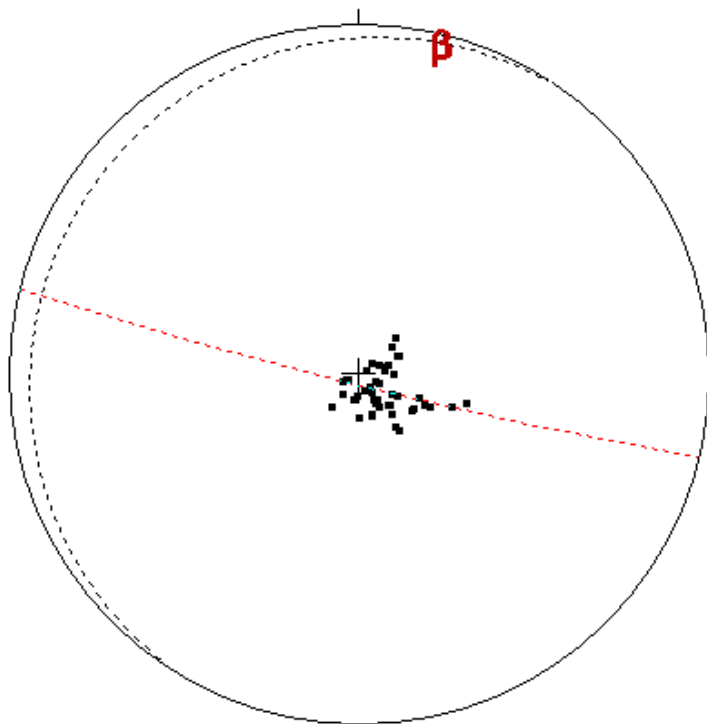


Figure 4-18
Equal-area stereonet plot
of poles to bedding on
Strawberry Mountain
anticline along
northwestern part of
roadcut

Number of data points
 = 41

Mean principal orientation
 = 034 07 NW

Calculated girdle:
 284 87 SW
 Calculated beta axis:
 3, 014

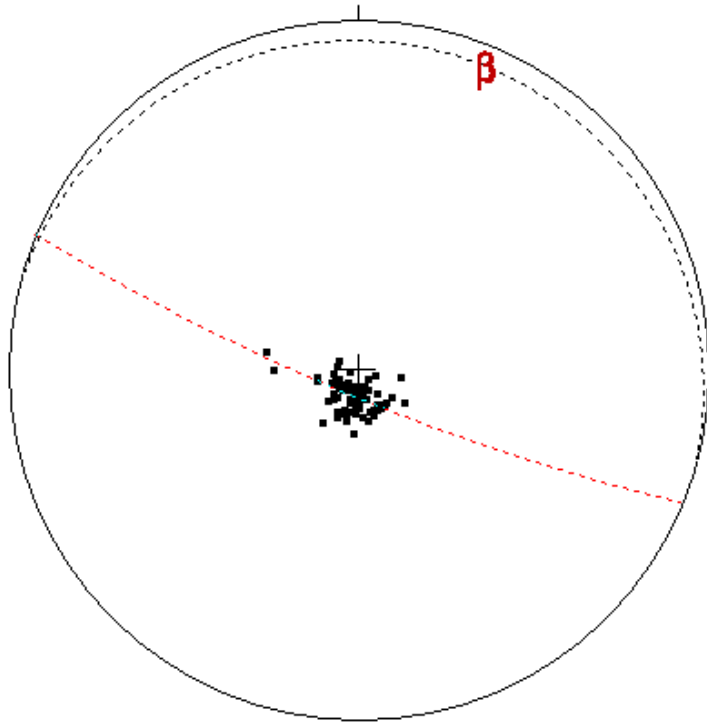


Figure 4-19
Equal-area stereoplot
of poles to bedding on
Strawberry Mountain
anticline along
southeastern part of
roadcut

Number of data points
 = 73

Mean principal orientation
 = 285 06 NE

Calculated girdle:
 293 84 SW

Calculated beta axis:
 6, 023

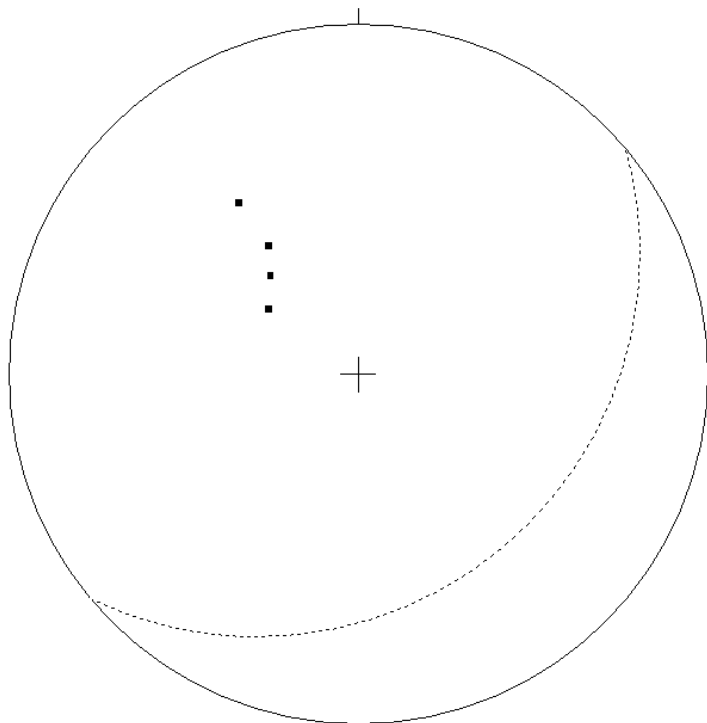


Figure 4-20
Equal-area stereoplot
of poles to bedding on
Taylor Ridge
monocline west of
intersection with
Strawberry Mountain
anticline

Number of data points
 = 4

Mean principal orientation
 = 050 36 SE

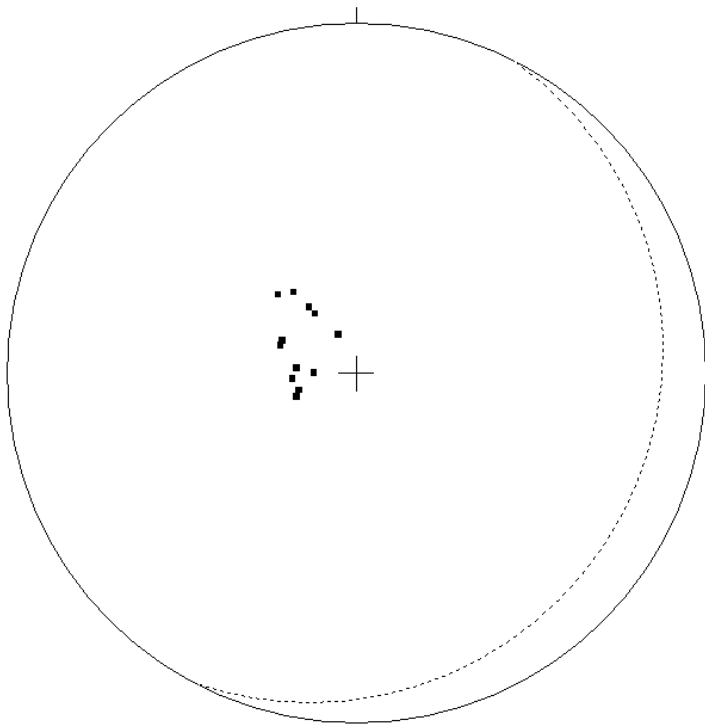


Figure 4-21
Equal-area stereonet plot
of poles to bedding on
Taylor Ridge
monocline north of
intersection with
Strawberry Mountain
anticline

Number of data points
 = 12

Mean principal orientation
 = 027 15 SE

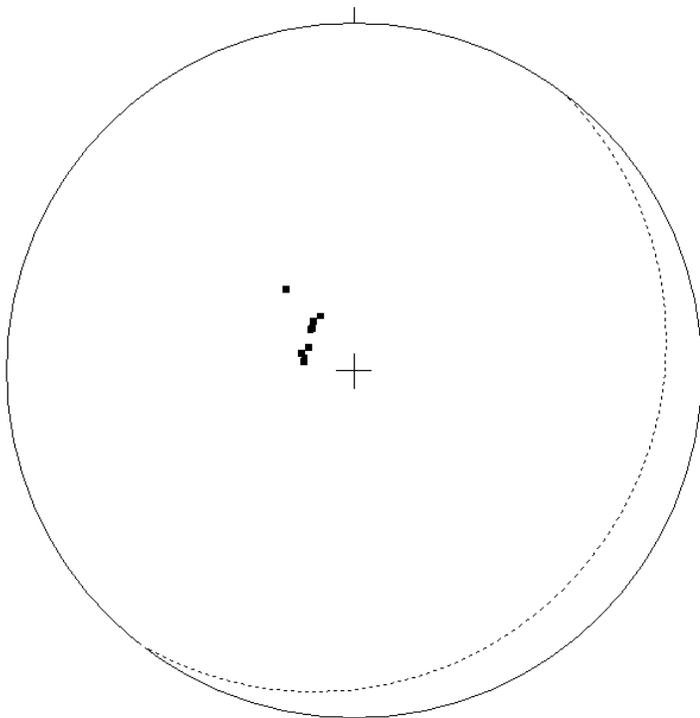


Figure 4-22
Equal-area stereonet plot
of poles to bedding on
Taylor Ridge
monocline south of
intersection with
Strawberry Mountain
anticline

Number of data
 = 9

Mean principal orientation
 = 038 14 SE

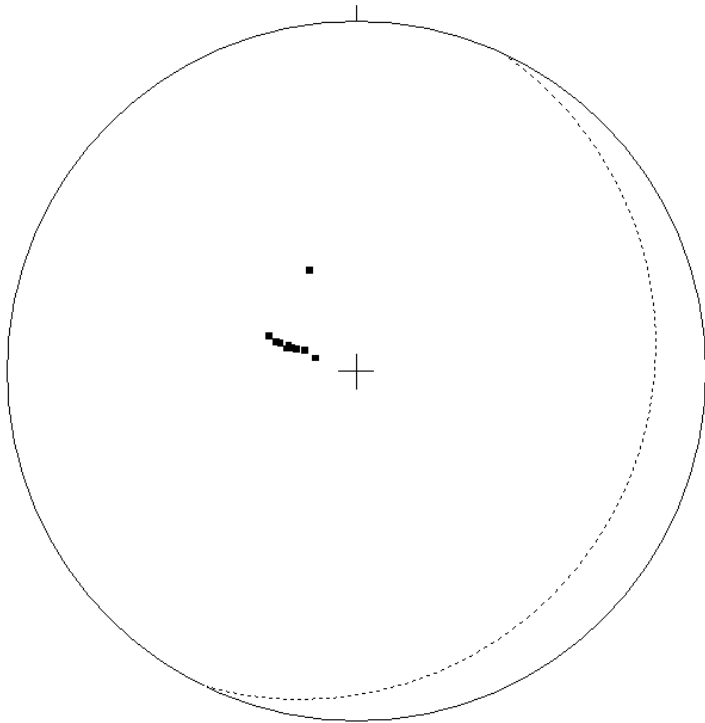


Figure 4-23
Equal-area stereonet plot of poles to bedding on Taylor Ridge monocline farther north of intersection with Strawberry Mountain anticline

Number of data points
 = 11

Mean principal orientation
 = 025 17 SE

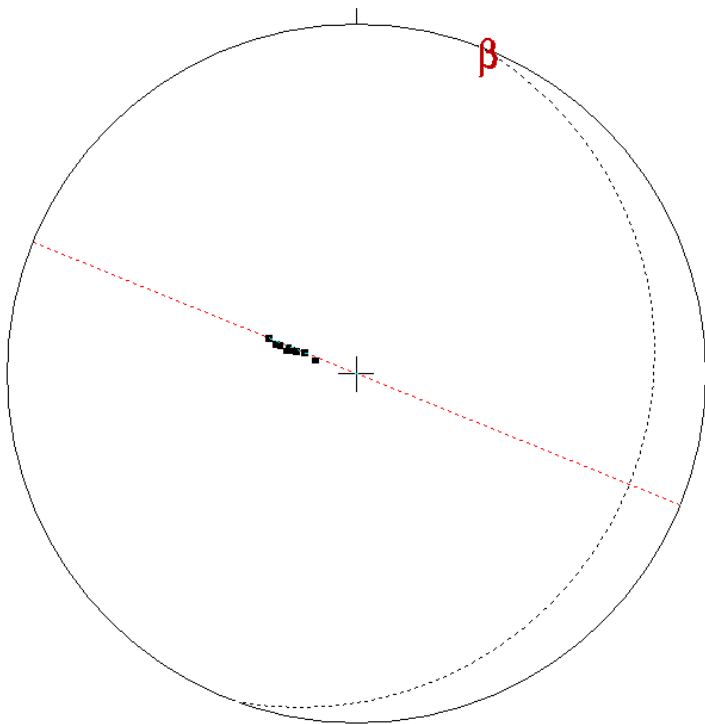


Figure 4-24
Equal-area stereonet plot of poles to bedding on Taylor Ridge monocline farther north of intersection with Strawberry Mountain anticline (omitting point from small fold)

Number of data points
 = 10

Mean principal orientation
 = 020 17 SE

Calculated girdle:
 292 89 SW

Calculated beta axis:
 1, 022

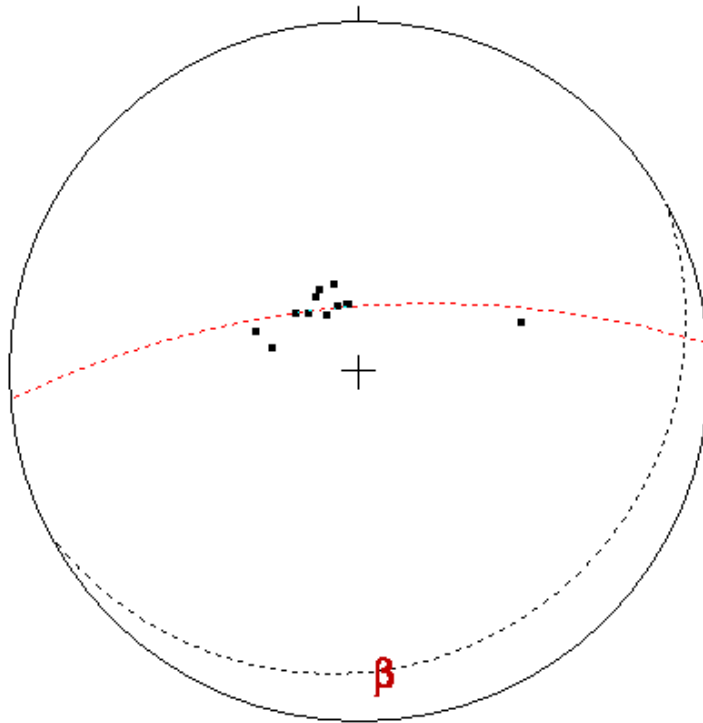


Figure 4-25
Equal-area stereoplot
of poles to bedding on
Strawberry Mountain
anticline at
intersection with Dick
Ridge anticline

Number of data points
 = 11

Mean principal orientation
 = 060 17 SE

Calculated girdle:
 085 75 NW

Calculated beta axis:
 15, 175

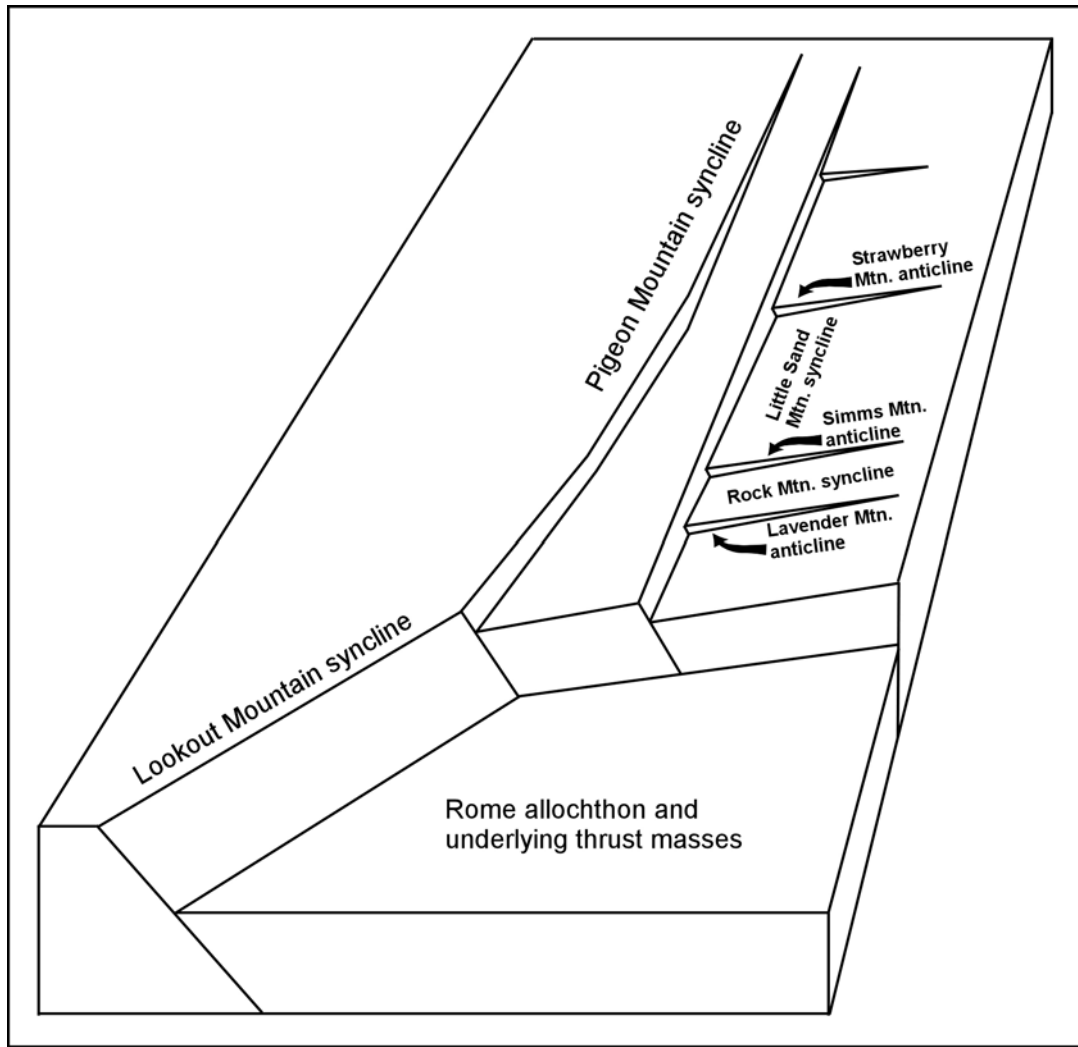


Figure 4-26. Basement fault map of northwestern Georgia, from Rich (1992). In this interpretation, basement faults directly correlate to position and orientation of surface structures.

Chapter V:

CROSS SECTIONS, SUBSURFACE STRUCTURE, VOLUME BALANCE

5.1 CROSS SECTIONS AND SUBSURFACE STRUCTURE

For this study, field measurements of structural orientation data and stratigraphic thickness have been obtained and compiled with structural data from other studies in the region (Butts, 1948; Cressler, 1963, 1964a, b, 1970, 1974; Georgia Geological Survey, 1976; Thomas and Cramer, 1979; Osborne *et al.*, 1988; Thomas and Bayona, 2005) to constrain construction of palinspastically restorable cross sections (Plate 2). The subsurface geology is interpreted from seismic reflection profiles and projection of surface data. The depths to basement and thickness of a basal weak layer are measured from seismic reflection profiles, and structures of the overlying units are constructed by extending surface measurements (*i.e.*, stratigraphic thickness and strike/dip, *etc.*) into the subsurface. The seismic profiles show two distinct packages of clear layered reflectors in most places. The lower package of layered reflectors corresponds to Unit 1, and the base of the package is near the base of the sedimentary cover above Precambrian crystalline basement (Figure 5-1). The top of the lower package of layered reflectors marks the top of Unit 1. Unit 2 is shown by seismic transparency with only weak, discontinuous internal reflectors. The upper package of layered reflectors evidently corresponds to Unit 3, and also defines the top of Unit 2.

On the northwest, the Kingston–Chattooga anticlinorium is a broad structural high bounded on the southeast by the Taylor Ridge monocline, which dips into the deeper Floyd synclinorium. Unit 2 is structurally lower within the Floyd synclinorium, which is partitioned on the southwest by east-northeastward-plunging anticlines of the Simms Mountain–Horseleg Mountain fold train and on the northeast by south-southwestward-plunging anticlines of the Little Sand Mountain–Horn Mountain fold train, including the Clinchport thrust ramp (Johns Mountain anticline). Seismic reflection profiles show that the top of Precambrian crystalline basement dips very gently southeastward and is broken by small steep normal faults (*e.g.*, Thomas and Bayona, 2005). In cross section, the difference in elevation between the base of Unit 2 in the Kingston–Chattooga thrust sheet

and the top of basement constitutes a large area to be filled (Plate 2 and Figure 5-1), requiring an interpretation of subsurface structure.

Previous interpretations have consistently included imbricate thrust sheets of Units 1 and 2 in the core of the Kingston–Chattooga anticlinorium, as well as blind thrusts in the cores of the anticlines of the Little Sand Mountain–Horn Mountain and Simms Mountain–Horseleg Mountain fold trains (*e.g.*, Thomas and Bayona, 2005). The dual fault traces of the Kingston fault and leading imbricate and the Chattooga fault and leading imbricate have been interpreted to be the surface expression of long imbricate thrust sheets in the core of the anticlinorium. Although this structural configuration satisfies the geometric form of the structures, other observations suggest that this interpretation may not be appropriate. The Chattooga fault and leading imbricate both end along strike, suggesting a relatively small magnitude of displacement. Furthermore, the Kingston fault and leading imbricate apparently terminate southwestward along strike and extend into an unfaulted detachment anticline (Thomas and Bayona, 2005). Seismic reflection profiles clearly image the southeastern limb of the Lookout Mountain syncline in the footwall of the Kingston fault; however, the profiles are ambiguous southeast of the Kingston fault, where no coherent reflectors are shown above the basal package of layered reflectors above the basement except for very shallow reflectors of Units 2 and 3 in the surface structures (Figure 5-1). The seismic reflection profiles lack resolution of any possible imbricate thrust sheets of Unit 2 beneath the surface-exposed thrust sheet (Figure 5-1).

Information applicable to the resolution of structural style in Georgia may be obtained by analogy from structures along strike to the southwest in the Appalachian thrust belt in Alabama. In Alabama, deep drilling in the Gadsden mushwad (Figure 1-3) has documented a minimum thickness of 2835 m of intensely deformed and tectonically thickened dark-colored shale and thin-bedded limestone of the Middle to lower Upper Cambrian Conasauga Formation (Unit 1) (Thomas, 2001). Seismic reflection profiles image dipping reflectors of the regional competent layer (Unit 2) both northwest and southeast of the Gadsden mushwad; however, the profiles show a distinct lack of coherent reflectors within the mushwad (*cf.* Figure 7 in Thomas, 2001). The internal structure of the mushwad is inferred to include thrust faults that partition the ductilely

deformed mass into internally deformed horses. Observations of outcrops and shallow core holes document disharmonic, tight, small-scale folds (amplitudes and wavelengths on the scale of a few meters) broken by faults of uncertain displacements. The mushwad structure is interpreted to be a ductile duplex beneath a roof thrust sheet of the regional competent layer (Unit 2) and a structurally attached uppermost part of Unit 1. The roof of the Gadsden mushwad has been eroded leaving the core of the duplex exposed; however, the structure of the roof can be inferred from bounding structures across strike (Thomas, 2001). Farther to the southwest in Alabama, the crest of the Birmingham anticlinorium (Figure 1-3) includes multiple thrust faults and folds, as well as backthrusts, exposed in Unit 2 (Thomas, 2001; Thomas and Bayona, 2005). These structures form the roof of a separate subsurface mushwad, which is also shown in seismic profiles as a zone lacking coherent reflectors. Interestingly, prior to drilling of the first well into the Gadsden mushwad in 1985, the common interpretation was that the structurally high rocks at the top of the exposed Unit 1 reflect a subsurface stack of imbricate thrust sheets of Unit 2 and younger rocks (Thomas, 1985; Figure 9 *in* Thomas, 2001).

By analogy with ductile duplexes that have been documented along strike in the Appalachians in Alabama (Thomas, 2001), the subsurface structure beneath the Kingston–Chattooga anticlinorium, as well as beneath the trailing part of the composite thrust sheet, is interpreted here as a ductile duplex. In this new interpretation, the mapped Kingston fault and leading imbricate, as well as the Chattooga fault and leading imbricate, are interpreted to be relatively low-magnitude thrust faults limited to the roof of the ductile duplex (Plate 2). An interval of layered reflectors beneath Unit 2 shows that some strata in the uppermost part of Unit 1 are attached to the competent layer in the thrust sheet, and that the detachment of the Kingston–Chattooga composite thrust sheet is within Unit 1. The roof thrust of the ductile duplex places Unit 1 strata in the Kingston–Chattooga composite thrust sheet over ductilely deformed, tectonically thickened Unit 1 in the ductile duplex. The ductile duplex fills the space between the base of the thrust sheet and the top of the autochthonous lower part of Unit 1 overlying Precambrian basement beneath the décollement (Plate 2 and Figure 5-1).

Seismic reflection profiles show that the leading edge of the ductile duplex forms a tectonic wedge under Unit 2 in the northwest-dipping limb of the Kingston–Chattooga anticlinorium (common limb with the Lookout Mountain syncline) (Plate 2 and Figure 5-1); a similar wedge is documented for the leading edge of the Gadsden mushwad in Alabama (Figures 5 and 7 *in* Thomas, 2001). The folds of the Little Sand Mountain–Horn Mountain and Simms Mountain–Horseleg Mountain fold trains are interpreted to be exaggerated detachment folds in the roof of the duplex, with the exception of the Clinchport fault-related fold (Johns Mountain anticline) and Horseleg Mountain anticline, which are interpreted to be translated detachment folds in the roof of the duplex (Plate 2).

5.2 VOLUME BALANCE IN THE DUCTILE DUPLEX

One of the primary objectives of this project is to compare the volume of rock in the ductile duplex in the present deformed state with the volume in a palinspastically restored state. Although the cross sections compiled for this research have been revised since Cook and Thomas (*in press*) was submitted, part of the following text was assembled for that manuscript.

In the cross sections (Plate 2), a large volume of ductilely deformed Unit 1 (Cambrian Conasauga shale) is shown to fill the space beneath the roof thrust at the base of the Kingston–Chattooga–Clinchport thrust sheet. A simplistic iteration of a palinspastically restored cross section, which employs only a line-length balancing of the competent layer (Unit 2), outlines the implications for an area-balanced reconstruction of the weak layer (Unit 1) (Panel 1 of Figure 5-2). Such a reconstruction is applicable to the evolution of a detachment fold, in which the regional weak layer is tectonically thickened to fill the cores of detachment anticlines as the overlying competent layer is translated. In this palinspastic reconstruction (Panel 1 of Figure 5-2), however, the restored area of Unit 1 is only about 50% of the deformed area of Unit 1 in the ductile duplex (Panel 2 of Figure 5-2), clearly requiring a different explanation for the large excess in the area of Unit 1.

The deformed-state cross sections assembled for this research were used to compile an isopach map of the ductile duplex (Figure 5-3). For this isopach map, the thickness of the ductile duplex was measured at 200 m intervals and at inflection points

in the mushwad; these data were contoured by hand in Canvas X. The contour map was exported as a shapefile into ESRI ArcMap, in which a triangulated irregular network (TIN) was created from the original values to yield a three-dimensional surface model representing the variations in thickness of the deformed-state ductile duplex (Figure 5-4). This TIN was then used to make grid calculations with a grid size of 50 m. The surface area of the deformed-state ductile duplex from these calculations is approximately $2.5 \times 10^9 \text{ m}^2$, and the calculated volume of the ductile duplex is $2.4 \times 10^{12} \text{ m}^3$ (Table 5-1).

A line-length balance of the base of the (Knox Group) in the array of deformed-state cross sections was used to create an array of restored-state cross sections. This restoration process required a palinspastic restoration of the configuration of the base of the Knox Group for the time prior to Appalachian thrusting. For this process, the top of the Mississippian succession was interpreted to be a horizontal depositional surface, which reflected the shallow-marine environment of deposition. The thickness of the Mississippian succession and of the underlying Unit 2 and 3 successions were palinspastically restored. These measurements yielded an average dip of approximately 0.41° southeastward for the base of the Knox Group. This angle also approximates the general dip of the basement from northwest to southeast.

An isopach map of the pre-deformation cross-section area of the ductile duplex was subsequently prepared (Figure 5-5). For this isopach map, the thickness of the ductile duplex was also measured at 200 m intervals and at inflection points in the mushwad; these data were also contoured by hand in Canvas X. In this restoration, some hinterland segments of some of the cross sections were restored at an angle from the orientation of the deformed-state cross section to approximate deformation perpendicular to structural trends. A TIN for this isopach map was constructed using the same method followed for the deformed-state isopach map, and was then used to make grid calculations also with a grid size of 50 m. The three-dimensional surface model representing the variations in thickness of the restored-state ductile duplex is shown in Figure 5-6. The surface area of the restored-state ductile duplex from these calculations is approximately $3.2 \times 10^9 \text{ m}^2$, and the calculated volume of the restored-state ductile duplex is $1.5 \times 10^{12} \text{ m}^3$ (Table 5-1).

From the surface-area calculations, the amount of bulk shortening in map view is estimated to be approximately 23%, which coincides well with the average shortening measured from line length of the base of the Knox Group in the cross sections (Table 5-2). From the volume calculations, the volume in the restored-state ductile duplex accounts for only about 64% of the volume in the deformed-state ductile duplex, which clearly creates a problem in the volume balance in the Unit 1 shale.

Two end-member solutions may be suggested for the excess volume of Unit 1 in the deformed-state cross sections. First, deformation/flow of the weak-layer shales from out of the cross-section planes could supply local excess volume. Secondly, a complex history of basement fault movement may have resulted in the sedimentary accumulation of locally thick weak-layer rocks as a source for the fill of a ductile duplex.

Tectonic thickening of Unit 1 as a result of out-of-plane flow requires convergence of material into the tectonically thickened ductile duplex. The intersection of the two structural trends (defined by the Little Sand Mountain-Horn Mountain and Simms Mountain-Horseleg Mountain fold trains) suggests possible convergence from the depression of the Floyd synclinorium into the Kingston-Chattooga anticlinorium. The calculated tectonic thickening of approximately 100% in the ductile duplex as seen in Figure 5-2 would require withdrawal of ductile rocks from an area as much as twice the size of the mapped area of the ductile duplex. Such a withdrawal would likely generate structural depressions (*e.g.*, structures in the competent layer plunging away from the center of the recess). The consistent plunges *toward* the center of the recess observed in the present outcrop geology, however, are contrary to a structural depression model. The documented plunge into the depression of the Floyd synclinorium suggests divergent (rather than convergent) flow. Given these observations, out-of-plane flow does not seem likely to account for more than a small fraction of the excess volume of Unit 1 in the ductile duplex.

Generally, the magnitude of tectonic thickening decreases southward from the northern end of the study area as shown in Table 5-3. This can be attributed to the overall southward-directed decreases in magnitude of shortening along the cross sections and in deformed-state mushroom surface areas.

5.2.1 Analogy with structures in Alabama

A complex history of basement fault movement has been demonstrated to be integral to the formation of the ductile duplexes in Alabama, where the boundary faults of the Birmingham basement graben are clearly imaged in seismic reflection profiles (Thomas, 2007). Large-scale frontal ramps rise northwestward over down-to-southeast basement faults, and thick disharmonic ductile duplexes (mushwads) underlie anticlinoria in which the competent-layer roof rocks are non-systematically faulted (Thomas, 2001). Palinspastic restorations of thrust-belt structures provide a framework to interpret stratigraphic variations in the context of episodic reactivation and inversion of the basement faults.

In palinspastic location, the Middle to lower Upper Cambrian Conasauga Formation includes a shale-dominated facies greater than 2000 m thick in the basement graben, and a much thinner carbonate facies that is less than 800 m thick outside the graben (Thomas, 2007). The differences in facies and thickness indicate synsedimentary fault movement, and the sedimentary variations document the time and magnitude of fault movement.

Upper Cambrian massive carbonate deposits (Unit 2) overstep the graben boundary faults, indicating cessation of fault movement during deposition of Unit 2 carbonate rocks (Thomas, 2007). The upper part of the Cambrian-Ordovician Knox Group (Unit 2), however, is unconformably absent over the palinspastically restored Birmingham graben. The unconformity is marked by a karstic paleotopography with tens of meters relief, as well as sporadically distributed chert-clast conglomerate at the base of the Middle Ordovician cover stratigraphy (Thomas, 2007). Middle Ordovician limestone units onlap the erosionally truncated Unit 2 and thin over the graben. These relationships indicate tectonic inversion of the Birmingham graben in the Middle Ordovician during Taconic tectonic loading (Bayona and Thomas, 2003; Thomas and Bayona, 2005). The amount of truncation of upper Unit 2 strata, paleotopography, and thinning by onlap combine to indicate as much as 700 m of reverse slip on the basement faults during inversion of the graben (Thomas, 2007). Stratigraphic and sedimentologic data indicate some minor episodic movement of the Birmingham graben faults during Silurian–Mississippian time, followed by > 900 m of normal slip during deposition of Upper

Mississippian–Lower Pennsylvanian synorogenic clastic strata. The ultimate composite vertical separation on the basement fault is approximately 2255 m (Thomas, 2007).

Propagation of Paleozoic, thin-skinned Appalachian thrust faults at a regional décollement in Unit 1 encountered the thick, mud-dominated facies (Conasauga shale) in the basement graben, as well as a basement-fault buttress at the northwestern boundary of the graben. Ductile deformation generated thick mushwads beneath large-scale frontal thrust ramps of the regional competent layer (Unit 2) (Thomas, 2001). The maximum structural relief on the roof of the mushwads is as much as 4500 m, indicating approximately 3:1 tectonic thickening of the depositionally thickened Conasauga Formation in the mushwad (Thomas, 2007).

5.2.2 Interpretation for structures in Georgia

No large-magnitude basement faults are seismically imaged in the region of the Kingston-Chattooga composite thrust sheet in Georgia; however, minor disruptions in the basal reflector package show the locations of faults that presently have small displacement of the top of the basement. By analogy with the history of mushwads (ductile duplexes) in Alabama, the present fault offset of the top of basement may reflect a composite of successive displacements, some of which are inverted. Assuming a history similar to that of the Alabama mushwads, an area balance of the ductile duplex beneath the Kingston-Chattooga composite thrust sheet (Kingston-Chattooga anticlinorium and fold trains) requires an original depositional thickness of the Conasauga Formation approximately 500 m greater than that in the foreland to the northwest (Figure 5-7). A basement graben approximately 500 m deeper than present basement elevation under the northern part of the ductile duplex will accommodate the greater thickness of Unit 1. Later inversion of the graben would have reversed part of the original slip. The lower basement elevation under the southern part of the ductile duplex (Figure 5-6) suggests an area in which inversion on the basement faults did not occur or was significantly smaller in magnitude. By analogy with stratigraphy in Alabama, inversion during Taconic (Middle Ordovician) loading may be recorded in erosion of the upper part of the Knox Group, Unit 2 (Figure 5-7) (Bayona and Thomas, 2003). Previously unexplained observations in Georgia include a local lack of the upper components that regionally comprise the Knox Group, specifically the absence of the

upper units of the Knox Group in parts of northwestern Georgia (*cf.* section 3.3.6). One of the same stratigraphic units (the Chepultepec Dolomite) is unconformably absent in the area of the Gadsden mushroom and along the Birmingham anticlinorium in Alabama, where the top of the Knox Group is marked by chert-clast conglomerates. Similar chert conglomerates are found sporadically at the top of Unit 2 in northwestern Georgia. These observations suggest that inversion occurred along basement faults in Georgia. Although the Birmingham graben shows subsequent reactivation in Alabama during late Paleozoic (Mississippian–Pennsylvanian) thrusting and tectonic loading (Thomas, 2007), this later episode of basement fault reactivation is not documented by stratigraphy in Georgia. The maximum structural relief on the roof of the mushroom in Georgia is approximately 2500 m, indicating approximately 2:1 tectonic thickening of the depositionally thickened Conasauga Formation.

Sequential diagrams (Figure 5-7) illustrate the interpreted origins of stratigraphic variations necessary to area balance the ductile duplex beneath the Kingston-Chattooga thrust sheet. The deformed state cross section (Panel 3 of Figure 5-7) shows the present location and geometry of the interpreted ductile duplex. The cross section in Panel 1 of Figure 5-7 illustrates the depositional framework of a thick Unit 1 succession in a synsedimentary graben; after the end of fault movement, Unit 2 was deposited across the graben with uniform thickness. The top of Unit 2 is drawn nearly horizontal to reflect the interpreted shallow-marine shelf deposition of the carbonate rocks. Area-balance restoration of the deformed state of the ductile duplex requires Unit 1 to be approximately 1700 m thick in the graben (for the cross section in Figure 5-7), in contrast to a regional average of 1200 m. The depositional thickening requires approximately 500 m of vertical separation along the normal fault boundary of the graben (Panel 1 of Figure 5-7). Panel 2 of Figure 5-7 shows inversion of the graben to elevate the thick graben fill (Unit 1) and cover (Unit 2), leading to erosion of the upper part of Unit 2. In this interpretation, the thickness of Unit 2 in the deformed-state cross section (approximately 660 m) constrains the thickness of the eroded upper part of Unit 2, which is on the order of 220 m. The amount of truncation, plus paleotopography and onlap, indicate approximately 500 m of reverse slip during inversion, and that magnitude of inversion places the top of basement at the present structural level (Figure 5-7).

The thickest part of the restored-state isopach and, thus, the highest volume in the ductile duplex, is in the southern part of the isopach map (Figure 5-6). This part of the restored-state ductile duplex represents a significant part of the restored-state volume. Some of this rock was likely transported northwestward into the thick deformed-state ductile duplex underlying the Kingston–Chattooga anticlinorium. On the contrary, one must recognize the limitations in how the thick part of the restored-state ductile duplex affects the overall volume budget with respect to the deformed-state ductile duplex (*i.e.*, material in the thick restored-state ductile duplex in the southern part of the map likely does not contribute any to the volume of the deformed-state ductile duplex in the far northern part of the map). Any transport of the thick ductile duplex material out of the plane of the cross section toward the southwest would also affect the volume budget and require more Unit 1 shale to have been deposited in the (later inverted) basement graben to the north.

A third isopach map was constructed to test the hypothesis of the inverted graben in the northern part of the study area (Figure 5-8). As illustrated in Figure 5-7, the cross sections used for this map are constructed such that the surface areas of the ductile duplex are equal to those in the deformed-state ductile duplex. The through-going cross sections used in this contour map were selected for their location—*i.e.*, in the northern part of the study area where the shale volume deficit is the greatest. As expected, the magnitude of offset along the graben in the model decreases southward. For this isopach map, the thickness of the ductile duplex was also measured at 200 m intervals and at inflection points in the mushwad; these data were also contoured by hand in Canvas X. In this restoration, some hinterland segments of some of the cross sections were restored at an angle from the orientation of the deformed-state cross section to approximate deformation perpendicular to structural trends. A TIN for this isopach map was constructed using the same method followed for the deformed-state and restored-state isopach maps, and was then used to make grid calculations also with a grid size of 50 m. The three-dimensional surface model representing the variations in thickness of the graben-state ductile duplex is shown in Figure 5-9. The surface area of the restored-state ductile duplex from these calculations is approximately $3.2 \times 10^9 \text{ m}^2$, and the calculated volume of the restored-state ductile duplex is $2.6 \times 10^{12} \text{ m}^3$ (Table 5-1). From these

volume calculations, the volume in the graben-state ductile duplex accounts for approximately 109% of the volume in the deformed-state ductile duplex. This surplus volume of Unit 1 may reflect, in part, the surplus of ductile duplex volume in the southern part of the field area over the part of the graben that has not been inverted. Also, the magnitudes of offset along the basement fault at the edge of the graben used for this model can be considered as estimates. This latter idea is especially important in light of the implied transfer of ductile shale out of the planes of cross section.

| | <u>deformed state</u> | <u>restored state</u> | <u>% deformed state</u> | <u>graben state</u> | <u>% deformed state</u> |
|-----------------------------------------------------|-----------------------|-----------------------|---------------------------------|----------------------|---------------------------------|
| 2-D surface area (m²) | 2,449,945,000.00 | 3,170,400,000.00 | ~129% | 3,211,447,500.00 | ~131% |
| 3-D surface area (m²) | 2,551,278,858.47 | 3,181,028,026.58 | ~125% | 3,230,457,057.34 | ~127% |
| 3-D volume (m³) | 2,355,834,235,288.83 | 1,506,170,500,651.18 | ~64% | 2,562,031,984,940.50 | ~109% |

Table 5-1. Calculations from the ductile duplex models. The deformed-state model is shown in Figure 5-4. The restored-state model is shown in Figure 5-6. The graben-state model is shown in Figure 5-9.

| <u>cross section</u> | <u>deformed length (m)</u> | <u>restored length (m)</u> | <u>shortening (%)</u> |
|----------------------|----------------------------|----------------------------|-----------------------|
| A-A' | 44322.35 | 52888.32 | 16.20 |
| B-B' | 41746.55 | 50020.74 | 16.54 |
| C-C' | 42520.84 | 49384.13 | 13.90 |
| D-D' | 43414.09 | 50825.07 | 14.58 |
| E-E' | 42226.87 | 48959.31 | 13.75 |
| H-H' | 56361.85 | 74519.72 | 24.37 |
| average | | | 16.56 |

Table 5-2. Calculations of shortening magnitudes from cross sections. Line lengths in the second and third columns are measured for the base of the Knox Group (Unit 2).

| <u>cross section</u> | <u>deformed-state area (m²)</u> | <u>restored-state area (m²)</u> | <u>imbalance (%)</u> |
|----------------------|--------------------------------------------|--------------------------------------------|----------------------|
| A-A' | 55210497.16 | 27593494.38 | 49.98 |
| C-C' | 51239454.89 | 26452891.56 | 51.63 |
| D-D' | 44201656.47 | 23031234.15 | 52.10 |
| E-E' | 39641668.36 | 20130528.55 | 50.78 |
| H-H' | 25197896.41 | 46998532.52 | 186.52 |

Table 5-3. Calculations of ductile duplex surface area from cross sections. Percentage values in the rightmost column reflect difference between the area in the restored state and the area in the deformed state.

| <u>cross section</u> | <u>deformed-state fold train area (m²)</u> | <u>restored-state fold train area (m²)</u> | <u>difference in fold train area (m²)</u> | <u>imbalance (%)</u> |
|----------------------|-------------------------------------------------------|-------------------------------------------------------|------------------------------------------------------|----------------------|
| D-D' | 535172758.54 | 852243411.99 | 267366761.66 | 49.96 |
| L-L' | 833347419.40 | 986963446.18 | 60671124.55 | 7.28 |
| average | | | | 28.62 |

Table 5-4. Calculations of thrust sheet surface area from cross sections as shown in Figure 5-10. The area of the fold train in the deformed state (second column) corresponds to the area in blue in Figure 5-10. The area values in the fourth column reflect the difference between the fold train area in the restored state and the fold train area in the deformed state, which is shown by the area in red in Figure 5-10. Percentage values in the rightmost column reflect proportion of the area difference (imbalance) to the deformed-state fold train area.

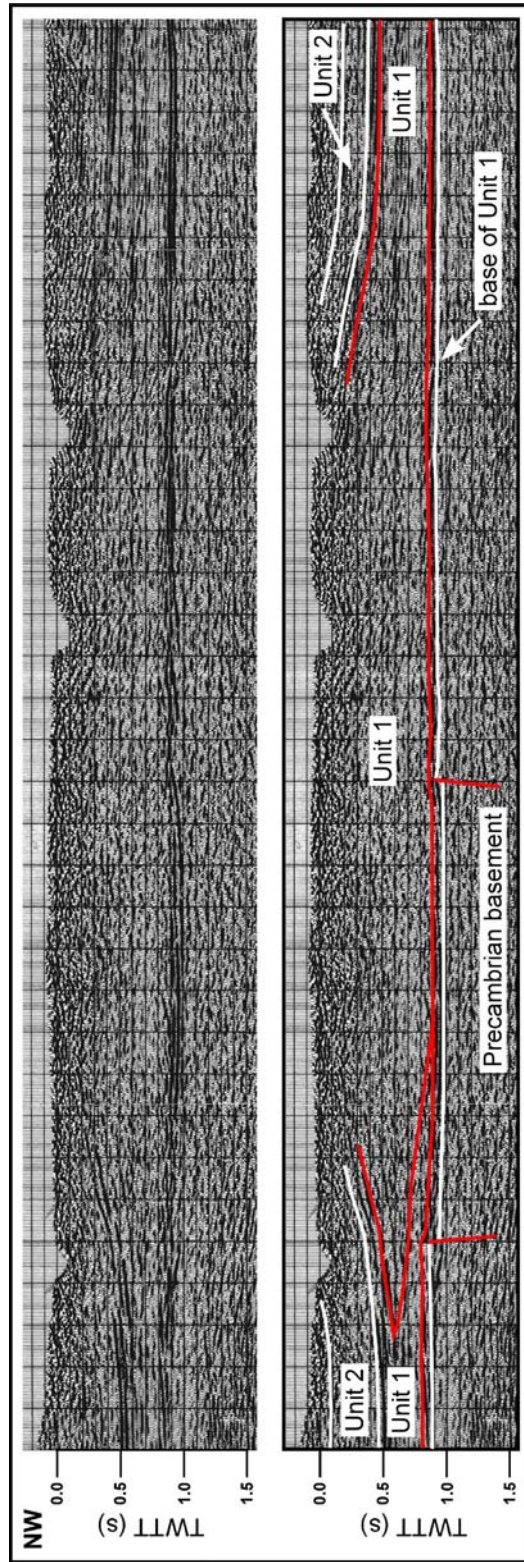


Figure 5-1. (previous page) Seismic reflection profile of the ductile duplex, interpretation shown in lower panel. Location of the profile is near the northwestern end of cross section A-A' in Plate 2, and the profile is oriented approximately parallel to the section.

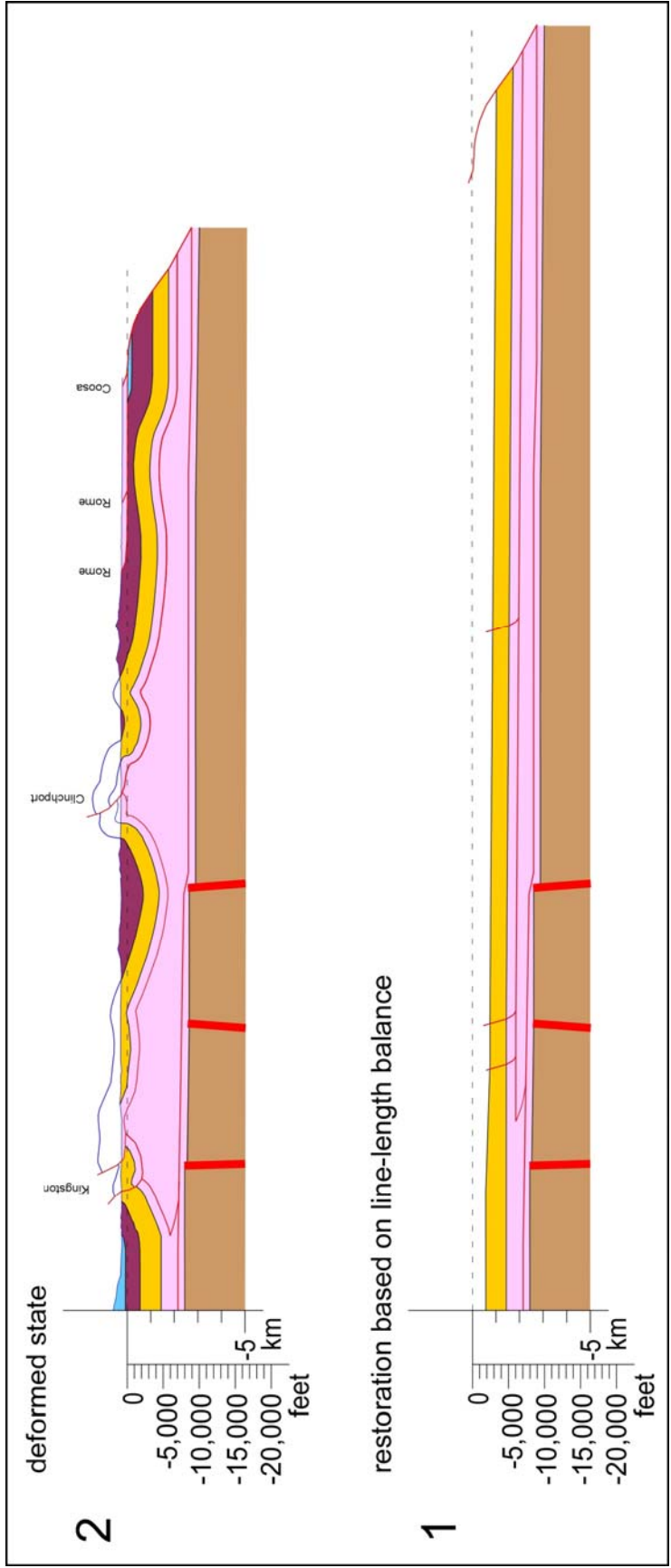


Figure 5-2. (previous page) Simplified palinspastic restoration (Panel 1) of cross section A–A' from Plate 2 based on line-length balance of the competent layer (Unit 2). Note that restored area of Unit 1 in the ductile duplex is approximately 50% of the area of the ductile duplex in the deformed-state cross section (Panel 2), showing that this interpretation of palinspastic restoration cannot be area balanced.

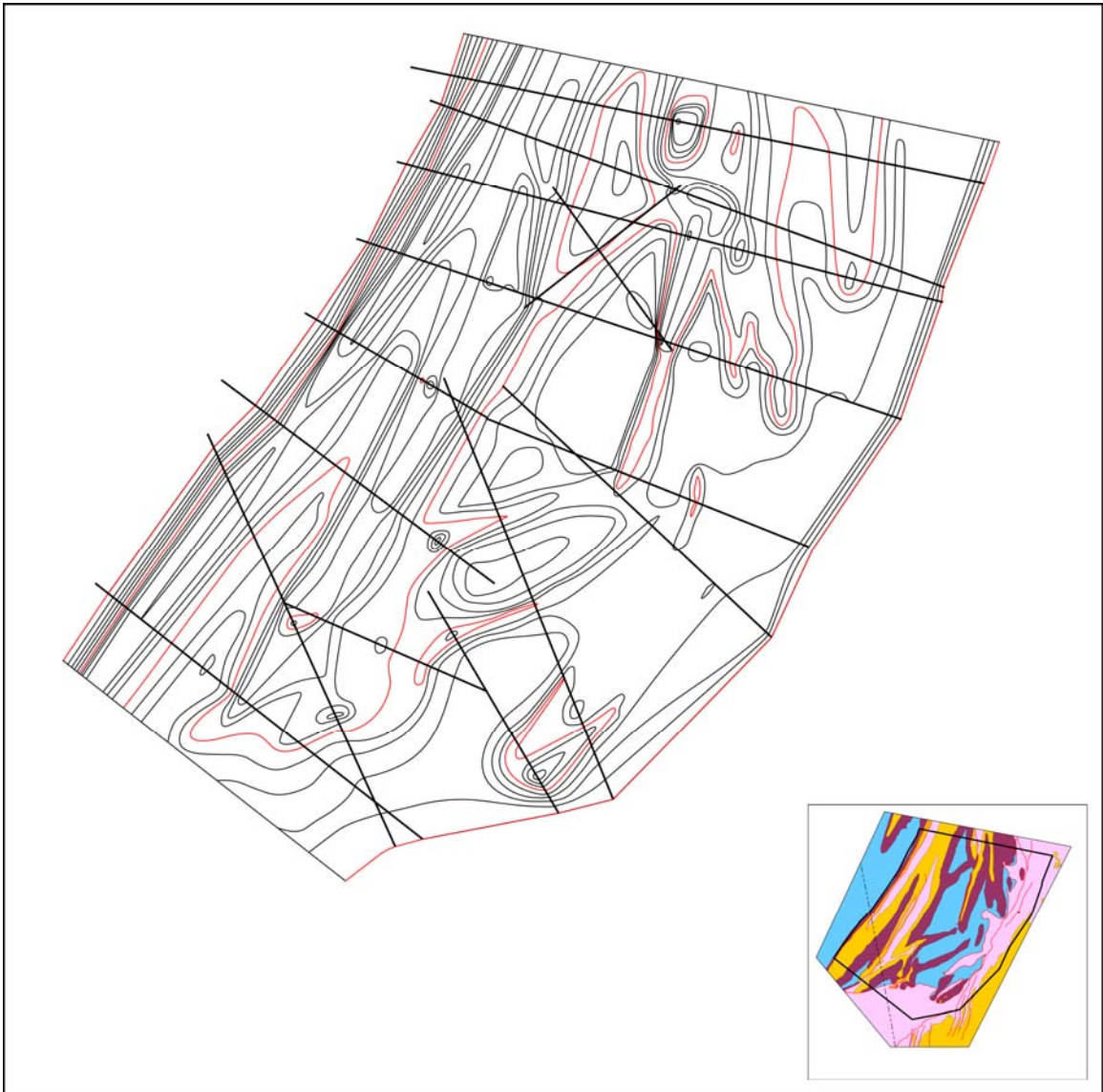


Figure 5-3. Isopach map of the deformed-state ductile duplex. Location of area is shown on inset map. Cross sections used for data are shown as black lines. Contour interval is 200 m and the contour lines for 0, 1000, and 2000 meters are in red.

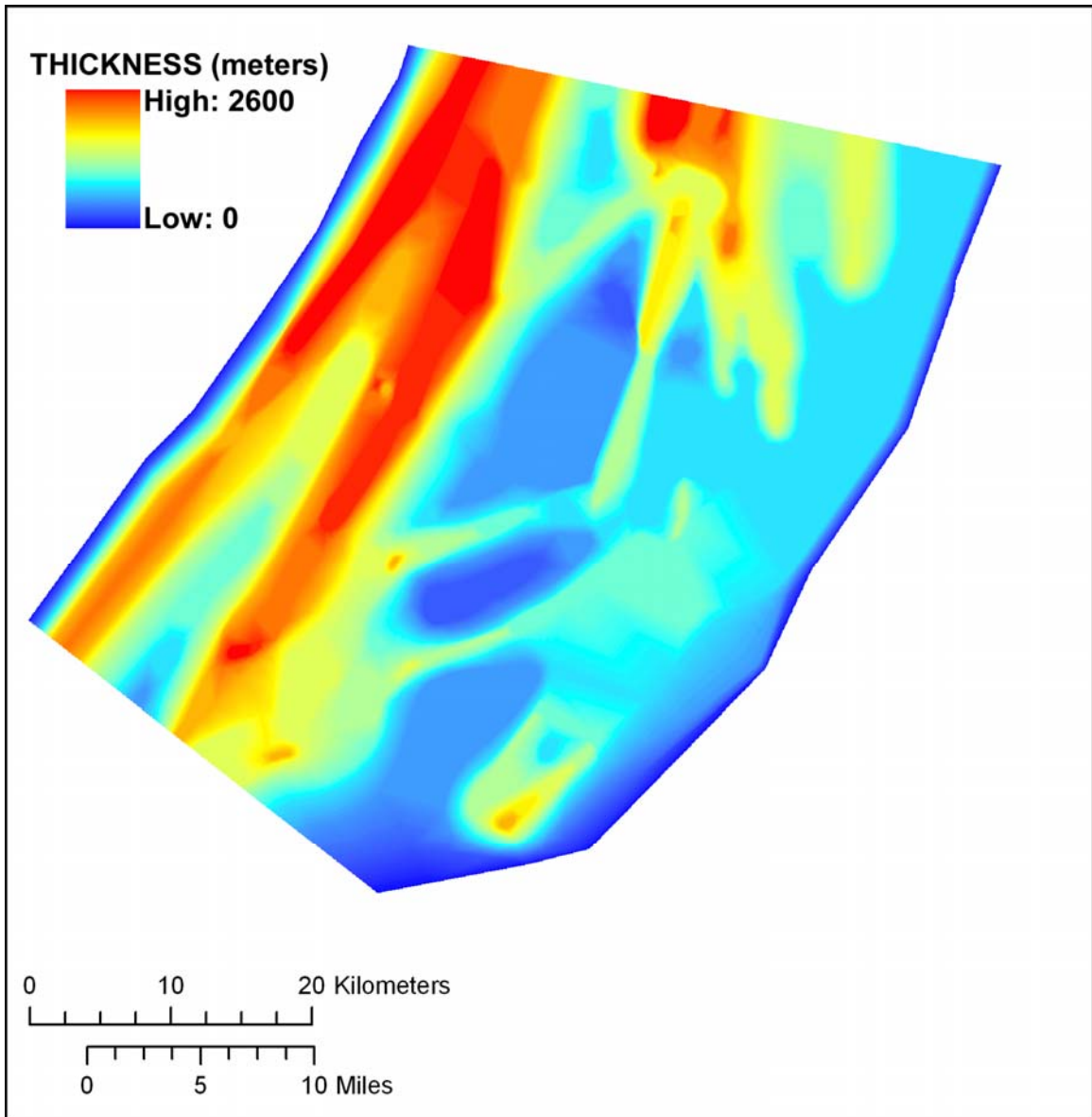


Figure 5-4. Three-dimensional surface model of the deformed-state ductile duplex constructed using the isopach map shown in Figure 5-3. Note that the leading (northwestern) edge is the “wedge” at the front of the ductile duplex and that the trailing edge represents the footwall cutoff of the base of the Knox Group (Unit 2) along the Coosa fault.

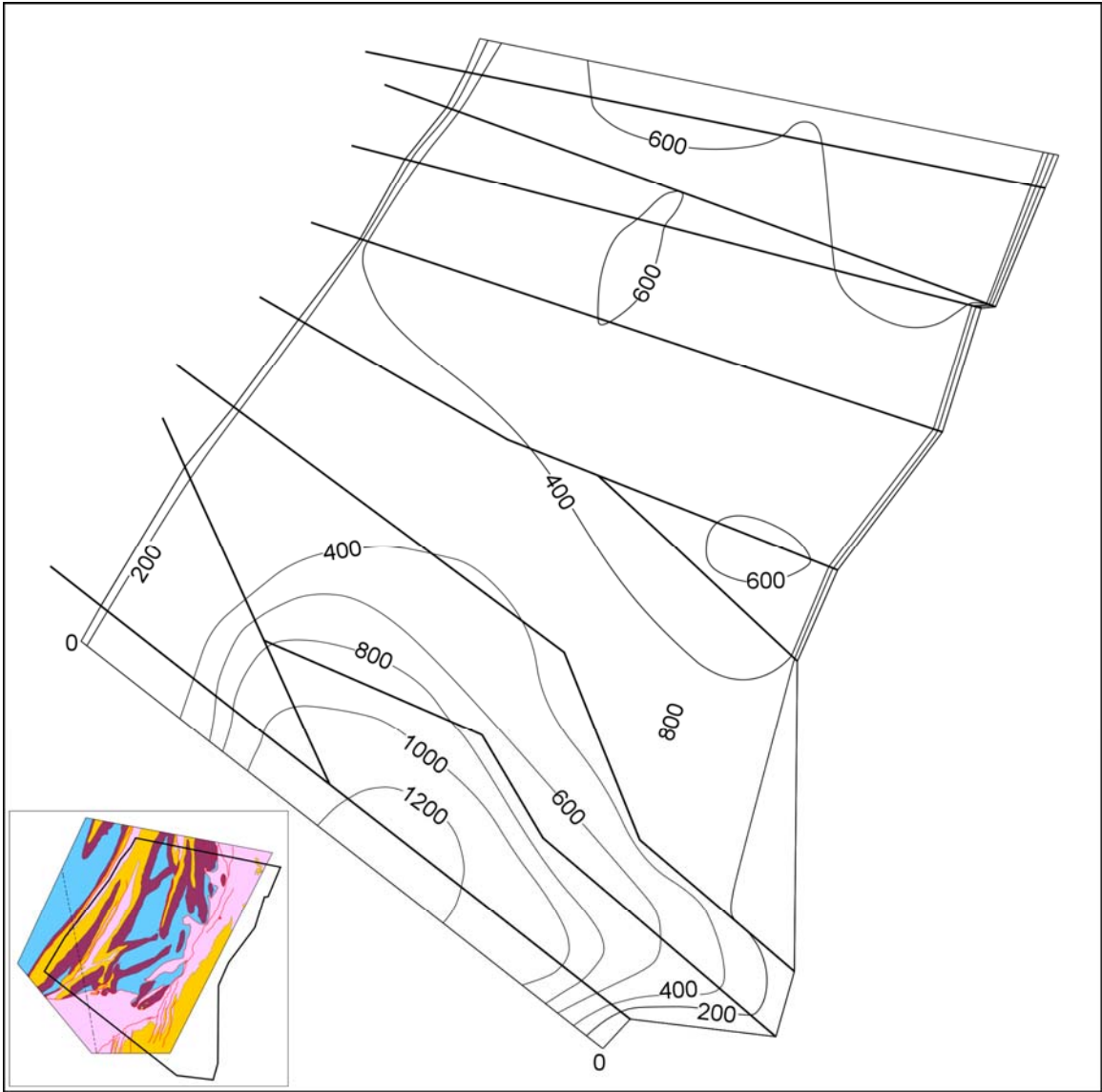


Figure 5-5. Isopach map of the restored-state ductile duplex using a simple line-length balance method for the base of the Knox Group (Unit 2). Location of area is shown on inset map. Cross sections used for data are shown as black lines. Contour values are in meters.

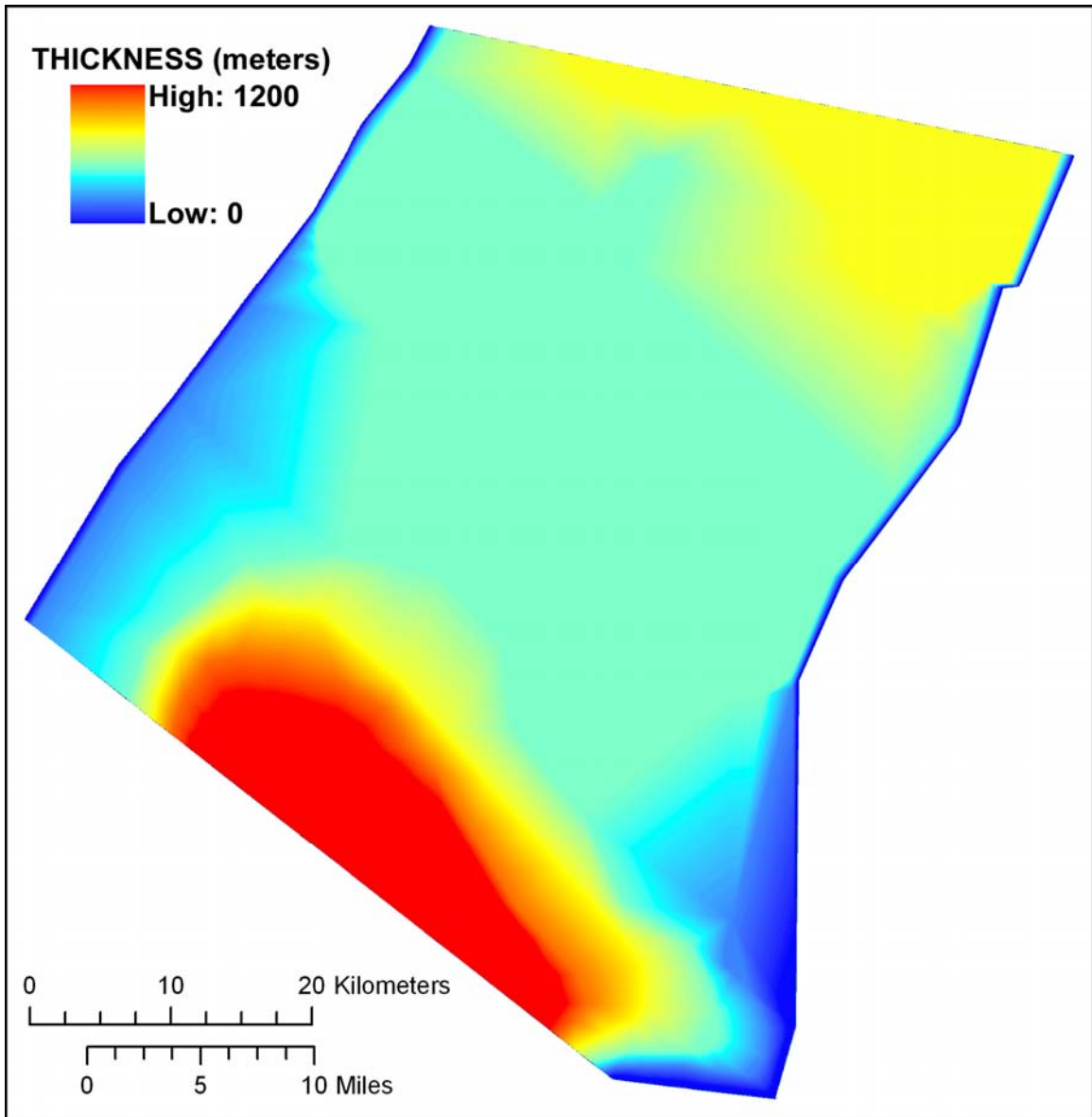


Figure 5-6. Three-dimensional surface model of the restored-state ductile duplex constructed using the isopach map shown in Figure 5-5. Note that the leading (northwestern) edge is the “wedge” at the front of the ductile duplex and that the trailing edge represents the footwall cutoff of the base of the Knox Group (Unit 2) along the Coosa fault.

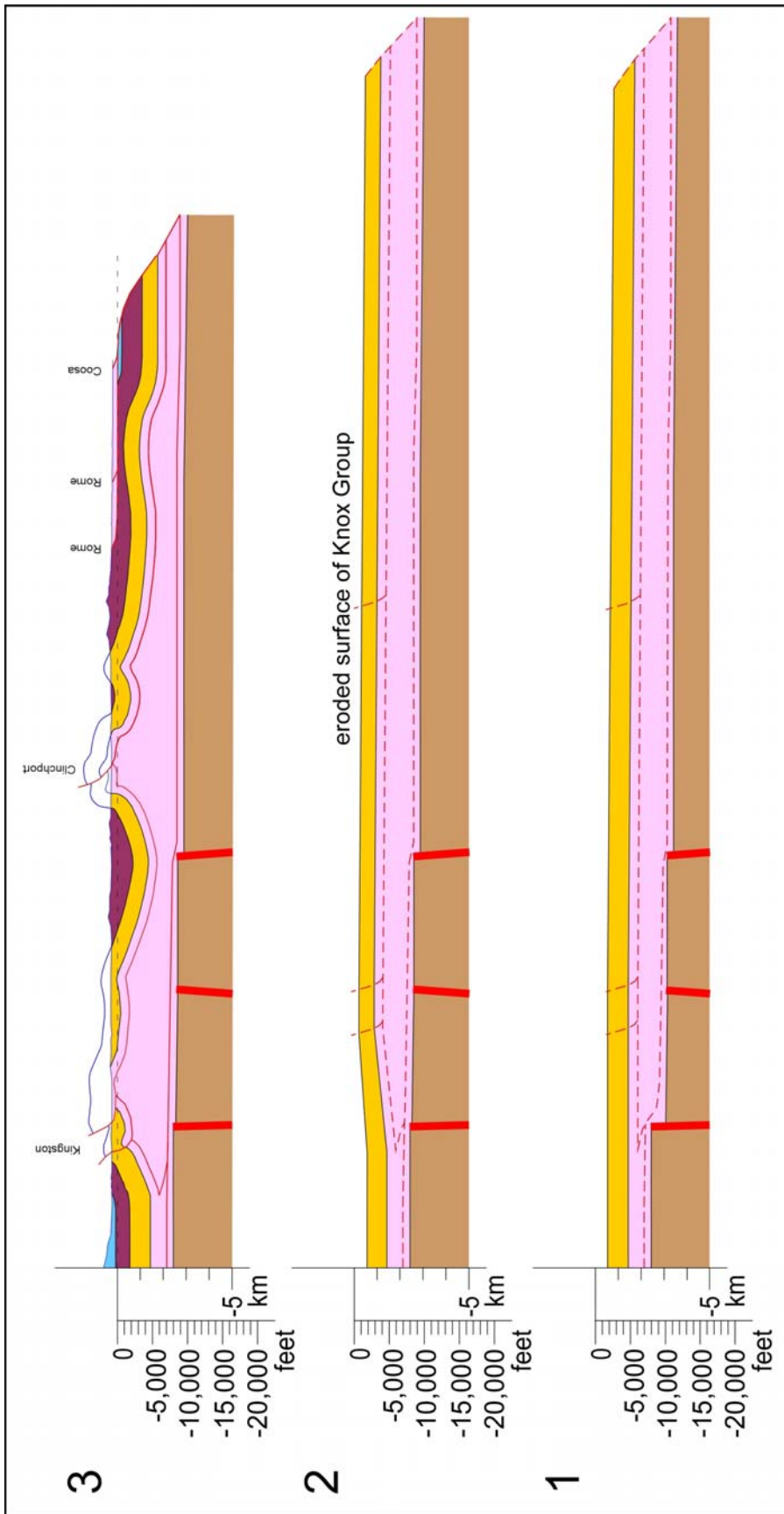


Figure 5-7. (previous page) Sequential cross sections illustrating a basement graben that is interpreted to be the source of the surplus volume of Unit 1 shales in the subrecess in Georgia. Panel 1 illustrates the thick Unit 1 succession in a synsedimentary graben, overlain by a uniform thickness of Unit 2 shallow-marine carbonates. Panel 2 illustrates graben inversion, leading to elevation of thickened Unit 1 and erosional truncation of the top of Unit 2 over the former graben. Panel 3 illustrates the deformed state cross section (cross section A-A' from Plate 2) in which the thickened Unit 1 is at the center of a ductile duplex. The dashed red lines in panels 1 and 2 represent future trajectories of thrust faults, including the floor and roof thrusts bounding the ductile duplex. The area of the ductile duplex is equal in all three diagrams.

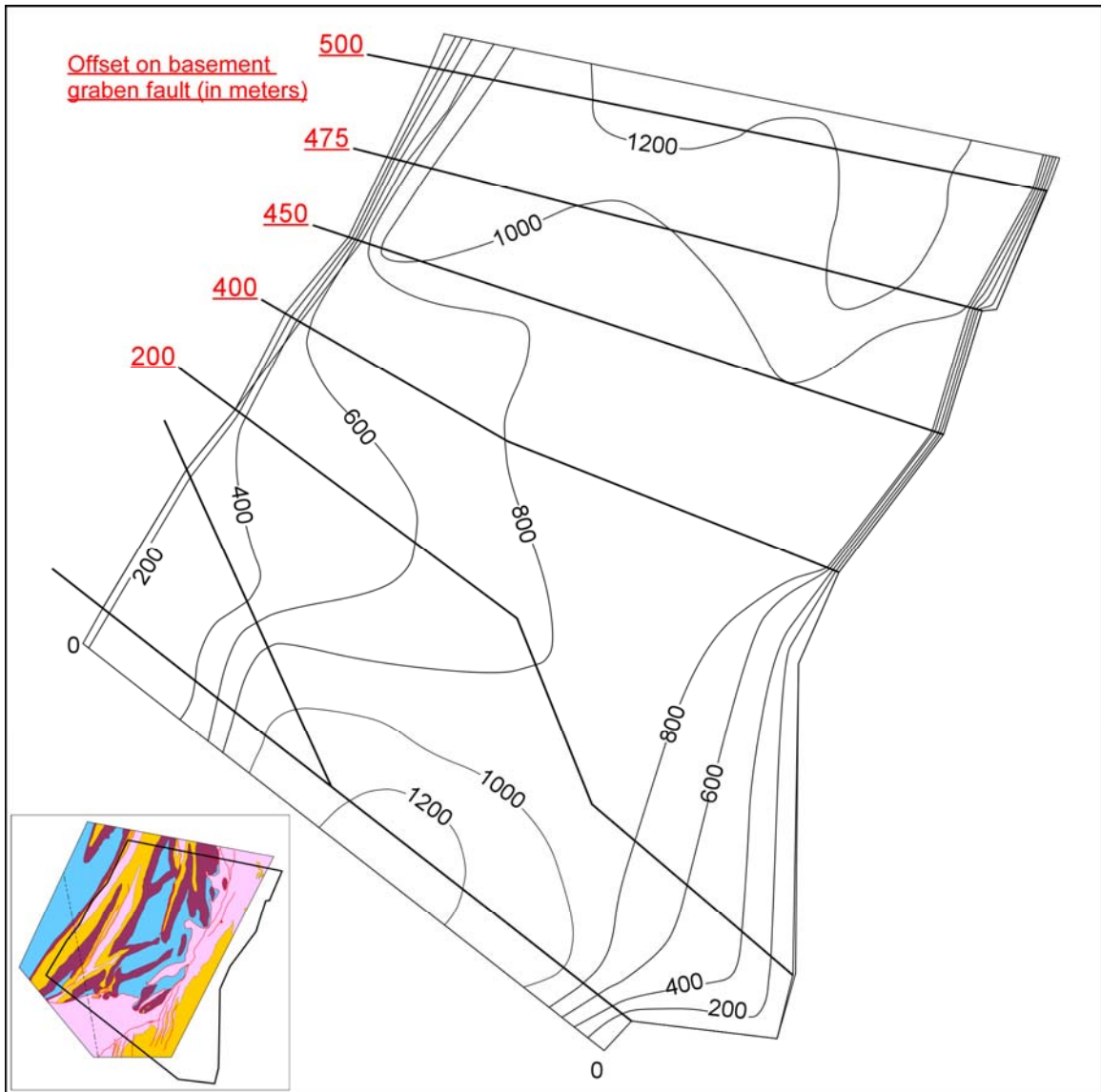


Figure 5-8. Isopach map of the graben-state ductile duplex. This map was constructed using a magnitude of offset along the basement fault that accommodates ductile-duplex surface area equal to that in the deformed state cross sections. Location of area is shown on inset map. Cross sections used for data are shown as black lines. Contour values are in meters. The magnitudes of offset (in meters) on the basement fault necessary to accommodate sufficient deposition of Unit 1 in the graben are shown in red numbers.

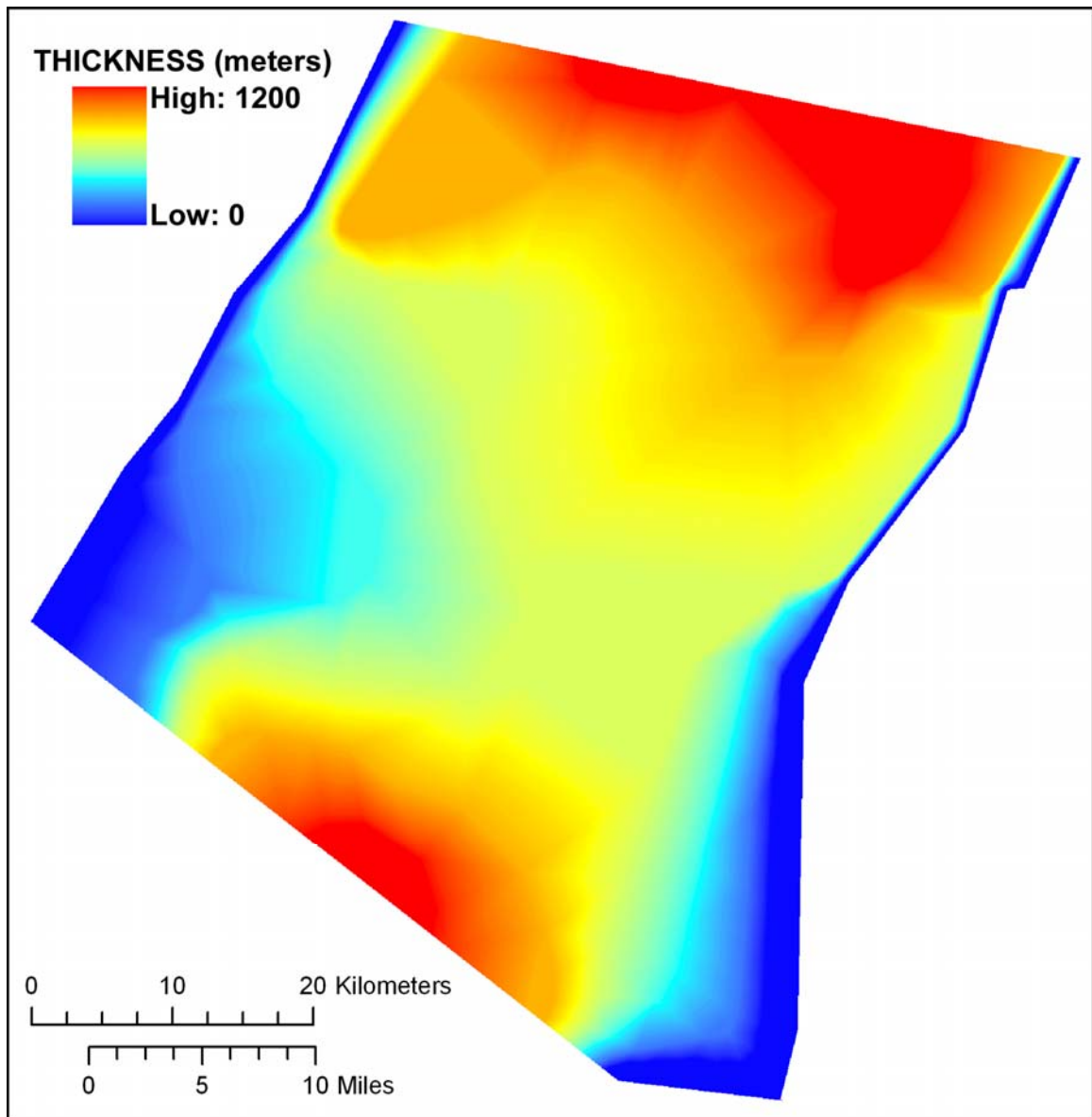


Figure 5-9. Three-dimensional surface model of the graben-state ductile duplex constructed using the isopach map shown in Figure 5-8. Note that the leading (northwestern) edge is the “wedge” at the front of the ductile duplex and that the trailing edge represents the footwall cutoff of the base of the Knox Group (Unit 2) along the Coosa fault.

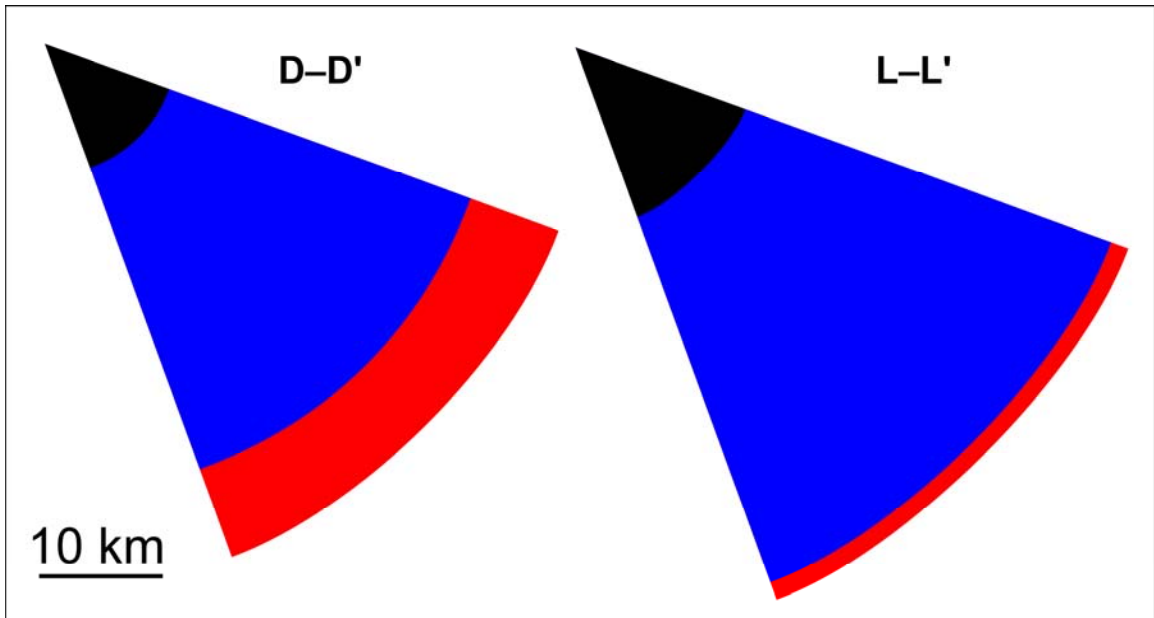


Figure 5-10. Calculations made from actual measurements on cross sections D–D' and L–L' in an attempt to compare results with the simplistic model in Figure 2-2. The area shown in black is a projection of the distance along each cross section between the intersection of the cross sections to the hinge of Taylor Ridge monocline. The area shown in blue is a projection of the deformed-state line length between the hinge of Taylor Ridge monocline to the trailing edge of the fold train through which the cross section is drawn. The area shown in red is the projection of the difference between the restored-state line length between the hinge of Taylor Ridge monocline to the trailing edge of the fold train through which the cross section is drawn and that same line-length in the deformed state.

Chapter VI:
INTERPRETATION AND DISCUSSION

6.1 STRUCTURAL INTERFERENCE IN THE GEORGIA SUBRECESS

The field research conducted as part of this project has demonstrated further details of the interference of the two prevalent structural trends in northwestern Georgia; but, no cross-cutting relationships between the structural fabrics were found to suggest distinct episodes of deformation that correspond to two non-coeval directions of thrust transport. Although Ramsay (1962) showed that interference folds can be produced by the overprint of one set of folds over another pre-existing set of folds, it stands to reason that such an overprint would create cross-cutting relationships in brittle structures such as the abundant fractures in the area of study. Two internally diachronous or overlapping episodes of deformation with distinct thrust translation directions, however, could have resulted in the structural interference pattern observed in northwestern Georgia.

Stewart (1993) demonstrated that a single deformation episode can result in interfering structural trends in the presence of other factors, such as footwall faults at oblique angles to thrust transport. Tull and Holm (2005) proposed that a north-northeast-striking oblique ramp in the footwall contributed to the formation of the abrupt bend in the Cartersville–Great Smoky fault in Georgia directly to the southeast of the study area (Figures 2-7 and 2-8). Tull and Holm (2005) referred to this oblique ramp as the Cartersville transfer fault, and it acts as part of the boundary between the Alabama promontory to the southwest and the Tennessee embayment to the northeast (Thomas, 1977). This fault is also a component of the Rising Fawn transverse zone, as described by Thomas (1990). The Cartersville–Great Smoky fault is the southeasternmost structure at the trailing edge of the sedimentary thrust belt in the Georgia subrecess, and also has one of the most abrupt bends in strike. The two structural trends of the subrecess are present to the foreland in the fault traces of the Coosa and Rome thrust sheets and the strikes of fold axes in the fold trains within the Kingston–Chattooga–Clinchport composite thrust sheet. The structural interference is thus accommodated toward the foreland from the Cartersville–Great Smoky fault intersection to the Kingston fault but does not affect structures to the northwest of the Kingston fault.

Furthermore, the mechanisms of basin control on salients can be applied to the Tennessee salient, which formed over the deep basin (referred to as the Ocoee basin in Figure 2-8) in the Tennessee embayment (*cf.* Thomas, 1977; Macedo and Marshak, 1999). The deeper detachment and the volume of sediment in the basin allowed for the (Tennessee salient) structures to propagate farther toward the foreland than those forming over the Alabama promontory. In this sense, the Georgia subrecess may be considered as the along-strike end of the Tennessee salient that lagged behind in terms of thrust transport magnitude.

Footwall obstacles in the foreland are another important factor in the formation of thrust belt curvature (*cf.* section 2.1.1.2). There are no significant basement highs documented in northwestern Georgia at present. The present research has demonstrated new evidence for a large volume of shale of the Conasauga Formation over an inverted graben in the foreland, the top of which would have had a small degree of topographic relief. This excess volume of mechanically incompetent shale, however, would not act as an obstacle, but rather readily deform ductilely and become mobile during thrust transport. The large mobile volume of shale contributed to the formation of the large ductile duplex demonstrated in this research. The ductile duplex is concentrated in the subsurface below the Kingston–Chattooga anticlinorium and the Floyd synclinorium and extends as far northwest to the subsurface beneath the area between the Kingston fault and Lookout Mountain syncline, where the ductile duplex ends as a subsurface tectonic wedge. Because none of the structures northwest of the Kingston fault bend across the Georgia subrecess, it can be suggested that the structural interference that begins southeastward at the Cartersville–Great Smoky fault intersection is accommodated and attenuated by deformation of the ductile duplex.

6.2 IMPLICATIONS OF VOLUME BALANCE OF THE DUCTILE DUPLEX

The volume balance of the ductile duplex is critical for palinspastic reconstruction of the recess, and the understanding of the kinematic and mechanical history of the local structures. The intersection and fold interference exemplify a long-standing problem in volume balancing of palinspastic reconstructions of sinuous thrust belts. Cross sections generally are constructed perpendicular to structural strike, parallel to the assumed slip

direction. An array of cross sections around a structural bend may be restored and balanced individually; however, restorations perpendicular to strike across intersecting thrust faults yield an imbalance in the along-strike lengths of frontal ramps. Similarly, the restoration leads to an imbalance in the surface area of a stratigraphic horizon. The line-length restorations along the lines of cross section measures one-dimensional shortening, which, in turn, leads to the surface-area imbalance demonstrated herein. The volumetric calculation in the models for the deformed-state and the restored-state ductile duplex demonstrates a volumetric imbalance of the Unit 1 shale. The inverted basement graben proposed herein accommodates the deposition a thicker Unit 1 across the region. In turn, the graben model provides a solution to the volume balance problems encountered in palinspastic restoration of the cross sections around the subrecess in Georgia.

As a final note, the application of the simplistic model shown in Figure 2-2 can be made to the Georgia subrecess. Actual measurements were taken from cross sections D–D' and L–L' and applied to the recess model depicted in Figure 2-2. These cross sections were selected because of mutual proximity and orientations that correspond to the two opposite arms of the subrecess. Calculation for a model similar to that in Figure 2-2 was not possible, however, because of imbalances of surface area of the thrust sheet and of magnitude of shortening between the two cross sections. Consequently, measurements from cross sections D–D' and L–L' were subsequently applied to the model in Figure 2-2 separately—as depicted in Figure 5-10—to illustrate the considerable differences between the two cross sections. In the left diagram of Figure 5-10, the palinspastic restoration lengths were measured from cross section D–D' and applied to both sides of the model from Figure 2-2; the right side of Figure 5-10 shows the same for cross section L–L'. The areas shaded blue Figure 5-10 illustrate that the width of the same segment of the thrust belt (between the hinge of Taylor Ridge monocline and the trailing edge of the fold train in this example) is significantly greater for cross section L–L'. Conversely, the amount of bulk shortening of the thrust belt segment between the hinge of Taylor Ridge monocline and the trailing edge of the fold train is substantially greater in cross section D–D'. As a result, the area of the surface area imbalance (shown in red in Figure 5-10) is considerably different. As shown by the calculations in Table 5-4, the proportion of the

surface area imbalance to the deformed-state surface area (percentage of area in red compared to the area in blue in Figure 5-10) is approximately 50% for cross section D–D', but only about 7% for cross section L–L'. In conclusion, the overall thrust belt architecture greatly differs on either arm of the Georgia recess, which may be revealed in future research as an essential feature of abrupt changes in structural trends in thrust belts.

Chapter VII:
SUMMARY AND CONCLUSIONS

Around the subrecess in northwestern Georgia, tectonically thickened weak sedimentary rocks of the Cambrian Conasauga Formation accommodated ductile deformation associated with the folding and brittle faulting of the overlying Cambrian-Ordovician regional competent layer. Ductile deformation of the underlying structurally thickened weak layer allows the shales to fill the cores of anticlines in the competent layer.

The ductile duplex (mushwad) in the core of the Kingston-Chattooga anticlinorium represents an excess volume of Unit 1 shales that elevates the structural level of the Kingston-Chattooga-Clinchport composite thrust sheet. The trailing limb of the anticlinorium is marked by the Taylor Ridge monocline, which dips into the structurally lower Floyd synclinorium. In the Floyd synclinorium, two fold trains of broad synclines and narrow anticlines plunge into the depression of the synclinorium with two distinct structural trends. Low-amplitude folds, which are the plunging ends of the fold trains, characterize the center of the abrupt bend in Appalachian structural trends in the subrecess in Georgia

The area of the mushwad in deformed-state cross sections is approximately twice the area of the corresponding Unit 1 in the restored cross sections, and cannot be explained solely by tectonic thickening parallel to the direction of apparent shortening of a conventional palinspastically restored cross section. Furthermore, the volume of the deformed-state ductile duplex is approximately 56% greater than the volume of the restored-state ductile duplex. This imbalance may result from some combination of two mechanisms: transport of Unit 1 shales into the plane of cross section, and activation/inversion of a basement graben. The out-of-plane transport of material implies an as yet unrecognized deficit in Unit 1 thickness elsewhere in the thrust belt to balance the surplus in the ductile duplex. A new interpretation proposes that a basement graben accommodated deposition of a locally thicker Unit 1 succession (approximately 1700 m for the cross section in Figure 5-7, in contrast to approximately 1200 m to the northwest of the graben) prior to thrust deformation, analogous to the Birmingham graben along

strike to the southwest in the Appalachian thrust belt in Alabama. Subsequent Middle Ordovician reactivation/inversion of part of the graben, related to Taconic loading, resulted in uplift and the erosion of the upper part of the overlying Unit 2 (Bayona and Thomas, 2003). Finally, thrusting and accretion of the weak layer into the ductile duplex occurred during tectonic shortening in the late Paleozoic. The exposed competent-layer structures in Georgia are analogous to those over shale-dominated ductile duplexes (mushwads; Thomas, 2001), which are being developed for natural gas in the Appalachian thrust belt in Alabama; however, the total thickness of the Unit 1 shale-dominated ductile duplex in Georgia is somewhat less than in those in Alabama. The high volume of the ductile duplex in the southern part of the restored-state isopach map (Figure 5-6) indicates a part of the graben in which little or no inversion occurred. Finally, the interpretation of a basement graben yields a solution to volume balance encountered during palinspastic restoration of the array of cross sections around the subrecess in Georgia. The basement graben herein allows for a thicker Unit 1 to have been deposited in the region that accounts for the volume of shale in the ductile duplex.

The reason for the abrupt bend in structural strike at the Georgia subrecess is likely multifold (as noted for the Meuse Valley recess by Lacquement *et al.*, 2005. No indication of two or more distinct translation episodes have been demonstrated for the region (*i.e.*, no consistent pattern of cross-cutting relationships between the two structural trends). Also, the vertical-axis rotation measured in the study area by Bayona *et al.* (2003) is insufficient to cause the bend in strike in northwestern Georgia. Thus, if the subrecess is the product of only one basic transport direction, other kinematic factors must have operated. Tull and Holm (2005) demonstrated that the two structural trends observed in northwestern Georgia could have been generated as a result of thrust translation over a transverse fault (Figure 2-8). Subsequently, the thick Unit 1 succession over the inverted graben in the foreland was transported and deformed into the ductile duplex (mushwad) as demonstrated herein. This ductile duplex likely served to blend the two structural trends towards the foreland and thus no structures northwest of the Kingston fault are affected by the bend in structural trend. As a final note, the considerable differences between the general architecture of the thrust belt on either side

of the subrecess may prove to be a common denominator in the structure of thrust belt recesses.

References Cited

- Algeo, T. J., 1985, Petrography and paleodepositional environment of the Bangor Limestone (Upper Mississippian) in northwest Georgia and southeast Tennessee: unpublished M.S. thesis, University of Georgia, Athens, 130 p.
- Allen, A. T., and Lester, J. G., 1957, Zonation of the Middle and Upper Ordovician strata in northwestern Georgia: Georgia Geological Survey Bulletin 66, 110 p.
- Alvarez-Marrón, J., 1991, 3D geometries and distribution of fault bend folds related to thrust topography: examples from the Cantabrian Zone, NW Spain: John Ramsay Meeting, ETH, Zurich, Neue Folge, v. 239b, p. 93.
- Apotria, T. G., Snedden, W. T., Spang, J. H., and Wiltshko, D. V., 1992, Kinematic models of deformation at an oblique ramp, *in* McClay, K. R., ed., Thrust Tectonics: London, Chapman and Hall, p. 141–154.
- Apotria, T. G., 1995, Thrust sheet rotation and out-of-plane strains associated with oblique ramps; an example from the Wyoming salient, USA: *Journal of Structural Geology*, v. 17, p. 647–662.
- Araújo, J.O. de, and Marshak, S., 1997, Formation of the Prineus syntaxis: Evidence for two episodes of Brasiliano (Pan-African) deformation in the Brasilia orogenic belt, central Brazil: Geological Society of America Abstracts with Programs, v. 29, p. 228.
- Baldwin, A. R., and Thomas, W. A., 1997, Intersecting structural trends in the Appalachian thrust belt in northwestern Georgia: Geological Society of America Abstracts with Programs, v. 29, no. 3, p. 3.
- Bayona, G., 2003, Controls on Middle to Late Ordovician synorogenic deposition in the southeastern corner of Laurentia: unpublished Ph.D. dissertation, University of Kentucky, Lexington, 268 p.
- Bayona, G., and Thomas, W. A., 2003, Distinguishing fault reactivation from flexural deformation in the distal stratigraphy of the peripheral Blountian foreland basin, southern Appalachians, USA, *Basin Research*, v. 15, p. 503–526.
- Bayona, G., and Thomas, W. A., 2006, Influence of pre-existing plate-margin structures on foredeep filling: Insights from the Taconian (Blountian) clastic wedge, Southeastern USA: *Sedimentary Geology*, v. 191, p. 115–133.
- Bayona, G., Thomas, W. A., and Van der Voo, R., 2003, Kinematics of thrust sheets within transverse zones: A structural and paleomagnetic investigation in the Appalachian thrust belt of Georgia and Alabama: *Journal of Structural Geology*, v. 25, p. 1193–1212.
- Boyer, S. E., and Elliott, D., 1982, Thrust systems: *American Association of Petroleum Geologists Bulletin*, v. 66, p. 1196–1230.
- Boyer, S. E., 1995, Sedimentary basin taper as a factor controlling the geometry and advance of thrust belts: *American Journal of Science*, v. 295, p. 1220–1254.
- Bridge, J., 1955, Disconformity between Lower and Middle Ordovician series at Douglas Lake, Tennessee: *Geological Society of America Bulletin*, v. 66, p. 725–730.
- Burg, J. P., Davy, P., Nievergelt, P., Oberli, F., Seward, D., Diao, Z., and Meier, M., 1997, Exhumation during crustal folding in the Namche-Barwa syntaxis: *Terra Nova*, v. 9, p. 53–56.
- Butler, R. W. H., 1982a, Hangingwall strain: A function of duplex shape and footwall topography: *Tectonophysics*, v. 88, p. 235–246.

- Butler, R. W. H., 1982b, The terminology of structures in thrust belts: *Journal of Structural Geology*, v. 4, p. 239-245.
- Butts, C., 1910, Description of the Birmingham quadrangle [Alabama]: United States Geological Survey Geologic Atlas, Folio 175, 24 p.
- Butts, C., 1926, The Paleozoic rocks, *in* Adams, G. I., Butts, C., Stephenson, L. W., and Cooke, W., *Geology of Alabama: Geological Survey of Alabama Special Report 14*, p. 41–230.
- Butts, C., 1948, Geology of the Paleozoic area in northwest Georgia, *in* Butts, C. and Gildersleeve, B., *Geology and mineral resources of the Paleozoic area of northwest Georgia: Georgia Geological Survey Bulletin 54*, p. 3–79.
- Callasou, S., Larroque, C., and Malaveille, J., 1993, Transfer zones of deformation in thrust wedges: and experimental study: *Tectonophysics*, v. 221, p. 325–344.
- Campbell, M. R., 1893, Geology of the Big Stone Gap coal field of Virginia and Kentucky: United States Geological Survey Bulletin 111, 106 p.
- Campbell, M. R., 1894, Description of the Estillville sheet [Kentucky–Virginia–Tennessee]: United States Geological Survey Geologic Atlas, Folio 12, 5p.
- Carter, B. D., and Chowns, T. M., 1988, Stratigraphic and Environmental Relationships of Middle and Upper Ordovician Rocks in Northwest Georgia and Northeast Alabama, *in* Keith, B. D., ed., *The Trenton Group (Upper Ordovician Series) of eastern North America: Deposition, diagenesis, and petroleum: American Association of Petroleum Geologists Studies in Geology 29*, p. 17–26.
- Chowns, T. M., 1972, Depositional environments in the Upper Ordovician of northwest Georgia and southeast Tennessee, *in* Chowns, T. M., ed., *Sedimentary environments in the Paleozoic rocks of northwest Georgia: Georgia Geological Society, Guidebook 11*, p. 3–12.
- Chowns, T. M., 1972b, Molasse sedimentation in the Silurian rocks of northwest Georgia, *in* Chowns, T. M., ed., *Sedimentary environments in the Paleozoic rocks of northwest Georgia: Georgia Geological Society, Guidebook 11*, p. 13–33.
- Chowns, T. M., compiler, 1972c, *Sedimentary environments in the Paleozoic rocks of northwest Georgia: Georgia Geological Society, Guidebook 11*, 100 p.
- Chowns, T. M., 1983, Stop 3: South end of Turnip Mountain, *in* Chowns, T. M., ed., *Geology of Paleozoic rocks in the vicinity of Rome, Georgia: Georgia Geological Society Guidebook for 18th Annual Field Trip*, p. 65.
- Chowns, T. M., 1989, Stratigraphy and major thrust sheets in the Appalachian thrust belt of Georgia, *in* Fritz, W. J., ed., *Excursions in Georgia Geology: Georgia Geological Society Guidebooks*, v. 9, no. 1, p. 211–238.
- Chowns, T. M., 2006, Sequence stratigraphy of the Red Mountain Formation; Setting for the origin of the Birmingham ironstones, *Alabama Geological Society Guidebook for 43rd Annual Field Trip*, p. 1-30.
- Chowns, T. M., *in press*, Stratigraphy of the Red Mountain Formation in its type area: Geological Survey of Alabama.

- Chowns, T. M., and Carter, B. D., 1983a, Stratigraphy of Middle and Upper Ordovician red beds in Georgia, *in* Chowns, T. M., ed., *Geology of Paleozoic rocks in the vicinity of Rome, Georgia: Georgia Geological Society Guidebook for 18th Annual Field Trip*, p. 1–15.
- Chowns, T. M., and Carter, B. D., 1983b, Karst topography and conglomerates at the base of the Greensport Formation (Middle Ordovician), *in* Chowns, T. M., ed., *Geology of Paleozoic rocks in the vicinity of Rome, Georgia: Georgia Geological Society Guidebook for 18th Annual Field Trip*, p. 68–70.
- Chowns, T. M., and Carter, B. D., 1983c, Middle Ordovician section along Mount Alto Road at southwest end of Horseleg Mountain, *in* Chowns, T. M., ed., *Geology of Paleozoic rocks in the vicinity of Rome, Georgia: Georgia Geological Society Guidebook for 18th Annual Field Trip*, p. 70–73.
- Chowns, T. M., and McKinney, F. K., 1980, Depositional facies in Middle-Upper Ordovician and Silurian rocks of Alabama and Georgia, *in* Frey, R. W., ed., *Excursions in southeastern geology*, v. 2: American Geological Institute, p. 323–348.
- Chowns, T. M., and Zeigler, E. L., 1989, Stratigraphy in the Clinchport thrust sheet, *in* Fritz, W. J., ed., *Excursions in Georgia Geology: Georgia Geological Society Guidebooks*, v. 9, no. 1, p. 231.
- Chowns, T. M., Sanders, R. P., Connell, D. A., O'Connor, B. J., and Friddell, M. S., 1989, Stratigraphy and sedimentology of the Knox Group at Graysville Gap, Catoosa County, Georgia, *in* Chowns, T. M., and O'Connor, B. J., eds., *Cambro-Ordovician Strata in Northwest Georgia and Southeast Tennessee; The Knox Group and the Sequatchie Formation: Georgia Geological Society Guidebook for 27th Annual Field Trip*, p. 5–38.
- Chowns, T. M., Holland, S. M., and Elliott, W. C., 1999, An introduction to sequence stratigraphy: Illustrations from the Valley and Ridge province in Georgia and Alabama: *Georgia Geological Society Guidebook for 34th Annual Field Trip*, p. 1–50.
- Coleman, J. L., Jr., 1988, Drilling on the CSD, *in* Coleman, J. L., Jr., Groshong, R. H., Jr., Rheams, K. F., Neathery, T. L., and Rheams, L. J., eds., *Alabama Geological Society, 25th Annual Field Trip Guidebook*, p. 52–53.
- Cook, B. S. and Thomas, W. A., 2009, Superposed lateral ramps in the Pell City thrust sheet, Appalachian thrust belt, Alabama: *Journal of Structural Geology*, v. 31, p. 941–949.
- Cook, B. S. and Thomas, W. A., *in press*, Ductile duplexes as potential natural gas plays: an example from the Appalachian thrust belt in Georgia, USA: *Hydrocarbons in Contractual Belts*, Geological Society of London.
- Cramer, H. R., 1979, Pennsylvanian stratigraphy of northwest Georgia, *in* Thomas, W. A., and Cramer, H. R., *The Mississippian and Pennsylvanian (Carboniferous) systems in the United States--Georgia: United States Geological Survey Professional Paper 1110-H*, p. H19–H34.
- Crawford, T. J., 1986, Pennsylvanian outliers in Georgia, *in* Rich, M., Crawford, T. J., and Grainger, G. S., *Carboniferous stratigraphy near Rome, in the Valley and Ridge province, western Georgia: Georgia Geological Society Guidebook for Field Trip No. 2, Society of Economic Paleontologists and Mineralogists Annual Meeting*, p. 7–15.
- Crawford, T. J., 1989, *Geology of the Pennsylvanian System of Georgia: Georgia Geological Survey Geologic Atlas 2*, 16 p.
- Crawford, T. J., Gillespie, W. H., and Waters, J. A., 1989, The Pennsylvanian system of Georgia, *in* Fritz, W. J., ed., *Excursions in Georgia Geology: Georgia Geological Society Guidebooks*, v. 9, no. 1, p. 1–27.

- Cressler, C. W., 1963, Geology and ground-water resources of Catoosa County, Georgia: Georgia Geological Survey Information Circular 28, 19 p.
- Cressler, C. W., 1964a, Geology and groundwater resources of the Paleozoic rock area, Chattooga County, Georgia: Georgia Geological Survey Information Circular 27, 14 p.
- Cressler, C. W., 1964b, Geology and ground-water resources of Walker County, Georgia: Georgia Geological Survey Information Circular 29, 15 p.
- Cressler, C. W., 1970, Geology and groundwater resources of Floyd and Polk Counties, Georgia: Georgia Geological Survey Information Circular 39, 95 p.
- Cressler, C. W., 1974, Geology and ground-water resources of Gordon, Whitfield, and Murray Counties, Georgia: Georgia Geological Survey Information Circular 47, 56 p.
- Croft, M. G., 1964, Geology and ground-water resources of Dade County, Georgia: Georgia Geological Survey Information Circular 26, 17 p.
- Culbertson, W. C., 1963, Pennsylvanian nomenclature in northwest Georgia: United States Geological Survey Professional Paper 450-E, p. E51–E57.
- Dahlstrom, C. D. A., 1969, Balanced cross sections: Canadian Journal of Earth Sciences, v. 6, p. 743–757.
- Dahlstrom, C. D. A., 1970, Structural geology in the eastern margin of the Canadian Rocky Mountains: Bulletin of Canadian Petroleum Geology, v. 18, p. 332–406.
- Dana, J. D., 1866, A Textbook of Geology: Philadelphia, Theodore Bliss, 354 p.
- Davis, D. M., and Engelder, T., 1985, The role of salt in fold-and-thrust belts: Tectonophysics, v. 119, p. 67–88.
- Davis, D. M., and Lillie, R. J., 1994, Changing mechanical response during continental collision: active examples from the foreland thrust belts of Pakistan: Journal of Structural Geology, v. 16, p. 21–34.
- de Beer, C. H., 1992, Structural evolution of the Cape fold belt syntaxis and its influence on syntectonic sedimentation in the SW Karoo Basin, *in* de Wit, J. J., and Ransome, I. G. D., eds., Inversion Tectonics of the Cape Fold belt, Karoo and Cretaceous Basins of Southern Africa: Rotterdam, Balkema, p. 197–206.
- Dean, S. L., and Kulander, B. R., 1978, Kinematic analysis of folding and pre-fold structures on the southwester flank of the Williamsburg anticline, Greenbriar County, WV: Geological Society of America Abstracts with Programs, v. 9, p. 132–133.
- Drahovzal, J. A., and Neathery, T. L., 1971, Middle and Upper Ordovician stratigraphy of the Alabama Appalachians, *in* Drahovzal, J. A., and Neathery, T. L., eds., The Middle and Upper Ordovician of the Alabama Appalachians: Alabama Geological Society Guidebook, 9th Annual Field Trip, p. 1–62.
- Drake, A. A., and Lyttle, P. T., 1980, Alleghanian thrust faults in the Kittatinny Valley, New Jersey, *in* Manspiezer, W., ed., Field Studies of New Jersey Geology and guide to field trips: 52nd Annual Meeting of the New York State Geological Association., p. 92–115.
- Englund, K. J., Gillespie, W. H., Cecil, C. B., and Windolph, J. F., Jr., 1985, Characteristics of the Mississippian–Pennsylvanian boundary and associated coal-bearing rocks in the southern Appalachians: United States Geological Survey Open-File Report 85-577, 84 p.

- Ferrill B. A. and Thomas, W. A., 1988, Acadian dextral transpression and synorogenic sedimentary successions in the Appalachians: *Geology*, v. 16, p. 604–608.
- Frey, M. G., 1973, Influence of Salina Salt on structure in New York–Pennsylvania part of Appalachian Plateau: *American Association of Petroleum Geologists Bulletin*, v. 57, p. 1027–1037.
- Geiser, P., and Engelder, T., 1983, The distribution of layer parallel shortening fabrics in the Appalachian foreland of New York and Pennsylvania: Evidence for two non-coaxial phases of the Alleghanian orogeny, *in* Hatcher, R. D., Jr., Williams, H., and Zietz, I., eds., *Contributions to the Tectonics and Geophysics of Mountain Chains: Geological Society of America Memoir 158*, p. 161–175.
- Georgia Geological Survey, 1976, Geologic map of Georgia: Georgia Geological Survey, scale 1:500,000.
- Gillespie, W. H., Crawford, T. J., and Waters, J. A., 1989, Plant fossils of the Pennsylvanian System of Georgia: 13 p.
- Grainger, G. S., 1983, Geology related to the powerhouse excavation of the Rocky Mountain pumped storage project, *in* Chowns, T. M., ed., *Geology of Paleozoic rocks in the vicinity of Rome, Georgia: Georgia Geological Society Guidebook for 18th Annual Field Trip*, p. 42–59.
- Gray, M. B., and Stamatakos, J., 1997, New model for evolution of fold and thrust belt curvature based on integrated structural and paleomagnetic results from the Pennsylvania salient: *Geology*, v. 25, p. 1067–1070.
- Harris, L. D., 1969, Kingsport Formation and Mascot Dolomite (Lower Ordovician) of East Tennessee: Tennessee Division of Geology Report of Investigations No. 23, p. 1–39.
- Harris, L. D., 1976, Thin-skinned tectonics and potential hydrocarbon traps—illustrated by a seismic profile in the Valley and Ridge Province of Tennessee: *Journal of Research of the United States Geological Survey*, v. 4, p. 379–386.
- Hass, W. H., 1956, Age and correlation of the Chattanooga Shale and the Maury Formation: United States Geological Survey Professional Paper 286, 47 p.
- Hasson, K. O., and Haase, C. S., 1988, Lithofacies and paleogeography of the Conasauga Group, (Middle and Late Cambrian) in the Valley and Ridge province of east Tennessee: *Geological Society of America Bulletin*, v. 100, p. 234–246.
- Hatcher, R. D., Jr., Thomas, W. A., Geiser, P. A., Snoke, A. W., Mosher, S., and Wiltschko, D. V., 1989, Alleghanian orogen, *in* Hatcher, R. D., Jr., Thomas, W. A., and Viele, G. W., eds., *The Appalachian-Ouachita orogen in the United States: Geological Society of America, The Geology of North America*, v. F-2, p. 233–318.
- Hayes, C. W., 1891, The overthrust faults of the southern Appalachians, with discussion by C. D. Walcott, W. M. Davis, and Bailey Willis: *Geological Society of America Bulletin*, v. 2, p. 141–154.
- Hayes, C. W., 1892, Geology of northeastern Alabama, and adjacent portions of Georgia and Tennessee: *Alabama Geological Survey Bulletin 4*, 85 p.
- Hayes, C. W., 1894, Geology of a portion of the Coosa Valley in Georgia and Alabama: *Geological Society of America Bulletin*, v. 5, p. 465–480.
- Hayes, C. W., 1902, Description of the Rome folio [Georgia]: United States Geological Survey Geological Atlas, Folio 78, 6 p.

- Hobday, D. K., 1974, Beach and barrier island facies in the Upper Carboniferous of northern Alabama: Geological Society of America Special Paper 148, p. 209-223.
- Hurst, V. J., 1953, Chertification in the Fort Payne Formation, Georgia: Georgia Geological Survey Bulletin, v. 60, p. 215-238.
- Jamison, W. R., 1992, Stress controls on fold thrust style, *in* McClay, K. R., ed., Thrust Tectonics: London, Chapman and Hall, p. 155-164.
- Jaumé, S. C., and Lillie, R. J., 1988, Mechanics of the Salt Range-Potwar Plateau, Pakistan: a fold-and-thrust belt underlain by evaporites: Tectonics, v. 7, p. 57-71.
- Jenkins, C., 1984, Depositional environments of the Middle Ordovician Greensport Formation and Colvin Mountain Sandstone in Calhoun, Etowah, and St. Clair Counties, Alabama: unpublished thesis, University of Alabama, Tuscaloosa, 156 p.
- Johnson, V. H., 1946, Coal deposits on Sand and Lookout Mountains, Dade and Walker Counties, Georgia: United States Geological Survey open-file report, scale 1 inch to 4,000 feet, text.
- Julivert, M., 1981, A cross section through the northern part of the Iberian massif: Geologie en Mijnbouw, v. 60, p. 107-128.
- Julivert, M., and Marcos, A., 1973, Superimposed folding under flexural conditions in the Cantabrian zone (Hercynian Cordillera, Northwest Spain): American Journal of Science, v. 273, p. 353-375.
- Kaygi, P. B., Cameron, T. E., and Raeuchle, S. K., 1983, Regional cross section and palinspastic reconstruction of the Alabama fold and thrust belt: Geological Society of America Abstracts with Programs, v. 15, p. 95.
- Keith, A., 1895, Description of the Knoxville sheet [Tennessee-North Carolina]: United States Geological Survey Geologic Atlas, Folio 12, 6 p.
- Keith, A., 1903, Description of the Cranberry quadrangle [North Carolina-Tennessee]: United States Geological Survey Geologic Atlas, Folio 90, 9 p.
- Kesler, T. L., 1975, Rome and Coosa faults in northwest Georgia: Geological Society of America Bulletin, v. 86, p. 625-631.
- Kidd, J. T., and Neathery, T. L., 1976, Correlation between Cambrian rocks of the southern Appalachian geosyncline and the interior low plateaus: Geology, v. 4, p. 767-769.
- Kulander, B. R., and Dean, S. L., 1986, Structure and Tectonics of Central and Southern Appalachian Valley and Ridge and Plateau Provinces, West Virginia and Virginia: American Association of Petroleum Geologists Bulletin, v. 70, p. 1674-1684.
- Kulander, B. R., and Dean, S. L., 1988, The North Mountain-Pulaski fault system and related thrust sheet structure, *in* Mitra, G., and Wojtal, S., eds., Geometries and Mechanisms of Thrusting: Geological Society of America Special Paper 222, p. 107-18.
- Kulik, D. M., and Schmidt, C. J., 1988, Region of overlap and styles of interaction of Cordilleran thrust belt and Rocky Mountain foreland, *in* Perry, W. J., Jr., and Schmidt, C. J., Interaction of Foreland and Thrust Belt, Western United States: Geological Society of America Memoir 171, p. 75-99.

- Kwon, S., and Mitra, G., 2004, Strain distribution, strain history and kinematic evolution associated with the formation of arcuate salients in fold-thrust belts: The example of the Provo salient, Sevier orogen, Utah, *in* Sussman, A., and Weil, A., eds., *Orogenic Curvature: Geological Society of America Special Paper 383*, p. 205–223.
- Lacquement, F., Averbuch, O., Mansy, J.-L., Szaniawski, R., and Lewandowski, M., 2005, Transpressional deformations at lateral boundaries of propagating thrust-sheets: the example of the Meuse Valley Recess within the Ardennes Variscan fold-and-thrust belt (N France–S Belgium): *Journal of Structural Geology*, v. 27, p. 1788–1802.
- Laubscher, H. P., 1972, Some overall aspects of Jura dynamics: *American Journal of Science*, v. 272, p. 293–304.
- Laubscher, H., 2008, The Grenchenberg conundrum in the Swiss Jura: a case for the centenary of the thin-skin décollement nappe model (Buxtorf 1907), *Swiss Journal of Geosciences*, v. 101, p. 41–60.
- Lawrence, R. D., Khan, S. H., DeJong, K. A., Farah, A., and Yeats, R. S., 1981, Thrust and strike-slip fault interaction along the Chaman transform zone, Pakistan, *in* McClay, K. R., and Price, N. J., eds., *Thrust and Nappe Tectonics: Geological Society of London Special Publication 9*, p. 363–370.
- Lisle, R. J., Styles, P., and Freeth, S. J., 1990, Fold interference structures: The influence of layer competence contrast: *Tectonophysics*, v. 172, p. 197–200.
- Lowry, W. D., 1971, Contrast in style of deformation of the southern and central Appalachians: Virginia Polytechnic Institute and State University guidebook no. 6, p. 1–22.
- Macedo, J. M., and Marshak, S., 1999, Controls on the geometry of fold-thrust belt salients: *Geological Society of America Bulletin*, v. 111, p. 1808–1822.
- Maples, C. G., and Waters, J. A., 1984, Algal-archaeocyathan patch reefs from the Cartersville mining district, Georgia: *Southeastern Geology*, v. 24, p. 159–167.
- Marrett, R., 1995, Structure, kinematics, and development of the Sierra Madre Oriental salient, Mexico: *Geological Society of America Abstracts with Programs*, v. 27, p. 73.
- Marshak, S., 1988, Kinematics of orocline and arc formation in thin-skinned orogens: *Tectonics*, v. 7, p. 73–86.
- Marshak, S., 2004, Salients, recesses, arcs, oroclines, and syntaxes--A review of idea concerning the formation of map-view curves in fold-thrust belts, *in* McClay, K. R., ed., *Thrust Tectonics and Hydrocarbon Systems: American Association of Petroleum Geologists Memoir 82*, p. 131–156.
- Marshak, S., and Flötmann, T., 1996, Structure and origin of the Fleurieu and Nackara arcs in the Adelaide fold-thrust belt, South Australia; salient and recess development in the Delamerian orogen: *Journal of Structural Geology*, v. 18, p. 891–908.
- Marshak, S., and Tabor, J., 1989, Structure of the Kingston orocline in the Appalachian fold-thrust belt, New York: *Geological Society of America Bulletin*, v. 101, p. 683–701.
- Marshak, S., and Wilkerson, M. S., 1992, Effect of overburden thickness on thrust-belt geometry and development: *Tectonics*, v. 11, p. 560–566.
- Martin, A. J., 1992, Stratigraphy and depositional environments of the Sequatchie Formation, *in* Chowns, T. M., and O'Connor, B. J., eds., *Cambro-Ordovician Strata in Northwest Georgia and Southeast Tennessee; The Knox Group and the Sequatchie Formation: Georgia Geological Society Guidebook for 27th Annual Field Trip*, p. 89–106.

- Maynard, T. P., 1912, A report on the limestones and cement materials of north Georgia: Georgia Geological Survey Bulletin 27, 293 p.
- McCallie, S. W., 1904, A preliminary report on the coal deposits of Georgia: Georgia Geological Survey Bulletin 12, 121 p.
- McDougall, J. W., and Khan, S. H., 1990, Strike-slip faulting in a foreland fold-thrust belt: The Kalabagh fault and western Salt Range, Pakistan: *Tectonics*, v. 9, p. 1061–1075.
- McLemore, W. H., 1971, The geology and geochemistry of the Mississippian System in northwest Georgia and southeast Tennessee: unpublished Ph.D. dissertation, University of Georgia, Athens, 251 p.
- McMaster, R. L., deBoer, J., and Barclay, P. C., 1980, Tectonic development of Southern Narragansett Bay and offshore Rhode Island: *Geology*, v. 8, p. 496–500.
- McQuarrie, N., 2004, Crustal scale geometry of the Zagros fold-thrust belt, Iran, *Journal of Structural Geology*, v. 26, p. 519–535.
- Melnyk, M. J., and Cameron, C. P., 1998, Structural geology of a portion of the Monterrey salient, northeastern Mexico; an analog to the Juras: *Geological Society of America Abstracts with Programs*, v. 30, p. 170–171.
- Milici, R. C., 1973, The stratigraphy of Knox County, Tennessee: *Tennessee Division of Geology Bulletin* 70, p. 9-24.
- Milici, R. C., 1974, Stratigraphy and depositional environments of Upper Mississippian and Lower Pennsylvanian rocks in the southern Cumberland Plateau of Tennessee, *in* Briggs, G., ed., *Carboniferous of the southeastern United States: Geological Society of America Special Paper* 148, p. 115–133.
- Milici, R. C., and Smith, J. W., 1969, Stratigraphy of the Chickamauga Supergroup in its type area: *Georgia Geological Survey Bulletin* 80, p. 1–35.
- Milici, R. C., and Wedow, H., Jr., 1977, Upper Ordovician and Silurian stratigraphy in the Sequatchie Valley and parts of the adjacent Valley and Ridge: *United States Geological Survey Professional Paper* 996, 38 p.
- Mitra, G., 1997, Evolution of salients in a fold-and-thrust belt: the effects of sedimentary basin geometry, strain distribution and critical taper, *in* Sengupta, S., ed., *Evolution of Geological Structures in Micro- to Macro- Scales: London, Chapman and Hall*, p. 59–90.
- Montgomery, J. M., Jr., 1993, The origin of structural curvature in the northern part of the Wyoming-Idaho thrust belt, Wyoming-Idaho: Lexington, University of Kentucky, unpublished M.S. thesis, 122 p.
- Mosher, S., 1981, Late Paleozoic deformation of the Narragansett Basin, Rhode Island: *Geological Society of America Abstracts with Programs*, v. 13, p. 515.
- Munyan, A. C., 1951, Geology and mineral resources of the Dalton Quadrangle, Georgia-Tennessee: *Georgia Geological Survey Bulletin* 57, 128 p.
- Murray, D. P., and Skehan, S. J., J. W., 1979, A traverse across the eastern margin of the Appalachian-Caledonide orogen, Southeastern New England, *in* Skehan, S. J., J. W., and Osberg, P. H., eds., *The Caledonides in the U. S. A.: Geological Excursions in the Northeast Appalachians*, *Weston Obsv.*, p. 1–35.

- Neathery, T. L., 1988, Stratigraphy and facies changes of the Paleozoic succession in Wills Valley, Etowah and De Kalb Counties, Alabama, in *Structure of the Wills Valley anticline-Lookout Mountain syncline between the Rising Fawn and Anniston CSD's, northeast Alabama: Alabama Geological Society Guidebook for the 25th Annual Field Trip*, p. 54–68.
- Nelson, W. A., 1925, The Southern Tennessee coal field: *Tennessee Division Geological Bulletin* 33-A, 239 p.
- Nunan, W. E., 1972, Sedimentary environment of the Armuchee Chert, northwest Georgia, *in* Chowns, T. M., ed., *Sedimentary environments in the Paleozoic rocks of northwest Georgia: Georgia Geological Society, Guidebook* 11, p. 57–68.
- Oder, C. R. L., 1934, Preliminary subdivision of the Knox dolomite in east Tennessee: *Journal of Geology*, v. 42, p. 469–497.
- Oder, C. R. L., and Miller, H. W., 1945, Stratigraphy of the Mascot-Jefferson City zinc district [Tennessee]: *American Institute of Mining and Metallurgical Engineers Technical Publication* 1818, 9p.
- Ortiz, A. S., and Chowns, T. M., 1978, A new reference section for the Knox Group in northwest Georgia: *Georgia Journal of Science*, v. 36, p. 89.
- Osborne, W.E., Szabo, M.W., Neathery, T.L., and Copeland, C.W., Jr., (compilers), 1988, Geologic Map of Alabama, northeast sheet. Geological Survey of Alabama Special Map 220, scale 1:250,000.
- Paulsen, T., and Marshak, S., 1998, Structure of the Mt. Raymond transverse zone at the southern end of the Wyoming salient, Sevier fold-thrust belt, Utah: *Tectonophysics*, v. 280, p. 199–211.
- Paulsen, T., and Marshak, S., 1999, Origin of the Uinta recess, Sevier fold-thrust belt, Utah: Influence of basin architecture on fold-thrust belt geometry: *Tectonophysics*, v. 312, p. 203–216.
- Peterson, M. N. A., 1962, The mineralogy and petrology of Upper Mississippian carbonate rocks of the Cumberland Plateau in Tennessee: *Journal of Geology*, v. 70, p. 1–31.
- Ramsay, J. G., 1962, Interference patterns produced by the superposition of folds of similar type: *Journal of Geology*, v. 70, p. 466–481.
- Ramsay, J. G., 1992, Some geometric problems of ramp-flat thrust models, *in* McClay, K. R., ed., *Thrust Tectonics*: London, Chapman and Hall, p. 191–200.
- Rankin, D. W., 1976, Appalachian salients and recesses: Late Precambrian continental breakup and the opening of the Iapetus Ocean: *Journal of Geophysical Research*, v. 81, p. 5605–5619.
- Raymond, D. E., 1993, The Knox Group of Alabama: An Overview: *Geological Survey of Alabama Bulletin* 152, 160 p.
- Repetski, J. E., 1992, Knox and basal Stones River Group conodonts from near Graysville, Catoosa County, Georgia, *in* Chowns, T. M., and O'Connor, B. J., eds., *Cambro-Ordovician Strata in Northwest Georgia and Southeast Tennessee; The Knox Group and the Sequatchie Formation: Georgia Geological Society Guidebook for 27th Annual Field Trip*, p. 39–46.
- Rich, M., 1984, Distribution of foraminifers in the Bangor Limestone (Upper Mississippian) in northwestern Georgia: *Geological Society of America Abstracts with Programs*, v. 16, p. 190.

- Rich, M., 1986a, Stop 2: Taylor Ridge, *in* Rich, M., Crawford, T. J., and Grainger, G. S., Carboniferous stratigraphy near Rome, in the Valley and Ridge province, western Georgia: Georgia Geological Society Guidebook for Field Trip No. 2, Society of Economic Paleontologists and Mineralogists Annual Meeting, p. 19.
- Rich, M., 1986b, Mississippian stratigraphy in northwestern Georgia, *in* Rich, M., Crawford, T. J., and Grainger, G. S., Carboniferous stratigraphy near Rome, in the Valley and Ridge province, western Georgia: Georgia Geological Society Guidebook for Field Trip No. 2, Society of Economic Paleontologists and Mineralogists Annual Meeting, p. 1–5.
- Rich, M., 1986c, Foraminifera, stratigraphy, and regional interpretation of the Bangor Limestone in northwestern Georgia: *Journal of Foraminiferal Research*, v. 15, p. 110–134.
- Rich, M., 1986d, Stop 1: Florida Rock Industries, Rome quarry, *in* Rich, M., Crawford, T. J., and Grainger, G. S., Carboniferous stratigraphy near Rome, in the Valley and Ridge province, western Georgia: Georgia Geological Society Guidebook for Field Trip No. 2, Society of Economic Paleontologists and Mineralogists Annual Meeting, p. 11–19.
- Rich, M., 1992, Structural and stratigraphic trends in the Floyd synclinorium, northwestern Georgia, and speculation on their relationship to reactivated basement faults: Georgia Geological Survey Geologic Report 6, 15 p.
- Rindsberg, A. K., 1983, Ichnology and paleoecology of the Sequatchie and Red Mountain Formations (Ordovician-Silurian), Georgia-Tennessee: unpublished M.S. thesis, University of Georgia, Athens, 365 p.
- Rindsberg, A. K., and Chowns, T. M., 1986, Ringgold Gap: Progradational sequences in the Ordovician and Silurian of northwest Georgia: *Geological Society of America Centennial Field Guide*, v. 6, p. 159–162.
- Rodgers, J., 1953, Geologic map of east Tennessee with explanatory text: Tennessee Division of Geology Bulletin, no. 58, pt. 2, 167 p.
- Rodgers, J., 1970, *The Tectonics of the Appalachians*: John Wiley and Sons, New York, 271 p.
- Rodgers, J., and Kent, D. F., 1948, Stratigraphic section at Lee Valley, Hawkins County, Tennessee: Tennessee Division of Geology Bulletin 55, 47 p.
- Royden, L., and Burchfiel, B. C., 1989, Are systematic variations in thrust belt style related to plate boundary processes? (the western Alps versus the Carpathians): *Tectonics*, v. 8, p. 51–61.
- Safford, J. M., 1869, *Geology of Tennessee*: State of Tennessee, Nashville, 550 p.
- Safford, J. M., and Killebrew, J. B., 1900, *The elements of the geology of Tennessee*: Nashville, 264 p.
- Sloss, L. L., 1963, Sequences in the cratonic interior of North America: *Geological Society of America Bulletin*, v. 74, p. 93–114.
- Smith, E. A., 1876, Report of progress for 1876: Alabama Geological Survey Report of Progress, Alabama Geological Survey Report of Progress 4, 99 p.
- Smith, E. A., 1890, Geology of the valley regions adjacent to the Cahaba coal field, *in* Squire, J., Report on the Cahaba coal field: Alabama Geological Survey Special Report 2, p. 133–180.
- Smith, E. A., 1894, *Geological map of Alabama*: Alabama Geological Survey Special Map 1.

- Spencer, J. W., 1893, The Paleozoic group: The geology of ten counties of northwestern Georgia: Geological Survey of Georgia, 406 p.
- Stauffer, M. R., 1988, Fold interference structures and coaptation folds: *Tectonophysics*, v. 149, p. 339-343.
- Stearns, R. G., 1963, Monteagle Limestone, Hartselle Formation, and Bangor Limestone; a new Mississippian nomenclature for use in Middle Tennessee, with a history of its development: Tennessee Division of Geology Information Circular 11, p. 3-8.
- Stewart, S. A., 1993, Fold interference structures in thrust systems: *Tectonophysics*, v. 225, p. 449-456.
- Stewart, S. A., 1999, Geometry of thin-skinned tectonic systems in relation to detachment layer thickness in sedimentary basins: *Tectonics*, v. 18, p. 719-732.
- Stose, G. W., 1923, Manganese deposits of east Tennessee: United States Geological Survey Bulletin 737, 154 p.
- Talbot, C. J., and Alavi, M., 1996, The past of a future syntaxis across the Zagros: Geological Society of London Special Publication 100, p. 89-109.
- Thomas, W. A., 1972, Mississippian stratigraphy of Alabama: Alabama Geological Survey Monograph 12, 121 p.
- Thomas, W. A., 1974, Converging clastic wedges in the Mississippian of Alabama: Geological Society of America Special Paper 148, p. 187-207.
- Thomas, W. A., 1977, Evolution of Appalachian-Ouachita salients and recesses from reentrants and promontories in the continental margin: *American Journal of Science*, v. 277, p. 1233-1278.
- Thomas, W. A., 1979, Mississippian stratigraphy of northwest Georgia, *in* Thomas, W. A., and Cramer, H. R., The Mississippian and Pennsylvanian (Carboniferous) systems in the United States--Georgia: United States Geological Survey Professional Paper 1110-H, p. H5-H18.
- Thomas, W. A., 1982, Stratigraphy and structure of the Appalachian fold and thrust belt in Alabama (Geological Society of America 95th Annual Meeting guidebook, field trip 13): Tuscaloosa, Alabama, Alabama Geological Survey, p. 55-66.
- Thomas, W. A., 1985, Northern Alabama sections, *in* Woodward, N. B., ed., Valley and Ridge Thrust Belt: Balanced Structural Sections, Pennsylvania to Alabama (Appalachian Basin Industrial Associates): University of Tennessee Department of Geological Sciences Studies in Geology, v. 12, p. 54-61.
- Thomas, W. A., 1989, Palinspastic restoration at bends in thrust belts: Appalachian Industrial Associates Program, v. 16, p. 171-184.
- Thomas, W. A., 1991, The Appalachian-Ouachita rifted margin of southeastern North America: Geological Society of America Bulletin, v. 103, p. 415-431.
- Thomas, W. A., 2001, Mushwad: Ductile duplex in the Appalachian thrust belt in Alabama: American Association of Petroleum Geologists Bulletin, v. 85, p. 1847-1869.
- Thomas, W. A., 2007, Role of the Birmingham basement fault in thin-skinned thrusting of the Birmingham anticlinorium, Appalachian thrust belt in Alabama: *American Journal of Science*, v. 307, p. 46-62.

- Thomas, W. A., and Bayona, G., 2005, The Appalachian thrust belt in Alabama and Georgia: Thrust-belt structure, basement structure, and palinspastic reconstruction: Geological Survey of Alabama Monograph 16. 48 p., 2 plates.
- Thomas, W. A., and Cramer, H. R., 1979, The Mississippian and Pennsylvanian (Carboniferous) systems in the United States--Georgia: United States Geological Survey Professional Paper 1110-H, 37 p.
- Thomas, W. A., and Whiting, B. M., 1995, The Alabama Promontory; an example of the evolution of an Appalachian-Ouachita thrust belt recess at a promontory of the rifted continental margin: Geological Association of Canada Special Paper 41, p. 1–20.
- Thomas, W. A., Astini, R. A., and Denison, R. E., 2001, Strontium isotopes, age, and tectonic setting of Cambrian salinas along the rift and transform margins of the Argentine Precordillera and southern Laurentia: *Journal of Geology*, v. 109, p. 231–246.
- Thorbjornsen, K. L., and Dunne, W. M., 1997, Origin of a thrust-related fold: geometric vs. kinematic tests: *Journal of Structural Geology*, v. 19, p. 303–319.
- Tull, J. F., and Holm, C. S., 2005, Structural evolution of a major Appalachian salient-recess junction: Consequences of oblique collisional convergence across a continental margin transform fault: *Geological Society of America Bulletin*, v. 117, p. 482–499.
- Twenhofel, W. H., Chairman of the Ordovician Subcommittee of the Committee on Stratigraphy of the National Research Council, and 14 others, 1954, Correlation of the Ordovician Formations of North America, Correlation Chart No. 2: *Geological Society of America Bulletin* v. 65, p. 247–298.
- Ulrich, E. O., 1911, Revision of the Paleozoic Systems: *Geological Society of America Bulletin*, v. 22, p. 281–680.
- Vail, P. R., 1959, Stratigraphy and lithofacies of Upper Mississippian rocks in the Cumberland Plateau: unpublished Ph.D. dissertation, Northwestern University, Evanston, Illinois, 143 p.
- Van der Voo, R., 2004, Paleomagnetism, oroclines, and growth of continental crust: *GSA Today*, v. 14, p. 4-9.
- Willis, B., 1893, The mechanics of Appalachian structure: U.S. Geological Survey, Annual Report 13, Part 2, p. 211–281.
- Wilson, C. W., Jr., 1949, Pre-Chattanooga stratigraphy in Central Tennessee: *Tennessee Division of Geology Bulletin* 56, 407 p.
- Wilson, C. W., Jr., Jewell, J. W., and Luther, E. T., 1956, Pennsylvanian geology of the Cumberland Plateau, Tennessee: Nashville, Tennessee Division of Geology Folio (Nashville), 21 p.
- Wilson, R. L., 1965, Pennsylvanian stratigraphy and sedimentation of the northern part of Sand Mountain, Alabama, Georgia, and Tennessee: unpublished Ph.D. dissertation, University of Tennessee, Knoxville, 110 p.
- Wilson, R. L., 1979, Geology of Hamilton County, Tennessee: *Tennessee Division of Geology Bulletin* 79, 128 p.
- Wilson, R. L., 1992, The Knox Group in Hamilton County, Tennessee, *in* Chowns, T. M., and O'Connor, B. J, eds., Cambro-Ordovician Strata in Northwest Georgia and Southeast Tennessee; The Knox Group and the Sequatchie Formation: *Georgia Geological Society Guidebook for 27th Annual Field Trip*, p. 47–54.

- Wiltschko, D., and Eastman, D., 1983, Role of basement warps and faults in localizing thrust fault ramps, *in* Hatcher, R. D., Jr., Williams, H., and Zietz, I., eds., *Contributions to the Tectonics and Geophysics of Mountain Chains*: Geological Society of America Memoir 158, p. 177–190.
- Wiltschko, D. V., and Eastman, D. B., 1988, A photoelastic study of the effects of preexisting reverse faults in basement on the subsequent deformation of the cover, *in* Schmidt, C. J., and Perry, W. J., Jr., eds., *Interaction of the Rocky Mountain Foreland and the Cordilleran Thrust Belt*: Geological Society of America Memoir 171, p. 111–118.
- Wise, D. U., 2004, Pennsylvania salient of the Appalachians: A two-azimuth transport model based on new compilations of Piedmont data: *Geology*, v. 32, p. 777–780.
- Wise, D. U., and Werner, M. L., 2004, Pennsylvania salient of the Appalachians: A two-stage model for Alleghanian motion based on new compilations of Piedmont data: *Geological Society of America Special Paper* 383, p. 109–120.
- Woodward, N. B., and Gray, D. R., 1985, Southwest Virginia, Tennessee, and northern Georgia sections, *in* Woodward, N. B., ed., *Valley and Ridge Thrust Belt: Balanced Structural Sections, Pennsylvania to Alabama (Appalachian Basin Industrial Associates)*: University of Tennessee Department of Geological Sciences Studies in Geology, v. 12, p. 40–53.

VITA

Brian Stephen Cook

born September 1, 1975, in Winston-Salem, North Carolina

Degrees conferred:

B.S. in Geology, 1999, from University of North Carolina at Chapel Hill,
minor in Linguistics

M.S. in Geological Sciences, 2001, from University of Kentucky

Professional positions held:

Teaching assistant and research assistant, University of Kentucky Department of
Geological Sciences, fall 1999 to fall 2001

Teaching assistant, Virginia Polytechnic Institute and State University Department of
Geological Sciences, fall 2001 to fall 2005

Teaching assistant and research assistant, University of Kentucky Department of Earth
and Environmental Sciences, fall 2005 to summer 2010

Geology intern, Equitable Resources (now EQT), fall 2008

Selected publications:

Cook, B. S., and Thomas, W. A., in press, Ductile duplexes as potential natural gas plays:
an example from the Appalachian thrust belt in Georgia, USA: Hydrocarbons in
Contractional Belts, Geological Society of London.

Cook, B. S., and Thomas, W. A., 2009, Superposed lateral ramps in the Pell City thrust
sheet, Appalachian thrust belt, Alabama: *Journal of Structural Geology*, v. 31, p.
941-949.

Cook, B. S., and Thomas, W. A., 2008, Potential natural gas plays in ductile duplexes: an
example from a recess in the Appalachian thrust belt in Georgia, USA: Geological
Society of London, Joint meeting of the Petroleum Group and the Tectonic
Studies Group--Fold-Thrust Belt Exploration. Geological Society, London, U.K.
14-16 May 2008.

Cook, B. S., and Thomas, W. A., 2007, Palinspastic reconstruction around a recess in the
Appalachian thrust in Georgia: *American Association of Petroleum Geologists*,
2007 Eastern Section Abstracts, p. 30.

- Law, R. D., Cook, B. S., Jessup, M., and Searle, M. P., 2004, Strain symmetry and vorticity of flow in mylonites from the Moine thrust zone and Greater Himalayan Slab: implications for space problems, extrusion and exhumation: Geological Society of London, Joint meeting of the Tectonic Studies Group and the Petroleum Group--Continental Tectonics: Discussion Meeting in Memory of the Life and Work of Mike Coward. Geological Society, London, U.K. 27-28 May 2004.
- Cook, B. S., and Thomas, W. A., 2002, Structural response of the Pell City thrust sheet to an oblique lateral ramp in the footwall, Appalachian thrust belt, Alabama: Geological Society of America Abstracts with Programs, v. 34, p. 118.